Université catholique de Louvain – Louvain Drug Research Institute

Metabolism and Nutrition Research Group

Hepatocyte endocannabinoid system and innate immunity influence whole-body lipid metabolism: investigation of the molecular mechanisms in the context of obesity

Charlotte Lefort

Thesis Director
Professor Patrice D. Cani

Thesis submitted in fulfilment of the requirements for a PhD degree in Biomedical and Pharmaceutical Sciences

Jury composition

Thesis Director

Professor Patrice D. Cani

President of the Jury

Professor Giulio G. Muccioli, UCLouvain, Belgium

Jury Members

Professor Isabelle Leclercq, UCLouvain, Belgium

Professor Xavier Stephenne, Cliniques Universitaires Saint-Luc, UCLouvain, Belgium

Professor André Marette, Université Laval, Canada

Doctor Philippe Gérard, INRAE Jouy-en-Josas, France

« Nommer c'est dévoiler. Et dévoiler, c'est déjà agir »
Simone de Beauvoir

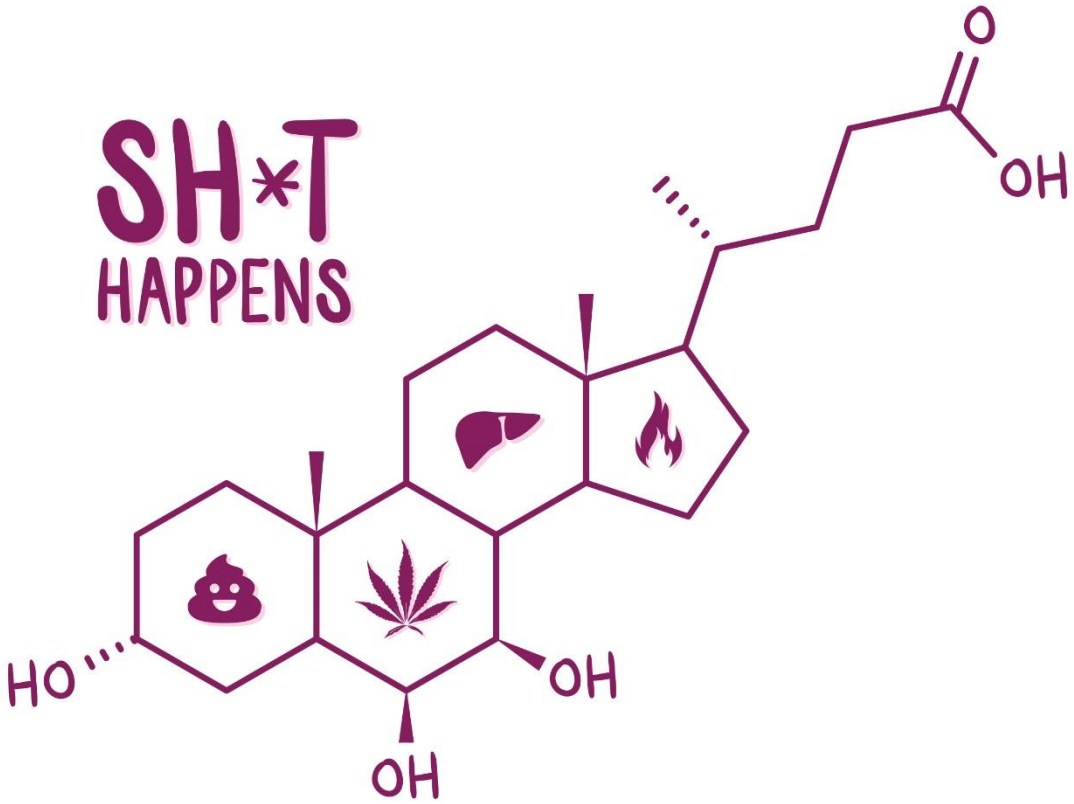

Figure 0 : Résumé de cette thèse en une image [Dheulin & Lefort, *Coloc du 69*, 2020]. Les jeux de mots aux connections multiples ont toujours été stimulants. Statistique : * représente une *P*<0.0000009 selon Lefort test. Abréviation : *, i.

MERCI

Bien que lors d'une thèse "Shit happens", il y a bien plus de moments remplis de good vibes et extraordinaires partagés avec des personnes uniques dont j'aimerais mettre l'emphase dans ces remerciements.

Partie scientifique sérieuse mais primordiale
J'aimerais tout d'abord remercier mon promoteur, le professeur **Patrice Cani**, qui m'a accueillie dans son équipe. Merci de m'avoir fait travailler dans un cadre si stimulant, de m'avoir accordé votre confiance et votre temps. Merci pour la formation scientifique de qualité. Travailler à vos côtés a été 10^9 enrichissant et vous avez, sans aucun doute, contribué à mon évolution durant ces 4 années. Quindi Grazie :)

Cette thèse n'aurait jamais vu le jour si elle n'avait pas été encadrée par mes membres de jury. Je tiens donc à remercier le président, le professeur **Giulio Muccioli** ainsi que les professeurs **Isabelle Leclercq** et **Xavier Stephenne** qui ont été présents dès le début de l'aventure. Merci pour les discussions scientifiques, vos conseils avisés et votre implication dans ce projet. Merci également aux membres externes, le docteur **Philippe Gérard** et le professeur **André Marette**, qui m'ont challengée en fin de parcours.

Merci également à tous les **collaborateurs** qui ont contribué de près ou de loin au développement de mon projet de thèse.

Partie toujours scientifique mais un peu moins sérieuse
Ensuite cette thèse n'aurait pas été si divertissante au quotidien sans certaines personnes composant ce labo.

Clara, ma partenaire de bureau depuis le 1er jour. Je sais que vivre autant d'heures au quotidien à mes côtés n'est pas toujours facile. Du coup, merci pour ta tolérance et de m'avoir fait éclater de rire au moins 1x par semaine que ce soit au labo ou en sortie. Je te certifie que les tomates orgasmiques et Mr "Bien à vous" restent mes moments préférés <3. Ça a été un réel plaisir de t'avoir rencontrée et de partager autant de temps ensemble. Merci aussi de m'avoir dépoucelée...si on nous avait dit que l'assistanat était un métier à risques.

Marialetizia (lo so che ti piace quando ti chiamo così). Abbiamo cominciato e terminato la tesi insieme mangiando un sacco di NAPE-PLD...e bevendo "un po" di limoncello. Grazie di averci invitate da te in Puglia. Sono stati dei giorni memorabili, veramente. E finalmente grazie di essere stata lì quando ne avevo bisogno. Sei una persona dal cuore d'oro.

Fra o l'uomo macho del ufficio. Meno male che sono lì per picchiarti e rimetterti sulla strada giusta quando dici delle cazzate (vuole dire ogni ora)... alla fine penso che forse sei un po maso ma vabbè ti rispetto cmq no worry.

Souph, **Marion**, **Alice**, **Flo**, **Camille** et **Quentin** ou comment passer des soirées mélangeant science et éthanol en passant parfois par des karaokés. Merci pour tous ces moments (in)oubliables … Il y a tellement d'anecdotes que je vais préférer les passer sous silence histoire que l'on garde un peu de crédibilité scientifique. Votre enthousiasme et dynamisme ont été des facteurs importants pour l'ambiance au laboratoire. Mais mis à part le côté festif, merci pour tous vos conseils (scientifiques et personnels), votre soutien et votre écoute. Votre amitié a été précieuse.

Ces années n'auraient pas été pareilles sans mon mentor **Alex** et son acolyte **Rémi**. Merci pour toutes ces heures passées en bio mol à me former dans un premier temps et à déconner dans un second temps (la plupart du temps comme j'apprends méga vite...keur). Vous ne serez pas là pour la défense mais sachez que votre présence me manque au labo. **Matthias** et **Amandine**, merci pour votre temps et vos recommandations. Merci également à toi **Henri** pour t'être occupé de mes progénitures murines comme un chef. Merci aux nouvelles recrues féminines de la Cani team, **Emilie** et **Paola**, pour apporter un élan de fraicheur dans l'institut. Et finalement, je tiens aussi à vous remercier **Isa**, **Bouazza** et **Antho** pour la bienveillance que vous dégagez au sein du laboratoire.

Merci également à toutes les personnes faisant partie ou ayant fait partie de la grande **famille MNut** et plus particulièrement de la **Cani Team** (nous sommes tellement nombreux que c'est difficile de citer tout le monde). Mais je n'en garde que du positif!

Il y a aussi quelques outsider d'MNut que je me dois de mentionner.
Martin ou comment passer des heures à se marrer en donnant TP ou à pester contre les HPLC. Honnêtement, je suis super contente que tu sois devenu mon binôme il y a 3 ans. Cela n'aurait pas été pareil avec quelqu'un d'autre, c'est sûr. Mon coup de foudre d'en face, **Claire**. Qui aurait cru qu'on accroche si fort et si vite lors d'un mariage… Aha Merci pour ton extravagance et ton écoute. Mon baby du 4ème, **Marine**. Merci pour toutes tes attentions et nos pauses sucrées (tes talents culinaires sont incroyables). Et enfin je ne pouvais pas passer à côté de toute **l'équipe de TP bio** en remerciant plus particulièrement **Marie**, **Sophie**, **Fanny**, **Audrey** et **Jean**. Avoir travaillé à vos côtés était extra. C'était efficace, dynamique et parfois challenging (tks to Covid) mais toujours dans la bonne humeur.

Partie patrimoine génétique et ses dérives
Evidemment, je tiens aussi à remercier **mes géniteurs**. Maman, Papa, faire fusionner vos gamètes au printemps 1992 et été 1995 a sûrement été la meilleure idée que vous avez eue ensemble (ahaha <3). Blague à part, merci d'avoir toujours été là. **Maman**, tu es une femme exceptionnelle, super positive et sachant gérer 10 000 trucs à la fois (Je n'ai malheureusement pas hérité de ton côté multitsaking). **Papa**, je sais que peux compter sur toi les yeux fermés. Merci de me soutenir dans ma passion, le pole dance et d'être venu me voir lors de mes représentations au cabaret. Ça me touche beaucoup. Merci également pour tous les voyages qu'on a faits ensemble, l'Italie, la France, Barcelone, St-Petersburg, New-York, la Floride, l'Afrique du Sud et le Cap-Vert. Cela restera de superbes souvenirs crois-moi.
Je sais que je reviens dans le sud que très rarement et que je vous perds parfois avec mes idées et mes raisonnements de vie mais sachez que je vous aime.

Alex mon frère de sang, le seul, l'unique (section drama). Merci pour tous ces moments de complicité qu'on a partagés et il y en a énormément. Je t'emmerderai toujours, sache-le.

Je voudrais aussi remercier mes beaux-parents. **Rol** merci d'exister et de rendre la madre heureuse. Tu es un sacré pilier et nos discussions sont toujours super intéressantes. **Marie**, les sorties sportives en vacances sont toujours les bienvenues et plus que challenging.

Cath et **Zo** je vous considère comme des soeurs. Cath, voisine et amie avant de partager une chambre (on l'avait rêvé mais on n'aurait jamais pu le prédire). Zo ta spontanéité et ta folie sont contagieuses. Love you. **Martin** il est encore temps de passer de l'autre côté de la force. Arrête la chimie et passe en bio. Traître. Je n'ai pas su sauver **Lucas** et **Thibaud** mais je pense qu'il y a encore une chance de te raisonner. Je vous remercie quand même d'avoir amélioré ma culture cinématographique car le côté positif de vivre avec une bande de geeks comme vous (et je vous réinclus Rol et Alex), c'est qu'on devient calé sur Star Wars et les Marvel.

Last but not least, mes grands-parents. **Mamy** et **Papy**, vous m'avez prouvé qu'un amour peut durer toute une vie (j'ai toujours du mal à le concevoir). Vous êtes un sacré exemple et je vous admire beaucoup.

Partie inébranlable (emoji danseuse)
Ensuite, l'aboutissement de cette thèse n'aurait jamais pu se réaliser sans ma vie extra-labo/familiale qui est tout aussi importante pour mon épanouissement personnel.

Cam, mon Minimoys d'amour, on va commencer par toi...il y a tellement de choses à dire. Ça fait maintenant 7 ans que tu es présente au jour le jour dans ma vie (ou presque, merci les vocs de Whatsapp). Tu as ma confiance et mon amitié et j'espère qu'elle continuera encore longtemps. Merci pour ta bienveillance, ton intelligence, ta positivité, ta disponibilité et ta fiabilité. Nos discussions à n'en plus finir sur le féminisme, nos objectifs de vie qui sortent un peu de la "normalité" et nos histoires de cœur m'ont fait évoluer +++ Merci pour tout belle gosse.

Loic (et **Pat**). Mon trouple. Merci à vous deux d'être entrés dans ma vie à l'unif. Je pense que vous êtes les personnes qui me conviennent le mieux pour vouloir vivre à 200 à l'heure, non-stop en quête de challenge, à vouloir toujours découvrir 1000 choses (l'Arak était une mauvaise idée), à repousser nos limites physiques et mentales (Mt Rinjani, MDS et LSO). Je vous en voudrais toujours de m'avoir caché que vous aviez la clé de ma chambre quand on habitait ensemble, sachez-le, la vengeance est un plat qui se mange froid. Mais merci d'avoir toujours été présents et plus particulièrement toi Loic, merci de m'encourager quand je sors de ma zone de confort et d'accepter et soutenir mes idées qui sont parfois farfelues

Clairus, qui aurait cru que partager une chambre au ski MDS nous lierait d'amitié à ce point? L'introduction de tes doigts dans ma cavité buccale a sûrement soulagé mon foie, mes intestins et mon cerveau d'un afflux trop élevé d'éthanol. Merci pour cette belle entrée en matière, c'était direct, j'ai aimé. Aïe mon cœur quand je pense à nos services bar, toutes les soirées à l'unif, à Lisbonne, Varsovie, Pisa, Valencia, Stockholm, Copenhague, Amsterdam et Bruxelles… Meuf tu me manques. Merci de n'avoir aucune limite et d'être toujours aussi présente dans ma vie. J'espère qu'on se retrouvera vite en Frouziland (emoji qui croise les doigts).

Camilla sei la mia più vecchia amica. Siamo cresciute insieme e non ci siamo mai lasciate. Conosci tutto della mia vita. A volte mi dispiace di non vivere in Italia con te. Sei la mia drama queen preferita. Non vedo l'ora di guardare le tue serie TV su Netflix. Sei una donna in gamba, talentuosa, unica, tanto aperta e con un cuore enorme. Spero che continueremo a vederci così spesso. Grazie di sempre esserci. Ci vedremo tra poco a Roma.

L'Arabe, mon **X**Y où attraction et répulsion se sont entremêlées durant ces 4 années. Tu es l'électron libre gravitant autour de mon être **XX** et changeant de couches électroniques en fonction de l'énergie qui nous habite. Notre relation pourrait être apparentée au chat de Schrödinger mais lorsque t'arrives à te rapprocher du noyau, l'attirance est tellement forte qu'elle en devient dangereuse. Merci pour ta douceur et ton excentricité. Peut-être qu'un jour j'arriverai à faire du surf sur un étang, qui sait.

Angèle, merci de m'avoir emmenée dans un univers nouveau, créatif et sans inhibition...où l'expression corporelle et l'ouverture psychique règnent en maître. Tu m'as fait découvrir le monde du cabaret, du pole dance, de l'expression scénique et de l'acceptation de toutes formes humaines avec ses envies aussi déjantées soient-elles. Sans toi, c'est certain que mon parcours sur Bruxelles n'aurait pas été aussi épanouissant et enrichissant.

Ensuite, il y a tous mes colocs qui ont partagé ma vie et qui doivent être remerciés à juste titre. Je sais que je suis parfois une autiste, solitaire et indépendante mais sachez que je vous apprécie énormément. Un big up particulier à **Chatty** et notre passion pour les concerts et festivals. De plus, sans toi je n'aurais jamais eu l'idée de faire mon doc dans cette équipe. **Quent'** et nos soirées sportives, houblonnées ou à dévorer une série Netflix en une soirée (jamais dans l'excès). Et **Charly**. Notre rencontre dans l'avion pour Sofia ne présageait rien de bon mais t'es devenu appréciable (<3). Merci pour tous tes jeux de mots, ton humour et tes œuvres artistiques dont ma couverture de thèse ;) En vrai la coloc du **69** me manquera beaucoup. Merci pour tous ces souvenirs.

Désolée pour tous les **potes** que je n'ai pas cités mais qui comptent également. Si je continue, je suis lancée pour écrire un livre de remerciements alors que ça ne doit faire que quelques pages… oups.

Finalement, merci **Salvador D**. et **Antoine V.** pour être une source d'inspiration permanente… il fallait marquer les annales.

Bisous.

[C'est comme les mails, il n'y a pas besoin de signature]

Summary

In an attempt to slow down the epidemic of obesity and associated comorbidities, several strategies have been tested to tackle these metabolic disorders (e.g. surgical, nutritional and physical programs). However, the efficacy of these numerous and diverse approaches is still limited thereby strengthening the emergency to find new therapeutic targets.

Interestingly, the immune system and several bioactive lipids (e.g. *N*-acylethanolamines (NAEs) and bile acids) were reported to be altered in obesity-related conditions. Therefore, the present thesis aimed to gain more insights into their implications in the onset of metabolic disorders and to discover new potential treatments. More precisely, the first objective of this thesis was to examine deeper the role of a central adaptor of the immune system named MyD88 while the second objective was to explore the function of the enzyme *N*-acylphosphatidylethanolamine-selective phospholipase D (NAPE-PLD), a key player of the endocannabinoid system in charge of generating important lipid mediators. Since the liver is an essential organ of metabolic relevance, it was chosen as tissue of interest to start the investigations.

The first chapter of this thesis was devoted to better examine the function of hepatocyte MyD88 on inflammation and lipid metabolism by extending the work undertaken by our laboratory. Indeed, we previously indicated that mice deleted for *MyD88* in hepatocytes (i.e. *MyD88*$^{\Delta Hep}$ mice) were prone to liver inflammation and displayed a compromised energy homeostasis. However, the molecular mechanisms underlying this phenotype remained to be elucidated. Hence, to further explore this phenotype, two experiments challenging the immune system and lipid metabolism were carried out. On the one hand, *MyD88*$^{\Delta Hep}$ mice and WT were exposed for 3 days to a high-fat diet (HFD). On the other hand, both groups were intraperitoneally injected with LPS to trigger an acute inflammation. Consistent with our previous findings, *MyD88*$^{\Delta Hep}$ mice exhibited an altered cholesterol-derived metabolite profile. We thereby went deeper and found that the concentration and composition of not only bile acids but also their precursors (i.e. oxysterols) were different in *MyD88*$^{\Delta Hep}$ mice compared to WT mice. By investigating key proteins involved in their synthesis, we discovered that some of them were altered at the mRNA level (e.g. *Cyp8b1 and Cyp7b1*) and that the phosphorylation of ERK, a key kinase involved in this process, was decreased in *MyD88*$^{\Delta Hep}$ mice compared to WT mice after a short-term HFD exposure. We therefore hypothesized that the enterohepatic feedback loop which is crucial to regulate properly bile acid synthesis and that includes both ERK and CYP8B1, might be impaired in *MyD88*$^{\Delta Hep}$ mice. Finally, we also suggested that the increased inflammatory response observed in

MyD88$^{\Delta Hep}$ mice may be explained by their higher level of 25-OHC, a specific oxysterol associated to inflammation and obesity.

The second objective of this manuscript was to decipher the role of hepatocyte NAPE-PLD on metabolism. To this end, we generated a new mouse model harboring an inducible *Napepld* hepatocyte-specific deletion using the Cre-lox system (i.e. *Napepld*$^{\Delta Hep}$ mice). After validating the model, we discovered that *Napepld*$^{\Delta Hep}$ mice displayed a HFD-like phenotype under normal diet. This was reflected by an increase in liver weight and lipid droplet size, fat deposits and adipocyte size, among others. Moreover, in addition to the variation of NAE levels observed in *Napepld*$^{\Delta Hep}$ mice, the results showed that the deletion of hepatocyte *Napepld* also affected both bile acid and oxysterol profiles. This suggests that, by influencing the regulation of a broad range of liver bioactive lipids, the role of hepatocyte NAPE-PLD goes beyond the mere synthesis of NAEs.

Taken together, this thesis revealed that a precise control of the liver immune and endocannabinoid system is essential to prevent metabolic disorders. A dysregulation of these two systems influenced the synthesis and the composition of critical lipid mediators (e.g. NAEs, bile acids and oxysterols) modulating host metabolism. Finally, this thesis shed light on the importance to push forward the research into a better understanding of the function and the regulation of these bioactive lipids in order to find new putative therapeutic targets to tackle obesity and ensuing complications.

List of abbreviations

ABC	ATP-binding cassette
ABCA	ABC subfamily A member
AA	arachidonic acid
ABCG	ABC subfamily G member
ABHD	α/β-hydrolase domain-containing protein
ACC	acetyl-CoA carboxylase
Acetyl-CoA	acetyl coenzyme A
AcG	2-acylglycerol
ACOX	peroxisomal acyl-coenzyme A oxidase
AEA	*N*-arachidonoylethanolamine
ALT	alanine aminotransferase
AMPK	AMP-activated protein kinase
AP-1	activator protein 1
ASBT	apical sodium-dependent bile salt transporter
AST	aspartate aminotransferase
ATP	adenosine triphosphate
BAAT	bile acid CoA:amino acid *N*-acyltransferase
BAL	bile acid CoA ligase
BAT	brown adipose tissue
B-arr 2	β-arrestin 2
BCAA	branched chain amino acids
BMI	body mass index
BSEP	ABC-transporter bile salt export pump
BSH	bile salt hydrolase
CA	cholic acid
cAMP	cyclic adenosine monophosphate
CAR	constitutive androstane receptor
CB	cannabinoid receptor
CD	cluster of differentiation
CDCA	chenodeoxycholic acid
CEACAM1	carcinoembryonic antigen-related cell adhesion molecule 1
ChORE	carbohydrate response element
ChREBP	carbohydrate responsive element binding protein
Cnone	7α-hydroxycholestenone
COX2	cyclooxygenase 2

CPT	carnitine palmitoyltransferase
CREB	cAMP response element-binding protein
CVD	cardiovascular disease
CYP	cytochrome P450 enzyme
CYP27A1	sterol 27-hydroxylase
CYP7A1	cholesterol 7α-hydroxylase
CYP7B1	oxysterol 7α-hydroxylase
CYP8B1	sterol 12α-hydroxylase
D2	2-iodothyronine deiodinase
DAG	diacylglycerol
DC	dehydrocholesterol
DCA	deoxycholic acid
DGL	diacylglycerol lipase
DHA	docosahexaenoic acid
DHEA	*N*-docosahexaenoylethanolamine
DIO2	type II iodothyronine deiodinase
EAT	epididymal adipose tissue
EC	epoxycholesterol
ECB	endocannabinoid system
eCBome	endocannabinoidome
EGP	endogenous glucose production
ELOVL	elongation of very long chain fatty acids protein
EPA	eicosapentaenoic acid
ER	endoplasmic reticulum
FAAH	fatty acid amide hydrolase
FABP	fatty acid–binding protein
FACS	fluorescence-activated cell sorting
FAS	fatty acid synthase
FFA	free fatty acids
FGF	fibroblast growth factor
FGFR	fibroblast growth factor receptor
FOXO	forkhead box O
FTO	fat mass and obesity-associated gene
FXR	farnesoid receptor X

G6Pase	glucose-6-phosphatase
GDE	glycerophosphodiesterase
GK	glucokinase
GLP	glucagon-like peptide
GLUT	glucose transporter
GPCR	G protein-coupled receptor
HCA	hyocholic acid
HCC	hepatocellular carcinoma
HDCA	hyodeoxycholic acid
HFD	high-fat diet
HMGCR	3-hydroxy-3-methylglutaryl coenzyme A reductase
HSC	hepatic stellate cells
IBABP	intestinal bile acid-binding protein
IDOL	inducible degrader of the LDLR
IGN	intestinal gluconeogenesis
IKK	iκB Kinase
IL	interleukin
INSIG	insulin-induced gene protein
IR	insulin receptor
IRAK	interleukin-1 receptor–associated kinase-1
IRS	insulin-receptor substrate
JNK	c-Jun N-terminal kinase
KC	Kupffer cells
Lan	lanosterol
LBP	LPS-binding protein
LCA	lithocholic acid
LDLR	low-density lipoprotein receptor
LEA	*N*-linoleylethanolamine
LPS	lipopolysaccharides
LSEC	liver sinusoidal endothelial cells
LXR	liver X receptor
MAMP	microbe-associated molecular pattern

MCA	muricholic acid
MCP1	monocyte chemoattractant protein 1
MD-2	myeloid differentiation factor 2
MDCA	murideoxycholic acid
MDR2	multidrug resistance protein 2
MGL	monoacylglycerol lipase
mTORC	mammalian target of rapamycin complex
MyD88	myeloid differentiation primary response gene 88
NAAA	*N*-acylethanolamine acid amidase
NADPH	nicotinamide adenine dinucleotide phosphate
NAE	*N*-acylethanolamine
NAFLD	nonalcoholic fatty liver disease
NAPE-PLD	*N*-acylphosphatidylethanolamine-selective phospholipase D
NAPE	*N*-acylphosphatidylethanolamine
NASH	nonalcoholic steatohepatitis
NAT	*N*-acyltransferase
NF-κB	nuclear factor-kappa B
NK	natural killers
NLR	nucleotide-binding oligomerization domain (NOD)-like receptor
NTCP	Na^+-dependent taurocholate transporter
OATP	organic anion transporter
OCA	obeticholic acid
OEA	*N*-oleoylethanolamine
OGTT	oral glucose tolerance test
OHC	hydroxycholesterol
OST	organic solute transporter
PA	phosphatidic acid
PDK1	3-phosphoinositide-dependent protein kinase 1
PE	phosphatidylethanolamine
PEA	*N*-palmitoylethanolamine
PEPCK	phosphoenolpyruvate carboxykinase
PGD2	prostaglandin D2
PI3K	phosphoinositide 3-kinase
PIP2	phosphatidylinositol-4,5-bisphosphate
PIP3	phosphatidylinositol-3,4,5-triphosphate

PKA	protein kinase A
PL	phospholipid
PLC	phospholipase C
PNPLA3	patatin-like phospholipase domain-containing protein-3
PP2A	protein phosphatase 2A
PPAR	peroxisome proliferator-activated receptor
PUFA	polyunsaturated fatty acid
PXR	pregnane X receptor
PYY	peptide YY
RIP	receptor interacting protein
ROR	retinoid-related orphan receptor
ROS	reactive oxygen species
RXR	retinoid X receptor
S6K	serine6 kinase
SAA	serum amyloid A
SAT	subcutaneous adipose tissue
SCAP	SREBP-cleavage activating protein
SCD	stearoyl-CoA desaturase
SCFA	short-chain fatty acid
SEA	*N*-stearoylethanolamine
SFA	saturated fatty acid
SHP	small heterodimer partner
SRE	sterol response element
SREBP	sterol regulatory element binding protein
StarD1	steroidogenic acute regulatory protein
T2DM	type 2 diabetes mellitus
T3	thyroxine
T4	3,3’ ,5-triiodothryonine
TAB1	transforming growth factor-β–activated kinase-1 binding protein 1
TAK1	transforming growth factor-β-activated kinase 1
TGR5	Takeda G-protein coupled receptor 5
THC	Δ^9-tetrahydrocannabinol
THDCA	taurohyodeoxycholic acid
TLR	toll-like receptor
TM6SF2	transmembrane 6 superfamily member 2
TMAO	trimethylamine N-oxide

TNF-α	tumor necrosis factor alpha
TRADD	TNF receptor–associated death domain
TRAF	TNF receptor–associated factor
TRIF	TIR domain containing adaptor protein inducing IFN-β
TRPV1	transient receptor potential cation channel subfamily V member 1
TUDCA	tauroursodeoxycholic acid
TXB2	thromboxane B2
UDCA	ursodeoxycholic acid
VAT	visceral adipose tissue
VDR	vitamin D receptor
VLCFA	very long chain fatty acid
VLDL	very low-density lipoprotein
WAT	white adipose tissue
WHO	world health organization
WT	wild-type
1/2-AG	1/2-arachidonoylglycerol
1/2-DHG	1/2-DHA-glycerol
1/2-LG	1/2-linoleoylglycerol
12S-HETE	12(S)-hydroxy-5Z,8Z,10E,14Z-eicosatetraenoic acid
13S-HODE	13(S)-hydroxy-9Z,11E-octadecadienoic acid
2-OG	2-oleoylglycerol

Table of contents

INTRODUCTION

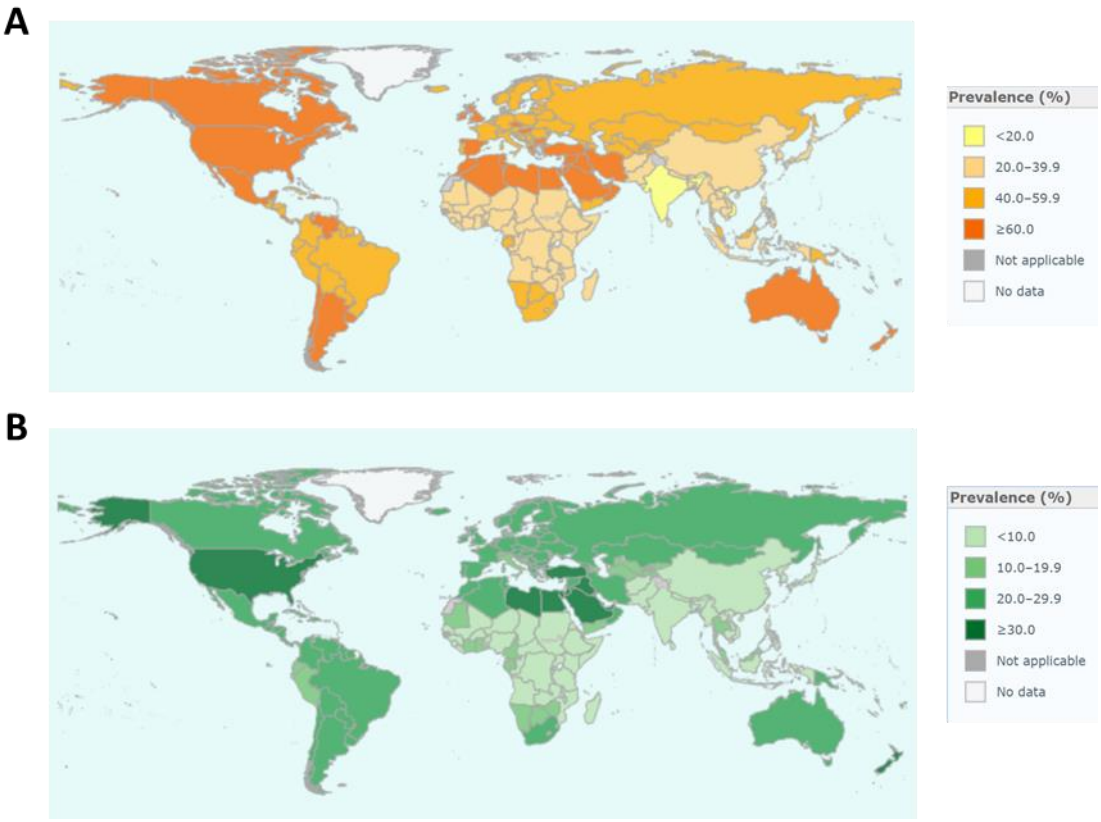

Figure 1: **Prevalence of (A) overweight and (B) obese adults including both sexes in the world according to the last epidemiological study of the WHO in 2017.**

1 Obesity

1.1 Pathogenesis and epidemiology

Obesity is characterized by an excessive and ectopic body fat mass deposition [1]. This elevated fat mass accumulation is commonly considered as the result of an imbalance between energy intake and expenditure [2]. Nowadays, efficient production and marketing have made caloric foods and drinks more tempting, affordable and readily available than ever, resulting in regular overconsumption, whereas our lifestyles have changed in recent years such that physical activity is often reduced. However, the etiology of obesity cannot be reduced to the unique contribution of such environmental factors since genetics are another key parameter that must be taken into account. For instance, mutations in the genes associated with the regulation of food intake, such as leptin, its receptor and melanocortin 4 receptor, as well as genetic variations in the fat mass and obesity-associated (FTO) gene region have been interconnected with a higher prevalence of obesity [3, 4]. Noteworthy, these are not the only genes involved in obesity. Finally, the influence of nurture versus nature is still under debate and is not easy to assess. At the present time, it is believed that the interaction of both environmental and genetic factors impacts the onset of this condition [2].

It is worth mentioning that obesity *per se* is not always a life-threatening condition. However, visceral obesity is one of the pathological criteria included in the definition of the metabolic syndrome. Indeed, a person is diagnosed with this syndrome when s·he displays at least three of the following parameters: visceral obesity, high fasting blood glucose levels, hypertriglyceridemia, hypertension and low serum high-density lipoprotein cholesterol level [1]. Moreover, obesity is a driving factor leading to other comorbidities including type 2 diabetes mellitus (T2DM), cardiovascular diseases (CVD), various types of cancer, steatohepatitis as well as other adverse health effects. The mortality risk associated with obesity is thereby substantial and is mainly due to cancer and CVD complications [1]. In the context of this thesis that has been realized in the laboratory of Metabolism and Nutrition, only the metabolic disorders with regards to obesity-relevant organs will be discussed later on (i.e. T2DM and hepatic steatosis).

Although some efforts have been taken to raise awareness among the worldwide population, the prevalence of obesity is still rising [5, 6]. This condition has become an epidemic disorder, reaching all continents. From a clinical point of view, obesity is classically evaluated by the body mass index (BMI) which is calculated based on the body weight expressed in kilograms divided by the height in meters squared (kg/m^2). According to the World Health Organization (WHO), a human being is considered overweight if her/his BMI ranges from 25 to 29.9 kg/m^2 while s·he is recognized as obese when her/his

BMI is equivalent or superior to 30 kg/m^2. Even though the BMI chart is a simplified tool that has its limitations, it remains the most widely used indicator [2]. The latest epidemiological study carried out by the WHO in 2017 reported that 39% of the adult world population was overweight or obese independently of the gender (Figure 1). This corresponds to more than 2 billion people (WHO data: https://www.who.int/gho/ncd/risk_factors/overweight/en/) [6]. In Belgium, the WHO has estimated that 59.5% of the adults were overweight and 22.1% were obese in 2016. Unfortunately, the global obesity epidemic does not show any signs of regression and it has been predicted that by 2030, overweight and obese adults will represent an estimated 3.3 billion people around the globe [7, 8]. The economic repercussions regarding the healthcare cost of obesity (i.e. hospitalization, drug consumption or consultation), which are already considerable today, would continue to increase. For instance, in the United Kingdom, public health authorities already spend approximately 2.3–2.6% of their budget for obesity-related purposes [9], while in the United States it accounts for more than 663 billion dollars a year [10].

Overall, obesity and ensuing complications are a clear worldwide health burden and having a better understanding of these disorders at the molecular level is crucial to find a way to tackle this problem. Accordingly, the next sections will describe the main molecular players and the crucial signaling pathways, known to be altered in obesity, with a first comment regarding the inflammation.

1.2 Origins of low-grade inflammation

There are roughly two types of inflammation. On the one hand, acute inflammation is a physiological immune response triggered by injury or pathogen infection, is generally short-termed and usually ceases once the stimulus has been removed. On the other hand, chronic inflammation is persistent and is usually associated with harmful outcomes [11]. As such, a low-grade inflammation may eventually lead to adverse health effects and is notably an important hallmark of obesity and associated comorbidities [12-16]. Therefore, this part of the thesis will provide a global overview of the various causes leading to this deleterious inflammation state and will introduce a pivotal ecosystem that shapes our metabolism, that is the gut microbiota.

1.2.1 Macrophage infiltration in metabolic-relevant tissues

It is well-described that one of the main functions of the adipose tissue is to store fat in form of triglycerides [17]. Since the development of obesity is correlated with an elevation of circulating free fatty acids (FFA), adipocytes will act as a sink by accumulating lipids to prevent abnormal and harmful fat deposition in lean tissues such as the liver or muscles. This will lead to the enlargement of adipose tissue cells (i.e. adipocytes) and adipose tissue expansion [18, 19]. Interestingly, the adipose tissue is also an important endocrine organ, able to produce a wide variety of biologically active molecules (i.e. adipokines) that modulate whole-body homeostasis [20]. As a consequence of fat accumulation, enlarged adipocytes will shift their metabolism and will become more prone to release inflammatory adipokines instead of anti-inflammatory adipokines. Moreover, hypertrophic adipocytes are more likely to become necrotic and cell membrane rupture further contributes to the inflammatory response by recruiting monocytes. The migration of immune cells initiates a feed forward loop promoting inflammation by secreting proinflammatory cytokines (e.g. interleukin(IL)-1β, tumor necrosis factor alpha (TNF-α), IL-6) and chemokines (e.g. monocyte chemoattractant protein 1 (MCP1)) [2, 21]. For example, when binding to its receptor, the cytokine TNF-α, elicits the inflammatory response by stimulating c-Jun N-terminal kinase (JNK) and iκB kinase (IKK) proteins that will in turn activate the transcription factors named nuclear factor-kappa B (NF-κB) and activator protein 1 (AP-1) respectively, leading to the transcription of proinflammatory genes including its own production, thereby creating a vicious circle (Figure 2; TNF-α cascade). In addition, this proinflammatory environment is also a driver of insulin resistance, a concept that will be described in the next sections [21].

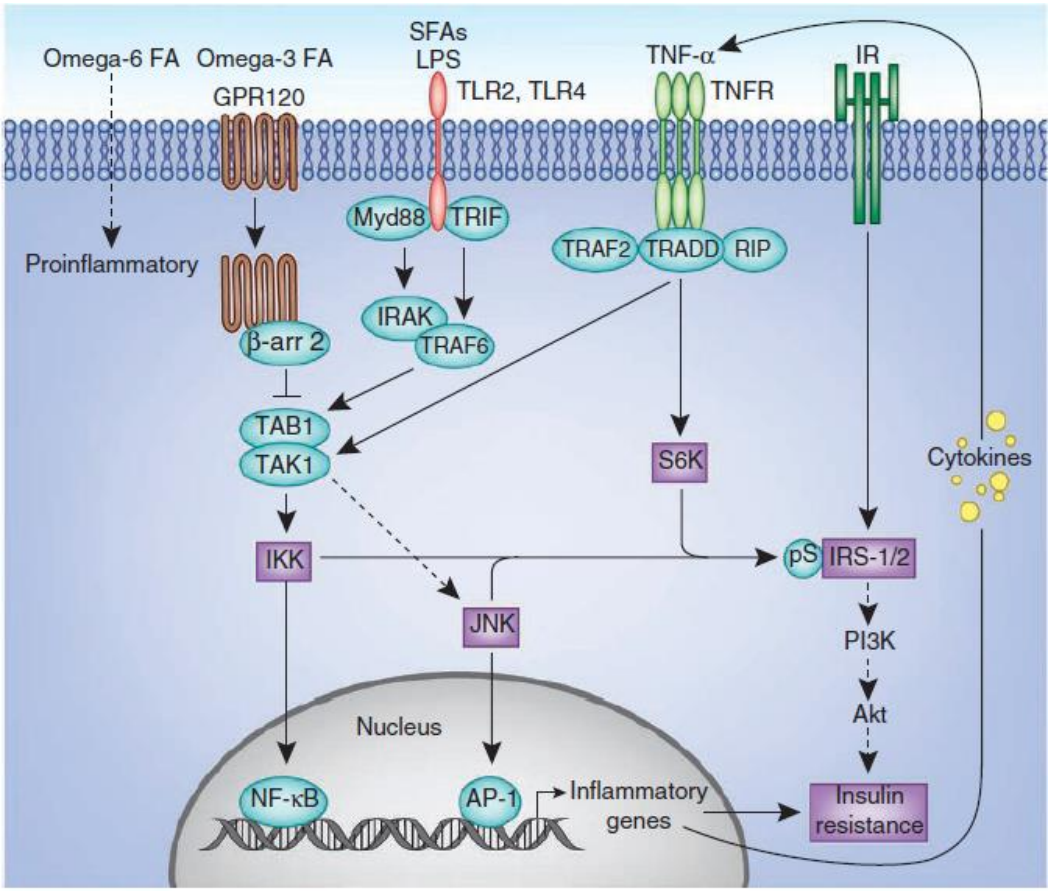

Figure 2: Proinflammatory signaling pathways and their contribution to insulin resistance [21]. Proinflammatory cascades can be initiated by several factors such as Omega-6 FA, SFAs, LPS or TNF-α. These drivers, by binding to specific receptors (i.e. TNFR and TLRs), induce the activation of specific kinases (i.e. JNK and IKK) through the involvement of a myriad of proteins (e.g. Myd88, TRIF, IRAK, TRAF6, TAB1, TAK1 or TRADD). In turn, JNK and IKK activate the transcription factors NF-κB and AP-1, respectively, leading to the transcription of inflammatory genes. Of note, Omega-3 FA exerts anti-inflammatory action by activating GPR120 which inhibits TAK activation. Finally, TNFR stimulation by TNF-α also activates S6K which in turn phosphorylates IRS-1/2 promoting insulin resistance. Abbreviations: AP-1, activator protein 1; β -arr 2, β-arrestin 2; GPR, G protein–coupled receptor; IKK, iκB Kinase; IR, insulin receptor; IRAK, interleukin-1 receptor–associated kinase-1; IRS, insulin-receptor substrate; JNK, c-Jun N-terminal kinase; LPS, lipopolysaccharides; Myd88, myeloid differentiation primary response gene 88; NF-κB, nuclear factor-kappa B; PI3K, phosphoinositide 3-kinase; pS, serine kinase phosphorylation; RIP, receptor interacting protein; S6K, serine6 kinase; SFA, saturated fatty acid; TAB1, transforming growth factor-β–activated kinase-1; TAK1, transforming growth factor-β-activated kinase 1; TLR, toll-like receptor; TNFR, TNF-α receptor; TNF-α, tumor necrosis factor alpha; TRADD, TNF receptor–associated death domain; TRAF, TNF receptor–associated factor; TRIF, TIR domain containing adaptor protein inducing IFN-β.

It is important to point out that overnutrition may also promote inflammation by participating to the polarization of macrophages from M2 to M1 phenotype. Indeed, different subpopulations of macrophages exist in the adipose tissue: the M1 population exhibits proinflammatory properties whereas the M2 contributes to the resolution of inflammation by releasing anti-inflammatory cytokines [17, 21]. Of note, although the concept of M1 and M2 macrophages is valuable to understand

some basic notions of inflammation, this classification into only two phenotypes is currently under debate as it actually oversimplifies the combinatorial spectrum of these cellular populations.

Finally, the inflammation may eventually spread and reach other organs through the secretion of proinflammatory cytokines in the bloodstream by the adipose tissue. Additionally, ectopic fat deposition due to the limited storage capacity of adipocytes and the excess of circulating FFA may also initiate inflammation in the concerned deposits [2, 22]. These events further trigger macrophage infiltration in various tissues relevant for obesity including the liver and further sustain the chronic low-grade inflammation induced by obesity.

1.2.2 The gut microbiota

The gut microbiota refers to the microorganism population (i.e. bacteria, viruses, phages, archaea yeast and fungi) residing in our intestine [23]. This last decade, huge progress has been made to decipher the role of the bacterial community. Scientists discovered that intestinal bacteria are able to regulate host homeostasis and are at the intersection of a vast array of disorders (Figure 3) [24, 25].

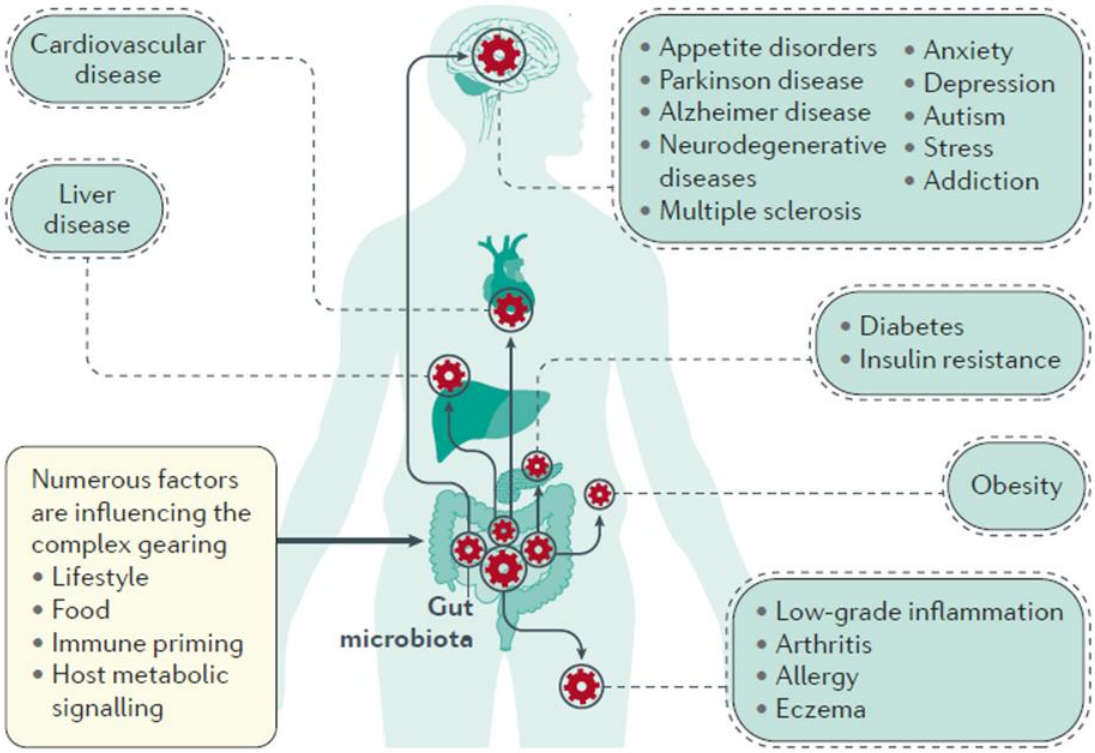

Figure 3: The gut microbiota composition is influenced by various factors and is closely intertwined with a plethora of diseases [25].

It is widely accepted that the amount of bacteria living in our body is substantial and exceeds or at least equals the quantity of human cells [26]. More importantly, it has been estimated that bacterial genes outnumber human genes by at least 40 times, suggesting that their metabolic activities are potentially greater than ours and deserve to be investigated in depth [27].

Interestingly, obesity and its relative comorbidities are characterized by changes in the gut microbiota composition and function that are considered deleterious and are therefore referred to as “dysbiosis” [28]. Concomitantly, the intestinal epithelium which is composed of a single-cell epithelial layer acting as a protector wall between the bacteria and the host, is also often compromised under these conditions (described below) [29]. Noteworthy, in healthy state, these different intestinal cells (i.e. enterocytes, goblet cells, endocrine cells and Paneth cells) are tightly connected together and some of them are specialized to produce mucus (i.e. goblet cells) or to secrete antimicrobial peptides (e.g. enterocytes and Paneth cells) in order to form the so-called gut barrier which limits the interactions between the microorganisms and the host [30] .

In an attempt to unravel the role of intestinal microorganisms in the context of obesity, Cani and colleagues were the first in 2007 to link the gut microbiota to low-grade inflammation associated with insulin resistance and obesity [31]. In this pioneering study, the authors demonstrated that mice fed a high-fat diet (HFD) displayed a higher plasma level of lipopolysaccharides (LPS), a major component of the outer membrane of gram-negative bacteria, capable of stimulating proinflammatory pathways [31, 32]. The increased translocation of endotoxins, primarily LPS, into the bloodstream is referred to as “metabolic endotoxemia” [31]. In the circulation, LPS interacts with LPS-binding protein (LBP), a protein secreted mainly by hepatocytes. This interaction enables LPS to be recognized by a glycoprotein named cluster of differentiation 14 (CD14) which in turn will transfer and present LPS to toll-like receptor (TLR)4-myeloid differentiation factor (MD)-2 complex [33, 34]. TLR4 activation induces complex signaling cascades involving a constellation of protein mediators. Two pathways could be activated: one dependent of the protein adaptor myeloid differentiation primary response gene (MyD)88 and another one that is MyD88-independent [35, 36]. The latter includes the endocytosis of the receptor and is responsible of Type I interferon production. However, both signaling cascades will ultimately result in the stimulation of transcription factors, AP-1 and NF-κB, that will elicit inflammation by inducing the expression of proinflammatory genes in diverse organs such as the intestine, the liver or the adipose tissue (Figure 2; LPS cascade) [36-39].

Obesity is usually associated with an increase in dietary fat intake. Ingested lipids could also exhibit inflammatory properties although data are somewhat controversial across studies (Figure 2; Fatty acid

cascade) [36, 40, 41]. Nevertheless, lipid ingestion promotes LPS absorption through the transcellular pathway via the formation of chylomicrons [42, 43]. During obesity, the paracellular route may also contribute to the translocation of this endotoxin to the blood since evidence suggests that obesity is accompanied with an increased intestinal barrier permeability [29]. Indeed, both the dysbiotic microbiota and the dietary constituents associated with obesity can lead to a compromised gut barrier function (Figure 4) [44, 45]. As such, the intestinal mucus layer thickness is decreased, the expression and localization of tight and adherence junctions are altered and the secretion of antimicrobial peptides is diminished [46, 47]. This phenomenon accentuates the translocation of other microbe-associated molecular patterns (MAMPs) such as flagellin or peptidoglycan which participate to the proinflammatory response by interacting with host receptors such as nucleotide-binding oligomerization domain (NOD)-like receptors (NLRs) and TLRs [48-51]. Finally, besides the role of fatty acids, other food components have been shown to contribute to the regulation of the gut barrier function. Indeed, it is worth noting that food additives commonly found in processed foods can also participate to the development of chronic inflammatory diseases. Indeed, it has been demonstrated that the consumption of dietary emulsifiers (e.g. polysorbate 80 (P80) and carboxymethylcellulose (CMC)) alters the composition of the gut microbiota and enhances bacterial encroachment into the mucus layer, increasing its proinflammatory capacity [52, 53].

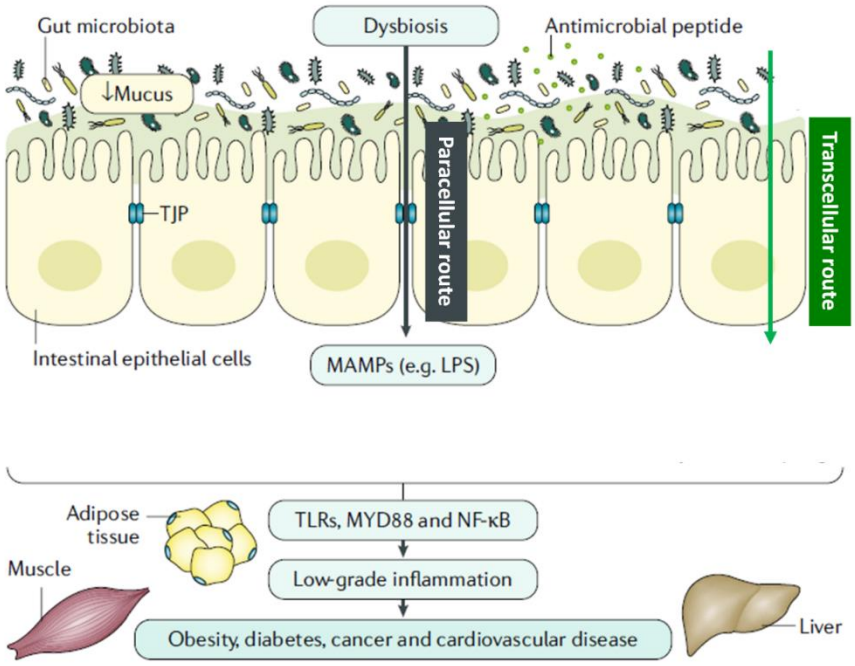

Figure 4: Impact of the gut microbiota on metabolic disorders (adapted from ref [54]). Dysbiosis alters the gut barrier function leading to an increased translocation of MAMPs in the bloodstream. By reaching organs relevant for obesity, they will contribute to the low-grade inflammation state. Abbreviations: LPS, lipopolysaccharide; MAMPs, microbe-associated molecular patterns; MyD88, myeloid differentiation primary response gene 88; NF-κB, nuclear factor-kappa B; TJP, tight junction protein; TLRs, toll-like receptors.

The discovery of the increased gut permeability, commonly referred to as the “leaky” gut, has led researchers in the field to wonder whether bacteria could also translocate and colonize other organs. This question has been examined by several laboratories but is still a matter of debate [46]. Nonetheless, a recent elegant study designed by Anhe and coworkers highlighted the presence of gut bacterial signatures in plasma and in different metabolic organs such as the liver or the adipose tissue in obese individuals. Noteworthy, gut bacterial genes harbored by obese individuals with T2DM were distinct from the obese control group, opening a brand new field of research on new potential targets [55].

Another hit that fuels metabolic inflammation comes from the presence or the absence of some metabolites synthesized by the bacterial community [54]. For example, the gut microbiota can metabolize primary bile acids, cholesterol-derived molecules produced in the liver, into secondary bile acids, which in turn can modulate inflammation through the farnesoid receptor X (FXR) and Takeda G-protein coupled receptor 5 (TGR5) [56]. In addition, these microorganisms can also produce endocannabinoid-like molecules which have been described as modulators of the gut barrier function and inflammation, among others [57-60]. The role of these bioactive lipids will be discussed further in the next chapters of this thesis.

It is also crucial to mention that the gut microbiota is not only involved in the stimulation of low-grade inflammation and its roles regarding host metabolism go far beyond this process. Because the number of metabolites is enormous, this paragraph is only intended to give a glimpse of their metabolic functions in the context of obesity to remain in the frame of this thesis topic [24].

A fundamental action of these host microorganisms is to digest the dietary components (e.g. fibres) that escape our digestion via a fermentation process, leading to the production of metabolites such as short-chain fatty acids (SCFAs) (i.e. acetate, butyrate, and propionate) [61, 62]. Even though SCFAs can be used as an energy source for other bacterial species (e.g. cross feeding) or host cells (e.g. colonocytes), they can also affect host homeostasis [63-65]. For example, an increase in SCFA levels could trigger the production of gut peptides such as glucagon-like peptide-1 (GLP-1) or peptide YY (PYY) by binding on G protein-coupled receptors (GPCRs; GPR41, GPR43) of enteroendocrine L-cells of the intestine to reduce food intake [66-68]. Furthermore, important metabolic pathways are influenced by SCFA concentrations, notably via GLP-1 secretion, such as gluconeogenesis and lipogenesis [69-72]. In addition, other bacterial metabolites such as bioactive lipids (e.g. endocannabinoids and bile acids), neurotransmitters or indole-derived compounds can also contribute to energy homeostasis by interacting with host cells [24, 60, 73].

Interestingly, despite the fact that bacterial components are usually associated with inflammatory response, a recent study by Plovier and colleagues demonstrated that a bacterial protein expressed on the membrane of a mucin-degrading bacterium, *Akkermansia muciniphila*, called Amuc_1100, exerts beneficial health effects in mouse model of obesity, potentially via TLR2 signaling [74].

Finally, it is also worth mentioning that depending on the diet and the intestinal microorganism composition, harmful metabolites can be produced such as trimethylamine N-oxide (TMAO), imidazole propionate or some branched chain amino acids (BCAA) and their concentration are positively correlated with an increased risk for developing metabolic complications [24].

Overall, the crosstalk between the gut microbiota, their metabolites and the host is complex and having a better insight on their interactions could hopefully lead to new therapeutic strategies.

1.3 Obesity-related comorbidities

Population studies have revealed that obesity is a major risk factor for the development of dyslipidemia, endocrine diseases, respiratory complications, cancers, cardiovascular problems as well as mood and cognitive disorders [1]. Since this thesis cannot pretend to be exhaustive, only the metabolic syndromes relevant for the topic of this manuscript will be introduced, that is T2DM and disorders related to hepatic steatosis.

1.3.1 Type 2 diabetes mellitus and insulin resistance

T2DM is characterized by an incapacity of the whole body to lower blood glucose in response to insulin. This metabolic disorder affects approximately 1 in every 11 adults worldwide and can contribute to vascular problems and fatty liver, thereby increasing mortality risks [75-77]. It has been indicated that obesity, alongside lifestyle and genetics, plays a major role in its development [75]. Therefore it is not surprising that approximately 50% of diabetic patients are also obese [1]. In order to understand the mechanistic connections underlying this complex metabolic disorder, having a better knowledge of the blood glucose dynamic is required and will be developed in the next paragraph.

Glucose homeostasis is finely regulated in order to maintain a normoglycemia (i.e. <100 mg/dL fasting blood glucose) [78]. This regulation is mainly orchestrated by insulin which is a hormone secreted by pancreatic islet β-cells following an elevation of blood glucose levels [79]. During fasting, individuals display low-to-normal blood glucose concentration and hypoinsulinemia. In this condition, the liver is stimulated and produces glucose through gluconeogenesis and glycogenolysis to avoid hypoglycemia.

Conversely, upon feeding, circulating glucose increases due to glucose uptake from the intestines and excess glucose are stored as glycogen in skeletal muscles and the liver through glycogenesis. Additionally, in the liver, glucose synthesis is inhibited whereas glycolysis is enhanced [80].

More specifically, insulin exerts its action by binding to its receptor, the insulin receptor (IR), which has an intrinsic tyrosine kinase activity [81]. Upon insulin binding, IR undergoes conformational changes which trigger its autophosphorylation and consequently the phosphorylation of its substrate protein, insulin-receptor substrate (IRS) [82, 83]. This event allows the association of the p85 regulatory subunit of phosphoinositide 3-kinase (PI3K) with the phosphorylated tyrosine residue of IRS. The resulting activation of the catalytic subunit of PI3K, p110, triggers the translocation of PI3K near the cell membrane which then leads to the phosphorylation of phosphatidylinositol-4,5-bisphosphate (PIP2) to phosphatidylinositol-3,4,5-triphosphate (PIP3). The transient generation of the second messenger PIP3 facilitates the recruitment and the interaction of two other proteins, 3-phosphoinositide-dependent protein kinase 1 (PDK1) and Akt/PKB. Once stimulated, PDK1 phosphorylates Akt that, in turn, phosphorylates several downstream proteins. In addition, another protein kinase is able to activate Akt, which is the mammalian target of rapamycin complex(mTORC)2 [76]. Numerous roles have been attributed to Akt [79], but in this thesis only the ones related to the pathophysiology of obesity and T2DM will be discussed. For instance, skeletal muscle is the main organ involved in postprandial glucose uptake (70-80%) and Akt activation leads to GLUT4 glucose-transporter translocation from the vesicles to the surface membrane, allowing the glucose to enter the cells and to undergo glycolysis [84-86]. Glycogen synthesis is also enhanced permitting the cell to store glucose [79]. In the liver, the activation of Akt suppresses gluconeogenesis and enhanced glycolysis by inhibiting forkhead box O(FOXO)1, a transcription factor regulating the expression key enzymes involved in these cascades. Indeed, inhibition of FOXO1 leads to the downregulation of gluconeogenic enzymes , namely phosphoenolpyruvate carboxykinase (PEPCK1*; gene Pck1*) and glucose-6-phosphatase (G6Pase; gene *G6pc*), and to the upregulation of glucokinase (*Gk*) [80]. Moreover, direct hepatic IR activation promotes glycogen synthesis by inhibiting GSK3, which consequently activates glycogen synthase [80]. Furthermore, Akt can also indirectly activate mTORC1 and then sterol regulatory element binding protein(SREBP)-1c which both control lipogenesis [80]. Finally, in the adipose tissue, a major action of insulin is to inhibit lipolysis, limiting the release of FFA and glycerol that are gluconeogenesis substrates (Figure 5) [76].

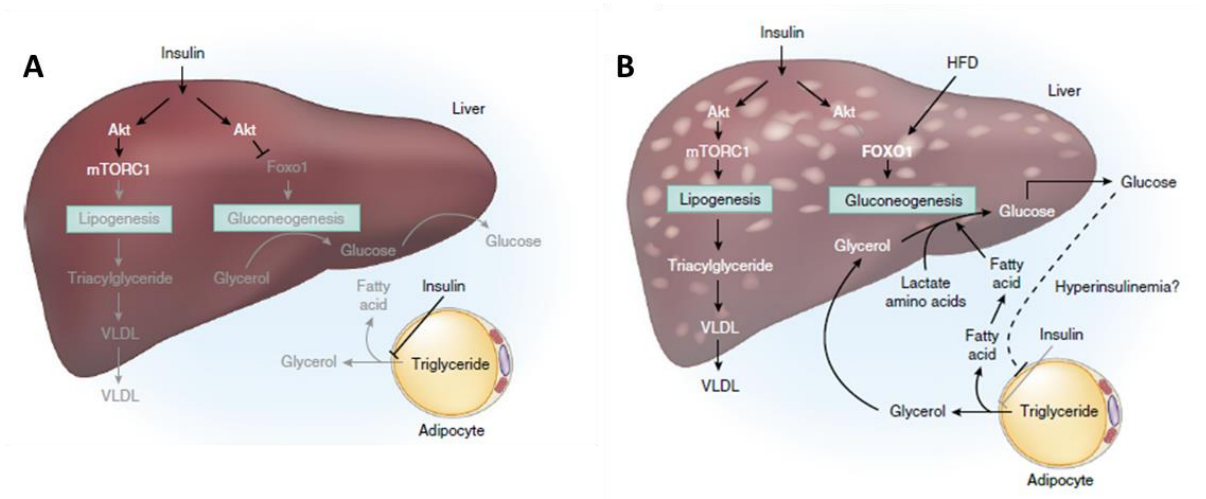

Figure 5: Actions of insulin in the liver and adipose tissues under (A) normal condition and (B) overnutrition (adapted from ref [76]). In non-pathological state, insulin inhibits gluconeogenesis in the liver and suppresses lipolysis in adipocytes. Under HFD, Akt activation is altered and is not able to suppress FOXO1 whereas Akt is still able to activate mTORC1 leading to increased gluconeogenesis and lipogenesis respectively, hence insulin is no longer able to suppress lipolysis in the adipose tissue. This increase in circulating fatty acids contributes to the development of obesity and hepatic steatosis. Abbreviations: FOXO1, forkhead box O 1; HFD, high-fat diet; mTORC1, mammalian target of rapamycin complex 1; VLDL, very low-density lipoprotein.

The circulating insulin level results from the balance between insulin secretion and insulin clearance [87]. Indeed, after being biosynthesized and secreted by the pancreas, this hormone reaches the liver through the portal circulation. During this first pass in the liver, the majority of insulin is cleared by the hepatocytes (i.e. ~50-80%) [88, 89]. Afterwards, the remaining unprocessed insulin exits the liver, is delivered to the rest of the body where it can exert its metabolic action in peripheral organs (e.g. skeletal muscles and adipose tissue), is further cleared by its second pass in the liver and the left-over insulin is finally degraded by the kidneys (~15-25%) [90]. The liver is thereby considered as the main organ responsible for insulin depletion from the blood. More precisely, when insulin binds to its receptor on the cell surface of hepatocytes, it phosphorylates notably the carcinoembryonic antigen-related cell adhesion molecule 1 (CEACAM1) leading to the formation of a protein complex insulin-IR-CEACAM1 [91]. This complex is taken up by the hepatocytes via endocytosis and is destabilized in the endosome. Eventually, insulin is enzymatically degraded and its receptor is recycle back to the surface membrane [87]. Noteworthy, although to a lower extent, peripheral cell types such as adipocytes and myoblasts can also participate to insulin internalization and degradation [90, 92].

T2DM develops when insulin-sensitive tissues such as the liver, the muscle and the adipose tissue become less responsive to insulin. This phenomenon is also referred to as “insulin resistance”. During the early stages of the disease, the insulin secretion is enhanced by the pancreatic cells in response to insulin resistance in order to maintain a proper glycemia. This results in hyperinsulinemia. In a more

advanced stage, the required amount of insulin becomes insufficient leading to a rise of both blood glucose levels and triglyceridemia. Eventually, β-cells will be exhausted and enter apoptosis promoted by a glucotoxic and lipotoxic environment. It is also worth mentioning that the increased ectopic fat accumulation in the muscle and the liver will contribute to the pathophysiology of obesity (e.g. triglycerides) and insulin resistance (e.g. diacylglycerols (DAG) and ceramides) [75, 80].

In order to treat this disease, extensive work has been done trying to understand the cause of insulin resistance from which several theories have emerged. This thesis will only focus on some of them which are discussed below. A first theory suggested that the reactive oxygen species (ROS) produced by the elevated FFA would be a major cause of insulin resistance [93, 94]. This is substantiated by the fact that upon HFD, hepatic ROS-producing enzymes, such as nicotinamide adenine dinucleotide phosphate (NADPH) oxidase, are increased whereas antioxidant activity is decreased [95, 96]. A similar trend has been reported to occur in skeletal muscles [97]. Other researchers proposed that insulin resistance might be due to an altered secretion of putative beneficial factors from adipocytes, which remain to be clearly determined. This has been pinpointed by the recovery of insulin sensitivity in obese mice following a transplantation of either a small quantity of subcutaneous adipose tissue from lean mice or human beige adipocytes [98-100].

A large and important body of literature has indicated that chronic low-grade inflammation, which is now considered a hallmark of obesity and T2DM, is a causal factor in the onset of the disease [21]. The first evidence came from a pioneering study of Feingold and Grunfeld that shed light on the raise of blood glucose upon TNF-α administration in rodents [101, 102]. Also, increased secretion of TNF-α was observed in obese rodents and neutralizing TNF-α improved insulin sensitivity [103]. In line with this, mice with impaired TNF-α function were protected against obesity-induced insulin resistance [104]. Moreover, genetic manipulations revealed that mice exposed to HFD with macrophage-specific deletion of *Jnk1*, *Ikkβ* or fatty acid–binding protein 4 (*Fabp4*) had improved insulin sensitivity compared to obese mice [105-108]. Several molecular mechanisms were put forward to explain the insulin resistance linked to inflammation. For instance, increased TNF-α levels were correlated to decreased *Glut4* and peroxisome proliferator-activated receptor(*Ppar*)γ expressions [109, 110]. Of note, PPARγ is a transcription factor that also mediates the production of anti-inflammatory cytokines and the deletion of *Pparγ* in macrophages impairs insulin responsiveness [111, 112]. TNF-α could also weaken the insulin signaling cascade by stimulating serine kinases which target IRS-1 [21]. Additionally, the accumulation of proinflammatory cytokines was related to the synthesis of ceramides [113]. These bioactive lipids were, in turn, able to dephosphorylate Akt by activating protein phosphatase 2A (PP2A) [114].

Research in that field introduced the hypothesis that inflammation-induced insulin resistance occurs in two steps. The first one is the infiltration and activation (i.e. M1 activation state) of macrophages in the insulin-sensitive organs, usually following nutrient overload [21, 115]. This effect leads to the increased proinflammatory cytokine release in the surrounding environment that in turn affects cells responsive to insulin action, which is the second step. The liver is a good example to illustrate this. It has been demonstrated that Kupffer cells (KC), resident hepatic macrophages, were activated upon HFD leading to the activation of inflammatory pathways in hepatocytes and thereby decreasing their insulin sensitivity [116]. Interestingly, after either KC depletion by intravenous clodronate administration or KC inhibition by gadolinium, the response to insulin was partially recovered in mice exposed to HFD suggesting that KC play a crucial role in the onset of liver insulin resistance [117, 118]. Aside from the increased macrophages recruitment in insulin-sensitive organs, the impact of the gut microbiota cannot be neglected either since we have previously shown that it contributes to obesity-induced inflammation and thereby accentuates insulin resistance (Figure 4) [31, 32, 119-121].

In addition, metabolites (e.g. lipids and amino acids) either coming from the diet, the gut microbiota or endogenously produced were reported to play a pivotal role in regulating insulin sensitivity. Obviously, all lipids, due to their numerous biological roles (e.g. cell membrane constituents, bioactive molecules and metabolic precursors) and their diverse chemical structures (e.g. chain length and saturation), do not act the same way and sometimes display opposite actions [122]. In more detail, saturated fatty acids are associated with insulin resistance given that they can exert inflammatory effects by activating TLR4 after binding to Fetuin A or by inducing endoplasmic reticulum stress and are substrates for DAG and ceramide molecules, two lipids known to inhibit insulin signaling [22, 113, 120, 123, 124]. In contrast, polyunsaturated fatty acids (PUFA), especially omega-3 PUFAs such as eicosapentaenoic acid (EPA) and docosahexaenoic acid (DHA) are linked to insulin sensitivity since they are able to counteract inflammation by binding to GPR120 which will inhibit JNK activity [125, 126]. To make the equation even more complicated, conflicting results exist in the literature, notably with regards to DAG which has been shown to also have beneficial health effects [127]. Other signaling lipids, in particular bile acids, are also involved in insulin resistance by modulating glucose and lipid metabolism [128]. Aside from lipids, it is worth noting that an elevated level of BCAA is also correlated to insulin resistance and obesity [129, 130]. However, deciphering whether it is a cause or a consequence remains to be further investigated.

So far, attention was focused on the downstream effectors of the insulin signaling pathway to understand the molecular bases related to insulin resistance. However, several studies have recently shifted their interest on the regulation of insulin receptor trafficking. Indeed, this regulation is altered

under diabetic and insulin resistance conditions [131]. Nevertheless, this field is still in its infancy and further investigations are warranted.

Although we have previously stated that insulin resistance leads to hyperinsulinemia, the fact that hyperinsulinemia triggers insulin resistance is also true. Experimentally, induction of hyperinsulinemia by insulin infusion in rodents caused insulin resistance [76, 132]. Moreover, it has been proposed that impaired insulin clearance can also induce insulin resistance. For instance, in mice it has been demonstrated that whole-body or hepatic-specific deletion of *Cc1*, the gene coding for the glycoprotein CEACAM1 involved in insulin uptake and degradation, leads to hyperinsulinemia and subsequently to insulin resistance, hepatic steatosis and visceral obesity [133-135]. Today, it remains difficult to assess the exact timeline in which these metabolic events take place and it cannot be excluded – in fact it is more than probable – that they often occur simultaneously.

Collectively, the mechanistic action causing this disease is still under debate and numerous studies are ongoing to elucidate the various cellular and signaling networks in order to find new therapeutic strategies.

1.3.2 Nonalcoholic fatty liver diseases

One of the repercussions of the global rising rates of obesity and type 2 diabetes is the increased prevalence of the nonalcoholic fatty liver disease (NAFLD) [136]. This disorder has emerged to be one of the most common chronic liver diseases worldwide and, to date, it has been estimated that its prevalence equals 24% in the general population, with South America and the Middle East being impacted the most (Figure 6) [137, 138].

NAFLD is defined by an excessive accumulation of triglycerides in hepatocytes and its pathological spectrum ranges from simple steatosis to different degrees of inflammation and liver cell damage. As such, NAFLD might progress to nonalcoholic steatohepatitis (NASH) that may ultimately lead to the development of cirrhosis. Of note, NASH has gained particular attention in recent years because of its association with hepatocellular carcinoma (HCC). NASH is a reversible state that occurs in approximately 25% of NAFLD patients and is characterized by lobular inflammation and hepatocyte ballooning. Fibrosis, which is the strongest predictive factor for the disease progression, can also develop and its degree of severity can vary from F1 (mild) to F4 (cirrhosis) [136, 139, 140].

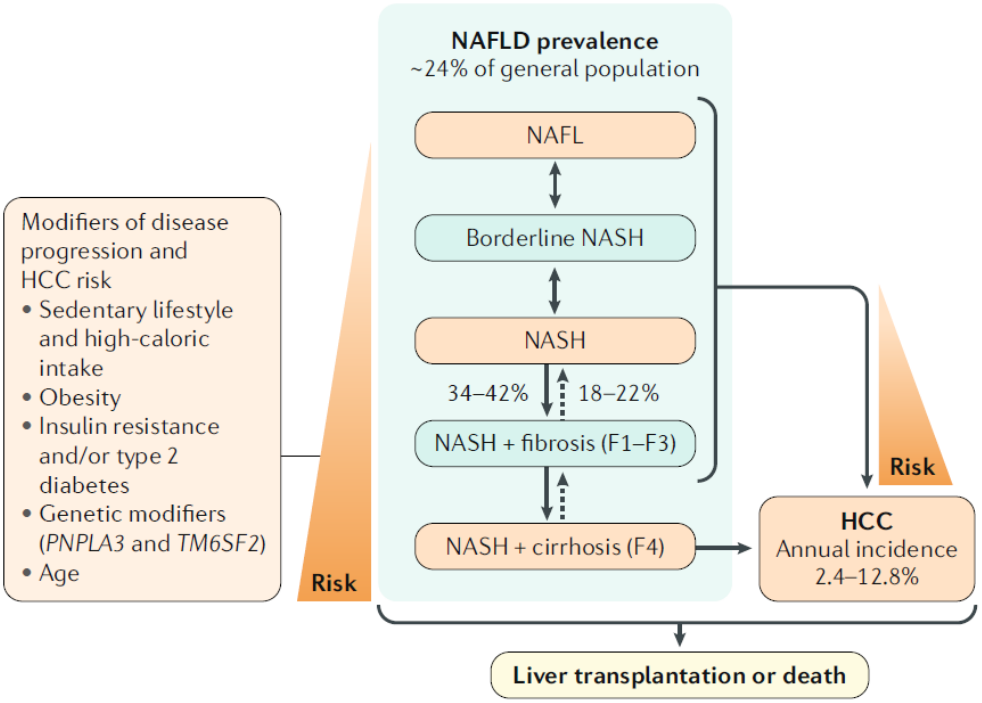

Figure 6: Schematic summary of the progression of NAFLD to HCC with the main drivers contributing to this range of liver disorders [139]. Abbreviations: HCC, hepatocellular carcinoma; NAFLD, nonalcoholic fatty liver disease; NASH, nonalcoholic steatohepatitis; PNPLA3, patatin-like phospholipase domain-containing protein-3; TM6SF2, transmembrane 6 superfamily member 2.

The etiology of this disorder is complex and, so far, several drivers have been identified to participate, probably in parallel, to the progression of this hepatic disease. First, the main source of fatty acids that accumulate in hepatocytes during hepatic steatosis come from the adipose tissue (59%) [86]. Even though lean individuals can also be affected by NAFLD, the majority (>80%) of patients are overweight or obese [13, 138, 141]. Indeed, obesity is strongly associated with insulin resistance as mentioned previously. This phenomenon promotes adipose tissue lipolysis resulting in an increased delivery of FFA to the liver [142]. Of interest, hyperinsulinemia, that is also linked to obesity, enhances hepatic *de novo* lipogenesis which is the second source of fatty acids during hepatic steatosis (26%), by overexpressing lipogenic genes [86, 143]. This ectopic liver fat accumulation induces lipotoxicity and oxidative stress leading to cellular damage and macrophage infiltration contributing to liver inflammation and fibrogenesis [139]. Accordingly, lipidomic studies revealed that the hepatic profile of cholesterol, triglycerides and eicosanoids were highly altered in NAFLD patients. More specifically, diacylglycerides, triglycerides and cholesterol were found to be increased, whereas some polyunsaturated fatty acids, phospholipids, eicosanoids and FFA were either decreased or unaltered [144-146]. Next, the diet, by being the third source of fatty acids in hepatic steatosis (15%) and by modulating the gut microbiota composition, is definitely another factor that must be considered [86].

In line with this, several recent studies indicated that ingestion of dietary saturated fat may contribute to the development of NAFLD in both humans and mice [147-149].

Since patients diagnosed with NAFLD and NASH often exhibit a dysbiosis, more and more studies have concentrated on the role of the gut microbiota [150, 151]. For instance, it has been reported that the gut barrier function was altered in NASH individuals, thus leading to an increased metabolic endotoxemia, which in turn promoted liver inflammation through TLR4 stimulation by LPS. In addition, several microbial metabolites such as SCFA or bile acids can also influence the progression of the disease notably by modulating FXR activity or binding to TGR5 and GPR43 [56, 152, 153]. Currently, some laboratories are looking for a specific microbial signature in NAFLD and NASH patients that could potentially be served as a biomarker of the disorder [136, 150, 154]. It is important to keep in mind, however, that it is not clear whether this dysbiosis is a cause or a consequence of the disease. Finally, genetic predisposition can also impact the development of the disease given that some variants in patatin-like phospholipase domain-containing protein-3 (PNPLA3) and in transmembrane 6 superfamily member 2 (TM6SF2) have been strongly correlated with NAFLD in substantial human cohorts [155-157].

From a research and clinical perspectives, two main challenges are faced. The first is studying this disease to understand better the underlying mechanisms in an appropriate animal model that fully recapitulates NASH [158]. The second is to develop a proper non-invasive technique allowing a clear diagnosis of the disease in humans. These challenges, the detection of the disease and the search for a cure, are both essential since, if left untreated, this hepatic disorder could progress into a more severe disease increasing the risk of mortality [139, 159]. Of interest, a non-invasive clinical test, the NAFLD fibrosis score which includes serum markers such as alanine aminotransferase (ALT), aspartate aminotransferase (AST), albumin, glycemia, platelet count, BMI and age, has been developed [160]. However, at the current stage, these data are not specific nor sensitive to NASH. Presently, most of the diagnostic procedures are done radiologically via abdominal ultrasound even though the gold standard method remains the invasive biopsy that provides histologic evidence on hepatocyte morphology, fibrosis and fat accumulation [136].

Altogether, over the course of the two past decades considerable progress has been made to decipher molecular mechanisms behind NASH. This has led to the discovery of potential pharmacological agents that are currently being tested in pivotal clinical trials. At the present time, it is still a field of intense research and hopefully an efficient drug will emerge from all these ongoing studies [136, 158].

1.4 Therapeutic strategies

Given the multifactorial origins of obesity, several strategies have been developed to overcome this metabolic disorder [2].

The first approach consists in changing the patient's lifestyle and implementing healthy habits. This is achieved by progressively increasing physical activities, changing eating patterns (e.g. lowering of the caloric intake and increasing food quality), modifying feeding behavior (e.g. eating slowly and at regular time), and following psychological therapy if needed. For instance, favoring certain types of diet such as the Mediterranean diet provides metabolic advantages (e.g. reduction of disease risk factors) [161]. Furthermore, several studies targeting the gut microbiota through prebiotics (i.e. *"a substrate that is selectively utilized by host microorganisms conferring a health benefit"*) such as certain polyphenols and non-digestible carbohydrates (e.g. inulin-type fructan), have evidenced that the use of such compounds ameliorated health status by reducing appetite and fat mass gain, among others [162-166]. Moreover, supplementing the diet directly with probiotics, which are "live microorganisms which when administered in adequate amounts confer a health benefit on the host", has also shown promising results [167, 168]. Finally, in our laboratory, Depommier and colleagues demonstrated that in overweight or obese and insulin resistant volunteers, daily administration of a next generation beneficial bacteria (*Akkermansia muciniphila*) during 3 months improved their metabolic parameters (i.e. insulin sensitivity, lower insulinemia and cholesterol) emphasizing the fact that gut microbiota is a potential new therapeutic target and that exploring its regulation and impacts should continue [169, 170]. At the present time, a personalized exercise and nutrition program remains the main recommendation to treat obesity and supplementation with pre- and/or probiotics and/or next generation beneficial bacteria could participate to the prevention of the development of metabolic disorders [24].

From a pharmacological point of view, some anti-obesity drugs have been designed and tested over the years [171]. Unfortunately, they were either poorly efficient or rapidly withdrawn due to important side-effects. The anti-obesity agent rimonabant (Acomplia®) is a good example of the latter. This molecule is an antagonist of cannabinoid receptor (CB)1 and was able to induce a significant weight loss by reducing food intake. Nonetheless, under its prescription, psychiatric issues such as depression and even some cases of suicide were reported [171, 172]. This drug was thereby withdrawn within 2 years after its commercialization.

Another approach resides in surgical interventions such as bariatric surgery. Although most of the patients lose weight and exhibit an amelioration of metabolic parameters, these operations remain criticized. Indeed, surgical complications following the intervention are frequently observed. Moreover, these interventions require a drastic adaptation to a specific diet that can be difficult to maintain throughout life. Hence, it is not rare that post-operative individuals regain weight and need to undergo a new surgical intervention [2, 173, 174].

Finally, it is my personal conviction that more global preventive approaches should also be considered if we want to tackle this worldwide problem. Indeed, obesity is as much a social phenomenon as it is nutritional/scientific one. Therefore, it will take a cultural shift and a great deal of political willingness to come to a real solution. We could start by trying to reduce the availability of “bad” food (e.g. reduce the number of fast foods, decrease portion sizes, limit advertising of junk food, increase prices of high-caloric processed foods) while make healthy ingredients more accessible and cheaper. This would in my opinion help to slow the progress of the epidemic. Obviously, from an economic point of view, these kinds of solutions would trigger another debate which is out of scope of the present work.

To conclude, the need for developing new treatments or improving the aforementioned strategies to cope with the obesity epidemic is still urgent. Hence, having a deeper insight into the molecular processes participating in this disorder is essential. In the frame of this thesis, the contribution of a key family of bioactive lipids produced in the liver will be further examined.

2 The liver

The liver, by displaying an extensive number of signaling pathways, is the most important metabolic hub of the body. This organ plays a vital role in the detoxification of harmful substances (e.g. toxins, xenobiotics), production of blood components and in the regulation of protein, carbohydrate and lipid homeostasis [175, 176]. In this section, only the main metabolic pathways related to obesity and energy homeostasis will be reviewed, that is glucose and lipid metabolism with an emphasis on bile acid regulation. But before going into details, the liver structure will be presented in order to have a better understanding of this intricate organ.

2.1 Structure of the liver

The liver is considered as the largest gland of the body and is positioned above the intestines and next to the stomach [177]. This organ receives blood from two vascular systems, the portal vein and the hepatic artery. The first carries blood from the mesenteric, pancreatic, splenic and gastric veins and supplies the majority of the blood flow (e.g. 70-75%) whereas the latter, coming from the aorta, is in charge of bringing most of the oxygen (e.g. 60%) to the liver [178]. These two blood supplies are mixed in the sinusoids and reach other organs by leaving the liver via the central vein [177]. This circulation establishes a gradient of not only nutrients or oxygen but also of cell types and functions. For instance, there are more macrophages in the periportal zone that are ready to defend this vital organ against harmful molecules coming from the portal vein [179]. Moreover, hepatocytes also harbor a functional gradient by taking up more bile acids, increasing their glucose-6-phosphatase activity or glycogen synthesis, when they are located in the periportal region [180]. Finally, the intrahepatic vascular system also includes lymph vessels and biliary canaliculi that convey bile salts from the hepatocytes to the gallbladder [177].

The structure of the liver is even more complex knowing that it comprises over a dozen of cell types in different proportions with distinct roles [180]. The hepatocytes are the major parenchymal cells of the liver. They are the functional units of this organ and represent 60% of the total liver cells but occupy 80% of the liver volume [177]. These cell types are essential and can manage numerous and various physiological processes (e.g. detoxification, bile acid synthesis, regulation of glucose and lipid metabolism). Hepatocytes are the biggest cell type of the liver (i.e. 20-40 µm) and have a life span of at least 150 to 200 days in humans and up to 450 days in rodents [177].

These cells are positioned next to each other and the presence of tight junctions (i.e. intermediate junctions and desmosomes) connects them together. Moreover, hepatocytes can directly and easily

communicate altogether due to gap junctions [181]. In addition, these cells are polarized. The basolateral side exhibits microvilli to enhance the absorption and secretion surface and is in contact with the perisinusoidal space (i.e. space of Disse), whereas the apical side refers to the canalicular surface [181].

Aside from hepatocytes, the liver is also composed of non-parenchymal cells such as biliary epithelial cells and sinusoidal cells. Specifically, sinusoidal cells constitute about 30-40% of total liver cell number and 6.5% of the liver volume. They include liver sinusoidal endothelial cells (LSEC), Kupffer cells (KC), PIT cells and hepatic stellate cells (HSC; Figure 7) [177].

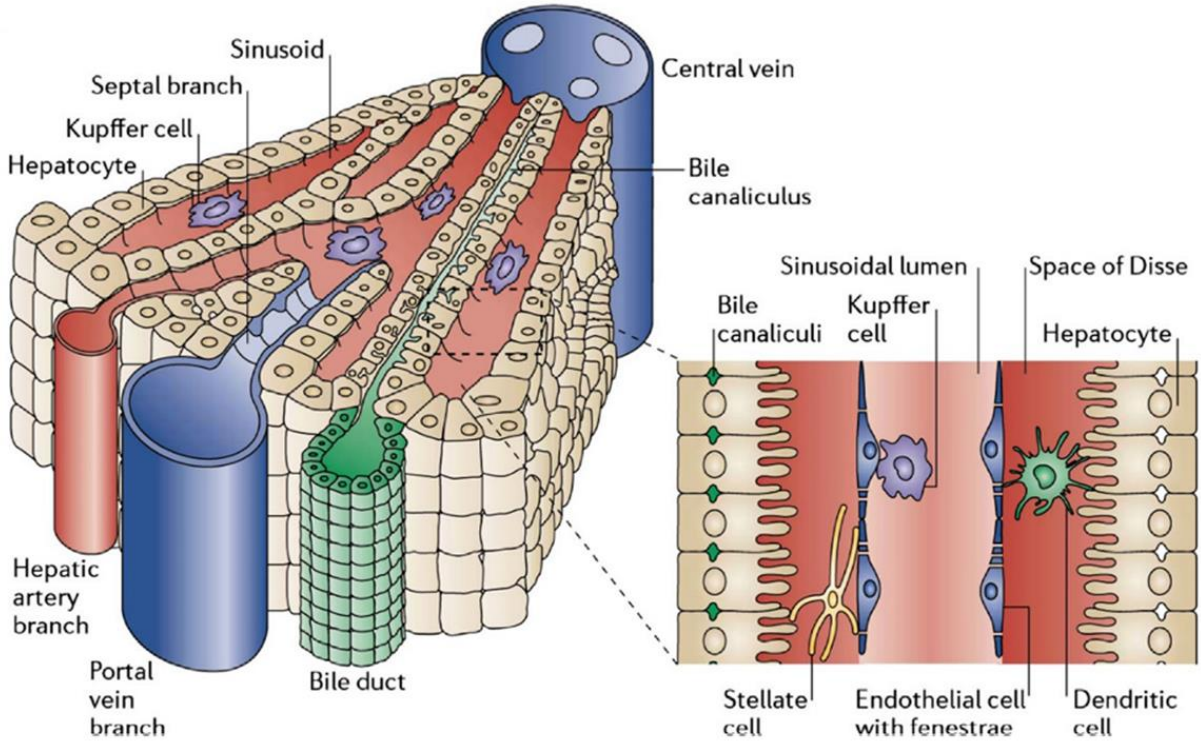

Figure 7: Schematic representation and localization of the main cells composing the liver [182].

LSEC make up 15-20% of total cell number and 2.8% of the liver volume [177]. LSEC lie along the sinusoids and have the particularity of possessing pores, also called fenestrae, which mainly filter the molecules of the blood for the hepatocytes [183]. Endothelial cells are also able to secrete diverse substances including cytokines, growth factors, vasoactive molecules and matrix constituents [184]. Of interest, the intercellular space between the hepatocytes and LSEC is called Disse's space and is also viewed as the major source of lymph [177]. KC are the resident macrophages of the liver and are located in the sinusoids, at a higher level near the periportal region [179, 185]. Indeed, they act as

sentinels and, under physiological conditions, they have the capacity, for instance, to clear endotoxins such as LPS coming from the gut lumen to defend the liver [186]. Even though KC are not close to hepatocytes, they can interact together due to ramifications of KC which can go through the endothelial pores [177]. Their proportion is 2.1% of the total liver volume and they comprise 8-15% of the total liver cells [180]. Another immune cell type that composes the liver are the PIT cells. These lymphocytes are 5 times less abundant than KC, are considered as liver-specific natural killers (NK) and thereby clear the blood from necrotic and tumor cells [177]. Last but not least, HSC lie in Disse's space and represent 3 to 8% of the total liver cells and 1.4% of the volume [187]. These cells are well-known to store fat and contain a high level of vitamin A within their cytoplasm [187]. More importantly, HSC contribute to fibrogenesis and play a major role in the production of the extracellular matrix that is composed of collagens, proteoglycans, glycoproteins, glycosaminoglycans and elastin [180, 188].

2.2 Pivotal liver metabolic pathways in the context of obesity

By being a major organ of biotransformation, the liver regulates crucial metabolic pathways involved in energy homeostasis that are closely intertwined and often altered in the context of metabolic disorders.

The liver is the main organ controlling glucose homeostasis and is the unique organ able to uptake, metabolize, store and produce glucose according to the needs of the body. As already mentioned above, the liver is one of the main tissues regulating glycemia. In short, when the level of blood glucose is high, the liver will take it up and oxidize it to provide energy (i.e. glycolysis). The excess of glucose will be stored first as glycogen (i.e. glycogenesis) or converted later into fatty acids (i.e. *de novo* lipogenesis). Conversely, when the level of blood glucose tends to decrease, the liver will synthesize it through first the glycogenolysis and second the gluconeogenesis [189].

Glucose is also a key driver for liver lipogenesis. During feeding, the glucose enters the liver via GLUT-2 and is either stored in the form of glycogen or metabolized first into pyruvate through glycolysis and further into acetyl coenzyme A (acetyl-CoA). Afterwards, acetyl-CoA enters Krebs cycle and is metabolized into citrate. Depending on the energy balance of the tissue, citrate can either continue Krebs cycle and produce adenosine triphosphate (ATP) or being used to generate lipids. In the latter case, citrate is converted back to acetyl-CoA that is utilized by acetyl-CoA carboxylase (ACC) to form malonyl-CoA which is then transformed into palmitic acid, a saturated fatty acid, by fatty acid synthase (FAS). Of note, the fatty acids generated can be desaturated by stearoyl-CoA desaturase (SCD1) which is able to introduce double bonds and they can further be elongated to form very long chain fatty acids (VLCFA; C<20) by other specific enzymes such as elongation of very long chain fatty acids proteins (ELOVL; Figure 8) [175, 176, 190, 191].

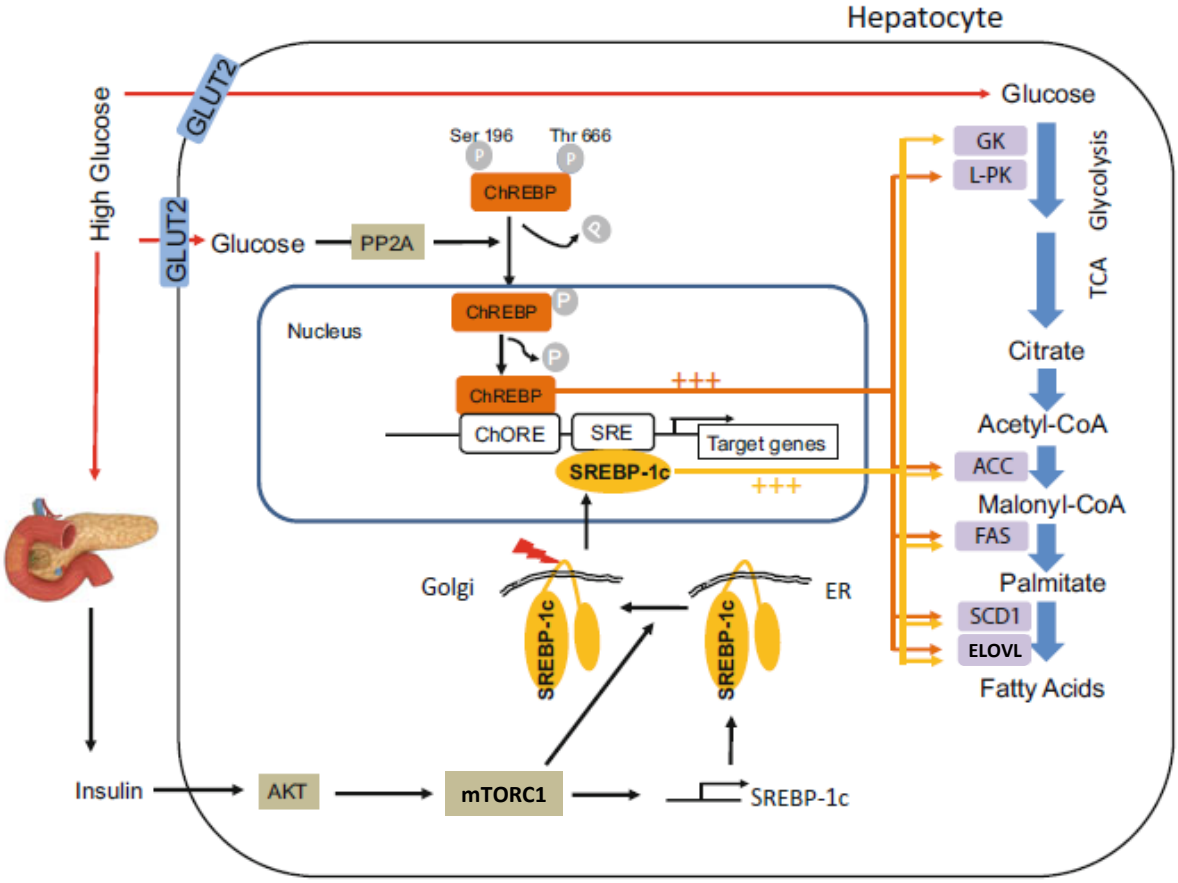

Figure 8: Glucose is the main driver of hepatic lipogenesis (adapted from ref [175]). During postprandial period, glucose blood level is high and this molecule could act as metabolic substrate and as a signaling molecule for fatty acid synthesis. For example, glucose activates ChREBP that in turn, enters the nucleus, binds to the consensus sequence called ChORE and induces the transcription of genes involved in the lipogenic and glycolytic cascades. Besides, a high glucose condition stimulates the release of insulin that induces the expression of SREBP-1c which is responsible for enhancing the transcription of key enzymes such as ACC, FAS, SCD1 or ELOVL. Abbreviations: ACC, acetyl-CoA carboxylase; ChORE, carbohydrate response element; ChREBP, carbohydrate responsive element binding protein; ELOVL, elongation of very long chain fatty acids proteins; ER, endoplasmic reticulum; FAS, fatty acid synthase; GK, glucokinase; GLUT2, glucose transporter 2; L-PK, liver-pyruvate kinase; mTORC1, mammalian target of rapamycin complex; PP2A, protein phosphatase 2A; SCD1, stearoyl-CoA desaturase; SRE, sterol response element; SREBP-1c, sterol regulatory element binding protein-1c; TCA, tricarboxylic acid.

Once synthesized, fatty acids will be associated with glycerol to form triglycerides. Here again, depending on the need of the cells, triglycerides can take different paths. These molecules can be released into the blood in the form of very low-density lipoprotein (VLDL) to provide energy to extrahepatic organs. Triglycerides can also be oxidized by the β-oxidation pathway in the mitochondria or peroxisomes to produce ATP. This metabolic pathway is mainly regulated by the transcription factor PPARα that mediates expression of genes such as peroxisomal acyl-coenzyme A oxidase (ACOX)1, or carnitine palmitoyltransferase (CPT)1. Finally, triglycerides can accumulate in the liver for long-term energy storage, generally resulting in steatosis when these cascades are altered or when there is an

excess of plasma triglyceride level due to an increase in lipolysis in the adipose tissue following insulin resistance [175, 192, 193].

Aside from providing carbon source for lipogenesis, glucose also activates transcription factors that promote fatty acid synthesis, both in a direct and an indirect manner. Briefly, glucose directly induces carbohydrate responsive element binding protein (ChREBP) through activation of PP2A, which dephosphorylates its Ser196 residue. This dephosphorylation drives the translocation of ChREBP from the cytosol to the nucleus. Once in the nucleus, ChREBP undergoes a second dephosphorylation by PP2A at Thr666 residue, that allows ChREBP to bind to a consensus sequence of the DNA called carbohydrate response element (ChORE), thereby leading to the transcription of both lipogenic and glycolytic enzymes. Of note, in low glucose conditions, ChREBP is highly phosphorylated (i.e. Ser196, Ser626, Thr666 and Ser568), which consequently inhibits its activation and nucleus translocation [175, 194]. By contrast, glucose indirectly stimulates SREBP-1c by enhancing the release of insulin which activates Akt, mTORC1 and *in fine* this transcription factor. Indeed, mTORC1 activation by Akt induces the translocation of SREBP-1c from the ER, where it is inactive, to the Golgi apparatus. In the Golgi, this transcription factor is cleaved and can thereby enter the nucleus to bind to sterol response element (SRE) and activate the transcription of its multiple target genes (e.g. *Gck*, *Acaca* and *Fasn*) [194-196].

It should also be pointed out that the regulation of both ChREBP and SREBP-1c is more complex than previously described in this paragraph. Furthermore, AMP-activated protein kinase (AMPK), an energy sensor that regulates the balance between ATP production and consumption, also plays a substantial role in these pathways. However, it will not be discussed in this thesis due to space limitation (for review [175, 176]).

Interestingly, the liver metabolism is also under the control of metabolic-relevant organs such as the intestine and the brain. In more detail, the liver is directly connected to the central nervous system and several studies have provided evidence that the hepatic sympathetic nerve participates in various liver metabolic pathways such as lipogenesis and glycogenolysis [197-199]. Moreover, over the last decade, interest toward intestinal gluconeogenesis (IGN) has increased considerably as this gut function was reported to ameliorate liver metabolic processes, among others. IGN accounts for 5-7 % of total endogenous glucose production (EGP) in post-absorptive state and it has been demonstrated that certain nutrients (i.e. fiber- and protein-enriched diets), bacterial metabolites (i.e. propionate and succinate) and bariatric surgery (e.g gastric bypass) have the capacity to promote IGN (i.e. 20% of EGP in the post-absorptive state in these conditions) which confers health benefits [69, 71, 200-202]. Indeed, Mithieux's team discovered that the glucose released into the portal blood produced by the

intestinal cells was crucial to control both liver lipid and glucose metabolism, likely through a gut-brain-liver neural circuit [200, 203]. As such, by feeding rodents with high-fat/high-sucrose diet supplemented with either succinate or fructo-oligosaccharides (i.e. a dietary fiber), De Vadder and coworkers showed that glucose homeostasis was improved (e.g. decreased hepatic glucose production, improved glucose and insulin tolerance) as compared with control groups. Moreover, they proved that these effects were IGN-dependent since mice harboring an inducible intestinal-specific deletion for *G6pc*, a key enzyme responsible for glucose production, did not exhibit these metabolic ameliorations [69, 71]. Besides, by working with 2 transgenic mouse lines (i.e. one overexpressing intestinal *G6pc* and the other deficient for intestinal *G6pc*) the same scientific group has recently indicated that IGN can prevent the development of liver steatosis in the context of obesity by regulating key liver genes involved in fibrosis (e.g. *Vimentin*, *Acta2*), inflammation (e.g. *Mcp1*, *Tnfa* and *Il6*) and *de novo* lipogenesis (e.g. *Fasn*, *Srebp1c* and *Acaca*). More precisely, *de novo* lipogenesis was decreased when intestinal *G6pc* was overexpressed whereas liver lipid synthesis was increased in the absence of intestinal glucose production. This latter phenotype was partially rescued when intestinal-specific *G6pc* knockout mice were infused with glucose into the portal vein demonstrating the causal effect of IGN on liver lipogenesis. Finally, the innervation of a certain type of neurons was increased in mice overexpressing *G6pc* suggesting that this control might occur through a gut-brain-liver axis [203].

2.3 Bile acid metabolism

The liver is the only organ able to synthesize primary bile acids, which are bioactive lipids that are not only involved in digestive processes, but also in the regulation of host homeostasis [204-206]. In the following section, biosynthesis of bile acids will be briefly presented through the description of their precursors (i.e. cholesterol and oxysterols), as well as their regulation and biological functions.

2.3.1 Regulation of cellular cholesterol in the liver

To fully understand the metabolism of bile acids, it is relevant to first introduce the regulation of their precursors in hepatocytes. Although cholesterol is a vital component of plasma membrane, this molecule can also be metabolized into lipid mediators (i.e. bile acids and steroid hormones) regulating metabolism [207]. Since an excess of cholesterol is toxic for the cells, a tight regulation of its cellular concentration is of the utmost importance. This is mediated by two transcription factors namely SREBP2 and liver X receptor (LXR) which are mutually antagonistic and integrate the need of the cell regarding cholesterol concentration (Figure 9) [208].

SREBP2 is a membrane protein taking part in the production and uptake of cholesterol [207, 208]. It is localized in the endoplasmic reticulum (ER) where it interacts with SREBP-cleavage activating protein (SCAP), which is itself associated to insulin-induced gene (INSIG) proteins [209]. Under conditions of cholesterol excess, SREBP2 is not activated and remains in the ER. Of particular interest, both cholesterol and desmosterol, its precursor, contribute to the retention of SREBP2 by binding to SCAP whereas some oxysterols, oxygenated derivatives of cholesterol, including 24(*S*)-hydroxycholesterol(OHC), 25-OHC and 27-OHC, interact with INSIG reinforcing its connection with SCAP. Conversely in response to a lower cellular level of cholesterol, SREBP2 is translocated to the Golgi apparatus where it is processed. Its activation leads to the transcription of 3-hydroxy-3-methylglutaryl coenzyme A reductase (*Hmgcr)*, an enzyme responsible of the synthesis of cholesterol, and low-density lipoprotein receptor (*Ldlr)*, the receptor involved in the uptake of LDL cholesterol [208, 210].

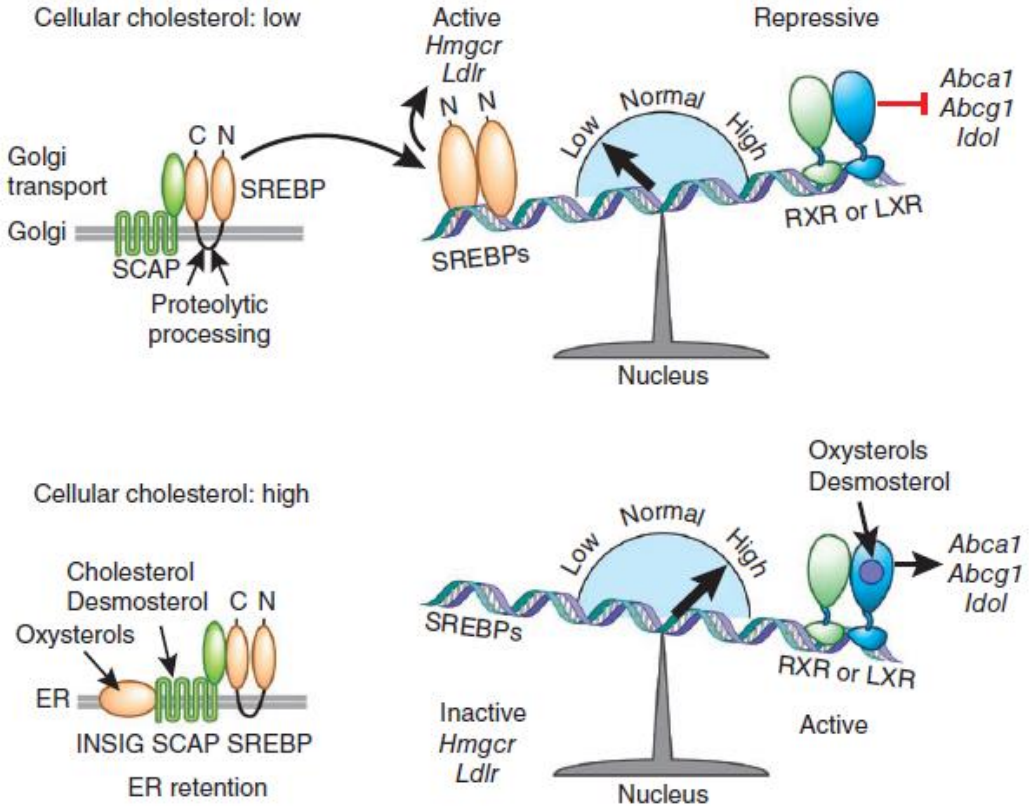

Figure 9: **Cellular regulation of cholesterol level in the cell [208]**. When the cellular cholesterol is low, SREBP is escorted by SCAP from the ER to the Golgi apparatus where it is processed. Activation of SREBP promotes the synthesis of cholesterol by enhancing the transcription of *Hmgcr* and *Ldlr* that are involved in the synthesis of cholesterol and the uptake of LDL respectively. In parallel, LXR-RXR heterodimer is repressed. In opposition, when the concentration of cellular cholesterol is high, SREBP is retained in the ER due to the binding of cholesterol/desmosterol and oxysterols on SCAP and INSIG respectively. This action suppresses the synthesis and the uptake of cholesterol. At the same time, oxysterols and desmosterol interact with LXR resulting in the enhancement of the excretion of cholesterol (ATP-binding cassette(ABC) subfamily A member(ABCA)1, ABC subfamily G member(ABCG)1 and the inhibition of the uptake (inducible degrader of the LDLR ;IDOL). Abbreviations: ABCA1, ATP-binding cassette subfamily A member 1; ABCG1, ATP-binding cassette subfamily G member 1; ER, endoplasmic reticulum; HMGCR, 3-hydroxy-3-methylglutaryl coenzyme A reductase; IDOL, inducible degrader of the LDLR; INSIG, insulin-induced gene protein; LDLR, low-density lipoprotein receptor; LXR, liver X receptor; RXR, retinoid X receptor; SCAP, SREBP-cleavage activating protein; SREBP, sterol regulatory element binding protein.

LXR family is the second main player in the regulation of cholesterol homeostasis and mediates the elimination of cholesterol excess [211]. This family includes two isotypes, LXRα and LXRβ. LXRα is expressed in metabolically active tissues (e.g. liver, adipose tissue and intestine) whereas LXRβ is ubiquitously expressed [212]. These nuclear receptors commonly form an heterodimer with the retinoid X receptor(RXR)-α and play a key role in the cholesterol efflux and conversion to bile acids by inducing the transcription of *Abcg5/8* and cytochrome P450 enzyme (*Cyp)7a1*, respectively [213, 214]. Interestingly, their transcriptional activity is also regulated by desmosterol and several oxysterols (e.g. 24(*S*)-OHC, 25-OHC, 27-OHC and 24(*S*),25-epoxycholesterol) [208, 211]. Additionally, LXR also controls

fatty acid metabolism by enhancing their synthesis through SREBP-1c and their remodeling via ELVOL5 and SCD1, among others [208].

2.3.2 Oxysterols, important signaling mediators derived from cholesterol

Oxysterols are mostly hydroxylated forms of cholesterol that are generated through enzymatic (e.g. CYP450) and non-enzymatic reactions (e.g. ROS; Figure 10) [215]. Although they were long considered as simple intermediates in the formation of bile acids and steroid hormones, they also act as signaling mediators. As such, it has been demonstrated that some oxysterols, through numerous molecular targets (e.g. LXR, GPCRs, retinoid-related orphan receptor (ROR) and estrogen receptor(ER)α), exert pleiotropic effects on inflammation and immunity as well as on glucose metabolism, lipogenesis and cholesterol homeostasis [208, 215-217]. More precisely, aside from the physiological effects already mentioned above regarding cholesterol homeostasis, LXR activation by some of its oxysterol agonists (e.g. 22(*R*)-OHC and 24(*S*),25-epoxycholesterol) also enhances *de novo* lipogenesis by inducing the expression of notably *Srebp1c* , *Fasn* and *Scd1* [212, 218-220]. In addition, LXR stimulation leads to the inhibition of gluconeogenesis by decreasing the expression of *Pck1* and *G6pc* [221, 222]. Of interest, a similar reduction has been indicated in murine primary hepatocytes treated with 7α-OHC, but this time, in a ROR-dependent manner [223].

The involvement of LXR in glucose and lipid metabolism has been further confirmed by using a non-endogenous oxysterol (i.e. 22(*S*)-OHC) which behaves as a LXR antagonist [217]. Indeed, incubation of 22(*S*)-OHC with human skeletal muscle cells from lean, obese and T2DM individuals enhanced glucose uptake and decreased lipogenesis as reflected by the reduced gene expression of *FASN* and *SCD1* in all groups [224]. Noteworthy, the reduction of lipid accumulation and *Fasn* mRNA expression have also been observed in murine adipocytes treated with 27-OHC [225].

Finally, LXR stimulation leads to the reduction of the inflammatory response by interfering with NF-κB and AP-1 [226, 227]. In line with this, it should be mentioned that 25-OHC is the most studied oxysterol regarding inflammation and its function is still debated since it exhibits both pro- and anti-inflammatory properties [228].

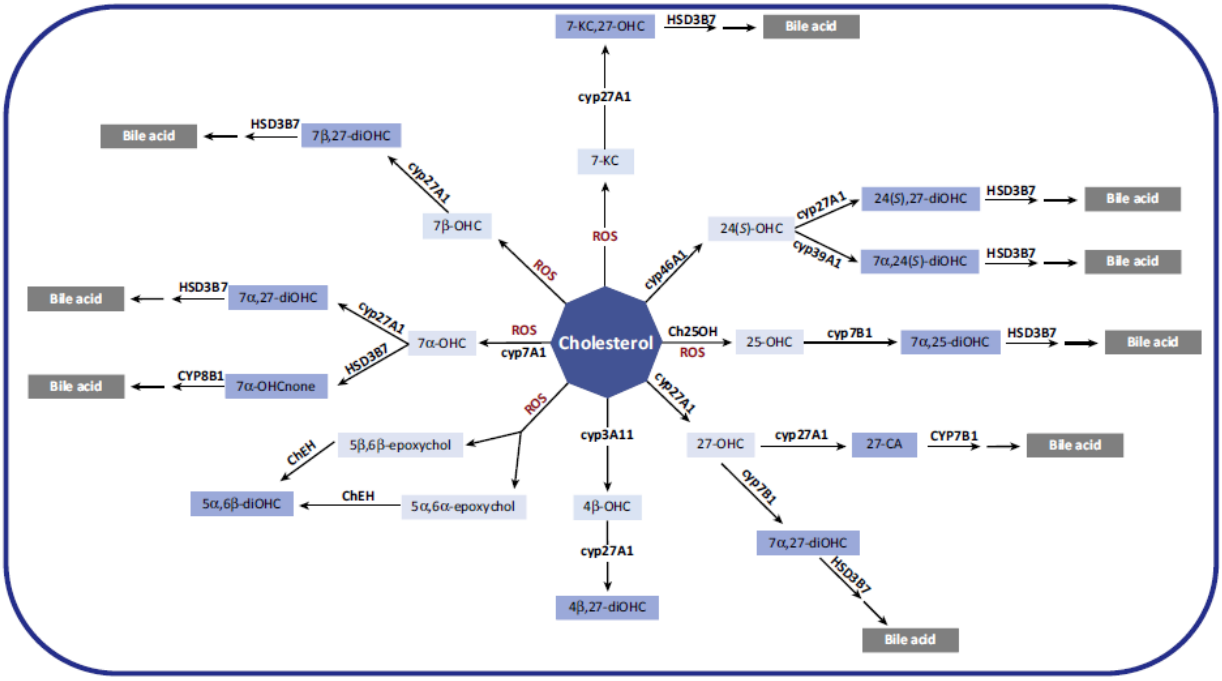

Figure 10: **Schematic overview of oxysterol metabolism [216].** Oxysterol are cholesterol metabolites produced either through multiple enzymes or ROS and are key intermediates for bile acid production as well as pivotal signaling molecules. Abbreviations: 27-CA, 27-cholestenoic acid; 7-KC, 7-ketocholesterol; 7α-OHCnone, 7α-hydroxycholestenone; Ch25OH, cholesterol 25-hydroxylase; ChEH, cholesterol-5,6-epoxide hydrolase; CYP, cytochrome P450 enzyme; Epoxychol, epoxycholesterol; HSD3B7, hydroxy-delta-5-steroid dehydrogenase, 3 beta- and steroid delta-isomerase 7; OHC, hydroxycholesterol; ROS, reactive oxygen species.

Bearing this in mind, it is thus not surprising that the level of oxysterols is altered under pathophysiological conditions ranging from obesity-related disorders (e.g. NAFLD, diabetes and cancer) to neurodegenerative diseases (e.g. Huntington's disease, Parkinson's disease and Alzheimer's disease) [229-235]. For instance, a reduction of serum 4β-OHC level has been associated with obesity in humans [229]. Accordingly, this diminution has also been noted in the liver and adipose tissue of both genetically and diet-induced obese mice [230]. Conversely, 4β-OHC as well as 25-OHC and 27-OHC were increased in the blood of NAFLD patients compared to control individuals [234]. In line with this, 25-OHC, 27-OHC and 7-KC levels were also higher in patients with diabetes or hyperlipidemia compared to healthy controls [232].

To conclude, despite their structural similarities, oxysterols exhibit a broad range of physiological effects and sometimes show opposite actions. It should be emphasized that it is quite difficult to assign a clear function to a specific oxysterol since this system is highly complex. Indeed, one oxysterol can target several receptors and these receptors are not specific to one oxysterol. Moreover, a single enzyme can be involved in the formation of several oxysterols (e.g. CYP27A1 and CYP7B1) and a specific oxysterol can either be generated by different pathways (e.g. 25-OHC) or metabolized through various

enzymes (e.g. 7α-OHC and 27-OHC) [216]. Nonetheless, given their involvement in key signaling pathways associated to metabolic disorders, research on these bioactive lipids should definitely be pushed forward.

2.3.3 Bile acid homeostasis

Unlike oxysterols, primary bile acids are only generated in hepatocytes through an elaborate network involving at least 17 enzymes [236]. There are two main routes producing primary bile acids: the classic and the alternative pathways. In humans, the classic pathway accounts for 90% of total bile acid production whereas the alternative pathway contributes for the remaining 10% under normal physiological condition. In rodents, however, both cascades participate equally to the synthesis of bile acids [204, 206].

On the one hand, the classic pathway initiates with the rate-limiting enzyme named cholesterol 7α-hydroxylase (CYP7A1) and aims to produce both cholic acid (CA) and chenodeoxycholic acid (CDCA) [236, 237]. The sterol 12α-hydroxylase (CYP8B1) is also a key enzyme of this cascade since it is required to form CA and is, therefore in charge of regulating the CA/CDCA ratio [238]. The alternative pathway, on the other hand, first regulates oxysterol levels by synthesizing 24(*S*)-OHC, 25-OHC and 27-OHC through the transporter steroidogenic acute regulatory protein (StarD1) and the enzyme sterol 27-hydroxylase (CYP27A1). These bioactive lipids are thereafter metabolized by oxysterol 7α-hydroxylase (CYP7B1) to predominantly generate CDCA. Noteworthy, in rodents CDCA is mostly converted to α-muricholic acid (MCA) and β-MCA [236, 239]. Once formed, primary bile acids are conjugated with glycine in humans and taurine in rodents by bile acid CoA:amino acid N-acyltransferase (BAAT) and excreted into the biliary canaliculi via the ABC-transporter bile salt export pump (BSEP) to ultimately be stored in the gallbladder. After meal ingestion, these amphipathic molecules are secreted into the duodenum and facilitate the digestion and absorption of dietary fat, steroids and fat-soluble vitamins. Most of the conjugated bile acids are actively reabsorbed in the distal ileum by the apical sodium-dependent bile salt transporter (ASBT), travelled back to the liver through the portal blood, are taken up by the Na^+-dependent taurocholate transporter (NTCP) in hepatocytes to finally be secreted in the gallbladder. This phenomenon is called the enterohepatic circulation. However, a small proportion of bile acids escapes this reabsorption and are profoundly affected by the gut microbiota in the ileum and colon. Conjugated bile acids are firstly deconjugated by bacterial bile salt hydrolases (BSH) present in members of bifidobacteria and lactobacilli, among others. Free bile acids can either cross the gut barrier through passive diffusion or be further processed by bacterial enzymatic activities (e.g. dehydrogenation and dehydroxylation), increasing the catalogue of bile acid molecules. Indeed CA and

CDCA are metabolized into cytotoxic secondary bile acids deoxycholic acid (DCA) and lithocholic acid (LCA), respectively [206]. Additionally, murine-specific primary bile acids, α-MCA and β-MCA, can be converted into secondary bile acids as well. Although both can generate murideoxycholic acid (MDCA), only β-MCA can be metabolized into ω-MCA, hyocholic acid (HCA) and hyodeoxycholic acid (HDCA) [206]. These bacterial metabolites can also be passively absorbed from the gut and can impact the whole organism by acting as signaling molecules (this will be discussed in a subsequent section of this manuscript). In total, ~95% of the total bile acids are reabsorbed at some point, whereas ~5% are excreted in the feces (Figure 11) [240]. Interestingly, a mutual crosstalk exists between these bioactive lipids and the intestinal bacteria. Although it has been demonstrated that gut bacteria influence bile acid profile thereby modulating host metabolism, bile acids can also impact the composition and the proliferation of these microorganisms, by notably exhibiting antimicrobial properties, hence preventing bacteria overgrowth [241, 242].

The synthesis of bile acids is under the control of a negative feedback loop. When entering in enterocytes, specific hydrophobic bile acids (i.e. CDCA, DCA, LCA and CA), free or conjugated, are able to activate FXR, which in turn, promote the production of the intestinal fibroblast growth factor(FGF)15 in mice (FGF19 in humans) [204]. Subsequently, this small molecule is conveyed to the portal circulation and reaches the liver to activate the fibroblast growth factor receptor(FGFR)4/β-Klotho receptor that represses CYP7A1 and CYP8B1 through ERK and JNK stimulation leading to the suppression of bile acid synthesis [243-245]. The inhibition of those two key enzymes is also mediated, to a lesser extent, by the activation of FXR in hepatocytes. This latter will induce the transcription of the nuclear receptor small heterodimer partner (SHP) resulting in the inhibition of CYP7A1 and CYP8B1 to avoid bile acid accumulation, which can induce liver inflammation and injury [239]. It is also worth noting that not all bile acids are FXR agonists and that Tα/β-MCA have been reported to be FXR antagonists [246].

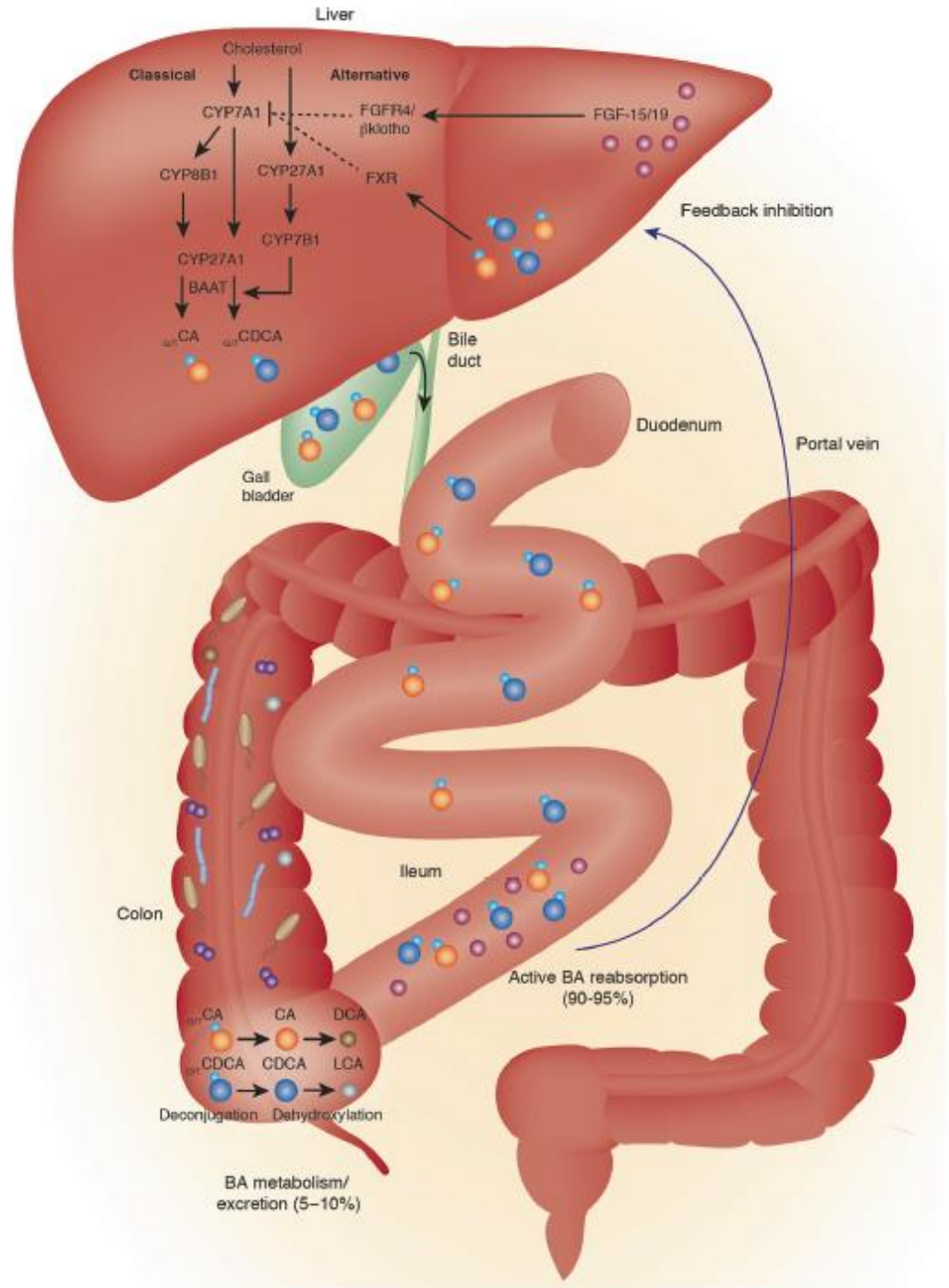

Figure 11: Enterohepatic circulation of bile acids [205]. Primary bile acids (e.g. CA and CDCA) are produced by hepatocytes through two different pathways (i.e. classic and alternative). Before being stored in the gallbladder, they are conjugated with taurine or glycine. After a meal, they are released in the intestine where they participate to the absorption of fat-derived molecules and are actively reabsorbed in the ileum to come back to the liver. Some bile acids, however, enter the colon and are biotransformed by the gut microbiota to generate secondary bile acids (e.g. DCA and LCA). Of note, this synthesis is tightly regulated via a negative feedback loop involving the activation of FXR by specific bile acids. In hepatocytes, FXR activation leads to the inhibition of CYP7A1 through SHP whereas in enterocytes, FXR activation stimulates the production of FGF15, which in turn, activates FGFR4 and suppresses bile acid production by inhibiting notably CYP7A1. Abbreviations: BA, bile acid; BAAT, bile acid CoA:amino acid N-acyltransferase; CA, cholic acid; CDCA, chenodeoxycholic acid; CYP, cytochrome P450 enzyme; DCA, deoxycholic acid; FGF15, fibroblast growth factor 15; FGFR4, fibroblast growth factor receptor 4; FXR, farnesoid receptor X; LCA, lithocholic acid.

As previously mentioned, bile acids are signaling mediators influencing host homeostasis by interacting with TGR5 and various nuclear receptors such as FXR, vitamin D receptor (VDR), constitutive androstane receptor (CAR) or pregnane X receptor (PXR). While PXR, VDR and CAR are mostly associated with drug metabolism and detoxification, it has been proven that FXR and TGR5 mediate pleiotropic effects in energy homeostasis as well as lipid and glucose metabolism [204, 237]. This thesis cannot be exhaustive regarding all the reported functions and will therefore focus on the most relevant ones for our topic.

FXR actions have been extensively studied and conflicting results are reported regarding its beneficial effects during pathological conditions. Many *Fxr* knockout animals were generated and several experiments demonstrated that the deletion of *Fxr* was deleterious for the regulation of bile acid homeostasis as well as lipid and glucose metabolism [247-250]. First, FXR activation has been indicated to prevent the hepatic accumulation of bile acids to toxic levels by inducing BSEP and BAAT in order to enhance bile acid efflux and conjugation, respectively. In addition of inhibiting bile acid synthesis, FXR stimulation may also lower the reuptake of plasma bile acids by downregulating NTCP [251-253]. It was also demonstrated that hepatic lipogenesis was decreased, through the repression of SREBP-1c and ChREBP, and that fatty acid oxidation was promoted, through PPARα stimulation, upon FXR activation [254-256]. Regarding glucose homeostasis, the role of FXR is less clear. One study showed that FXR stimulation inhibited gluconeogenesis by repressing *Pck1* and *G6pc in vitro* whereas another study demonstrated the opposite [257, 258]. In spite of this inconsistency, most of the studies on mice indicated that FXR activation lowers blood glucose level and enhances insulin sensitivity [249, 250, 259]. Finally, anti-inflammatory properties have been also described upon FXR activation in the liver. The decrease in proinflammatory cytokines was likely due to the inhibition of NF-κB [260, 261]. All these studies led to the design of a FXR agonist drug, the obeticholic acid (OCA) which when administered in animals displayed all the beneficial health effects of FXR activation [260, 262, 263]. It is currently a good candidate for the treatment of NASH and T2DM [237]. From a clinical point of view, administration of OCA in a phase II trial in NAFLD and T2DM patients resulted in an amelioration of insulin sensitivity and a decrease in liver proinflammatory markers [264]. Moreover, in a phase III clinical trial for treating NASH, the administration of 25 mg of OCA on a daily basis during 18 months improved fibrosis in NASH patients [265].

After having introduced the good sides of FXR activation, it should be noted that its inactivation can also be beneficial. Indeed, Prawitt and colleagues demonstrated, in mice, that the deletion of *Fxr* conferred a protection against insulin resistance as well as obesity induced either genetically or by the diet [266]. Additionally, another study indicated that mice fed HFD gained more weight upon FXR

agonist administration [267]. In view of all these discrepancies, researchers went further and succeeded in targeting or inhibiting only intestinal FXR in an effort to assess the tissue-dependent FXR functions. Unfortunately, once again, paradoxical effects were reported [268-271]. Additional studies are clearly warranted to clarify the beneficial versus deleterious effects of FXR in different pathological conditions.

Aside from FXR, TGR5 is also a good potential therapeutic target since its activation has been correlated with increased thermogenesis and insulin sensitivity and decreased inflammatory response (Figure 12). Interestingly, its strongest endogenous agonist includes LCA and, to a lesser extent, (un)conjugated DCA, CDCA, UDCA and CA [272, 273].

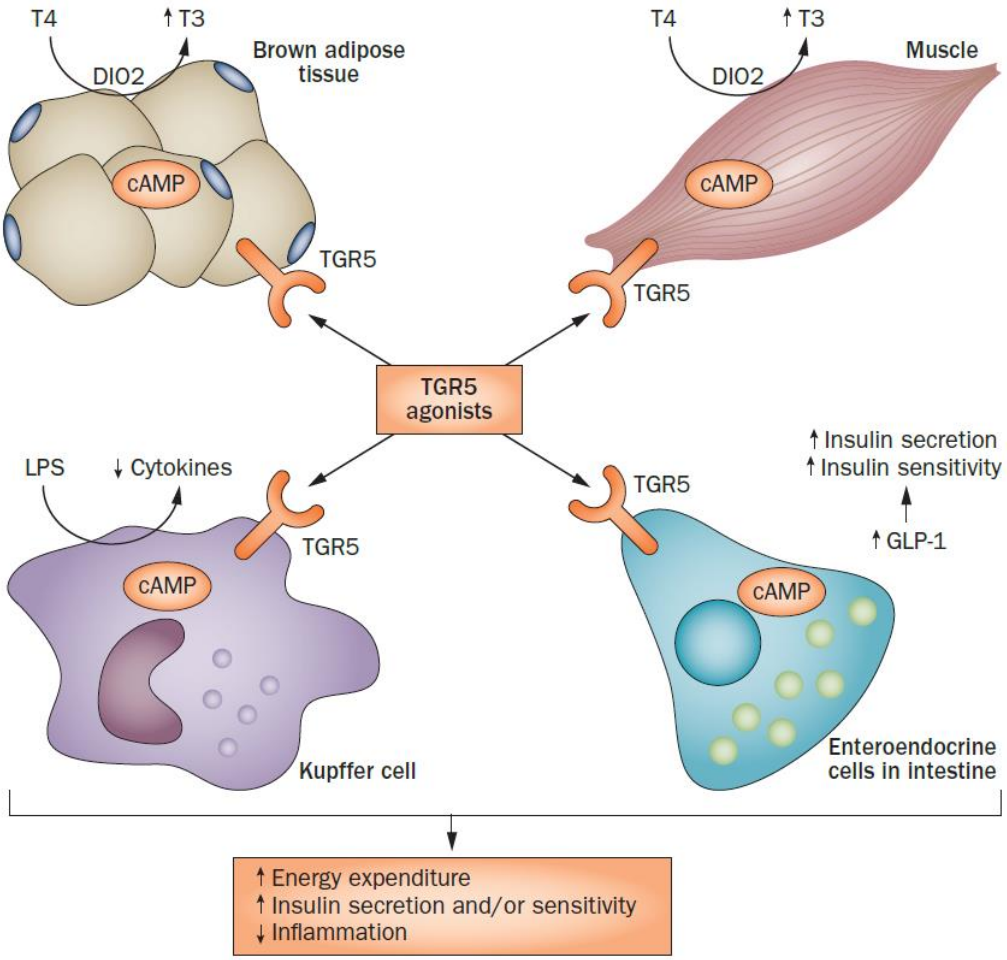

Figure 12: Metabolic actions of TGR5 [237]. TGR5 activation promotes health benefits by increasing energy expenditure in muscles and adipose tissues, by enhancing GLP-1 secretion and by reducing liver inflammation. Abbreviations: cAMP, cyclic adenosine monophosphate; DIO2, type II iodothyronine deiodinase; LPS, lipopolysaccharide; T3, 3,3' ,5-triiodothryonine; T4, inactive thyroxine ; TGR5, Takeda G-protein coupled receptor 5.

Paragraph adapted from Cani, P. D., Van Hul, M., Lefort, C., Depommier, C., Rastelli, M., & Everard, A. (2019). Microbial regulation of organismal energy homeostasis. Nature Metabolism, 1(1), 34-46.

TGR5 stimulation leads to intracellular cyclic adenosine monophosphate (cAMP) accumulation, which activates protein kinase A (PKA) and further downstream cascades. For instance, in thermogenically competent tissues, such as brown adipose tissue (BAT) and muscles, PKA phosphorylates the co-activator cAMP response element-binding protein (CREB), which induces the transcription of type II iodothyronine deiodinase (DIO2). The product of this gene is the enzyme 2-iodothyronine deiodinase (D2). D2 generation triggers the conversion of inactive thyroxine (T4) into 3,3' ,5-triiodothryonine (T3), the active form of thyroid hormone, thus increasing thermogenesis [274]. TGR5 activation also promotes GLP-1 secretion in enteroendocrine cells of the gut enhancing insulin secretion and contributes to the reduction of liver inflammation by inhibiting the nuclear translocation of NF-kB in Kupffer cells [275-278].

Overall, the liver is a vital and metabolically complex organ that contributes to the synthesis of a constellation of molecules that take part in the regulation of host homeostasis. The studies reviewed in the context of this manuscript were chosen to illustrate the possible physiological actions in which these molecules are involved, but are by no means a comprehensive listing. In the next section, another intriguing family of bioactive lipids, ubiquitously expressed, will be described in order to be able to fully appreciate the results and discussion of this thesis.

3 The endocannabinoid system

The endocannabinoid system is a key regulator of host metabolism and mediates several important physiological functions such as appetite, energy balance, stress, inflammation and pain [60, 279-281]. Studying this system is therefore necessary to better understand the underlying mechanisms of metabolic disorders. In this section, the endocannabinoid system will first be defined, with a specific focus on *N*-acylphosphatidylethanolamine-selective phospholipase D (NAPE-PLD), which is one of the main enzymes of this system able to generate specific bioactive lipids. Next, the second part of this chapter will review the metabolic actions associated with these lipid mediators in peripheral organs, especially during obesity.

3.1 Description of the endocannabinoid system

The term "endocannabinoid" was introduced in the 1990s when CB1 and CB2, the receptors of the psychoactive molecule of *Cannabis sativa* named Δ^9-tetrahydrocannabinol (THC), were discovered [282, 283]. After the isolation of these two GPCRs, their two endogenous ligands, *N*-arachidonoylethanolamine (AEA), also known as anandamide, and 2-arachidonoylglycerol (2-AG) were quite rapidly characterized and called endocannabinoids [284-288]. Interestingly, AEA, which has been one of the most studied endocannabinoid, can bind to other receptors either membrane-bound (e.g. transient receptor potential cation channel subfamily V member 1 (TRPV1)) or nuclear (e.g. PPARγ) and exerts a variety of biological actions that goes beyond the psychoactive effect of THC (discussed later) [289]. AEA belongs to the *N*-acylethanolamine (NAE) family which also includes *N*-palmitoylethanolamine (PEA), *N*-oleoylethanolamine (OEA), *N*-linoleylethanolamine (LEA), *N*-stearoylethanolamine (SEA) and *N*-docosahexaenoylethanolamine (DHEA). Noteworthy, AEA is one of the least abundant (i.e. ~tenfold lower) NAEs present in the organs that have been examined so far. This is due to the fact that, its precursor, arachidonic acid (AA), is one of the least represented *sn*-1 esterified fatty acids [281, 290-292]. Strictly speaking, the AEA congeners listed above are not endocannabinoids since they do not bind to CB1 or CB2, but they are still considered as endocannabinoid-related molecules and are therefore included as members of the endocannabinoid system. They can also bind to a wide variety of receptors and are identified as bioactive lipids [60]. However, their intra- and intercellular trafficking are still unclear. Indeed, several NAE carriers within the cells were discovered and even though NAEs are lipophilic and could diffuse through membranes, a specific transporter has been proposed for AEA [293, 294]. Although, specific reservoirs in which AEA is stored (i.e. adiposomes) have also been found, it is widely accepted that NAEs are short-lived molecules (i.e. ~15 min) that are not stored in vesicles but are rather produced "on demand" in

response to cellular stimuli [293, 295]. Therefore, since they are signaling molecules influencing the host homeostasis, a tight control of their synthesis and degradation is mandatory.

NAEs consist in an ethanolamine linked to a specific acyl chain that can differ in length and saturation (Figure 13). These bioactive lipids are biosynthesized from membrane phospholipids and free fatty acids. Specifically, they are mostly formed through the sequential action of *N*-acyltransferases (NATs) which transfer an acyl chain from the *sn*-1 position of phospholipids to the NH_2 group of phosphatidylethanolamines generating *N*-acylphosphatidylethanolamines (NAPEs), which are subsequently hydrolyzed principally by NAPE-PLD to produce NAEs [281, 296].

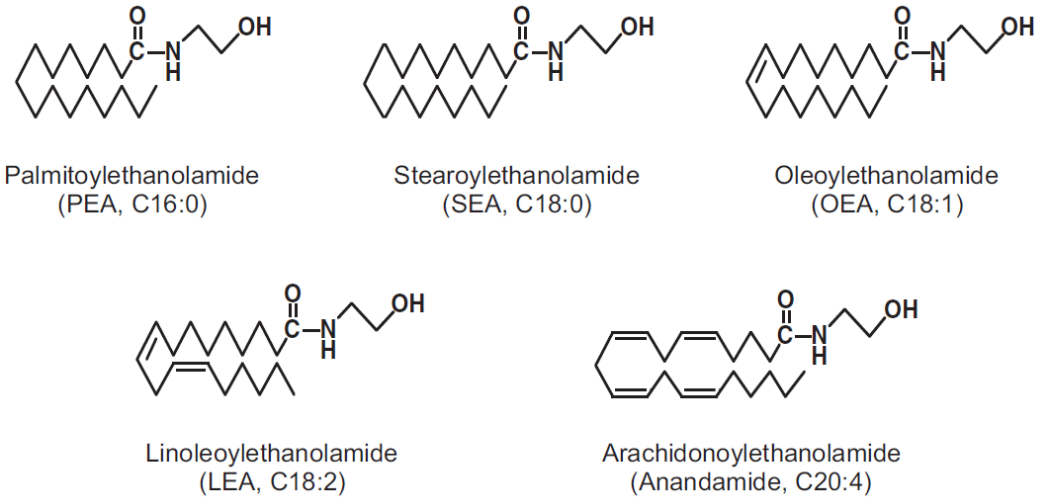

Figure 13: Chemical structure of the various NAEs [297].

It is also worth noting that alternative pathways have been discovered, which slightly contribute to NAE biosynthesis by indirectly converting NAPE to NAE (Figure 14) [298]. Indeed, when investigating constitutive whole-body *Napepld*-deficient mice, researchers were still able to detect small amounts of NAEs, suggesting the existence of NAPE-PLD independent pathways. Accordingly, different cascades have been pinpointed including the one involving α/β-hydrolase domain-containing protein (ABHD)4 and glycerophosphodiesterase (GDE) family proteins [298-300].

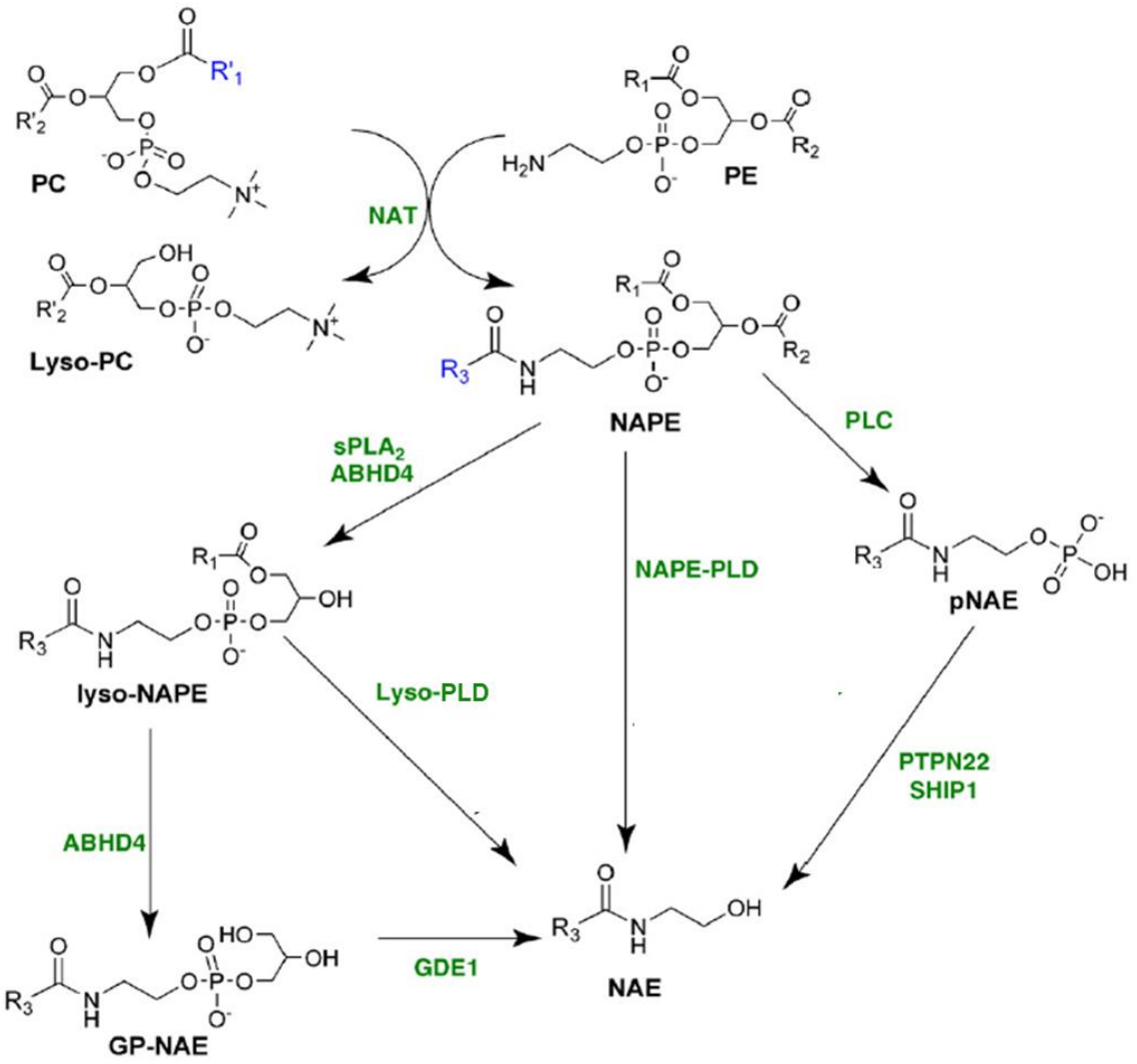

Figure 14: The different pathways contributing to the synthesis of NAEs (adapted from ref [301]). NAEs are mainly biosynthesized from the direct hydrolysis of NAPEs by the NAPE-PLD enzyme. However, alternative pathways have also been identified as illustrated in this figure. Abbreviations: ABHD4, α/β-hydrolase 4; GDE1, glycerophosphodiesterase 1; GP-NAE, glycerophospho-NAE; NAE, *N*-acylethanolamine; NAPE, *N*-acylphosphatidylethanolamine; NAPE-PLD, *N*-acylphosphatidylethanolamine-selective phospholipase D; NAT, *N*-acyltransferase; PC, phosphatidylcholine; PE, phosphatidylethanolamine; PLC, phospholipase C; pNAE, phospho-NAE; PTPN22, phosphatase protein tyrosine phosphatase 22; SHIP1, SH2 domain-containing inositol phosphatase; $sPLA_2$, secreted phospholipase A_2.

NAEs can be inactivated by two different enzymes: fatty acid amide hydrolase (FAAH) and *N*-acylethanolamine acid amidase (NAAA). These enzymes are present at different cellular localizations and exhibit specific NAE affinities [302, 303]. FAAH is present in the membrane of the ER and principally hydrolyzes long-chain NAEs into corresponding fatty acids and ethanolamine [302]. By contrast, NAAA is localized in lysosomes and predominantly inactivates saturated NAEs, in particular PEA [281, 304].

The other well described endocannabinoid, 2-AG, is part of another lipid family named 2-acylglycerols (2-AcGs; Figure 15). Aside from 2-AG, that is one of the main abundant family member, 2-AcGs also

include palmitoylglycerol (2-PG) and oleoylglycerol (2-OG) [60, 281, 293]. 2-AcGs are also derived from cellular phospholipids but are processed by diacylglycerol lipase (DAGL)α and DAGLβ [305]. Unlike the inactivation of NAEs, the hydrolysis of 2-AcGs is rather unspecific and particularly involves the monoacylglycerol lipase (MGL), as well as other esterases, such as ABHD6 and ABHD12 [306, 307].

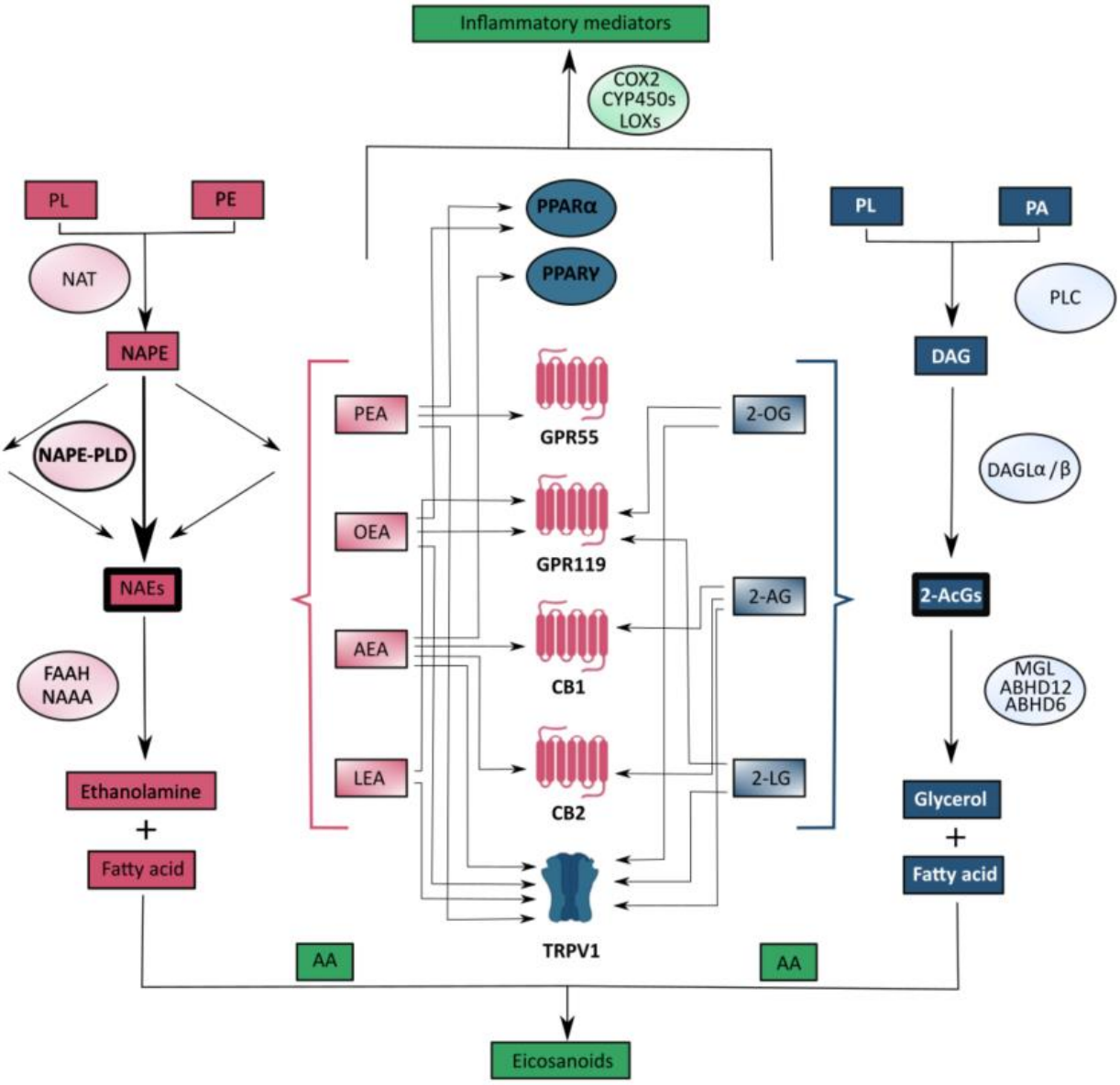

Figure 15: Simplified overview of the endocannabinoidome (adapted from ref [281]). The two main bioactive lipid families composing this system are the NAE family, including PEA, OEA, AEA, LEA, among others, as well as the 2-AcG family that is composed of 2-OG, 2-AG and 2-LG for instance. These lipid mediators can bind to a wide variety of receptors (e.g. CB1, CB2, GPR119, GPR55, PPARα, PPARγ and TRPV1) and mediate a myriad of metabolic processes. All these lipid mediators are synthesized from membrane phospholipids. NAEs are generated through the sequential action of NAT and NAPE-PLD whereas 2-AcGs are formed by the consecutive enzymatic activity of PLC and DAGLa/b. Of note, alternative pathways exist for both families. Finally, NAEs are metabolized into their corresponding fatty acids and ethanolamines by FAAH or NAAA while several enzymes (e.g. MGL, ABHD6 and ABHD12) are involved in the degradation of 2-AcGs. Interestingly, AA, the product of degradation of some eCBome mediators such as AEA and 2-AG, can be used as precursors of eicosanoids which are other bioactive lipids mostly involved in inflammation (e.g. prostaglandins and leukotrienes). It should be

also mentioned that NAEs and 2-AcGs can also be inactivated by oxidation through the actions of several enzymes (e.g. COX2, CYP450s and LOXs) leading to the production of other inflammatory mediators such as lipoxins and prostaglandins. Abbreviations: 2-AcGs, 2-acylglycerols; 2-AG, 2-arachidonoylglycerol; 2-LG, 2-linoleylglycerol; 2-OG, 2-oleoylglycerol; AA, arachidonic acid; ABHD, α/β-hydrolase domain-containing protein; AEA, *N*-arachidonoylethanolamine; CB, cannabinoid receptor; COX2, cyclooxygenase 2; CYP450s, cytochrome p450; DAG, diacylglycerol; DAGL, diacylglycerol lipase; FAAH, fatty acid amide hydrolase; GPR, G protein-coupled receptors; LEA, *N*-linoleylethanolamine; LOXs, lipoxygenases; MGL, monoacylglycerol lipase; NAAA, *N*-acylethanolamine acid amide hydrolase; NAE, *N*-acylethanolamines; NAPE, *N*-acylphosphatidylethanolamine; NAPE-PLD, *N*-acylphosphatidylethanolamine-selective phospholipase D; NAT, *N*-acyltransferase; OEA, *N*-oleoylethanolamine; PA, phosphatidic acids; PE, phosphatidylethanolamine; PEA, *N*-palmitoylethanolamine; PL, phospholipid; PLC, phospholipase C; PPAR, peroxisome proliferator-activated receptor; TRPV1, transient receptor potential cation channel subfamily V member 1.

Globally, the endocannabinoid system encompasses the aforementioned enzymes, receptors and bioactive lipids. However, this system revealed its true complexity when it was discovered that NAEs and 2-AcGs can also be oxidized and thus inactivated by specific enzymes including cyclooxygenase 2 (COX2), cytochrome p450 oxygenases (CYP450s) and lipoxygenases (LOXs), resulting in the generation of bioactive molecules involved in inflammation regulation (e.g. prostaglandins, thromboxanes, lipoxins) [308-311]. Hence, another important term, “the endocannabinoidome” (eCBome), was recently introduced and refers to the endocannabinoid system along with its related signaling molecules, molecular targets and enzymes (Figure 15). As such, bioactive endocannabinoid metabolites from the oxidative pathway, as well as the endocannabinoid precursors (e.g. NAPEs and DAG) are members of the eCBome [281, 312]. At the present time, although intensive research has provided a better overview of the components and regulatory mechanisms of this network. It is quite clear that more studies are required in order to acquire a greater appreciation of the all subtleties underlying these pathways.

3.2 NAPE-PLD, a key enzyme of the endocannabinoid system

Since the levels of NAEs are altered in various neurological disorders and metabolic diseases, deciphering their physiological function is essential to better understand their specific involvement in those disorders and potentially open the way to future therapeutic targets [279, 281].
To this aim, one important approach, among others, has been to focus on the main enzyme synthesizing these molecules, namely NAPE-PLD.

Even though NAPE-PLD was already identified in the mid 1980s [313], this enzyme was only cloned in 2004 [296], and structurally characterized by Magotti and colleagues in 2015 [314]. This protein is expressed in a wide variety of organisms including mammals and plants, and is composed of 396 and 393 amino acids in mice and humans, respectively. These two species share 89,1% homology and the molecular size of this enzyme varies between 45 to 46 kDa [315, 316]. NAPE-PLD belongs to the metallo-β-lactamase family, which includes various hydrolases and is able to recognize all NAPEs, regardless of their N-acyl group [317]. NAPE-PLD is ubiquitously expressed as reflected by the detection of its activity and mRNA expression in a broad range of mouse tissues. Of interest, the brain is the organ with the highest NAPE-PLD activity followed by the kidneys and testis [296]. Although its exact localization is still unknown, its activity has been detected in microsomal fraction including plasma membrane as well as ER and Golgi vesicles, and at a lower level in the mitochondrial fraction [313].

The crystallization of the human NAPE-PLD allowed Garau's team to determine its molecular structure and to better understand its regulation. They have discovered that this enzyme forms a homodimer associated to cell membranes and possesses a hydrophobic cavity which conveys NAPE into the active site. In this active site, anionic NAPE is hydrolyzed into NAE, a process which is coordinated by a binuclear Zn^{2+} center. Interestingly, Garau's laboratory has also highlighted that bile acids are endogenous modulators of NAPE-PLD and bind with high affinity in a specific cavity closed to the active site [314]. As such, DCA (K_D ~43 µM) and CDCA (K_D ~25 µM) have been described to stabilize the dimer assembly and drive its catalytic activity whereas LCA (K_D ~20 µM), which showed the highest affinity for the enzyme, has been indicated to inhibit its activation [318]. In line with this, in vitro LCA inhibits the enzyme at a low concentration (~68µM) whereas the bile acid concentration required to activate NAPE-PLD and to induce a half-maximal response varies from ~2 to 4mM [318]. Although the physiological meaning of this study remains to be assessed in vivo, these results seem promising since bile acid concentration spans from ~2 to 10mM in the ileum after meal ingestion and at lower range (µM) in the blood and the liver [319-321]. More recently, tauroursodeoxycholic acid (TUDCA),

taurohyodeoxycholic acid (THDCA) as well as α/β-MCA and their taurine-conjugated forms have also been identified as NAPE-PLD inhibitors, although slightly less potent than LCA [322]. These studies paved the way to the design of specific NAPE-PLD modulators [323] and a first study demonstrating *in vivo* the efficacy of a potent and selective NAPE-PLD inhibitor in the brain was published in May of the current year [324].

To gain more insight into the function of NAPE-PLD *in vivo*, three independent groups (i.e. Cravatt's, Deutsch's and Luquet's groups) generated mice with a constitutive whole-body deletion of *Napepld*. Even though, *Napepld*$^{-/-}$ mice exhibited a normal phenotype, were fertile and were born at the expected Mendelian ratio, brain lipidomic analyses revealed an altered lipid profile in mutant mice compared to wild-type (WT) mice. Indeed, an increase and a decrease in NAPEs and NAEs respectively, have been found in brain tissue of mice deficient for NAPE-PLD, thereby demonstrating that this protein is indeed a pivotal enzyme converting NAPEs to NAEs directly [299, 300, 325]. However, it should be mentioned that one out of the three groups (i.e. Cravatt's team) has observed that the brain level of AEA was not altered in *Napepld*$^{-/-}$ mice compared to WT indicating the existence of alternative pathways [299]. This discrepancy in the findings might be due to the different constructs and/or the various analytical methods regarding NAE quantification among the three *Napepld* knockout lines. Interestingly, a recent study, carried out by Luquet's lab, went further and characterized the lipid profile in 8 brain regions by screening more than 70 lipids in *Napepld*$^{-/-}$ and WT mice. Aside from the already mentioned difference of NAPEs and NAEs, they have surprisingly found that a dysregulation of NAPE-PLD expression could impact other lipid families than NAE family in a region-dependent manner. For instance, prostaglandin levels were increased in most of the tested brain regions (i.e. 6 in 8). Moreover, both 2-AG and AA levels were elevated in *Napepld*$^{-/-}$ mice but only in one part of the brain, namely the brainstem [325]. In 2017, the profile of these bioactive lipids has also been investigated and described in peripheral organs such as the heart, kidney, liver and jejunum in *Napepld*$^{-/-}$ mice from Ueda's line. The study indicated that the level of NAPEs was significantly higher in all tested *Napepld*$^{-/-}$ tissues except the jejunum whereas the level of NAEs did not differ between *Napepld*$^{-/-}$ and WT mice. This suggests the presence of NAPE-PLD-independent cascades in the examined organs [326].

In the meantime, several studies have reported that the expression of *Napepld* was increased in the adipose tissue of genetically obese mice as well as influenced by food intake and inflammation [58]. In more detail, *Napepld* mRNA expression and activity were enhanced in rat jejunum following food ingestion whereas its transcription was suppressed in murine macrophage cell line treated with LPS [327, 328]. In addition, in 2011, a human study revealed that a variant of *Napepld* gene was associated with obesity in a Norwegian population [329]. Hence, all these results emphasized the fact that this

enzyme might play a key role in obesity. It should also be pointed out that the regulatory role of bile acids on NAPE-PLD was unknown at the time the aforementioned studies were conducted. Yet, it is also an argument to consider which strengthens the possible involvement of NAPE-PLD in metabolic disorders.

Consequently, convinced of the contribution of this enzyme in the regulation of host metabolism, our research team generated a conditional *Napepld* deficient mouse model in which the deletion was specific to adipocytes (i.e. *Napepld*$^{lox/lox}$ mice x *Fabp4-Cre* mice). We discovered that, by deleting the enzyme only in this specific tissue, *Napepld*-deleted mice exhibited an obese phenotype even when fed a normal diet. This was accompanied by glucose intolerance, adipose tissue inflammation and an altered lipid metabolism. As expected, a reduction of NAE levels (i.e. PEA, OEA and SEA) in subcutaneous adipose tissue (SAT) was reported, but not for AEA, corroborating previous findings regarding the existence of alternative pathways. Interestingly, the level of ceramides was increased whereas the concentration of several prostaglandins and eicosanoids were decreased in SAT tissue of mutant mice. This altered lipid metabolism was also underlined by an increased plasma cholesterol and triglyceride contents in these mutant mice. Finally, our lab was able to demonstrate that the phenotype was, at least partially, mediated by a shift in the gut microbiota composition by transferring these bacteria into germ-free mice, which partially recapitulated the phenotype. Altogether, these data revealed an important role of adipocyte NAPE-PLD in the regulation of basal and lipid metabolism [291].

Next, our group generated another mouse model. This time in an effort to elucidate the role of NAPE-PLD from the gut in the context of obesity. To this end, an inducible intestinal epithelial cell (IEC)-specific deletion of *Napepld* (*Napepld*$^{\Delta IEC}$ from *Napepld*$^{lox/lox}$ mice x Villin-Cre^{ERT2}) was created. The resulting *Napepld*$^{\Delta IEC}$ mice were hyperphagic upon the first exposure to HFD and that they were more prone to develop obesity and steatosis. In contrast to the previous study, glucose metabolism was not impaired and all the measured intestinal NAEs were reduced in *Napepld*$^{\Delta IEC}$ mice, suggesting that the contribution of alternative pathways might be organ-dependent. Remarkably, intestinal 2-AG was also reduced whereas no change was indicated for other 2-AcGs (i.e. 2-OG and 2-PG). Of note, these modifications were less marked in the blood, suggesting that this enzyme might play an important role, first locally before its effects can also influence other organs. Interestingly, the gut microbiota was also found to be altered in *Napepld*$^{\Delta IEC}$ mice [292].

Taken together, these experiments show that NAPE-PLD is a key regulator of host homeostasis and that a dysfunction of this enzyme can result in several metabolic complications. Moreover, it seems

that its function could be organ/tissue-dependent. Therefore, understanding its mechanism of action would require the investigation of its role in the different tissues separately. Indeed, having a better insight into the processes by which this enzyme can play a role in the development of metabolic diseases will allow future researchers to develop specific and targeted innovative treatments.

3.3 NAEs as bioactive lipids

It is now acknowledged that members of the eCBome, in particular NAEs, are widely produced bioactive lipids which display a myriad of metabolic functions that sometimes show opposite actions [60]. For a long period of time, however, AEA was the only NAE that has been investigated in metabolic disorders and an incredible amount of work has been published on this topic. To unravel its functions, genetically deleting and pharmacologically inhibiting or activating its receptors, CB1 and CB2, was the main strategy used. Nevertheless, studies focusing on CB1 and CB2 receptors are not able to distinguish between the actions of their two ligands, the "real" endocannabinoids AEA and 2-AG. However, it should be noted that AEA has a lower affinity with CB2 compared to CB1, but that 2-AG, on the other hand, binds equally to both receptors [330].

It took several years before the endocannabinoid-like NAEs received the attention they deserve. For instance, by generating the first tissue-specific *Napepld* deletion, Geurts and coworkers proved in a study published in 2015, that a disturbed metabolism was induced by a decrease in PEA, OEA and SEA levels without affecting AEA level, highlighting the physiological importance of other NAEs on metabolism [291]. In this section, the most relevant roles of these bioactive molecules and their related proteins in the context of metabolic diseases will be summarized (Figure 16). Some proteins, like TRPV1, for which the roles are still unclear because conflicting and controversial conclusions have been drawn from knockout mouse studies, will not be discussed in detail for the sake of brevity [331, 332]. Finally, a specific part on inflammation will be developed to close the section.

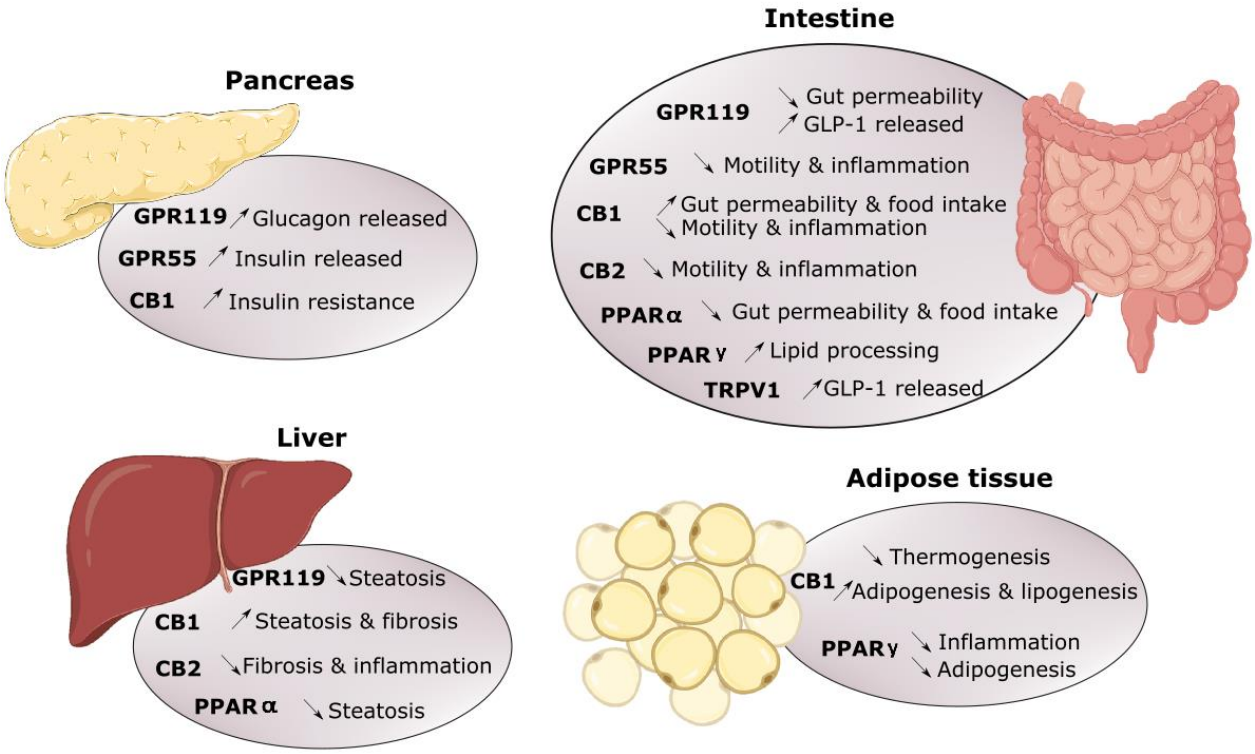

Figure 16: Biological actions of NAEs and their associated receptors in several peripheral organs of metabolic relevance. Abbreviations: CB, cannabinoid receptor; GPR, G protein-coupled receptor; PPAR, peroxisome proliferator-activated receptor; TRPV1, transient receptor potential cation channel subfamily V member 1.

3.3.1 The intestine

The intestine, by being directly in contact with the ingested food and the gut microbiota, is unquestionably one of the main organs involved in host homeostasis. Within the intestine, eCBome mediators control various pivotal functions involved in host homeostasis such as food intake, intestinal permeability, peptide secretion, gut motility and inflammation.

Interestingly, it has been demonstrated that the nutrients can impact intestinal NAE profile, that in turn, influence appetite. More specifically, several studies have proposed that different types of dietary fat modulate NAE levels distinctively by providing the necessary substrates for their biosynthesis. For example, feeding rats with fat in the form of corn oil increased the synthesis of 2-AG and AEA in the jejunum, thereby leading to gut nerves CB1 activation and stimulation of food intake [333]. In line with this, it has been recently suggested that CB1 activation was important for the regulation of food preferences. Indeed, when exposed to both western diet and standard chow diet for only few hours, WT mice had a clear preference for the palatable food whereas this effect was transiently abolished in mice deleted for *Cb1* in the intestine [334]. Conversely, the production of the following NAE, OEA and to a lesser extent LEA and PEA, has been indicated to exhibit anorexigenic

properties predominantly through PPARα signaling via the vagus nerve [335, 336]. These examples perfectly illustrate the opposite actions that NAEs can exert on energy balance.

Another example of the antagonist effects of eCBome mediators concerns the gut barrier function, which is mediated mainly by CB1, GPR119 and PPARα receptors. For instance, increased expression of intestinal CB1, which has been proposed to be under the control of the gut microbiota, altered the gut barrier function leading to a "leaky" gut [58]. In line with this result, blocking CB1 has been proved to restore intestinal integrity [58]. In another work, the gut barrier function was enhanced following the administration of *Akkermansia muciniphila*, a bacterium associated with health benefits in HFD fed mice [337]. In this study, an elevation of 2-AG, 2-OG and 2-PG levels was observed in ileum of treated mice. The underlying mechanism hypothesized by Everard and colleagues was that 2-OG, by binding to GPR119 present in enteroendocrine L cells, enhanced the release of GLP-2, which is known to ameliorate the gut barrier function [47]. Finally, an *in vitro* study performed on Caco-2 cells showed that PEA may also contribute to the improvement of the gut barrier function in a PPARα-dependent manner [338]. To sum up, AEA could be considered as a "gate opener" while 2-OG and PEA as "gate keepers" [60].

Interestingly, the release of the gut peptide GLP-2 is not the only one mediated by eCBome mediators. Indeed, GLP-1 and PYY secreted by enteroendocrine L cells are also enhanced by GPR119 agonists (i.e. OEA and 2-OG), leading to an improvement of glucose metabolism by increasing insulin secretion and by decreasing food intake [339, 340]. Additionally, TRPV1 activation in the gut has also been proposed to promote GLP-1 secretion [341]. Finally, the release of cholecystokinin, an anorexigenic hormone playing also a pivotal role in digestion by inducing the release of bile acids and pancreatic enzymes, has also been reported to be mediated in a CB1-dependent manner [342, 343].

The role of intestinal PPARγ has also been investigated by generating mice with intestinal-specific deletion of *Pparγ*. In this study, Duszka and coworkers reported that PPARγ was involved in lipid metabolism by regulating LCFA processing in enterocytes [344].

Ultimately, activation of CB1, CB2 and GPR55 receptors has been associated with a reduced gut motility and, surprisingly, with a decreased intestinal inflammation [345-348]. This latter finding is a bit counterintuitive since usually CB1 activation is mostly associated with inflammation in other organs such as the liver, the muscle or the adipose tissue [349]. Nevertheless, several studies have demonstrated a protective and anti-inflammatory role of AEA and 2-AG in gastrointestinal diseases

through CB1 activation [350]. This observation challenges the hypothesis that peripheral CB1 antagonist drug would only confer health benefits.

3.3.2 The liver

The liver, as previously described in the previous chapter, is essential regarding host metabolism and is the first organ directly exposed to the molecules absorbed from the gut. Under normal condition, the endocannabinoid system is considered to be mostly quiescent as reflected by the low expression of endocannabinoid receptors and the low activity of NAPE-PLD. By contrast, under pathological conditions, the expression of CB1 and CB2 significantly increases, which suggests that they might play an important function in metabolism regulation [299, 351-353]. CB1 is expressed on hepatocytes, HSC and vascular endothelial cells whereas CB2 is not expressed in hepatocytes but rather in HSC and immune cells such as KC [351].

It is commonly accepted that liver CB1 activation is deleterious and leads to steatosis development and promotes fibrogenesis as well as insulin resistance [351]. CB1 function has been deeply investigated *in vivo* in mice globally deleted for *Cb1* which were protected against diet-induced obesity suggesting that CB1 activation caused adverse health effects [352, 354]. In line with these findings, experiments in mice and on cultured hepatocytes have demonstrated that CB1 agonist administration induced lipogenic gene expression, in turn enhancing liver lipid accumulation. Importantly, this effect was abolished in mice deleted for *Cb1* [352]. The contribution of hepatic CB1 on lipid metabolism has been further confirmed using hepatocyte-specific *Cb1* knockout mice. Indeed, even though mice were still gaining weight under HFD, they did not develop liver steatosis [353]. In addition, CB1 activation can also impact insulin concentration since its hepatic activation leads to a suppression of insulin clearance, which can provoke hyperinsulinemia [355]. Moreover, stimulation of CB1 has also been reported to induce liver fibrosis [356]. Finally, after having discovered the aforementioned effects, CB1 antagonists were rapidly designed and many studies have proved that CB1 blockade, not only improved liver function such as insulin sensitivity or glucose tolerance but also global metabolic parameters in the context of obesity [357-360].

By contrast, the role of liver CB2 is a rather protective one and shows inverse effects compared to CB1 activation. For instance, it has been indicated that CB2 activation displays antifibrogenic properties. This has been highlighted by *Cb2*-knockout mice which developed enhanced liver fibrosis than WT after treatment with hepatoxin carbon tetrachloride [361]. In line with this, the administration of CB2 agonists in a mouse model of fibrosis has been shown to counteract this liver dysfunction [362].

Moreover, CB2 stimulation on KC attenuates inflammation by inducing anti-inflammatory cytokine production and thereby improving liver function [363].

Two other key receptors having protective effects in the liver are GPR119 and PPARα. They both constitute good potential candidates to reduce liver steatosis. Indeed, as mentioned earlier, hepatic PPARα stimulation contributes to fatty acid oxidation, thereby limiting liver lipid accumulation [364]. Moreover, recent studies demonstrated that mice specifically deleted for *Pparα* in hepatocytes are more prone to develop NAFLD in the context of obesity [365, 366]. GPR119 activation, on the other hand, inhibits lipogenesis. As such, GPR119 agonist administration has been shown to reduce lipogenesis by decreasing SREPB-1c expression through AMPK activation in *in vitro* (i.e. hepatocytes) and *in vivo* (i.e. mice) experiments [367].

3.3.3 The pancreas

The action of the pancreas is mandatory for a proper digestion and control of glycemia. Of interest, several receptors of the eCBome (e.g. GPR55, CB1/2 and GPR119) are also found in pancreatic islets and are believed to play a role in glucose homeostasis. For instance, it has been reported that GPR119 activation triggered glucagon release in response to hypoglycemia in diabetic rodents [368]. Other studies have revealed that GPR55 substantially contributed to insulin sensitivity and that insulin secretion was enhanced following GPR55 agonist treatment [369, 370]. Conversely, CB1 activation has been shown to promote insulin resistance and CB1 blockade to enhance insulin sensitivity [371]. Finally, it has been highlighted that CB2 agonist administration via osmotic minipump in diabetic mice had a beneficial role on β-cell function resulting in an increased insulin sensitivity [372]. However, it should be noted that the beneficial effect of CB2 stimulation is still under debate since controversial data coexist in the literature. Additional studies are therefore required to fully unravel its function [373].

3.3.4 The adipose tissue

In line with the deleterious actions of CB1 in the previously described metabolic active tissues under pathological conditions, CB1 activation in white adipose tissue (WAT) has been reported to enhance lipogenesis and adipogenesis [374]. Moreover, by using specific genetic tools and CB1 antagonists, several studies have demonstrated that the blockade of CB1 improved mitochondrial function and promoted beiging in WAT which was mirrored by an increased gene expression of genes involved in thermogenesis such as *Ucp1* and *Pgc1α* [375, 376]. In accordance with this finding, the specific and inducible inactivation of the *Cb1* gene in adipocytes protected the mice against diet-induced obesity

by promoting energy dissipation and by reducing WAT lipid storage [377]. In opposition to CB1 actions, activation of PPARγ in adipose tissues has been shown to confer positive effects on insulin sensitivity as well as to avoid ectopic fat accumulation, regulate properly adipokine production (i.e. leptin and adiponectin) and reduce inflammation [378]. Finally, it is worth noting that GPR55 and TRPV1 are also expressed in WAT but since their respective functions remains to be clearly established, they will not be further developed in the present work [279, 331].

As previously mentioned, inflammation can be elicited in many organs and is a hallmark of obesity and associated comorbidities. Interestingly, the endocannabinoid system also has its role in this context. The most characterized NAE displaying anti-inflammatory effects is, without any doubt, PEA through PPARα and TRPV1 receptors [364, 379, 380]. Studies including *Pparα* knockout mice and isolated macrophages have evidenced that PEA can exert anti-inflammatory properties through the activation of PPARα leading to the inhibition of NF-κB [381-383]. Although, CB1 activation is widely associated with proinflammatory responses, AEA administration in the intestine can also confer health benefits regarding intestinal inflammatory disorders [349]. Finally, activation of either CB2, PPARα or PPARγ has been reported to attenuate inflammatory responses [364, 380, 384, 385].

In conclusion, this section has summarized the main players of the endocannabinoid system with regards to obesity and demonstrated both the importance and the complexity of this system. These bioactive lipids are undoubtedly key molecules involved in metabolic disturbances and act by regulating gut barrier function and insulin sensitivity, by modulating anorexigenic and orexigenic signals, and by inducing both pro- and anti-inflammatory effects. Of course, many questions remain and further studies are clearly required to better understand the roles and regulation of these lipid mediators. One of the key issues to address in order to develop therapeutic drugs against metabolic disorders such as obesity and its complications, is the fact that their functions seem to be organ-dependent.

AIMS & OBJECTIVES

Obesity is a major risk factor for developing metabolic diseases and has reached epidemic proportion. At the present time, it is also considered as a multifactorial disorder since genetic, social and environmental factors have been reported to contribute to the onset of this condition. In accordance with this, several strategies have been tested and implemented to overcome its progression such as dietary intervention, surgical operation, anti-obesity drug therapy or exercise program. However, the effectiveness of these different approaches is still limited. Furthermore, in spite of intense research in this field, which substantially shed light on the development of this disorder, deciphering the exact molecular mechanisms underlying obesity-related diseases remains challenging. Therefore, the aim of the present thesis was to contribute to a better understanding of the etiology of obesity at the molecular level in order to potentially find new therapeutic targets. This investigation was focus on the liver which is an essential organ of metabolic regulation.

Since obesity is usually associated with a chronic low-grade inflammation, the first objective of this thesis was to gain a better insight into the role of the innate immunity on this metabolic disorder. In this specific context, one project of our lab was to examine the physiological function of a key component of the immune system called MyD88. Noteworthy, MyD88 is an adaptor protein of, notably, almost all TLR and is thereby crucial to elicit the inflammatory response linked to their activation. Accordingly, our lab succeeded in generating a genetic mouse model deleted for *MyD88* in hepatocytes (i.e. *MyD88*$^{\Delta Hep}$ mice) and outlined its phenotype in an article published in 2017 by Duparc and colleagues. This primary investigation brought lights on the involvement of hepatocyte MyD88 not only in inflammation but also in glucose and lipid metabolism. However, the molecular events leading to these alterations remained to be elucidated. Therefore, in order to pursue the work initiated by our lab, the first chapter of this thesis was devoted to a deeper analysis of the action of hepatocyte MyD88. To reach this objective, two different strategies described to challenge the immune system and lipid metabolism were performed. On the one hand, *MyD88*$^{\Delta Hep}$ and WT mice were exposed to a short-term exposure of HFD, that are 3 days. On the other hand, both groups were injected with LPS, a potent proinflammatory compound well-known to trigger an acute inflammation. Lipidomic analyses, protein quantifications and gene expression measurements, among other assays, were thereafter carried out.

The second chapter of this thesis was dedicated to deciphering the role of hepatocyte NAPE-PLD, an essential enzyme of the endocannabinoid system, on host metabolism. NAPE-PLD belongs to the endocannabinoid system and is the main enzyme synthesizing specific bioactive lipids (i.e. NAEs) regulating energy homeostasis. Interestingly, NAEs have been reported to be altered in obesity-related disorders suggesting that NAPE-PLD might be a potential therapeutic target. It is therefore not surprising that these last two decades several research teams, including ours, have tried to evaluate

its metabolic impact by generating several *Napepld* knockouts. Although the effects of a whole-body *Napepld* deletion in mice led to a normal phenotype, our lab discovered opposite results by inducing the deletion of *Napepld* in specific organs of metabolic relevance (i.e. the adipose tissue and the intestine). Indeed, we revealed that NAPE-PLD played a central role in the pathophysiology of obesity. More specifically, in 2015, Geurts and colleagues demonstrated that the absence of NAPE-PLD in adipocytes induced an obese-like phenotype whereas in 2019, Everard, Plover, Rastelli and coworkers proved that its deletion in intestinal epithelial cells affected appetite regulation in rodents. However, the role of NAPE-PLD and associated lipid mediators in the liver remained unclear. Therefore, another objective of this thesis was to generate a new mouse model of inducible *Napepld* hepatocyte-specific deletion using the Cre-lox system and explore the function of this enzyme in the context of obesity.

RESULTS & DISCUSSION

1 Chapter: Hepatic MyD88 regulates liver inflammation by altering synthesis of oxysterols

Am J Physiol Endocrinol Metab 317: E99–E108, 2019.
First published April 30, 2019; doi:10.1152/ajpendo.00082.2019.

RESEARCH ARTICLE | *Immunometabolic Cross-Talk and Regulation of Endocrine and Metabolic Functions*

Hepatic MyD88 regulates liver inflammation by altering synthesis of oxysterols

Charlotte Lefort, Matthias Van Hul, Nathalie M. Delzenne, Amandine Everard, and Patrice D. Cani
Metabolism and Nutrition Research Group, Louvain Drug Research Institute, UCLouvain, Université Catholique de Louvain and Walloon Excellence in Life Sciences and Biotechnology, Brussels, Belgium

The results related to this chapter have been published in Am J Physiol Endocrinol Metab 317: E99–E108, 2019

1.1 Abstract

This study aimed to investigate the function of hepatic myeloid differentiation primary response gene 88 (MyD88), a central adaptor of innate immunity, in metabolism. Although its role in inflammation is well known, we have recently discovered that MyD88 can also mediate energy, lipid, and glucose metabolism. More precisely, we have reported that mice harboring hepatocyte-specific deletion of *MyD88* (*Myd88*$^{\Delta Hep}$) were predisposed to glucose intolerance, liver fat accumulation, and inflammation. However, the molecular events explaining the onset of hepatic disorders and inflammation remain to be elucidated. To investigate the molecular mechanism, *Myd88*$^{\Delta Hep}$ and wild-type (WT) mice were challenged by two complementary approaches affecting liver lipid metabolism and immunity. The first approach consisted of a short-term exposure to high-fat diet (HFD), whereas the second was an acute LPS injection. We discovered that upon 3 days of HFD *Myd88*$^{\Delta Hep}$ mice displayed an increase in liver weight and liver lipids compared to WT mice. Moreover, we found that bile acid and oxysterol metabolism were deeply affected by the absence of hepatic MyD88. Our data suggest that the negative feedback loop suppressing bile acid synthesis was impaired (i.e., ERK activity was decreased) in *Myd88*$^{\Delta Hep}$ mice. Finally, the predisposition to inflammation sensitivity displayed by *Myd88*$^{\Delta Hep}$ mice may be caused by the accumulation of 25-hydroxycholesterol, an oxysterol linked to inflammatory response and metabolic disorders. This study highlights the importance of MyD88 on both liver fat accumulation and cholesterol-derived bioactive lipid synthesis. These are two key features associated with metabolic syndrome. Therefore, investigating the regulation of hepatic MyD88 could lead to discovery of new therapeutic targets.

1.2 Introduction

The liver is an essential organ that is involved in many metabolic features such as lipid and glucose metabolism, xenobiotic detoxification, and bile production. Over the last decade the incidence of liver diseases has increased, becoming epidemic. The most common is nonalcoholic fatty liver disease, which is clearly linked with the increased prevalence of obesity and its comorbidities [386]. Different drivers are contributing to liver diseases, including diet, innate immunity stimulation, gut microbiota, and host genetic background [386-389]. Although the numbers of metabolic-related liver disorders are rising, the molecular mechanisms and triggering factors are not yet fully deciphered.

Myeloid differentiation primary response gene 88 (MyD88) is a key player in the innate immune system. It is the main adaptor protein not only of IL-1 and IL-18 receptors but also of all Toll-like receptors (TLRs) except TLR3. TLR stimulation initiates an immune response and leads to proinflammatory cytokine production by activating several proteins and transcription factors such as c-Jun NH2-terminal kinase (JNK) and nuclear factor-κB (NF-κB) [390]. MyD88 is thus considered a central hub of the inflammatory signaling cascades. Although its role in inflammation and immunity is well established, we have recently shown that MyD88 can also modulate metabolism (e.g., energy, glucose, and lipid metabolism) [37, 391]. Indeed, we reported that intestinal epithelial MyD88 acts as a nutrient sensor and controls energy expenditure [37]. More recently we have discovered that mice harboring hepatocyte-specific deletion of *MyD88* (*Myd88*$^{\Delta Hep}$) are predisposed to liver fat accumulation and inflammation [391]. Besides this observation, *Myd88*$^{\Delta Hep}$ mice also exhibited altered gut microbiota and bile acid metabolism [391]. However, this phenotype has only been studied upon a prolonged exposure to a high-fat diet (HFD), and the molecular events explaining the onset of hepatic disorders and inflammation remain to be elucidated.

Therefore, this study aimed to investigate the mechanisms behind the *Myd88*$^{\Delta Hep}$ phenotype in order to find new putative targets responsible for the onset of metabolic liver disorders. Hence, we designed two complementary approaches known to challenge liver lipid metabolism and immunity. The first consists of a short-term exposure to HFD and the second of an acute injection of lipopolysaccharide (LPS), the major component of the outer membrane of gram-negative bacteria.

1.3 Results

Hepatocyte Myd88-Deleted Mice Are Predisposed to Accumulate Lipids in the Liver

In the present study, we exposed WT and *Myd88*$^{\Delta Hep}$ mice to 3 days of HFD. We hypothesized that ingestion of a hyperlipidic diet for a short-term period would trigger bioactive lipid production without the potential compensation effect observed during a prolonged HFD exposure (i.e., 8 wk). Interestingly, upon 72 h of HFD exposure *Myd88*$^{\Delta Hep}$ mice showed a significant increase in liver weight compared with WT mice (Fig. 1*A*). Accordingly, both liver lipid and triglyceride levels were markedly increased in *Myd88*$^{\Delta Hep}$ mice compared with WT mice under HFD ($P < 0.01$, *t*-test; Fig. 1, *B* and *C*). However, we did not observe any modification of liver cholesterol levels (Fig. 1*D*).

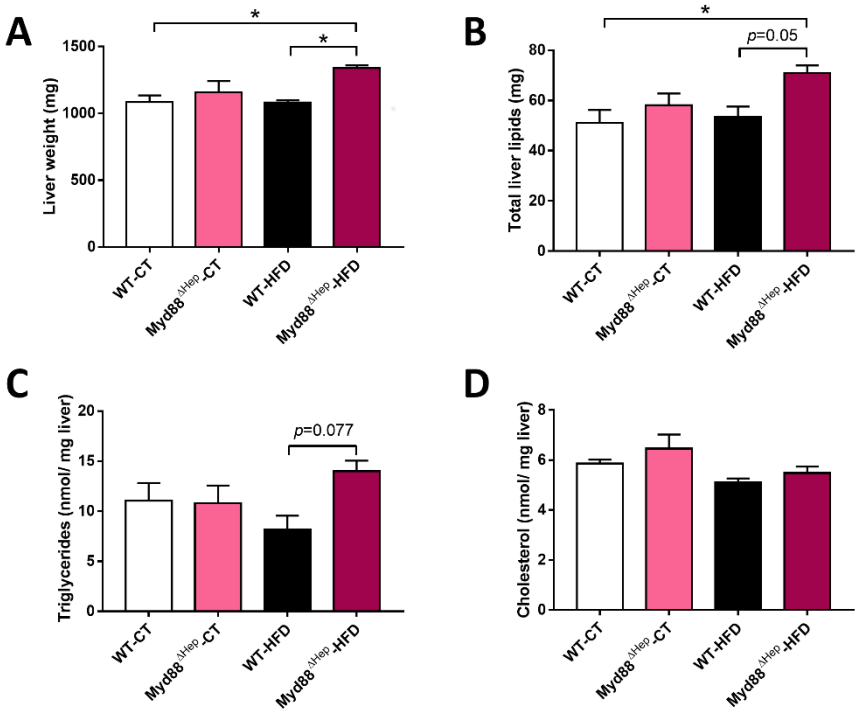

Figure 1: Hepatocyte myeloid differentiation primary response gene 88 (MyD88) deletion (*Myd88*$^{\Delta Hep}$) worsens high-fat diet (HFD)-induced fat accumulation. **A**: mean liver weight. **B**: total lipid levels measured in the liver. **C**: liver triglyceride measurement. D: liver cholesterol measurement. Data are presented as means ± SE (n = 6–9 mice). CT, control diet; WT, wild type. Significantly different according to 2-way ANOVA followed by Tukey post hoc test: **P* < 0.05.

Altogether, these data indicate that hepatocyte MyD88 modulates liver lipid storage after a short exposure to HFD.

Myd88 Deletion Strongly Modifies Bile Acid Metabolism

Our first data confirmed an impairment of liver lipid regulation in *Myd88*$^{\Delta Hep}$ mice also after a short HFD exposure. Since we previously reported that bile acid metabolism was altered in *Myd88*$^{\Delta Hep}$ mice during long-term HFD (8 wk) [391], we wondered whether bile synthesis was already affected under short-term HFD in *Myd88*$^{\Delta Hep}$ mice.

First, we analyzed the expression of key enzymes regulating bile acid production, and we observed that the enzyme synthesizing cholesterol, *Hmgcr,* was significantly increased in *Myd88*$^{\Delta Hep}$-HFD compared with WT-HFD mice (Fig. 2*A*). *Cyp8b1* mRNA expression followed the same expression pattern (Fig. 2*A*). Additionally, the rate-limiting enzyme of bile acid synthesis, *Cyp7a1,* was also overexpressed in *Myd88*$^{\Delta Hep}$-CT versus WT-CT mice ($P < 0.05$, *t*-test; Fig. 2*A*). It is worth noting that among all the enzymes measured, *Cyp7b1* was the only one to be found significantly decreased in Myd88$^{\Delta Hep}$ mice in both conditions (Fig. 2A).

Second, to further explore the impact of MyD88 on bile acid regulation, we examined the bile acid profile in the cecal content and the portal vein blood of *Myd88*$^{\Delta Hep}$ and WT mice (Fig. 2, *B* and *C*). The results showed that, in general, all mice exposed to HFD had an overall increase in bile acid concentration in both portal vein and cecal content. Of note, the primary bile acids [cholic acid (CA), chenodeoxycholic acid (CDCA), a- and b-muricholic acid (MCA)] and some secondary bile acids [ursodeoxycholic acid (UDCA), hyodeoxycholic acid (HDCA), and o-MCA] from the portal vein were the only bioactive lipids measured displaying a lower level upon HFD exposure (Fig. 2*C*). Strikingly, although HFD has a clear impact on bile acid metabolism, the alteration pattern of bile acid levels in *Myd88*$^{\Delta Hep}$ mice was almost identical independently of diet and was clearly different compared with WT mice. Hence, our data indicate that the genotype has a stronger influence on bile acid pathways than diet per se. Indeed, in the portal vein the detection of conjugated bile acids [e.g., TDCA, TCDCA, TUDCA (in HFD), TCA (in CT, $P < 0.01$, Mann-Whitney test)] were mostly decreased (Fig. 2*C*). In line with this result, a higher proportion of conjugated bile acids were measured in the cecal content of *Myd88*$^{\Delta Hep}$ mice (Fig. 2*B*).

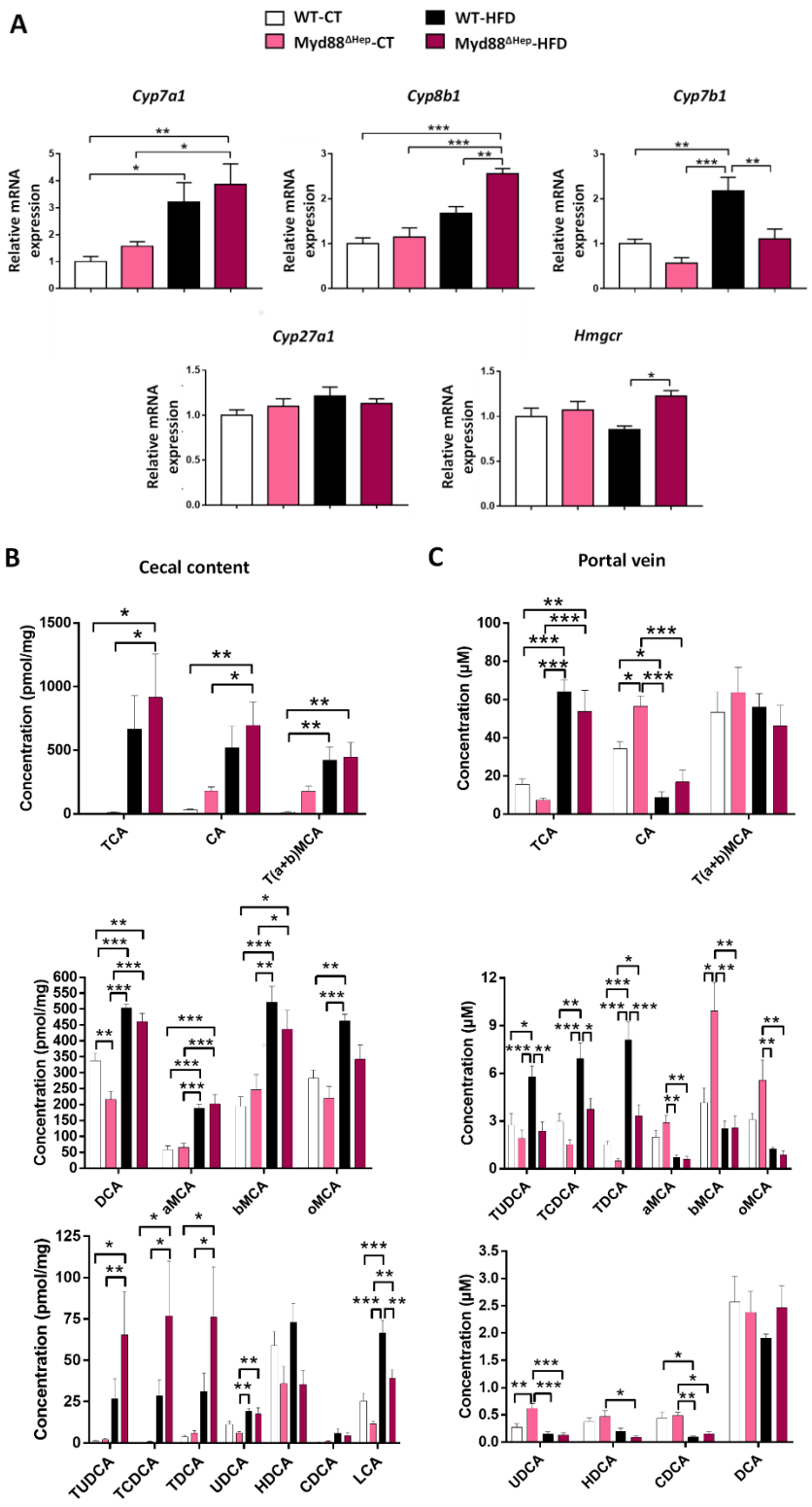

Figure 2: Hepatocyte myeloid differentiation primary response gene 88 (Myd88) deletion (*Myd88*$^{\Delta Hep}$) profoundly impacts bile acid metabolism. **A**: liver mRNA expression of bile acid synthesis enzymes measured by real-time qPCR in wild-type (WT) and *Myd88*$^{\Delta Hep}$ mice fed with either control diet (CT) or high-fat diet (HFD). **B**: cecal bile acid content. **C**: plasma (portal vein) bile acid content. Data are presented as means ± SE (n = 6–9 mice). CA, cholic acid; CDCA, chenodeoxycholic acid; DCA, deoxycholic acid; HDCA, hyodeoxycholic acid; LCA, lithocholic acid; MCA, muricholic acid; T, taurine; UDCA, ursodeoxycholic acid; a, α, b, β, o, ω conjugated species. Significantly different according to 2-way ANOVA followed by Tukey post hoc test: **P* < 0.05, ***P* < 0.01, ****P* < 0.001.

It is also worth noting that in cecal content the levels of secondary bile acids were mainly lower in *Myd88*$^{\Delta Hep}$ mice (Fig. 2*B*). Indeed, under CT diet UDCA ($P < 0.05$, *t*-test) and DCA were markedly decreased in *Myd88*$^{\Delta Hep}$ mice, whereas under HFD HDCA and o-MCA ($P < 0.05$, *t*-test) and lithocholic acid concentrations were significantly lower. Finally, CA was the only bile acid following the same trend in both cecal content and portal vein (Fig. 2, *B* and *C*). Interestingly, a strong elevation of CA concentration was observed in *Myd88*$^{\Delta Hep}$-CT compared with WT-CT mice. Upon HFD, the levels were also elevated in *Myd88*$^{\Delta Hep}$ mice, but this effect did not reach significance.

Altogether, this set of data confirms a clear impact of MyD88 on the control of bile acid production and levels in both cecum and blood.

Enterohepatic Loop Repressing Cyp7a1 and Cyp8b1 Is Impaired in Myd88$^{\Delta Hep}$ Mice

Since our data indicated that *Myd88*$^{\Delta Hep}$ mice overexpressed *Cyp7a1* and *Cyp8b1* mRNA, we wondered whether the enterohepatic feedback loop controlling bile acid synthesis could be altered in *Myd88*$^{\Delta Hep}$ compared with WT mice. The regulation of bile acid production is mediated by the stimulation of intestinal fibroblast growth factor 15 (FGF15; FGF19 in humans) expression thanks to farnesoid X receptor activation by specific bile acids [392]. FGF15 then reaches the liver through the portal vein and activates the hepatic fibroblast growth factor receptor 4 (FGFR4) [392]. FGFR4 stimulation induces the phosphorylation of JNK and ERK to activate them. In turn, p-JNK and p-ERK promote the repression of CYP7A1 and CYP8B1, suppressing bile acid production. It is important to note that the proper molecular mechanism underlying this hepatic signaling pathway still remains elusive [245]. Because we have previously demonstrated that Myd88$^{\Delta Hep}$ mice express normal levels of both FGF15 and FGFR4 [391], we hypothesized that the deletion of *Myd88* would impact this feedback loop downstream of FGF15/FGFR4, at the hepatic level. We discovered that p-ERK was lower in *Myd88*$^{\Delta Hep}$-HFD versus WT-HFD mice ($P < 0.05$, *t*-test), whereas a trend was observed for p-JNK (Fig. 3, *A* and *B*, respectively).

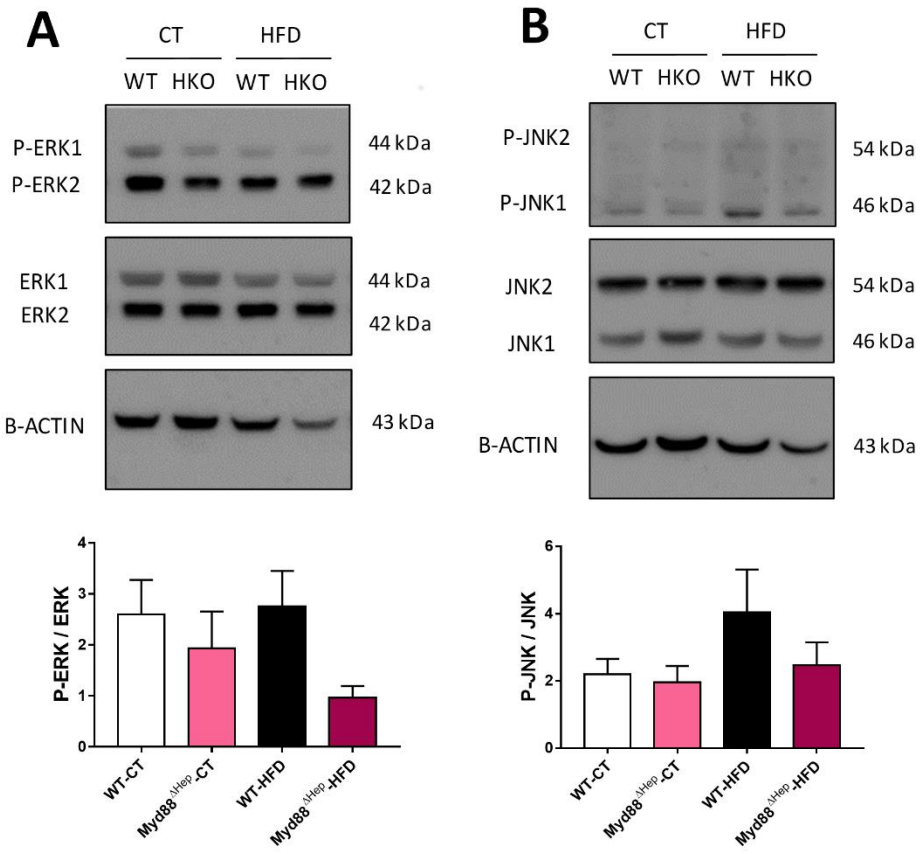

Figure 3: Hepatocyte myeloid differentiation primary response gene 88 (Myd88) deletion (*Myd88*$^{\Delta Hep}$) affects ERK activity: Western blot analysis of liver protein extracts from *Myd88*$^{\Delta Hep}$ and wild-type (WT) mice fed with either control diet (CT) or high-fat diet (HFD). Ratio quantification is measured by densitometry and is expressed relative to β-actin. **A**: expression of ERK1/2 and its active form, phosphorylated (p-)ERK1/2. **B**: expression of JNK1/2 and its active form, p-JNK1/2. Quantification data are presented as means ± SE (n = 6–7).

Taken together, a decreased activity of ERK in Myd88$^{\Delta Hep}$-HFD mice highlights the importance of MyD88 in modulating the hepatic feedback loop responsible for the repression of bile acid synthesis. These results are in line with the increase in mRNA expression of bile acid synthesis enzymes.

Predisposition to Liver Inflammation Observed in Myd88$^{\Delta Hep}$ Mice Is Linked with Altered Oxysterol Metabolism

Although one may intuitively expect a decreased inflammatory response in mice lacking hepatic MyD88, we have recently reported that *Myd88*$^{\Delta Hep}$ mice are in fact more sensitive to inflammation [391].

To investigate the molecular action behind this inflammation sensitivity, *Myd88*$^{\Delta Hep}$ and WT mice were injected with LPS. When challenged with LPS, *Myd88*$^{\Delta Hep}$ mice exhibited a worsened inflammation compared with WT. Indeed, the hepatic mRNA expressions of *Tnfa*, *Il6*, and *Il1b* were markedly increased (fold change of 1.3, 3, and 1.5, respectively) in *Myd88*$^{\Delta Hep}$-LPS compared with WT-LPS mice (Fig. 4*A*). In addition, *Cd11c* and *F4/80* mRNA expression levels tended to be more elevated in *Myd88*$^{\Delta Hep}$ compared with WT mice (Fig. 4*A*). Since liver lipid regulation was affected in mice deleted for *Myd88* in the hepatocyte, we measured two important families of bioactive lipids contributing to host homeostasis and to the regulation of inflammation. The first family includes prostaglandins, whereas the second is related to cholesterol derivatives, namely oxysterols. Although it is well established that prostaglandins mediate inflammation, we did not find relevant alterations between *Myd88*$^{\Delta Hep}$ and WT mice (Fig. 5*B*). In contrast, the levels of several oxysterols were deeply altered by the absence of hepatic MyD88 (Fig. 5*A*). Interestingly, among all the oxysterols measured we found that 25-hydroxycholesterol (25-OHC) was the only one following the same pattern of expression as proinflammatory cytokines (Fig. 4*B*). It is important to mention that 25-OHC has been described as a modulator of immune functions and inflammatory markers [228]. To further investigate this finding, we measured the main enzyme degrading 25-OHC (i.e., *Cyp7b1*) and found that its expression was significantly decreased in *Myd88*$^{\Delta Hep}$ mice in both conditions (Fig. 4*C*).

Therefore, these results suggest that hepatocyte deletion of *Myd88* predisposes mice to inflammation and this effect is strongly linked with an alteration of oxysterol metabolism.

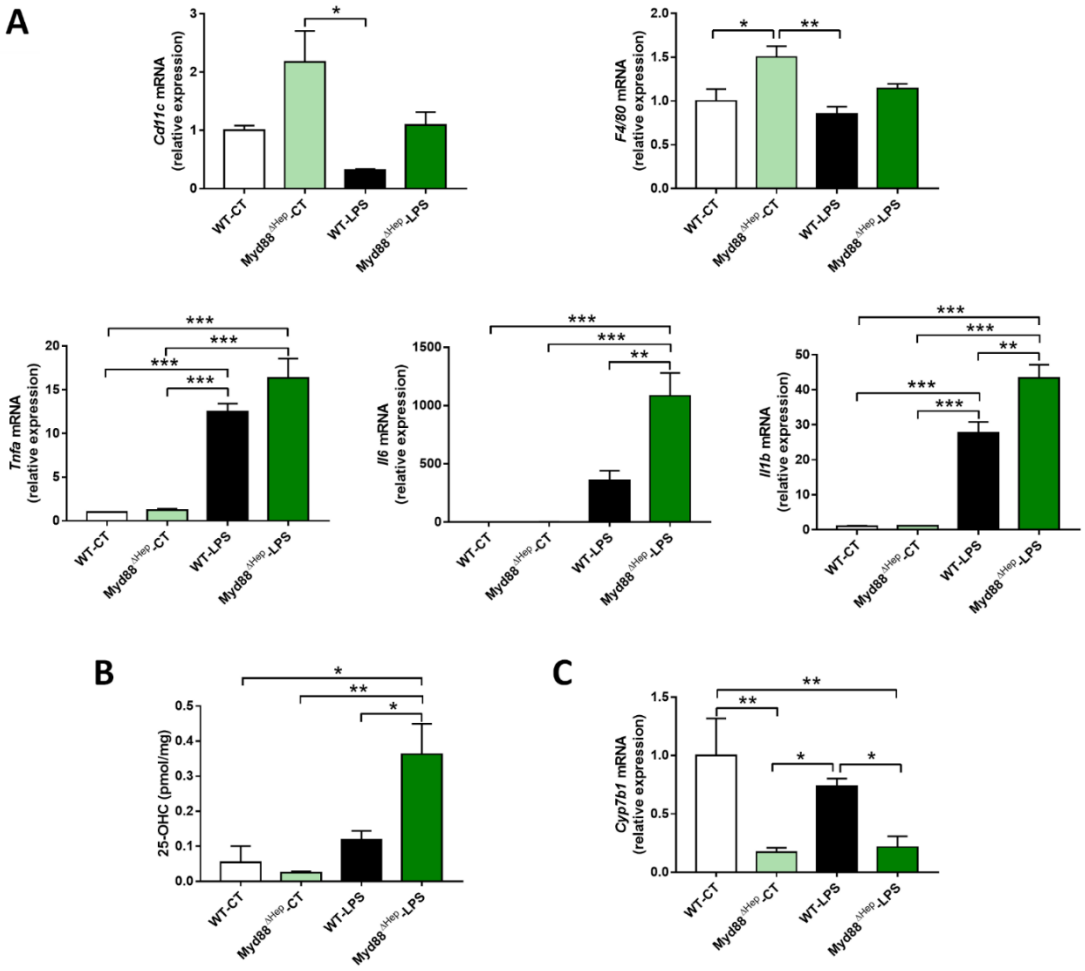

Figure 4: Myeloid differentiation primary response gene 88 (Myd88)-deleted mice are predisposed to inflammation, presumably due to the alteration of oxysterol metabolism. **A**: liver mRNA expression of inflammatory markers measured by real-time qPCR in wild-type (WT) and *Myd88*$^{\Delta Hep}$ mice injected with either saline solution [control (CT)] or LPS. **B**: liver 25-hydroxycholesterol (25-OHC) concentration. **C**: liver *Cyp7b1* mRNA expression measured by real-time qPCR. Data are presented as means ± SE (n = 3–5 mice). Significantly different according to 2-way ANOVA followed by Tukey post hoc test: **P* < 0.05, ***P* < 0.01, ****P* < 0.001.

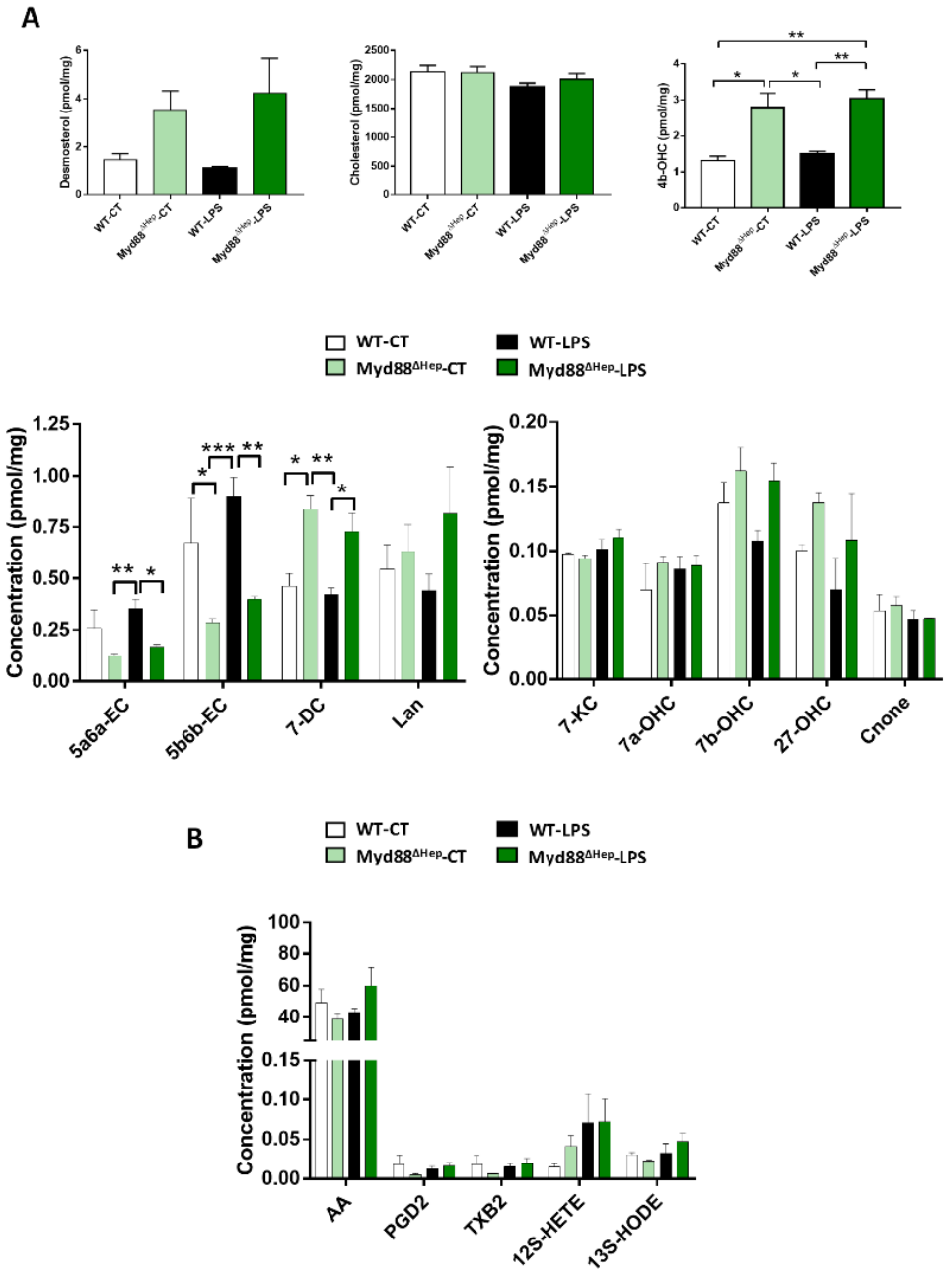

Figure 5: Hepatocyte myeloid differentiation primary response gene 88 (Myd88) deletion (*Myd88*$^{\Delta Hep}$) strongly impacts cholesterol-derived bioactive compound synthesis in the liver. **A**: liver measurements of cholesterol and its relative compounds in wild-type (WT) and *Myd88*$^{\Delta Hep}$ mice injected with either saline solution [control (CT)] or LPS. **B**: prostaglandins and relative molecule measurements in liver extract of *Myd88*$^{\Delta Hep}$ and WT mice injected with either saline solution or LPS. Data are presented as means ± SE (n = 3–5 mice). 4b-OHC, 4β-hydroxycholesterol; 5a6a-EC, 5α,6α-epoxycholesterol; 5b6b-EC, 5β,6β-epoxycholesterol; 7-DC, 7-dehydrocholesterol; 7-KC, 7-ketocholesterol; 7a-OHC, 7α-hydroxycholesterol; 7b-OHC; 7β-hydroxycholesterol, 27-OHC, 27-hydroxycholesterol; Cnone, 7α-hydroxycholestenone; Lan, lanosterol. AA, arachidonic acid; PGD2, prostaglandin D2; TXB2, thromboxane B2; 12S-HETE, 12(S)-hydroxy-5Z,8Z,10E,14Z-eicosatetraenoic acid; 13S-HODE, 13(S)-hydroxy-9Z,11E-octadecadienoic acid. Significantly different according to 2-way ANOVA followed by Tukey post hoc test: **P* < 0.05, ***P* < 0.01, ****P* < 0.001.

1.4 Discussion

The incidence of metabolic disorders is constantly rising and is often associated with liver fat accumulation [386]. In the present study, we discovered that mice lacking MyD88 in the hepatocytes are prone to liver fat accumulation. Indeed, when challenged with a HFD for 3 days, *Myd88*$^{\Delta Hep}$ mice displayed higher liver weight and an elevation of lipid and triglyceride contents. Next, we demonstrated that MyD88 controls the synthesis of cholesterol-derived bioactive lipids in both HFD and LPS challenge conditions. Moreover, we discovered that the profiles of bile acids or their precursors, namely oxysterols, were profoundly affected by the absence of hepatic MyD88.

Unexpectedly, liver levels of cholesterol were not higher in any experiments, even though the enzyme responsible for its synthesis was increased (HFD study) and its precursor, desmosterol, tended to be more elevated in Myd88$^{\Delta Hep}$ mice (Fig. 5*A*; LPS study). Given that *Myd88*$^{\Delta Hep}$ mice displayed an increased rate of bile acid synthesis, our results suggest that the putative excess of cholesterol might be directly metabolized into oxysterols and/or bile acids. Indeed, intracellular accumulation of cholesterol is toxic, and one way to remove extra cholesterol from the liver is to increase bile acid and oxysterol synthesis [236].

Our data show that the feedback loop controlling bile acid production was altered. Indeed, the main enzymes repressed by the negative feedback loop involved in bile acid synthesis were overexpressed in *Myd88*$^{\Delta Hep}$ mice, suggesting that the FGF15-FGFR4-JNK-ERK-CYP7A1/CYP8B1 pathway was affected by *Myd88* deletion. Because we have previously demonstrated that FGF15 and FGFR4 levels were normal in *Myd88*$^{\Delta Hep}$ compared with WT mice [391], we focused our attention on the downstream effectors regulating this signaling cascade. We found that activated ERK, p-ERK, which has been described to inhibit CYP7A1 and CYP8B1 in parallel with p-JNK [204, 245], was lower in Myd88$^{\Delta Hep}$ mice fed with HFD compared with WT mice. Since *Cyp8b1* is strongly overexpressed in Myd88$^{\Delta Hep}$-HFD mice, it might indicate that p-ERK is more potent at inhibiting it than *Cyp7a1*. Finally, the reason why we did not observe significant changes regarding p-JNK could result from the fact that the FGF15-FGFR4 pathway activates ERK strongly than JNK [245].

Collectively, our data support the hypothesis that hepatic MyD88 is involved in the fine-tuning of bile acid synthesis by interacting with the enterohepatic feedback loop.

In line with the fact that hepatic MyD88 mediates cholesterol-derivative bioactive lipid metabolism, we propose that the increased sensitivity to inflammation observed in *Myd88*$^{\Delta Hep}$ mice injected with

LPS may be due to the accumulation of one specific oxysterol, namely, 25-OHC. In fact, in the last decade this oxysterol has emerged as a regulator of immune cell function by displaying antiviral activities, regulating IgA formation, inducing macrophage foam cell production, and controlling inflammation (see Ref. [228] for review). However, its impact on inflammation is still debated because 25-OHC has been shown to exhibit both pro- and anti-inflammatory properties. On one hand, the production of type 1 interferon by viral or bacterial infection induces 25-OHC production, whereby this oxysterol exerts an anti-inflammatory activity by inhibiting sterol regulatory element-binding protein, resulting in the feedback inhibition of IL-1 family production [393, 394]. On the other hand, other studies have reported the importance of 25-OHC to amplify inflammation by promoting some inflammatory gene expression, likely via NF-kB signaling pathways [228, 395, 396]. It is also suggested that the mediation of this immune process is complex, and we may speculate that the impact of 25-OHC depends on its concentration, the cell types involved, and the type of receptors promoting its formation [228, 397, 398]. Previous findings clearly demonstrated that 25-OHC is induced by LPS [397, 399]. Here we found that the accumulation of 25-OHC observed in the liver of Myd88$^{\Delta Hep}$ mice was even worsened after LPS injection. This is likely due to the decreased expression of its degrading enzyme, *Cyp7b1*, compared with WT mice. Since we observed a significant increase in mRNA expression of *Il1b* and other proinflammatory markers in the liver of *Myd88*$^{\Delta Hep}$-LPS mice, we might suggest that at this concentration the anti-inflammatory effect of 25-OHC is probably not effective. However, this assumption warrants further investigations.

Strikingly, a similar decrease in *Cyp7b1* mRNA expression as well as an increase in 25-OHC level have also been reported in the liver of both *ob/ob* and *db/db* mice, strengthening the fact that the dysregulation of hepatic MyD88 might be involved in metabolic syndrome [230].

In addition to the data described above, we have also found an increase in 4β-hydroxycholesterol (4b-OHC) in both basal and challenged conditions in *Myd88*$^{\Delta Hep}$ mice (Fig. 5). An elevation of this oxysterol has been associated with indole alleviating liver inflammation after LPS injection [400]. Moreover 4b-OHC is a liver X receptor (LXR) agonist, and activation of LXR induces anti-inflammatory effects [217, 401]. Besides the increase in 4b-OHC, we found that other putative regulators of LXR activity (i.e., desmosterol, 25-OHC, 5α,6α-epoxycholesterol) were changed in *Myd88*$^{\Delta Hep}$ mice (Fig. 5*A*). One key LXR target gene, *Cyp7a1*, was also upregulated. Therefore, although we did not assess precisely the LXR activity, we may hypothesize that MyD88 is involved in the regulation of liver metabolism by affecting various key metabolites such as bile acids and oxysterols, both involved in inflammatory response and glucose and lipid metabolism.

Altogether, our results suggest that hepatocyte-specific *Myd88* deletion predisposed mice to inflammation by altering liver oxysterol levels (Fig. 6).

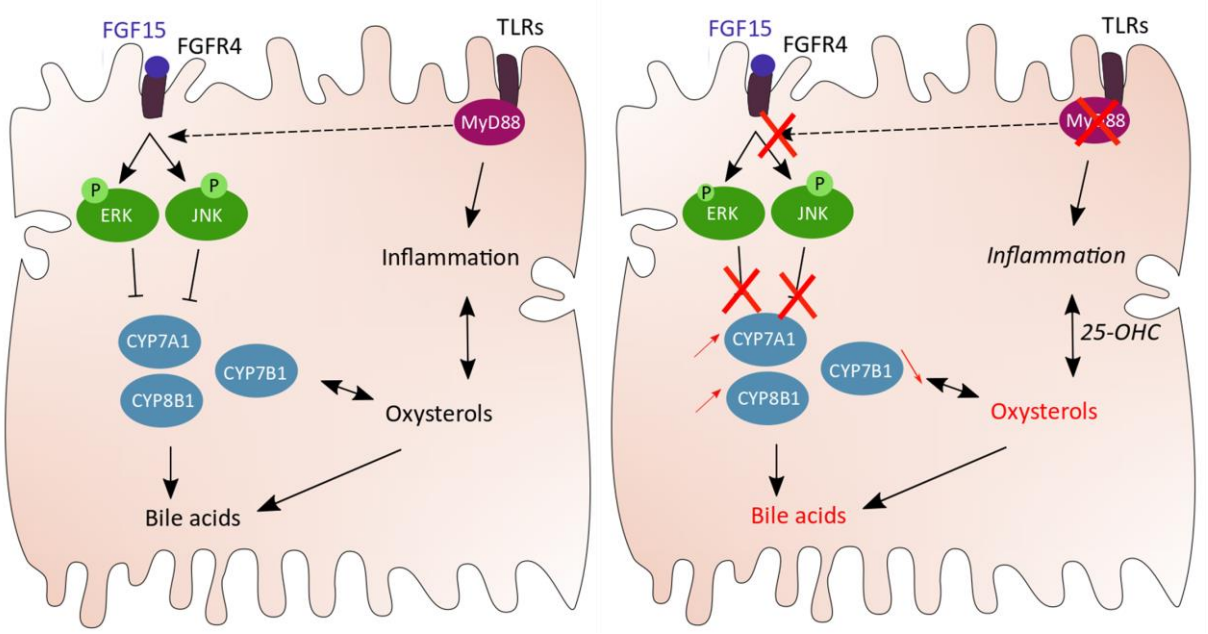

Figure 6: Illustration of the findings and working hypothesis. Our data show that hepatic myeloid differentiation primary response gene 88 (MyD88), in addition to being involved in immunity, can regulate metabolism. In addition, we demonstrate that hepatic MyD88 controls cholesterol-derived bioactive lipid synthesis, presumably by regulating the negative feedback loop inhibiting bile acid production. Finally, an accumulation of 25-hydroxycholesterol (25-OHC) would predispose hepatocyte *Myd88*-deletion (*Myd88*$^{\Delta Hep}$) mice to inflammation. Thus, we discovered a novel mechanism of interaction between the innate immune system and the synthesis of different bioactive lipids thereby controlling host metabolism. FGF15; fibroblast growth factor 15; FGFR4, fibroblast growth factor receptor 4; JNK, c-Jun NH2-terminal kinase; P, phosphorylated; TLRs, Toll-like receptors.

Finally, emerging evidence has also described an interesting interaction between the liver and the gut microbiota through the gut-liver axis, contributing to liver homeostasis [389, 402]. As a matter of fact, modification of bile acids can affect gut microbiota population and proliferation. In turn, these intestinal bacteria are able to mediate bile acid composition by converting primary bile acids into secondary bile acids. These observations highlight a reciprocal regulation between those two key factors [402]. In the present study, we found that *Myd88*$^{\Delta Hep}$ mice exhibited an enhanced bile acid synthesis. It has been established that an increased bile acid concentration exerts bactericidal effects [128]. In accordance with this observation, we have previously shown that *Myd88*$^{\Delta Hep}$ mice displayed an altered gut microbiota composition [391]. We can thus speculate that the microbial community present in *Myd88*$^{\Delta Hep}$ is disturbed. In line with this hypothesis, we found that the concentration of secondary bile acids in the cecum was lower in *Myd88*$^{\Delta Hep}$ compared with WT mice. Hence, we cannot rule out that the *Myd88*$^{\Delta Hep}$ phenotype may also be due to the indirect effect of *Myd88* deletion on gut microbiota and its metabolites.

In summary, in this study we identify a novel role for hepatic MyD88 in host metabolism. We reveal an unexpected link between this key player of the immune system and liver lipid metabolism independent of its role on inflammation. We demonstrated that in the absence of hepatic *Myd88*, mice were prone to liver fat accumulation and were sensitive to inflammation due to a dysregulation of cholesterol-derivative bioactive lipid synthesis (Fig. 6). Since metabolic syndrome is usually associated with increased liver fat and low-grade inflammation, investigating the exact regulation of MyD88 in the liver might lead to finding some relevant target to tackle metabolic diseases.

1.5 Materials and Methods

Mice

Generation of Myd88$^{\Delta Hep}$ mice. Hepatocyte *Myd88*-deleted (*Myd88*$^{\Delta Hep}$) mice were generated as previously described in Duparc et al. [391]. Briefly, mice harboring *Cre* recombinase expressed under the *albumin* promoter (*Albumin*-Cre) (C57BL/6 background; Jackson Laboratory, Bar Harbor, ME) were crossed with mice bearing a *loxP*-flanked *Myd88* allele (C57BL/6 background; Jackson Laboratory). Genotyping and validation of the deletion in the offspring were performed as described in Duparc et al. [391]. The control mice were wild-type (WT) littermates harboring the *Myd88 loxP*-flanked allele but not the *Cre* recombinase.

Mice were housed in a controlled environment (12-h daylight cycle, lights off at 6 PM) and in specific pathogen-free conditions in groups of two mice per cage (filter-top cages), with free access to irradiated food and autoclaved water. The mice were fed a normal control diet (AIN93Mi; Research Diets, New Brunswick, NJ).

Short-term high-fat diet experiment. A cohort of 10-wk-old male *Myd88*$^{\Delta Hep}$ and WT mice were fed either a control diet (CT) (10% fat, AIN93Mi; Research Diets) (WT-CT or *Myd88*$^{\Delta Hep}$-CT) or a HFD (60% fat, D12492i; Research Diets) (WT-HFD or *Myd88*$^{\Delta Hep}$-HFD) for 3 days.

LPS injection experiment. A cohort of CT-fed male *Myd88*$^{\Delta Hep}$ and WT mice were injected intraperitoneally with either 300 µg/kg LPS solution (LPS from *Escherichia coli* O55:B5; Sigma L2880) or saline solution (CT). Mice were euthanized 4 h after the injection.

Tissue Sampling

At the end of the treatment period, fed animals were anesthetized with isoflurane (Forene; Abbott) and blood was sampled from the portal vein. After blood sampling mice were killed by cervical dislocation, and both liver and cecum were immediately immersed in liquid nitrogen and stored at −80°C for further analysis.

RNA Preparation and Real-Time qPCR Analysis

Total RNA was prepared from tissues with TriPure Reagent (Roche). Quantification and integrity analysis of total RNA were performed by running 1 µl of each sample on an Agilent 2100 Bioanalyzer (Agilent RNA 6000 Nano Kit; Agilent). The cDNA was prepared by reverse transcription, and real-time

qPCR was performed as previously described by Everard et al. [37]. *Rpl19* RNA was chosen as housekeeping gene. Sequences of the primers used for real-time qPCR are shown in Table 1.

Table 1: Primers used for real-time qPCR.

Gene	Forward primer sequence (5'-3')	Reverse primer sequence (5'-3')
Rpl19	GAAGGTCAAAGGGAATGTGTTCA	CCTTGTCTGCCTTCAGCTTGT
Il6	ACAAGTCGGAGGCTTAATTACACAT	TTGCCATTGCACAACTCTTTTC
Cd11c	ACGTCAGTACAAGGAGATGTTGGA	ATCCTATTGCAGAATGCTTCTTTACC
F4/80	TGACAACCAGACGGCTTGTG	GCAGGCGAGGAAAAGATAGTGT
Il1b	TCGCTCAGGGTCACAAGAAA	CATCAGAGGCAAGGAGGAAAAC
Tnfa	TCGAGTGACAAGCCTGTAGCC	TTGAGATCCATGCCGTTGG
Hmgcr	CCTGACACTGAACTGAAGCG	TCTTTCCAGAACACAGCACG
Cyp7a1	GGGATTGCTGTGGTAGTGAGC	GGTATGGAATCAACCCGTTGTC
Cyp27a1	TCTGGCTACCTGCACTTCCT	GTGTGTTGGATGTCGTGTCC
Cyp8b1	GATCCGTCGCGGAGATAAGG	CGGGTTGAGGAACCGATCAT
Cyp7b1	TAGGCATGACGATCCTGAAA	TCTCTGGTGAAGTGGACTGAAA

Western Blotting

For detection of proteins, liver tissues were homogenized with TissueLyser II (Qiagen) in ice-cold buffer [in mM: 20 Tris, 270 sucrose, 5 EGTA, 1 EDTA, 1 sodium orthovanadate, 50 sodium β-glycerophosphate, 5 sodium pyrophosphate, 50 sodium fluoride, and 1 1,4-dithiothreitol, with 1% Triton X-100 and 10% protease inhibitor cocktail 10× (Roche Applied Science, Vilvoorde, Belgium)]. Homogenates were centrifuged at 10,000 *g* for 10 min at 4°C. Supernatants were immediately stored at −20°C. Equal amounts of proteins were separated by SDS-PAGE and transferred to nitrocellulose membranes. Membranes were incubated overnight at 4°C with antibodies diluted in Tris-buffered saline-Tween 20 containing 1% bovine serum albumin: JNK (1:1,000; 9252S, Cell Signaling), phosphorylated (p-)JNK (1:200; 9251S, Cell Signaling), ERK (1:1,000; 4695S, Cell Signaling), and p-ERK (1:1,000; 9101S, Cell Signaling). The loading control was β-actin (1:10,000; ab6276, Abcam). The difference in protein loading is taken into account when signal quantification is analyzed. Signal quantification was acquired with an Amersham Imager 600 (GE Healthcare) and analyzed by ImageQuant TL software.

Liver Lipid Content

Total lipid content was measured in the liver tissue after extraction with chloroform-methanol according to the Folch method, as previously described by Duparc et al. [391] and Folch et al. [403].

Triglyceride and cholesterol concentrations were measured with kits coupling enzymatic reaction and spectrophotometric detection of reaction end products (Diasys Diagnostic and Systems, Holzheim, Germany).

Lipidomic Analysis

Lipid measurements were performed in collaboration with Biocrates (Innsbruck, Austria).

Bile acid quantification was performed with a commercial Bile Acids Kit from Biocrates. A selective reverse-phase LC-MS/MS analysis method in negative ion multiple reaction monitoring (MRM) detection mode was used to measure bile acid levels. Analyses were performed via LC-electrospray ionization (ESI)-MS/MS with a SCIEX 4000 QTRAP (SCIEX, Darmstadt, Germany) instrument. Seven-point external calibration curves and 10 stable isotope-labeled internal standards were used.

Prostaglandins were purified from 20 µl of biological sample with a methanolic protein precipitating solution. A MRM mode using negative ESI was applied to detect prostaglandins. An online solid phase extraction-HPLC-MS/MS on a SCIEX 5500 QTRAP (SCIEX) instrument was used to carry out the analysis. Several deuterated metabolites were used as internal standards; quantitation was performed with a seven-point calibration.

Extractions of sterols and oxysterols from samples were performed with methanol and the Biocrates Kit filter plate. A UHPLC-MS/MS with MRM in positive mode using a SCIEX API 5500 QTRAP (SCIEX) instrument with ESI was applied to determine the concentration of sterols and oxysterols.

All data were quantified with MS software (ThermoFisher Scientific Xcalibur) and Biocrates MetIDQ software.

Ethics Statement

All mouse experiments were reviewed and approved by and performed in accordance with the guidelines of the local ethics committee for animal care of the Health Sector of the Université Catholique de Louvain under the specific agreement numbers 2014/UCL/MD/022 and 2017/UCL/MD/005. Housing conditions were as specified by the Belgian Law of 29 May 2013 regarding the protection of laboratory animals (agreement number LA1230314). Every effort was made to minimize animal pain, suffering, and distress.

Statistical Analysis

Data are expressed as means ± SE. Differences between more than two groups were assessed by two-way ANOVA, followed by the Tukey post hoc test. Data were analyzed with GraphPad Prism (GraphPad Software).

1.6 Acknowledgments

We thank A. Barrois, H. Danthinne, and R. M. Goebells for excellent technical assistance.
The raw data supporting the conclusions of this report will be made available by the authors, without undue reservation, to any qualified researcher.

1.7 Grants

This work is supported by the Funds Baillet Latour (Grant for Medical Research 2015) and European Research Countil Starting Grant 2013 (Starting Grant 336452-ENIGMO). P. D. Cani is a senior research associate at FRS-FNRS (Fonds de la Recherche Scientifique), Belgium. A. Everard is a research associate at FRS-FNRS, Belgium. P. D. Cani is the recipient of grants from FRS-FNRS: under a Projet de Recherche (convention: T.0138.14), FRFS-Walloon Excellence in Life Sciences and Biotechnology (WELBIO) (under Grant WELBIO-CR-2017-C02), and The Excellence of Science (EOS) (EOS 30770923).

1.8 Disclosures

No conflicts of interest, financial or otherwise, are declared by the authors.

1.9 Author Contributions

C.L., M.V.H., and P.D.C. conceived and designed research; C.L., M.V.H., A.E., and P.D.C. performed experiments; C.L., M.V.H., A.E., and P.D.C. analyzed data; C.L., M.V.H., A.E., and P.D.C. interpreted results of experiments; C.L. and P.D.C. prepared figures; C.L. and P.D.C. drafted manuscript; C.L., M.V.H., N.M.D., A.E., and P.D.C. edited and revised manuscript; C.L., M.V.H., N.M.D., A.E., and P.D.C. approved final version of manuscript.

Graphical abstract

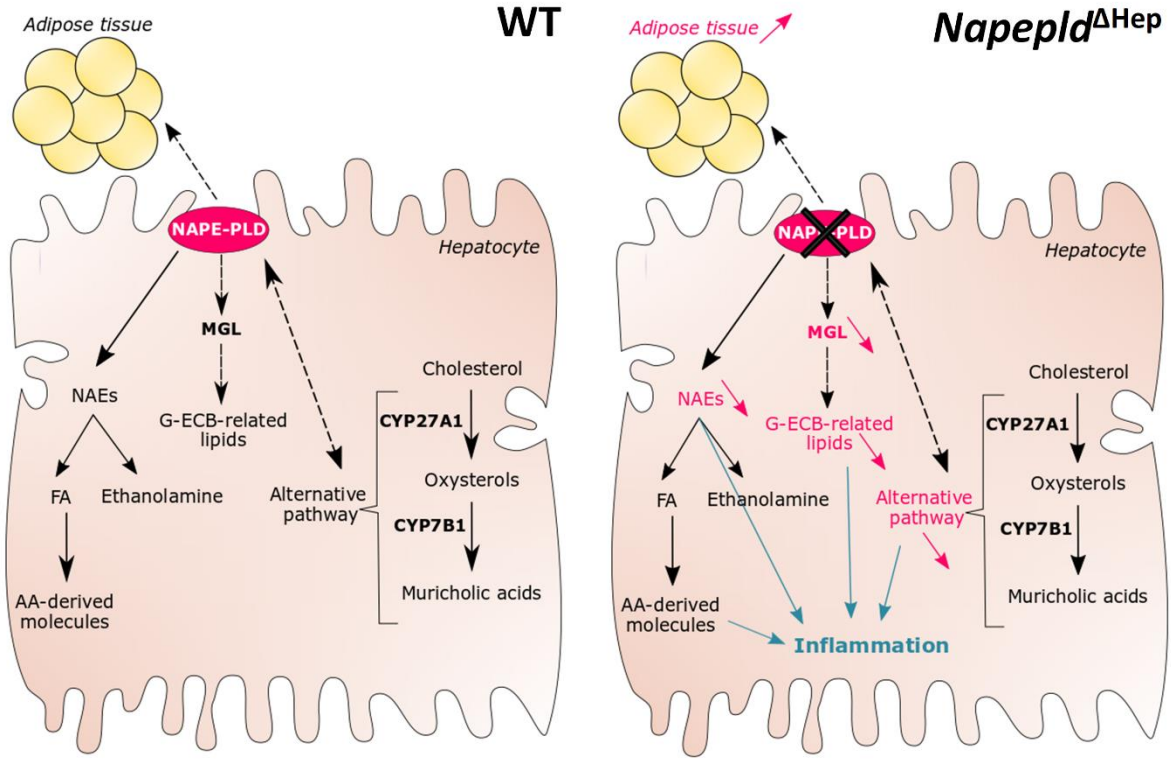

2 Chapter: Hepatic NAPE-PLD Is a Key Regulator of Liver Lipid Metabolism

cells

MDPI

Article

Hepatic NAPE-PLD Is a Key Regulator of Liver Lipid Metabolism

Charlotte Lefort [1], Martin Roumain [2], Matthias Van Hul [1], Marialetizia Rastelli [1], Rita Manco [3], Isabelle Leclercq [3], Nathalie M. Delzenne [1], Vincenzo Di Marzo [4,5,6], Nicolas Flamand [4], Serge Luquet [7], Cristoforo Silvestri [4], Giulio G. Muccioli [2] and Patrice D. Cani [1,*]

The results related to this chapter have been published in Cells, 9(5):1247, 2020

2.1 Abstract

Diverse metabolic disorders have been associated with an alteration of *N*-acylethanolamine (NAE) levels. These bioactive lipids are synthesized mainly by *N*-acylphosphatidylethanolamine-selective phospholipase D (NAPE-PLD) and influence host metabolism. We have previously discovered that NAPE-PLD in the intestine and adipose tissue is connected to the pathophysiology of obesity. However, the physiological function of NAPE-PLD in the liver remains to be deciphered. To study the role of liver NAPE-PLD on metabolism, we generated a new mouse model of inducible *Napepld* hepatocyte-specific deletion (*Napepld*$^{\Delta Hep}$ mice). In this study, we report that *Napepld*$^{\Delta Hep}$ mice develop a high-fat diet-like phenotype, characterized by an increased fat mass gain, hepatic steatosis and we show that *Napepld*$^{\Delta Hep}$ mice are more sensitive to liver inflammation. We also demonstrate that the role of liver NAPE-PLD goes beyond the mere synthesis of NAEs, since the deletion of NAPE-PLD is associated with a marked modification of various bioactive lipids involved in host homeostasis such as oxysterols and bile acids. Collectively these data suggest that NAPE-PLD in hepatocytes is a key regulator of liver bioactive lipid synthesis and a dysregulation of this enzyme leads to metabolic complications. Therefore, deepening our understanding of the regulation of NAPE-PLD could be crucial to tackle obesity and related comorbidities.

2.2 Introduction

Over the last few years, interest in specific bioactive lipids, the *N*-acylethanolamines (NAEs), has increased exponentially as accumulating evidence demonstrated an association between variations in NAE levels and diverse pathological conditions such as obesity, inflammation or hepatic disorders [60, 351, 404]. NAEs belong to the expanded endocannabinoid system, or endocannabinoidome (eCBome), which is composed of several enzymes, receptors and bioactive lipids involved in energy homeostasis [24, 60]. The best-known NAEs include anandamide (*N*-arachidonoylethanolamine, AEA, an endocannabinoid), *N*-palmitoylethanolamine (PEA), *N*-stearoylethanolamine (SEA), *N*-linoleylethanolamine (LEA) and *N*-oleoylethanolamine (OEA). In the context of metabolic disorders, some NAEs have been reported to regulate food intake [405-407], to mediate inflammation [381, 382] or to contribute to the development of steatosis [352, 408]. Even though many of their physiological actions have been discovered, understanding the molecular mechanisms that link NAEs to metabolic diseases remains challenging.

Since *N*-acylphosphatidylethanolamine-selective phospholipase D (NAPE-PLD) is the main enzyme producing NAEs [296], inhibiting its action, represents an efficient way to explore the function of NAEs. However, the mechanisms of regulation of NAPE-PLD activity, especially in vivo, are not yet fully deciphered. Interestingly, recent studies have made progress in that perspective and have elegantly shown that natural bile acids, and specific steroidal hydroxylation pattern were key elements for modulating the enzyme activity [318]. These data suggesting a link between NAPE-PLD and steroid acids open the floor to design putative small-molecule modulators with potential therapeutic applications [314].

Nevertheless, in order to better understand the physiological role of NAPE-PLD, deleting this enzyme in the whole-body has been the initial strategy. Although whole-body *Napepld*-knockouts displayed controversial brain lipid profiles, they did not exhibit a peculiar phenotype [299, 325, 326, 409, 410], suggesting that compensatory mechanisms come into effect when this vital system is deficient in early developmental stages. To overcome this problem, we generated *Napepld*-deleted mouse models in which NAPE-PLD could be inactivated in specific organs from adult mice, using the Cre-lox system [411]. This allowed us to previously discover that mice deleted for *Napepld* in the adipose tissue developed an obese-like phenotype, with higher fat mass, glucose intolerance and low-grade inflammation, when fed a normal diet [291]. In addition, we also demonstrated that the deletion of *Napepld* in the intestinal epithelial cells affected food intake regulation [292]. These two studies highlighted that NAPE-PLD and the bioactive products it generates are involved in host homeostasis and that the

phenotypes observed were organ-specific. Interestingly, in humans, a single nucleotide polymorphism in *Napepld* has been linked to obesity [329]. Since obesity is associated with a cluster of metabolic complications including liver disorders [6, 388, 412], and both organ-specific *Napepld* knockout mouse models previously investigated were prone to develop obesity-associated steatosis, we next wondered what would be the role of NAPE-PLD in the liver. In the present study, we therefore generated a new mouse model of inducible hepatocyte-specific deletion of *Napepld* in hepatocytes (*Napepld*$^{\Delta Hep}$) to further investigate the physiological functions of this enzyme in the context of metabolic diseases.

2.3 Results

Hepatocyte-Specific Deletion of Napepld

To explore the role of liver NAPE-PLD on metabolism, *Napepld*$^{\Delta Hep}$ mice were generated by crossing Albumin-Cre^{ERT2} mice [413] with *Napepld*$^{lox/lox}$ mice [291]. The liver specificity of the deletion upon tamoxifen treatment was assessed by quantifying *Napepld* messenger RNA (mRNA) expression in the liver and in several organs including adipose tissues, brain, intestine, muscle or the kidney of wild-type (WT) and *Napepld*$^{\Delta Hep}$ mice fed a control diet (Figure 1A). As expected, the liver was the unique organ exhibiting a strong reduction of *Napepld* mRNA expression confirming the liver specificity of the model. In accordance with this data, the deletion was also observed by in situ hybridization performed on liver slices of both genotypes since the *Napepld*-specific probe was not detected in *Napepld*$^{\Delta Hep}$ hepatocytes (Figure S1A).

Next, we measured the NAEs produced by NAPE-PLD in the liver of WT and *Napepld*$^{\Delta Hep}$ mice (Figure 1B). The levels of OEA and LEA were significantly lower, as mirrored by the 20% reduction, in *Napepld*$^{\Delta Hep}$ livers compared to WT whereas no change was reported regarding AEA and PEA levels. These data support the existence of alternative pathways, possibly tissue- and cell-specific for NAE biosynthesis. This alternative pathway has been largely described for AEA biosynthesis, which is also consistent with our previous studies [291, 299-301, 409, 414]. Surprisingly, almost all the lipid congeners related to the eCBome (i.e., acylglycerols) were affected in the liver of *Napepld*$^{\Delta Hep}$ mice, suggesting that NAPE-PLD could, albeit indirectly, control the biosynthesis of a larger group of bioactive lipids in the liver than initially thought (Figure 1C and Figure S1B). The altered lipid profile could not be explained by a major impact on the other biosynthetic and degrading enzymes for these mediators because the monoacylglycerol lipase (*Mgll)* was the only enzyme significantly altered at the mRNA level, as reflected by a 25% decreased expression, in *Napepld*$^{\Delta Hep}$ livers as compared to WT (Figure 1D).

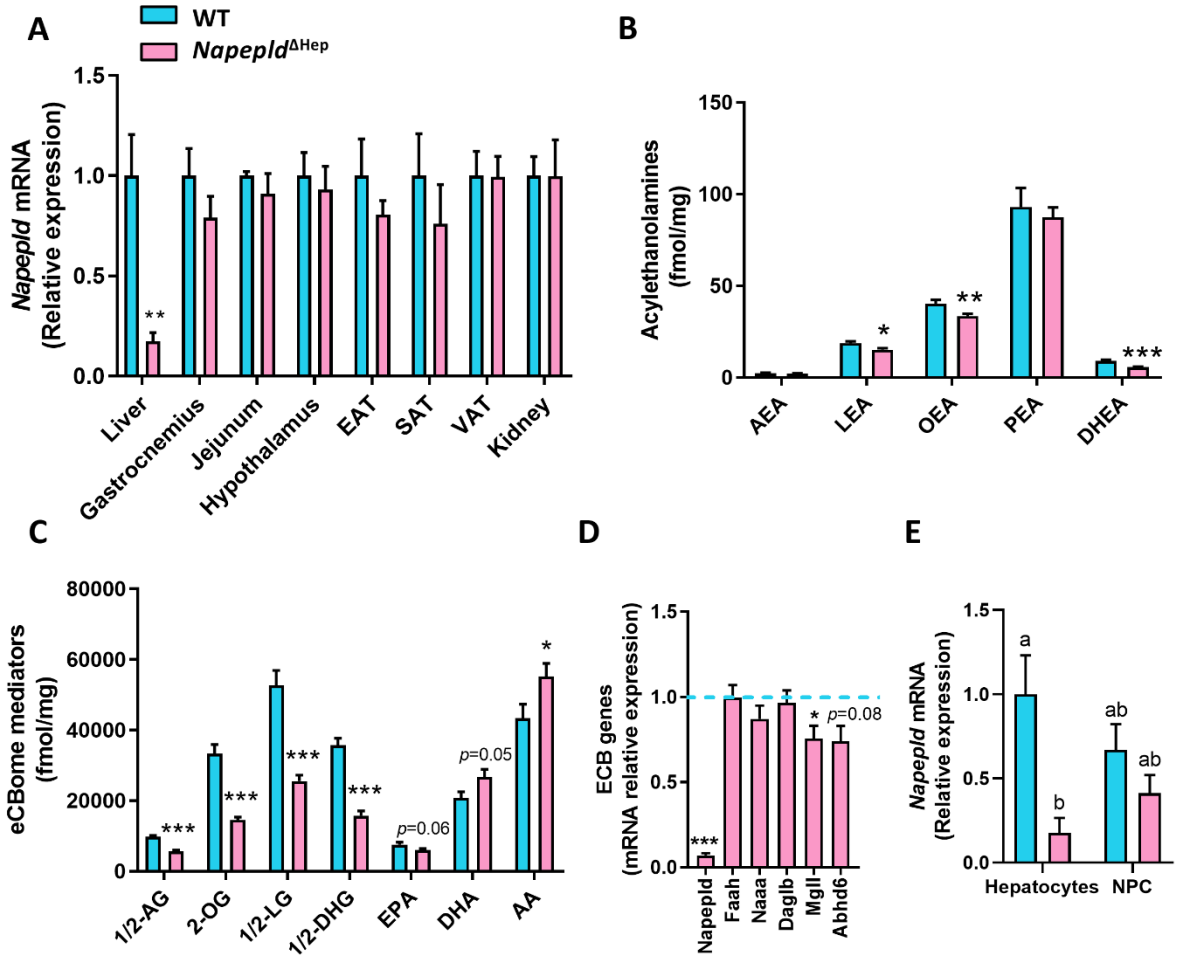

Figure 1: Hepatocyte-specific deletion of *Napepld*. (**A**) *Napepld* mRNA expression measured by real-time qPCR in the liver, gastrocnemius muscle, jejunum, hypothalamus, epididymal adipose tissue (EAT), subcutaneous adipose tissue (SAT), visceral adipose tissue (VAT) and kidney (n = 6). (**B–C**) Levels of *N*-acylethanolamines and other eCBome mediators in the liver (fmol/mg; n = 8–10). (**D**) mRNA expression of key enzymes of the endocannabinoid system (ECB) measured by real-time qPCR in the liver (n = 8–10). (**E**) *Napepld* mRNA expression in hepatocytes and hepatic non-parenchymal cells (NPC; n = 4–5). Blue: wild-type (WT) normal diet (ND) mice. Pink: *Napepld*$^{\Delta Hep}$ ND mice. Data are presented as the mean ± s.e.m. *, ** and *** indicate a significant difference versus WT ND (Respectively $p < 0.05$, $p < 0.01$ and $p < 0.001$) according to the *t*-test. Data with different superscript letters are significantly different ($p < 0.05$) according to two-way ANOVA followed by Tukey post hoc test. Lipid abbreviations: 1/2-AG, 1/2-arachidonoylglycerol; 1/2-DHG, 1/2-DHA-glycerol; 1/2-LG, 1/2-linoleoylglycerol; 2-OG, 2-oleoylglycerol; AA, Arachidonic acid; AEA, N-arachidonoylethanolamine; DHA, Docosahexaenoic acid; DHEA, N-docosahexaenoylethanolamine; EPA, Eicosapentaenoic acid; LEA, N-linoleylethanolamine; OEA, N-oleoylethanolamine; PEA, N-palmitoylethanolamine.

To further validate the specific deletion of NAPE-PLD in hepatocytes, we separated these cells from the hepatic non-parenchymal cells (NPC). Of interest, the purity of both fractions was measured by various markers: the NPC fraction was assessed by an increased mRNA expression of *F4/80*, *Cd31*, *Acta2* and *Ck19,* which are specific to Kupffer cells, sinusoidal endothelial cells, stellate cells and cholangiocytes respectively whereas a higher expression of *Hnf4a* was unique to the hepatocyte fraction (Figure S1C) [415-418]. Our data showed that the expression of *Napepld* was

markedly decreased in the hepatocyte-enriched fraction from *Napepld*$^{\Delta Hep}$ mice, while the NPC were not significantly affected (Figure 1E).

Altogether, these data confirm the invalidation of the *Napepld* gene in hepatocytes and highlight a new role of NAPE-PLD in the regulation of liver lipid metabolism.

Napepld$^{\Delta Hep}$ *Mice Develop a High-Fat Diet-Like Phenotype upon Normal Diet*

To assess whether the *Napepld* deletion in hepatocytes affects the whole-body metabolism, we followed a cohort of WT and *Napepld*$^{\Delta Hep}$ mice fed a control diet for 7 weeks. Strikingly, although the body weight of the two genotypes was equivalent at the end of the experiment, nuclear magnetic resonance (NMR) revealed that *Napepld*$^{\Delta Hep}$ mice tended to have a higher percentage of fat mass and a significantly lower percentage of lean mass compared to WT mice (Figure 2A–C). The fat mass accumulation was reflected by increased adipose tissue weights in *Napepld*$^{\Delta Hep}$ mice, obtained after precise dissection. The liver weight of *Napepld*$^{\Delta Hep}$ mice was also higher compared to WT mice, while a significant reduction of the cecal content was observed in *Napepld*$^{\Delta Hep}$ mice (Figure 2D). All the aforementioned measures observed in *Napepld*$^{\Delta Hep}$ mice are usually reported in the animal model of diet-induced obesity and this effect could not be attributed to an increase in food intake (Figure 2E). Therefore, we evaluated the impact of hepatocyte *Napepld* deletion on whole-body glucose metabolism by performing an oral glucose tolerance test (OGTT). The glycemia of WT and *Napepld*$^{\Delta Hep}$ mice was similar during the test (Figure 2F). However, *Napepld*$^{\Delta Hep}$ mice exhibited a higher insulin resistance index (Figure 2G), mainly explained by elevated plasma insulin levels (Figure S2).

Overall, *Napepld*$^{\Delta Hep}$ mice display a high-fat diet-like phenotype without developing glucose intolerance.

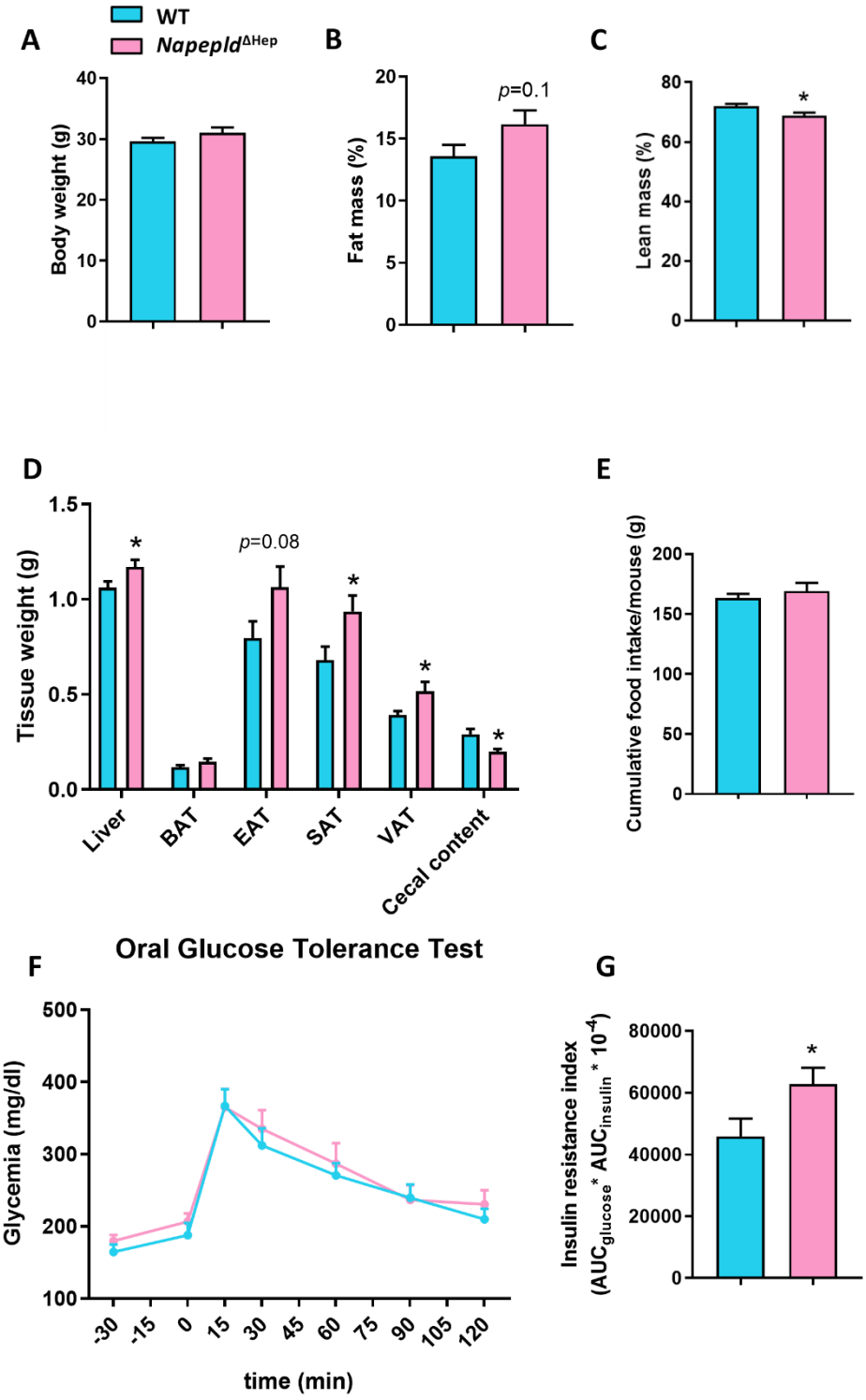

Figure 2: *Napepld*$^{\Delta Hep}$ mice develop a high-fat diet-like phenotype upon normal diet. (**A**) Body weight (g), (**B**) fat mass (%) and (**C**) lean mass (%) after a 7 weeks period on normal diet. (**D**) Weight (g) of different tissues: liver, brown adipose tissue (BAT), epididymal adipose tissue (EAT), subcutaneous adipose tissue (SAT), visceral adipose tissue (VAT) and cecal content. (**E**) Cumulative food intake per mouse (g) after a 7 weeks period. (**F**) Plasma glucose profile (mg/dl) measured between 30 min before and 120 min after oral glucose loading (**G**) Insulin resistance index determined by multiplying the area under the curve (AUC) of blood glucose by the AUC of insulin. Blue: WT ND mice. Pink: *Napepld*$^{\Delta Hep}$ ND mice (n = 8–10). Data are presented as the mean ± s.e.m. *and ** indicate a significant difference versus WT ND (Respectively $p < 0.05$ and $p < 0.01$) according to the *t*-test.

Napepld$^{\Delta Hep}$ *Mice Are More Sensitive to Liver Lipid Accumulation*

Since *Napepld*$^{\Delta Hep}$ mice displayed an altered liver lipid metabolism as well as a higher liver weight, we wondered whether this latter was due to an accumulation of liver lipids. To address this question, we first performed histology analysis by staining liver slices of WT and *Napepld*$^{\Delta Hep}$ mice with oil red O dye, which highlights lipid droplet in red. Although the global liver morphology was similar between both genotypes, the lipid droplet size was larger in *Napepld*$^{\Delta Hep}$ liver compared to WT (Figure 3A). In parallel, gravimetric and biochemical measurements were conducted to quantify liver lipid content in WT and *Napepld*$^{\Delta Hep}$ mice. In accordance with the 10% increased of liver mass, the results, albeit not significant, showed a slight elevation in total liver lipid (15%) and triglyceride (11%) levels in *Napepld*$^{\Delta Hep}$ liver (Figure 3B and Figure S3A). To gain a better insight into the origins of the higher liver lipid accumulation, we investigated the enzymes involved in the β-oxidation pathway including peroxisomal acyl-coenzyme A oxidase 1 (*Acox1*), carnitine O-palmitoyltransferase 1α (*Cpt1a*) and peroxisome proliferator-activated receptorα (*Ppara*; Figure 3C). Strikingly, all studied genes were downregulated at the mRNA level indicating that the absence of *Napepld* in hepatocytes could contribute to this phenomenon. Besides, we also explored the adipose tissue metabolism given that this organ plays a pivotal role on lipid storage and release. By carrying out hematoxylin and eosin staining on SAT deposits, we discovered that the size of adipocytes was larger in *Napepld*$^{\Delta Hep}$ mice strengthening the high-fat diet-like phenotype exhibited by these mutant mice (Figure 3D). Additionally, because insulin resistance can be linked with a higher release of circulating free fatty acids promoted by the lipolysis and that *Napepld*$^{\Delta Hep}$ mice had a higher insulin resistance index, we quantified plasma lipid levels. We discovered that plasma triglyceride level tended to increase (p = 0.05) whereas plasma non-esterified fatty acids (NEFA) and cholesterol levels were unchanged in both groups (Figure S3B–D).

All the aforementioned results indicate that deletion of NAPE-PLD in hepatocytes contributes to liver lipid accumulation by affecting β-oxidation pathway rather than lipolysis.

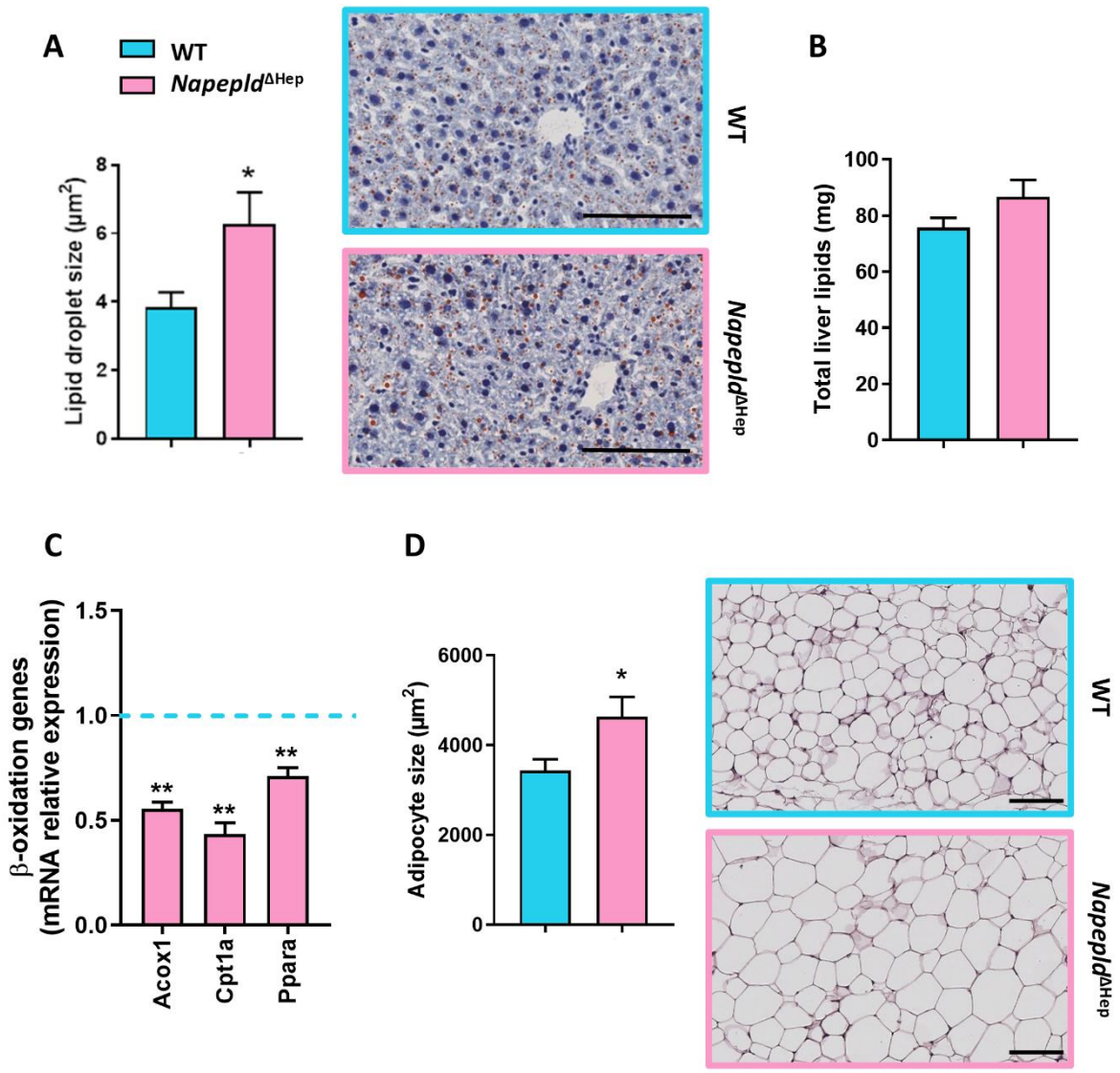

Figure 3: *Napepld*$^{\Delta Hep}$ mice are more sensitive to liver lipid accumulation. (**A**) Representative liver oil red O staining (scale bar: 100 µm) and average lipid droplet size (µm²). (**B**) Liver lipid content measured by gravimetry (mg). (**C**) mRNA expression of genes involved in β-oxidation measured by real-time qPCR in the liver. (**D**) Representative hematoxylin and eosin-stained pictures of SAT deposits (scale bar: 100 µm) and mean adipocyte size (µm²). Blue: WT ND mice. Pink: *Napepld*$^{\Delta Hep}$ ND mice (n = 8–10). Data are presented as the mean ± s.e.m. *and ** indicate a significant difference versus WT ND (Respectively $p < 0.05$ and $p < 0.01$) according to the *t*-test.

Hepatocyte Napepld Deletion Modifies Liver Bioactive Lipid Metabolism

Our first liver lipidomic analysis regarding NAEs and eCBome mediators comparing WT and *Napepld*$^{\Delta Hep}$ mice revealed that NAPE-PLD deletion impacts lipid regulation beyond NAEs synthesis. To investigate the effect of NAPE-PLD deletion on additional lipid mediators in the liver, we quantified two important liver lipid families derived from cholesterol oxidation, namely the bile acids and their precursors, the oxysterols. Surprisingly, almost all bioactive lipids belonging to both families were strongly decreased in *Napepld*$^{\Delta Hep}$ mice in comparison to WT (Figure 4A,C). To better characterize this altered lipid profile, we studied the gene expression of enzymes responsible for the synthesis of cholesterol and bile acid metabolism. We found a significant downregulation of *Cyp7b1* and *Hmgcr* mRNA and a tendency for decreased *Cyp27a1* mRNA (p = 0.06; Figure 4B). This finding is in line with the reduced concentrations of these bioactive lipids in the liver of *Napepld*$^{\Delta Hep}$ mice. We also explored the enterohepatic feedback loop of bile acid metabolism by examining the mRNA expression of receptors and transporters related to the recirculation of bile acids to the liver (Figure 4E). After their synthesis in hepatocytes and prior to secretion into the biliary canaliculi, bile acids must be conjugated with taurine in mice or glycine in humans. Interestingly, the enzymes involved in bile acid conjugation, bile acid CoA ligase (*Bal*) and bile acid CoA:amino acid N-acyltransferase (*Baat*), were already altered in this first step in *Napepld*$^{\Delta Hep}$ mice. Following conjugation, bile acids cannot diffuse across membranes and need specific transporters to go through hepatocyte membrane. As such, the organic solute transporter (OST)β mediates bile acid efflux and the bile salt export protein (BSEP) allows them to reach biliary canaliculi. In this study, we found that *Ostb* tended to be reduced (p = 0.07) while *Bsep* was significantly downregulated *in Napepld*$^{\Delta Hep}$ mice suggesting a decreased secretion of bile salts. Of interest, the bile is also composed of phospholipids and cholesterol, which are transported from hepatocytes to the gallbladder by respectively multidrug resistance protein 2 (MDR2) and ATP-binding cassette sub-family G member (ABCG)5 and ABCG8. *Mdr2* mRNA expression was significantly decreased in *Napepld*$^{\Delta Hep}$ livers whereas cholesterol transporters were reported unchanged. In addition, transporters in charge of the reabsorption of bile acids in hepatocytes such as the sodium (Na^+)-taurocholate cotransporting polypeptide (NTCP) and the organic anion transporter (OATP)1B2 were also investigated. Although *Ntcp* mRNA expression was similar in both groups, *Oatp1b2* tended to be reduced in *Napepld*$^{\Delta Hep}$ mice (p = 0.06). In the jejunum and ileum, however, we found no significant difference in mRNA level of bile acid transporters such as the apical sodium-dependent transporter (ASBT) or OSTα/OSTβ that would have indicated a change in bile acid reabsorption. Besides, the expression of intestinal bile acid-binding protein (*Ibabp*) that facilitates the travel of bile acids from the apical to the basolateral membrane of enterocytes was not different either between groups.

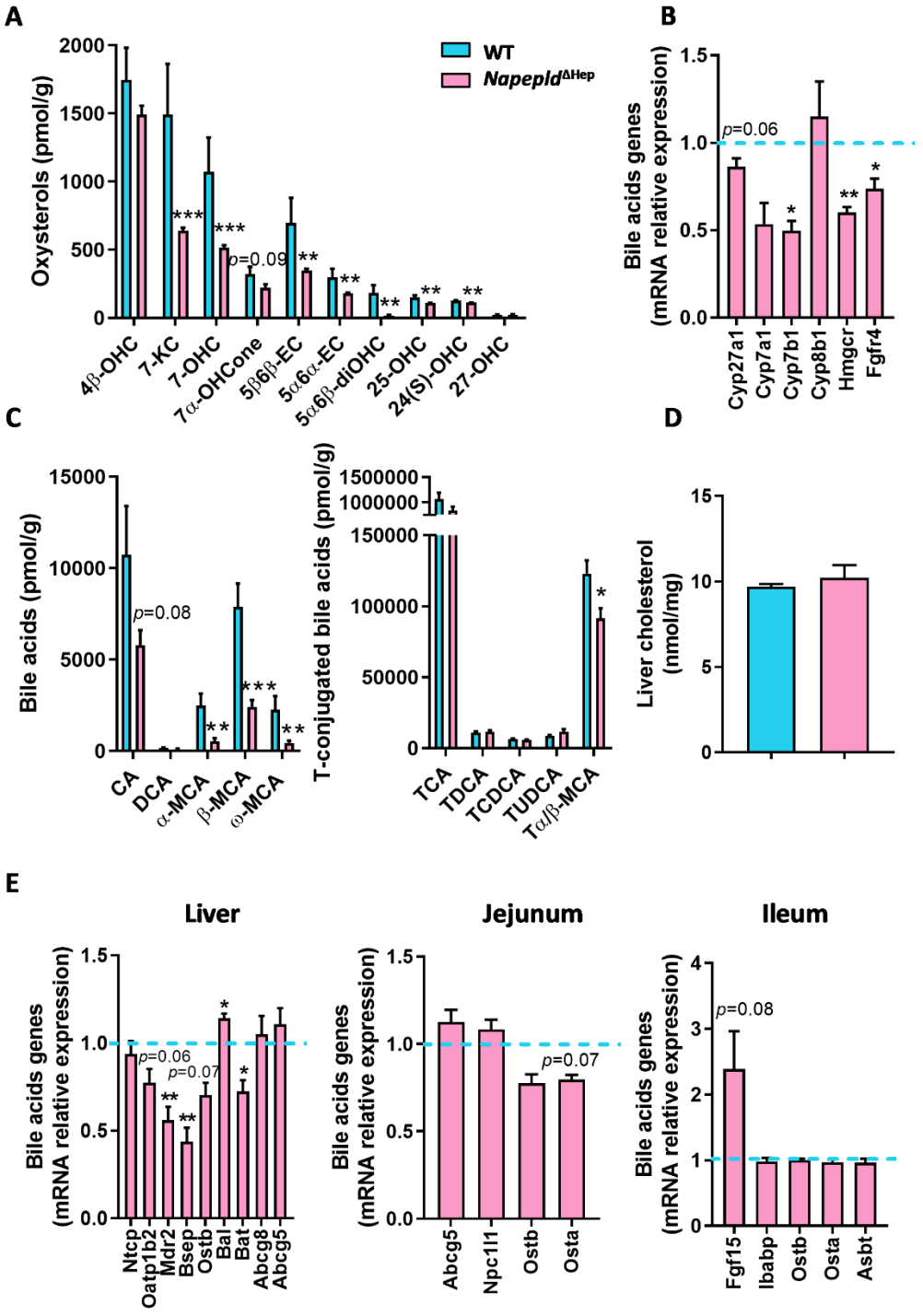

Figure 4: Hepatocyte *Napepld* deletion modifies liver bioactive lipid metabolism. (**A**) Liver oxysterol concentration (pmol/g). (**B**) Key markers of bile acid metabolism measured by real-time qPCR in the liver. (**C**) Liver bile acid concentration (pmol/g). (**D**) Liver cholesterol concentration (nmol/mg). (**E**) Markers of the enterohepatic feedback loop involved in bile acid metabolism measured by real-time qPCR in the liver, jejunum and ileum. Blue: WT ND mice. Pink: *Napepld*$^{\Delta Hep}$ ND mice (n = 8–10). Data are presented as the mean ± s.e.m. *, ** and *** indicate a significant difference versus WT ND (Respectively $p < 0.05$, $p < 0.01$ and $p < 0.001$) according to the *t*-test. Lipid abbreviations: 24(S)-OHC, 24(S)-hydroxycholesterol; 25-OHC, 25-hydroxycholesterol; 27-OHC, 27-hydroxycholesterol; 4β-OHC, 4β-hydroxycholesterol; 5α6α-EC, 5α,6α-epoxycholesterol; 5α6β-diOHC, 5α,6β-dihydroxycholesterol; 5β6β-EC, 5β,6β-epoxycholesterol; 7-KC, 7-ketocholesterol; 7-OHC, 7-hydroxycholesterol; 7α-OHCone, 7α-hydroxycholestenone; CA, Cholic acid; CDCA, Chenodeoxycholic acid; DCA, Deoxycholic acid; (α, β or ω)-MCA, (α, β or ω)-Muricholic acid.

Of note, the enterohepatic feedback loop is also driven by the stimulation of the endocrine hormone fibroblast growth factor (FGF)-15. This latter is induced by the activation of farnesoid receptor X (FXR) by specific bile acids in the enterocyte and then secreted into the portal circulation to repress bile acid synthesis by inhibiting cytochrome P450 enzyme (CYP)7A1 and (CYP)8B1 via fibroblast growth factor receptor (FGFR)4 receptor expressed in the liver. We found that *Fgf15* expression doubled in the ileum of *Napepld*$^{\Delta Hep}$ mice as compared to WT (p = 0.08) whereas *Fgfr4* was downregulated. Although the increased level of *Fgf15* could contribute mildly to the slight decrease in *Cyp7a1* expression, no significant repression was reported regarding *Cyp7a1* and *Cyp8b1* mRNA expressions in the liver of *Napepld*$^{\Delta Hep}$ mice. This suggests that the enterohepatic feedback loop is functional in enterocytes but not properly active in the liver. Finally, the deletion of hepatocyte *Napepld* did not change total liver cholesterol content (Figure 4D) nor the expression of cholesterol transporters measured both in the liver (*Abcg5* and *Abcg8*) and in the intestine (*Abcg5* and *Npc1l1).* Thereby, it indicates that hepatocyte NAPE-PLD influences bile acid and oxysterol production without affecting cholesterol secretion and absorption.

Taken together, these findings demonstrate a strong link between hepatic *Napepld* and the regulation of cholesterol-derived lipid metabolism.

Deletion of Napepld Partially Accentuates the Obese Phenotype Induced by a High-Fat Diet

Given that, in the absence of *Napepld* in hepatocytes, the mice fed control diet developed a high-fat diet-like phenotype, we wondered whether challenging the mice with a high-fat diet (HFD) would worsen the phenotype. After 8 weeks of HFD, *Napepld*$^{\Delta Hep}$ mice had a higher percentage of fat mass and a decreased percentage of lean mass compared to WT. This was independent of food intake or body weight (Figure 5A–C,E). Subcutaneous adipose tissue (SAT) was significantly increased and visceral adipose tissue (VAT) tended to be larger (p = 0.1) in *Napepld*$^{\Delta Hep}$ mice. Similarly to what observed upon the normal diet, in this experiment the cecal content also tended to be reduced in *Napepld*$^{\Delta Hep}$ mice as compared to WT mice exposed to HFD (Figure 5D). Moreover, biochemical analyses showed an elevated concentration of plasma cholesterol in *Napepld*$^{\Delta Hep}$ mice whereas no change was reported for plasma triglycerides (Figure 5F and Figure S4F).

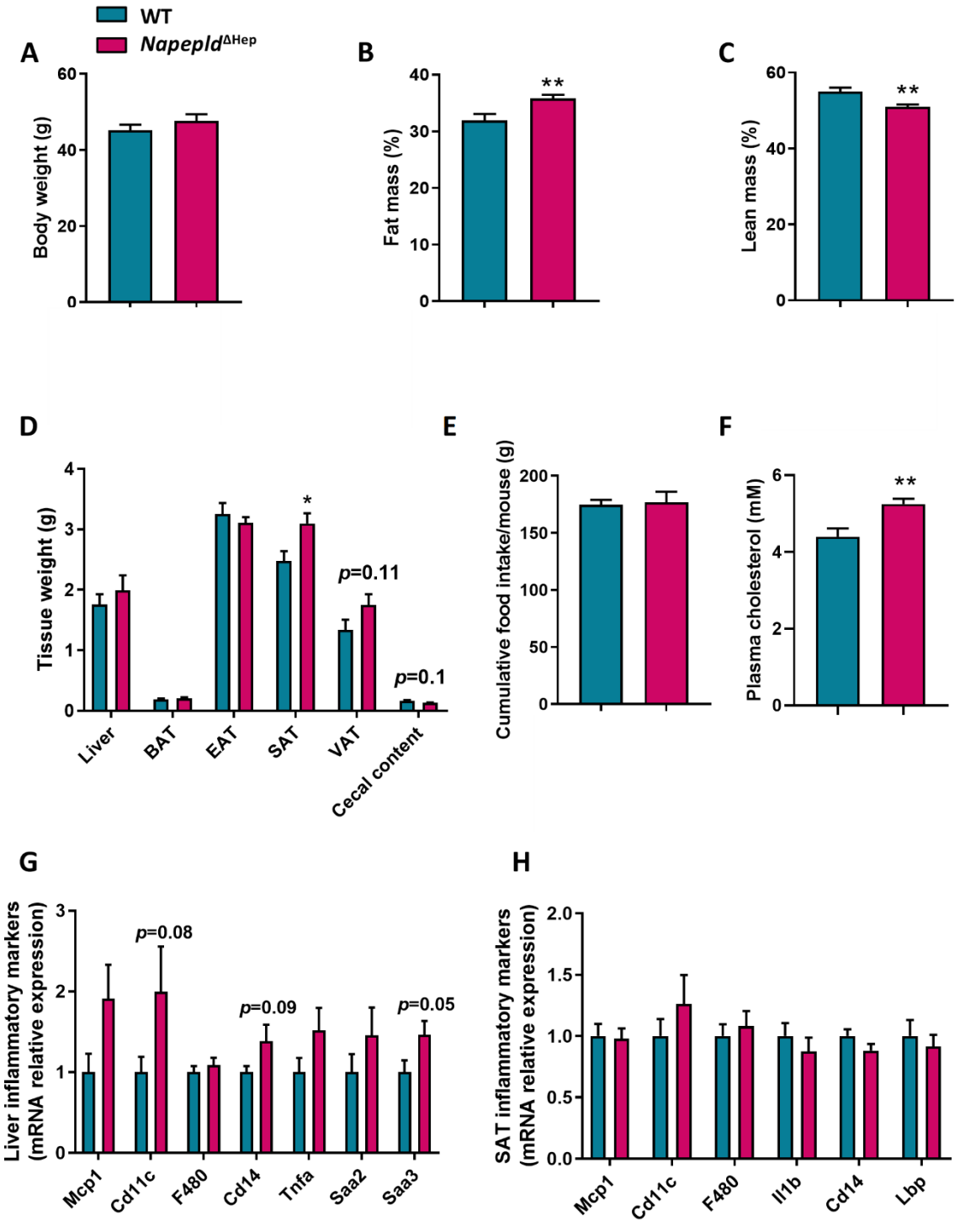

Figure 5: Deletion of *Napepld* partially accentuates the obese phenotype induced by a high-fat diet. (**A**) Body weight (g) after an 8 weeks period. (**B**) Fat mass (%) over an 8 weeks period. (**C**) Lean mass (%) after an 8 weeks period. (**D**) Weight (g) of different tissues: liver, brown adipose tissue (BAT), epididymal adipose tissue (EAT), subcutaneous adipose tissue (SAT), visceral adipose tissue (VAT) and cecal content. (**E**) Cumulative food intake per mouse (g) after an 8 weeks period. (**F**) Plasma cholesterol concentration (mM). (**G**) Liver and (**H**) SAT inflammatory markers measured by real-time qPCR. Dark blue: WT HFD mice. Dark pink: *Napepld*$^{\Delta Hep}$ HFD mice (n = 11). Data are presented as the mean ± s.e.m. * and ** indicate a significant difference versus WT HFD (Respectively $p < 0.05$ and $p < 0.01$) according to the *t*-test (except for (**B**) that is according to a two-way ANOVA followed by a Tukey post hoc test).

Although, *Napepld*$^{\Delta Hep}$ mice exhibited an exacerbated fat mass accumulation, they did not develop a worsened glucose intolerance nor higher plasma insulin level compared to WT during the OGTT suggesting that the potential effect of NAPE-PLD on insulin level might be hidden by the diet itself, which could be the main driver (Figure S4A–E). However, the inflammatory tone in the liver of *Napepld*$^{\Delta Hep}$ mice tended to be higher as reflected by RT-qPCR measurements of inflammatory markers such as cluster of differentiation 11c (*Cd11c; p* = 0.08) that reflects activated macrophages, cluster of differentiation 14 (*Cd14; p* = 0.09) that contributes to endotoxin-induced inflammation or serum amyloid A3 (*Saa3; p* = 0.05) which encodes an acute phase protein that increases upon inflammation (Figure 5G). Of interest, this trend was not observed in adipose tissue suggesting that hepatocyte NAPE-PLD exerts a substantial function locally rather than distally regarding the inflammatory response (Figure 5H).

Collectively, the results show that following a nutritional stress, *Napepld*$^{\Delta Hep}$ mice store a greater amount of fat and seem predisposed to develop high-fat diet-induced inflammation.

***Napepld*$^{\Delta Hep}$ Mice are More Sensitive to Inflammation**

To better evaluate the involvement of hepatocyte *Napepld* in the inflammatory response, we injected WT and *Napepld*$^{\Delta Hep}$ mice with lipopolysaccharides (LPS), a known potent proinflammatory compound. LPS challenge induced an acute inflammation in the liver of both WT and *Napepld*$^{\Delta Hep}$ mice (Figure 6A), but the inflammatory tone was worsened in the liver of *Napepld*$^{\Delta Hep}$ mice as reflected by the increased mRNA expression of inflammatory markers. Even though, proinflammatory cytokines interleukin-1β (*Il1β*) and interleukin-6 (*Il6*) did not reach the significance, tumor necrosis factor alpha (*Tnfα*) was significantly upregulated in *Napepld*$^{\Delta Hep}$ livers. In line with this, gene expression of proteins contributing to the inflammatory response triggered by LPS such as LPS-binding protein (*Lbp*) and *Cd14* were both significantly increased in *Napepld*$^{\Delta Hep}$ mice. Interestingly, the expression of *Cd11c*, a marker of activated macrophages, tended to be more elevated in *Napepld*$^{\Delta Hep}$ mice already in basal conditions (*p* = 0.06) compared to WT mice. This might explain the predisposition of these mice to develop a higher inflammatory tone when challenged by a chronic or acute inflammation.

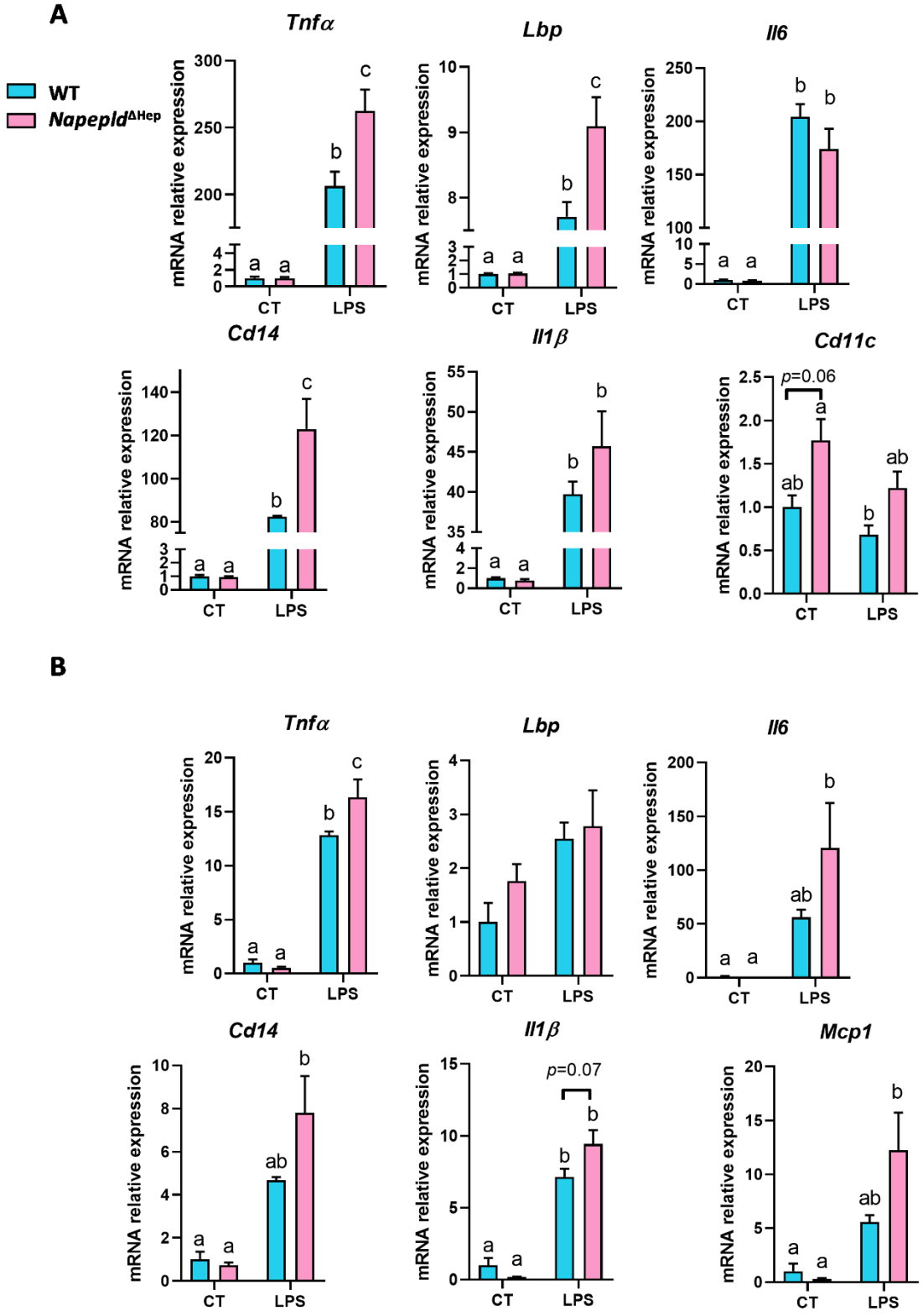

Figure 6: *Napepld*$^{\Delta Hep}$ mice are more sensitive to inflammation. mRNA expression of inflammatory markers measured by real-time qPCR in WT and *Napepld*$^{\Delta Hep}$ mice injected with either saline solution (control (CT)) or LPS (**A**) in the liver and (**B**) in the subcutaneous adipose tissue (SAT). Blue: WT ND mice. Pink: *Napepld*$^{\Delta Hep}$ ND mice. Data are presented as the mean ± s.e.m. (n = 4–6). Data with different superscript letters are significantly different ($p < 0.05$) according to a two-way ANOVA followed by a Tukey post hoc test.

Additionally, we examined the inflammation in the subcutaneous adipose tissue to investigate whether hepatocyte *Napepld* also affects inflammatory response in another peripheral organ involved in obesity. The magnitude of the increase in the LPS-induced inflammation markers was lower in the adipose tissue as compared to the liver. Although only *Tnfα* expression was significantly higher in *Napepld*$^{\Delta Hep}$ mice, a consistent trend was observed for the other inflammatory markers when compared to WT mice (Figure 6B).

These data suggest that the marked reduction in the different bioactive lipids that regulate inflammation, caused by the deletion of *Napepld* in the liver, affects primarily the immune response in the liver itself and to a lesser extent that in the periphery.

2.4 Discussion

The bioactive lipids belonging to the eCBome are involved in numerous metabolic functions, including lipid and glucose metabolism, energy homeostasis and regulation of inflammatory tone [60, 419]. In this study, we discovered that hepatocyte NAPE-PLD plays a major role in most of these physiological processes.

Regarding the direct targets of NAPE-PLD, the NAEs [293, 301, 420], we found a significant decrease in OEA and LEA concentrations in the liver of *Napepld*$^{\Delta Hep}$ mice, whereas AEA and PEA levels remained unchanged. The lack of reduction of PEA and AEA levels could not be explained by a downregulation of the enzyme in charge of their degradation since the expression of both fatty acid amide hydrolase (*Faah)* and *N*-acylethanolamine acid amide hydrolase (*Naaa*) was unaltered in *Napepld*$^{\Delta Hep}$ mice [302, 421]. However, alternative biosynthetic pathways have already been demonstrated for some NAEs and especially for AEA [291, 299-301, 409, 414]. Even tough NAPE-PLD is the main enzyme producing NAEs, we cannot rule out that the serine hydrolase α/β -hydrolase 4 (ABHD4) and the glycerophosphodiesterase 1 (GDE1) may also partially contribute to their synthesis [301]. Finally, among the different roles of PEA, it is well-documented that this NAE displays anti-inflammatory properties and is produced by immune cells [328, 383, 422-425]. As we observed that NPC also expressed *Napepld*, we could not exclude that the absence of a decreased concentration of this mediator, or even AEA, in the tissue was due to compensatory mechanisms from cells unaffected by the deletion construct, possibly immune cells (i.e., Kupffer cells).

More surprisingly, NAPE-PLD deletion led to a robust and consistent reduction of almost all other eCBome mediators investigated here, suggesting that hepatocyte NAPE-PLD controls bioactive liver lipid metabolism that goes beyond NAEs production, which is the only reported function of NAPE-PLD so far [293]. Our data showed that the absence of NAPE-PLD in hepatocytes did not alter the expression of other key enzymes of the eCBome except one, the monoacylglycerol lipase (*Mgll*), which was downregulated. Since this enzyme is an endocannabinoid-glycerol lipase, as well as *Abhd6* that tended to be decreased (p = 0.08), one would have expected an accumulation of monoacylglycerols into *Napepld*$^{\Delta Hep}$ livers. Strikingly, the results indicated the opposite effect. As other endocannabinoid-glycerol lipases have recently been discovered in human leukocytes [426], we cannot rule out that they do not take part into the degradation of monoacylglycerols in the mouse liver. This assumption deserves however further investigations. Interestingly, *Mgll*, aside from degrading monoacylglycerols is also involved in the hydrolysis of triglycerides to fatty acid and glycerol [301, 427]. As *Napepld*$^{\Delta Hep}$ mice did not accumulate monoacylglycerols in the liver, we hypothesized that the

decreased *Mgll* mRNA expression may restrict glycerol availability and contribute to the reduction of the concentrations of glycerol-associated lipids. This was also reflected by the increased levels of arachidonic acid (AA) in *Napepld*$^{\Delta Hep}$ mice whereas its glycerol-conjugated forms, 1/2-AG, were strongly decreased.

The hypothesis that NAPE-PLD acts as a hub controlling, albeit indirectly, the levels of a large range of liver lipids was further confirmed by the lipidomic analysis of two essential liver bioactive lipid families, namely the bile acids and the oxysterols. Strikingly, although most of the bile acids and the oxysterols were strongly reduced in *Napepld*$^{\Delta Hep}$ mice, the level of cholesterol, which is the precursor of these lipids was not affected by the lack of *Napepld* in hepatocytes. Besides, the expression of cholesterol transporters measured in the liver and in the intestine (*Abcg5/8* and *Npc1l1*) was similar between *Napepld*$^{\Delta Hep}$ mice and WT. However, several enzymes involved in bile acids synthesis were significantly, or tended to be, downregulated in *Napepld*$^{\Delta Hep}$ mice. Interestingly, these enzymes (*Cyp27a1* and *Cyp7b1*) are involved in the alternative pathway of bile acids (as opposed to the classic pathway) and produce muricholic acids in rodents [204, 236]. This is in line with the marked reduction in muricholic acids (i.e., α-MCA, β-MCA, ω-MCA and to a lower extent Tα/β-MCA) observed in *Napepld*$^{\Delta Hep}$ mice.

The enterohepatic feedback loop also contributes to the reduction of bile acid synthesis [237, 392]. By investigating this pathway we discovered that the main transporters of bile acids regulating their reabsorption in the ileum (*Osta/b* and *Asbt*) [428] were not altered, whereas the majority of the liver-specific transporters were reduced in *Napepld*$^{\Delta Hep}$ mice (*Oatp1b2*, *Bsep* and *Ostb*). This negative feedback loop also involves a bile acid–FXR–FGF15 axis, in which specific bile acids bind to FXR in the intestine to induce the secretion of FGF15 into the portal circulation. FGF15 then binds to the heterodimeric FGFR4/βKlotho receptor and inhibits CYP7A1 and CYP8B1 expression in hepatocytes thereby limiting de novo synthesis of bile acids [244, 245, 429]. In *Napepld*$^{\Delta Hep}$ mice, *Fgf15* was strongly expressed in the enterocyte, confirming the absorption of bile acids in the intestine. Yet, we did not see a significant decrease in *Cyp7a1* and *Cyp8b1* mRNA expression in the liver of *Napepld*$^{\Delta Hep}$ mice, possibly due to a downregulation of the intermediate, *Fgfr4*. Of interest, the elevated *Fgf15* expression might be explained by a significant decrease in a well-characterized FXR antagonist, Tα/βMCA [246]. In comparison, FXR agonists such as TCDCA, TCA and TDCA were not significantly reduced. All the aforementioned results suggest that the enterohepatic loop was not altered in the intestine while it was impacted in the liver. Therefore, we may conclude that the reduced production of bile acids was not likely due to FGF15/FGFR4 signaling pathway but rather to an altered regulation in the liver itself. Since cholesterol levels in WT and *Napepld*$^{\Delta Hep}$ mice were similar but the cholesterol-derived

metabolites were deeply modified in *Napepld*$^{\Delta Hep}$ livers, we hypothesized that hepatic NAPE-PLD modulates the cascade participating to cholesterol oxidation and specifically the alternative pathway of bile acid synthesis rather than the classic pathway given that this latter was only slightly affected. This possibility, and the underlying molecular mechanisms, will need to be explored in future studies.

It is also worth mentioning that secondary bile acids (i.e., LCA and DCA) are potential structural cofactors regulating NAPE-PLD activity [314, 318]. Interestingly, in our study, by deleting NAPE-PLD we discovered that *Napepld*$^{\Delta Hep}$ mice were characterized by a specific change in bile acid profile. Hence, given that bile acid metabolism is highly affected in *Napepld*$^{\Delta Hep}$ mice and that different data have linked bile acids with the regulation of NAPE-PLD activity [314, 318], we speculated on the existence of a mutual regulation between bile acids and NAPE-PLD activity. Nonetheless, this assumption deserves further investigations.

One of the remarkable outcomes of this study is that a targeted deletion for *Napepld* in hepatocytes is sufficient to induce a high-fat diet-like phenotype. Indeed, we showed that *Napepld*$^{\Delta Hep}$ mice were more sensitive to accumulate liver lipids as mirrored by the increased liver weight and the larger vacuolar lipid droplets highlighted by oil-red O staining. We indicated that this phenomenon was likely due to a decreased expression of genes involved in the β-oxidation process rather than an increase in circulating fatty acid level. Indeed, since *Napepld*$^{\Delta Hep}$ mice also accumulated fat mass in various adipose tissues, had larger adipocytes and exhibited a higher insulin resistance index compared to WT mice, the lipolysis pathway could have been promoted. Nevertheless, the plasma NEFA level was similar in both genotypes suggesting that adipose tissue was still responsive to insulin action. This obesity-prone phenotype in *Napepld*$^{\Delta Hep}$ mice existed already in basal conditions under a normal chow diet and was partially accentuated upon HFD exposure. These observations corroborate a central role of NAPE-PLD in lipid metabolism as a higher accumulation of fat mass has also been reported in mice lacking *Napepld* in either the adipose tissue or the intestinal epithelial cells [291, 292]. Interestingly, in this present study, we could hypothesize that this higher body fat content might be linked to the decreased levels of monoacylglycerols in *Napepld*$^{\Delta Hep}$ mice since mice globally deleted for *Mgll* accumulate monoacylglycerols and display a leaner phenotype [430]. However, the exact molecular mechanisms behind this connection remain to be elucidated.

Although glucose metabolism is also regulated by the endocannabinoid system [291, 419, 431, 432], the liver glucose metabolism was not affected by the absence of *Napepld* in hepatocytes, neither under basal (i.e., control diet) nor under pathological conditions (i.e., diet-induced obesity). This absence of hyperglycemia in *Napepld*$^{\Delta Hep}$ mice indicated that these mice were not yet strongly resistant

to insulin despite their increased insulin resistance index under control diet. Since the timeline of events regarding hyperinsulinemia and insulin resistance is still under debates, we proposed that the hyperinsulinemia displayed by *Napepld*$^{\Delta Hep}$ mice would be the cause of a future insulin resistance [76]. This suggests that *Napepld*$^{\Delta Hep}$ mice were at the early stage of a diabetic disorder when exposed to a normal diet for seven weeks. Given that glucose metabolism and bile acids are intertwined, we speculated that the alteration of bile acids might be responsible of hyperinsulinemia. For instance, Jiang and colleagues demonstrated an improvement of glucose metabolism and a reduction of plasma insulin level in mice treated with glycine-β-MCA [269]. Interestingly, MCA were strongly reduced in *Napepld*$^{\Delta Hep}$ mice. Nonetheless, the relationship between glucose metabolism and these bioactive lipids are not that clear and further investigations are needed in that field to fully identify the molecular interconnections [433]. Under HFD, *Napepld*$^{\Delta Hep}$ mice and WT exhibited a similar level of insulin. This could be explained by the fact that HFD per se induces hyperinsulinemia and hyperglycemia suggesting that this factor is the major driver contributing to this phenotype and might hide the potential effect caused by *Napepld* deletion. Of note, intestinal *Napepld*-deleted mice do not develop glucose intolerance either unlike mice deleted for *Napepld* in the adipose tissue [291, 292], reinforcing our hypothesis that NAPE-PLD plays an organ-dependent role in regulating lipid and glucose metabolism. These various roles might be explained with the fact that the enzyme controls the concentrations of different lipid mediators in specific cells: different NAEs in hepatocytes, adipocytes and epithelial intestinal cells as well as monoacylglycerols, bile acids and oxysterols in hepatocytes. These bioactive lipids display different or even opposite effects, mediated by different receptors (i.e., CB1, GPR119, GPR55, FXR and LXR), on lipid and glucose metabolism [216, 237, 434].

In addition to excessive fat mass, obesity is also linked to a low-grade inflammation [31]. Interestingly, we reported that when exposed to a nutritional stress such as a high-fat diet, *Napepld*$^{\Delta Hep}$ mice tended to be more sensitive to liver inflammation compared to WT mice. To further explore this phenomenon, we challenged the mice with an acute exposure to LPS. We found that, following this treatment, *Napepld*$^{\Delta Hep}$ mice exhibited a worsened inflammatory response in the liver. One explanation for this predisposition to inflammation may be found in the altered liver lipid profile of the *Napepld*$^{\Delta Hep}$ mice. Indeed, AA, a polyunsaturated fatty acid, accumulated in the liver of *Napepld*$^{\Delta Hep}$ mice. AA may come from the degradation of endocannabinoids such as AEA or 2-AG and is a precursor of prostaglandins, leukotrienes or lipoxins, which are involved in the inflammatory response [40, 435-437]. Besides, eCBome mediators as well as oxysterols and bile acids regulate inflammation [40, 208, 216, 438]. The relationship between immunity, inflammation, oxysterols and bile acids has also been described in our lab since we recently demonstrated that deletion of hepatocyte myeloid differentiation primary response gene 88 (MyD88) led to a profound alteration of

bile acid and oxysterol profiles, which contributed to the increased inflammation sensitivity displayed by the mutant mice [391, 439]. Hence, we may not exclude that the reduced levels of these molecules detected here in *Napepld*$^{\Delta Hep}$ mice also participated to the observed sensitivity. Likewise, the decrease, found in these mice, in the hepatic levels of OEA, previously observed also in obese Zucker rats [440], in view of the PPARα agonist action of this NAE [436], may underlie both the excessive hepatic lipid accumulation and inflammation that are typical of both animal models. However, as both pro- and anti-inflammatory lipids were decreased in *Napepld*$^{\Delta Hep}$ mouse livers, understanding their role in this context, particularly in view of their different relative potencies, would be rather complicated at this stage, thus calling for further research. Finally, it is important to note that the higher inflammatory tone was not observed in the adipose tissue, suggesting that the involvement of hepatocyte NAPE-PLD is restricted to local regulation of inflammation.

In conclusion, by generating a mouse model harboring a liver specific deletion of NAPE-PLD, we discovered that hepatocyte NAPE-PLD orchestrates the synthesis of a large range of bioactive lipids in the liver. We also found that hepatocyte NAPE-PLD acts as a crucial player on energy homeostasis since *Napepld*$^{\Delta Hep}$ mice are prone to develop an obese-like phenotype and are predisposed to inflammation. These findings contribute to the understanding of the physiological and pathological roles of hepatocyte NAPE-PLD, and, when combined with our previous studies, shed light on the broad contribution of this enzyme in the development and the progression of metabolic disorders.

2.5 Supplementary Materials

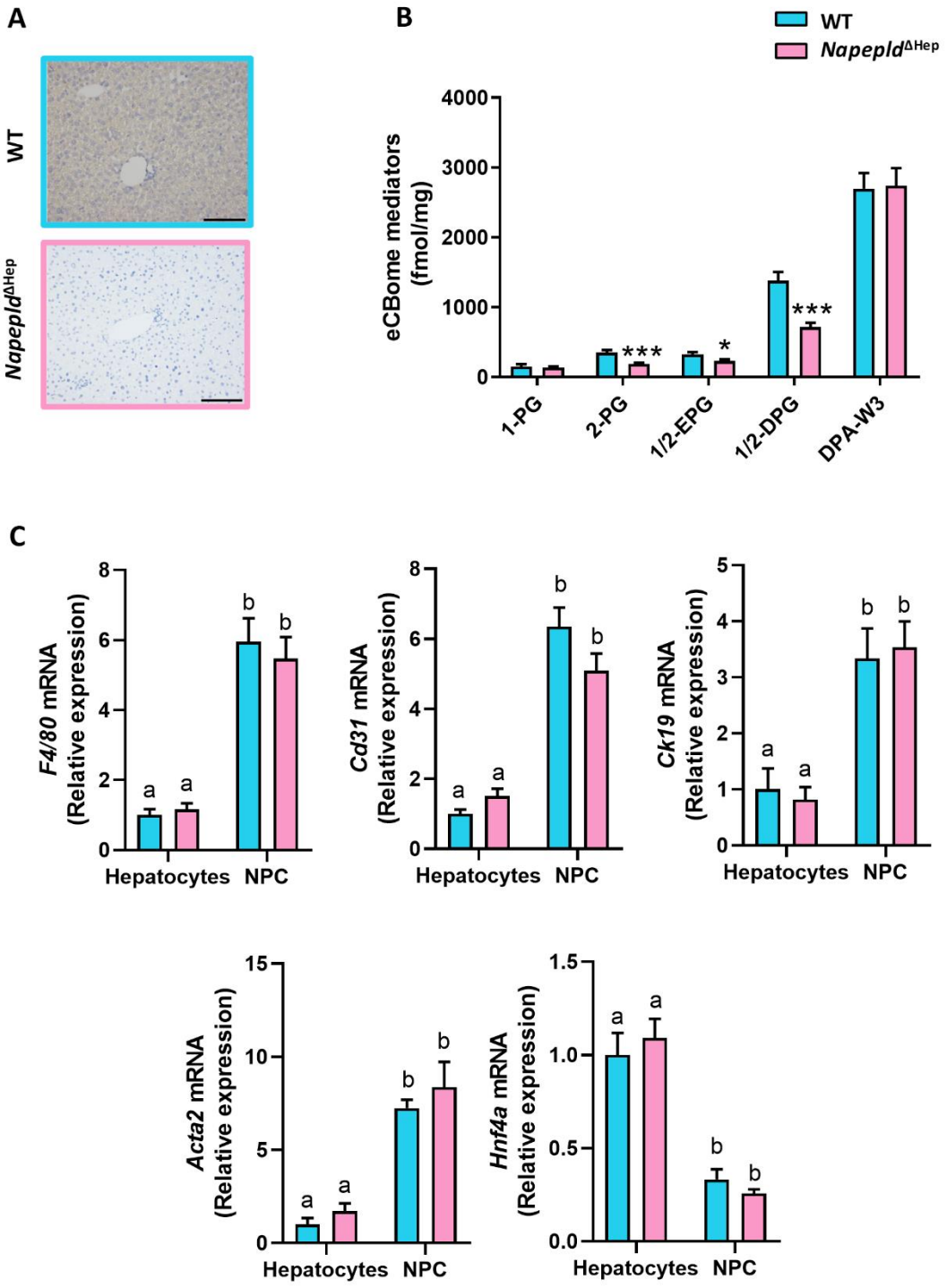

Figure S1: *Napepld* deletion is specific to hepatocytes. (**A**) Localization of *Napepld* mRNA by in situ hybridization in the liver (scale bar: 100 µm; *n* = 4–5). (**B**) eCBome mediator levels in the liver (fmol/mg; *n* = 8–10). (**C**) Specific markers of NPC (*F4/80, Cd31, Ck19* and *Acta2*) and hepatocytes (*Hnf4a*) measured by real-time qPCR (*n* = 4–5). Blue: WT ND mice. Pink: *Napepld*$^{\Delta Hep}$ ND mice. Data are presented as the mean ± s.e.m. * and *** indicate a significant difference versus WT ND (Respectively $p < 0.05$ and $p < 0.001$) according to the *t*-test. Data with different superscript letters are significantly different ($p < 0.05$) according to a two-way ANOVA followed by a Tukey post hoc test. Lipid abbreviations: 1/2-DPG; 1/2-DPA-glycerol; 1/2-EPG, 1/2-EPA-glycerol; 1-PG, 1-palmitoylglycerol; 2-PG, 2-palmitoylglycerol; DPA-ω3, DPA-omega3.

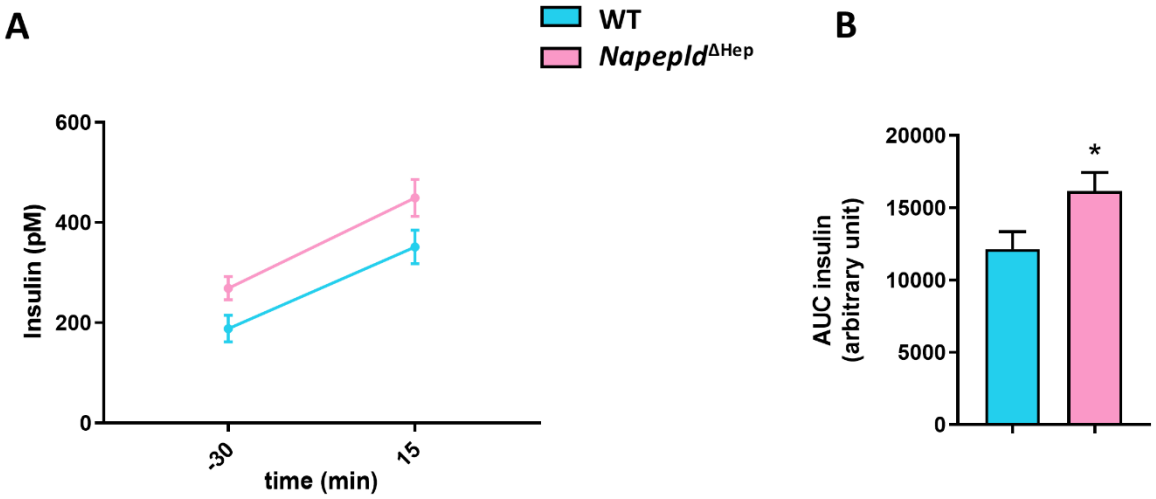

Figure S2: *Napepld*$^{\Delta Hep}$ mice develop a high-fat diet-like phenotype upon normal diet. (**A**) Plasma insulin levels (pM) at 30 min before and 15 min after oral glucose loading. (**B**) Mean area under the curve (AUC) of insulin measured between 30 min before and 15 min after oral glucose loading. Blue: WT ND mice. Pink: *Napepld*$^{\Delta Hep}$ ND mice (n = 8–10). Data are presented as the mean ± s.e.m. * indicate a significant difference versus WT ND (p < 0.05) according to t-test.

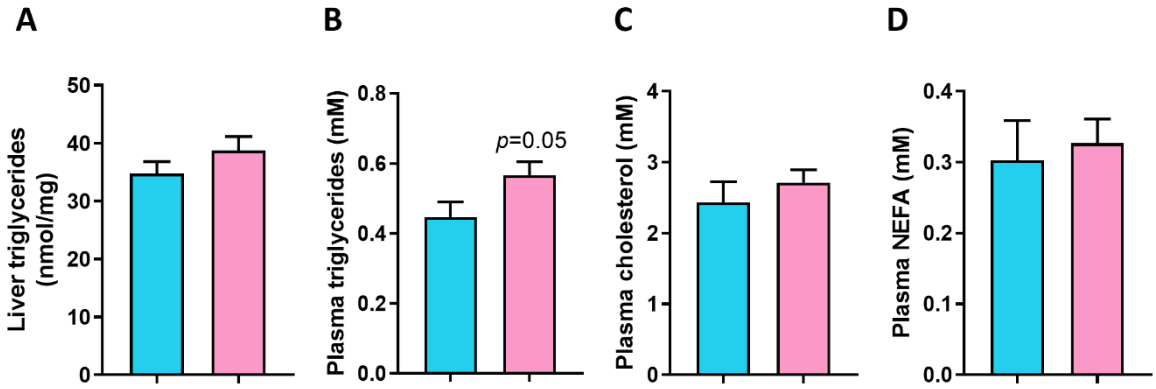

Figure S3: *Napepld*$^{\Delta Hep}$ mice are more sensitive to liver lipid accumulation. (**A**) Liver triglycerides (nmol/mg). (**B**) Plasma triglycerides (mM). (**C**) Plasma cholesterol (mM). (**D**) Plasma NEFA (mM). Blue: WT ND mice. Pink: *Napepld*$^{\Delta Hep}$ ND mice (n = 8–10). Data are presented as the mean ± s.e.m.

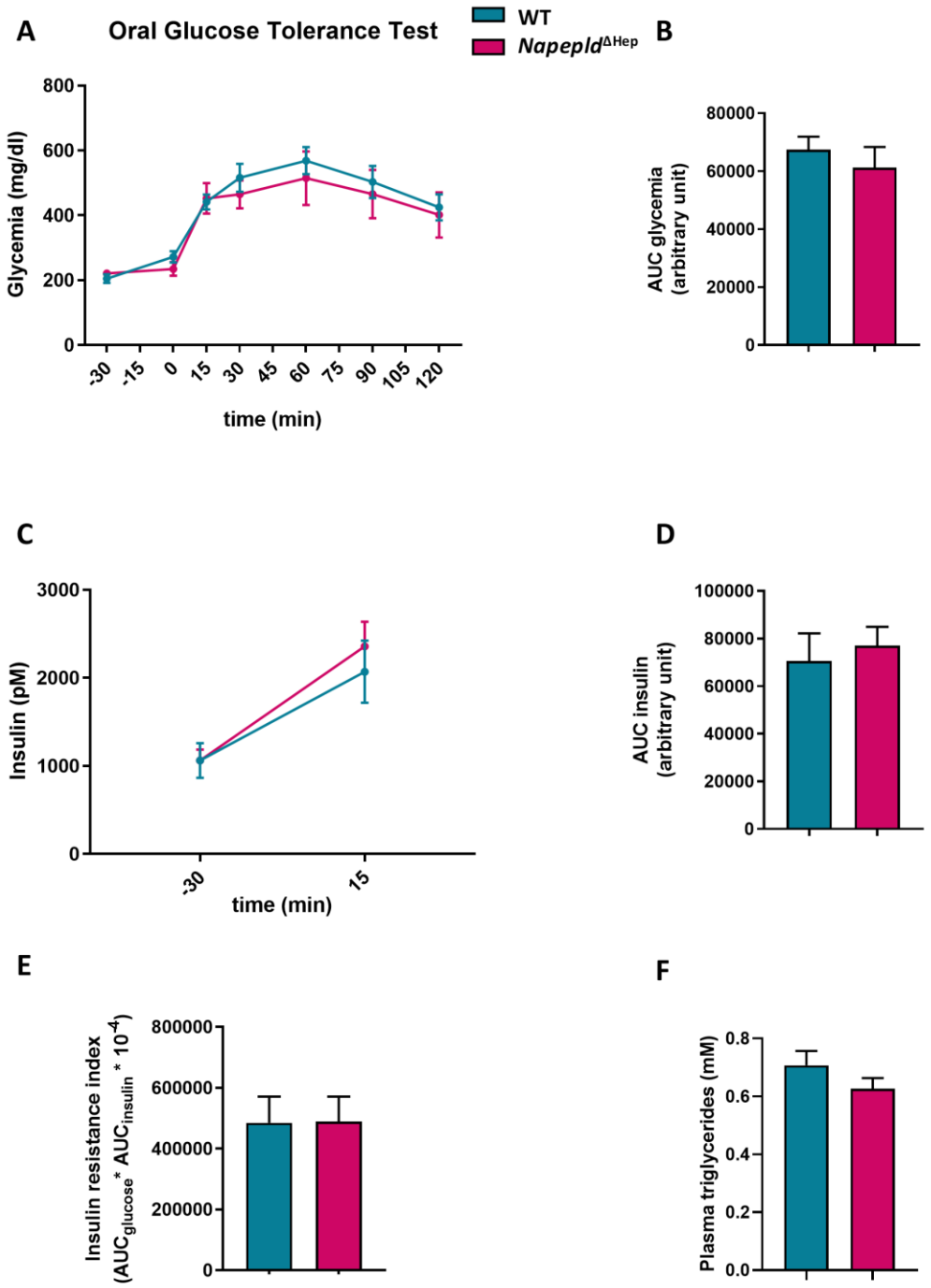

Figure S4: Deletion of *Napepld* partially accentuates the obese phenotype induced by a high-fat diet. (**A**) Plasma glucose profile (mg/dl) measured between 30 min before and 120 min after glucose loading. (**B**) Mean area under the curve of glycemia measured between 30 min before and 120 min after glucose loading. (**C**) Plasma insulin levels (pM) at 30 min before and 15 min after glucose loading. (**D**) Mean area under the curve (AUC) of insulin measured between 30 min before and 15 min after glucose loading. (**E**) Insulin resistance index determined by multiplying the AUC of blood glucose by the AUC of insulin. (**F**) Plasma triglyceride concentration (mM). Dark blue: WT HFD mice. Dark pink: *Napepld*$^{\Delta Hep}$ HFD mice (*n* = 11). Data are presented as the mean ± s.e.m

2.6 Materials and Methods

Mice

All mice were bred in our specific opportunistic and pathogen free (SOPF) animal facility. Animals were housed filter-top cages kept in a controlled environment (room temperature of 22 ± 2 °C, humidity 55% ± 10%, 12 h daylight cycle) in groups of two mice per cage, with free access to irradiated food and autoclaved water. Mice were fed a normal diet (ND; AIN93Mi, Research Diets, New Brunswick, NJ, USA). Body composition (lean and fat mass) was assessed by using 7.5 MHz time domain-nuclear magnetic resonance (TD-NMR; LF50 Minispec, Bruker, Rheinstetten, Germany). This technique allows one to follow in vivo the development of adipose tissue, fat-free mass in non-anesthetized mice throughout the experimental treatment.

Generation of Napepld$^{\Delta Hep}$ Mice

Inducible hepatocyte *Napepld*-deleted C57Bl6/J mice (*Napepld*$^{\Delta Hep}$) were generated by crossing mice harboring a tamoxifen-dependent Cre recombinase expressed under the control of the albumin promoter (Albumin Cre-ERT2 mice were kindly provided by Prof. Pierre Chambon, GIE-CERBM (IGBMC), Illkirch, France) with mice bearing a *loxP*-flanked *Napepld* allele [291, 413]. After verification of the genotype by PCR, littermate mice were randomly assigned to the different experimental groups. The deletion was induced at 8 weeks of age by intra-peritoneal (i.p.) injection of 100 µL tamoxifen (10 mg/mL) for 5 consecutive days. The control mice (wild-type (WT) that is *Napepld*$^{lox/lox}$ × Albumin Cre-ERT2) were injected by an i.p. injection of 100 µL of vehicle (filtered sunflower oil with ethanol) for 5 consecutive days. Tamoxifen was prepared by addition of ethanol to 100 mg of tamoxifen (tamoxifen-free base, MP Biomedicals) to obtain a 100 mg/mL of tamoxifen suspension. A 10 mg/mL tamoxifen solution was prepared by addition of filtered sunflower oil, followed by 30 min sonication. The 10 mg/mL solution of tamoxifen solution was stored at 4 °C for up to 1 week and was sonicated 5 min before use. After the 5 days of injections, mice were allowed to rest for two weeks to recover from any stress or discomfort they may have experienced due to the injections and to allow any residual oil and ethanol to wash out.

Phenotyping in Normal Diet (ND) Condition

A cohort of 11-week-old male *Napepld*$^{\Delta Hep}$ and WT mice were fed a control diet (AIN93Mi, Research Diets) for 7 weeks.

Phenotyping in High-Fat Diet (HFD) Condition

A cohort of 11-week-old male *Napepld*$^{\Delta Hep}$ and WT mice were fed a HFD (60% fat, D12492i, Research Diets) for 8 weeks.

Oral Glucose Tolerance Test

One week before the end of the experiments, mice were fasted for 6 h prior to be given an oral glucose load (2 g glucose per kg body weight). Blood glucose levels were measured 30 min before, just prior to gavage, and 15, 30, 60, 90 and 120 min after oral glucose load using a standard glucose meter (Accu Check, Roche, Basel, Switzerland) on the tip of the tail vein. Plasma samples were collected from the tip of the tail vein in heparinized tubes 30 min before and 15 min after oral glucose load for determination of insulin concentration.

Insulin Resistance Index

Plasma insulin concentration was determined using an ultrasensitive mouse insulin ELISA kit (Mercodia, Uppsala, Sweden) according to the manufacturer's instructions. Insulin resistance index was determined by multiplying the area under the curve of both blood glucose (−30 and 15 min) and plasma insulin (−30 and 15 min) obtained following the oral glucose tolerance test.

LPS Injection Experiment

A cohort of 14-week-old ND-fed male *Napepld*$^{\Delta Hep}$ and WT mice were injected, as previously described [439], intraperitoneally with either 300 µg/kg LPS solution (LPS from *Escherichia coli* O55:B5; Sigma L2880) or saline solution (CT). Mice were killed 4 h after the injection.

Tissue Sampling

At the end of the experiment, mice were anesthetized with isoflurane (Forene, Abbott, Queenborough, Kent, England) after a fasting period of 6 h. Blood was sampled from the portal and cava veins. After exsanguination, mice were killed by cervical dislocation. Tissues were precisely dissected, weighed and immediately immersed in liquid nitrogen followed by storage at −80 °C for further analysis.

Hepatocyte Isolation

A cohort of 11-week-old ND-fed male *Napepld*$^{\Delta Hep}$ and WT mice were anesthetized with Ketamine-Xylazine (Nimatek, Eurovet Animal Health BV, Bladel, Netherlands-Rompun, Bayer Healthcare, Loos, France) solution. The mice were surgically opened and the liver was infused with a PBS solution containing EGTA and HEPES buffer injected in the portal vein via a 26 g needle at a rate of 9 mL/min

for 10 min. Warm (37 °C) digestion medium including DMEM/F12, no glutamine (Thermo Fisher, Waltham, MA, USA), Penicillin-Streptomycin, HEPES buffer, thermolysin (Promega, Madison, WI, USA), collagenase G (Abiel, Palermo, Italy) and collagenase H (Abiel, Palermo, Italy) was then added for 7 min. The liver was then removed and incubated with the medium at 37 °C for 15 min for further digestion. The obtained solution was then filtered (70 µm) and centrifuged twice (4 °C, 50 g, 2 min) to allow the separation between hepatocytes and non-parenchymal cells (NPC). The resulting pellet contained the hepatocytes whereas NPC were enriched in the supernatant. After isolating the two fractions in different tubes, they were centrifuged (4 °C, 10,000× *g*, 10 min) and pellets were stored in −80 °C prior TriPure RNA extraction.

RNA Preparation and Real-Time qPCR Analysis

Total RNA was prepared from tissues using TriPure reagent (Roche Diagnostics, Penzberg, Germany). Quantification and integrity analysis of total RNA were performed by analyzing 1 µL of each sample in an Agilent 2100 Bioanalyzer (Agilent RNA 6000 Nano Kit, Agilent). cDNA was prepared by reverse transcription of 1 µg total RNA using the GoScript Reverse Transcriptase kit (Promega, Madison, WI, USA). Real-time PCR was performed with the QuantStudio 3 real-time PCR system (Thermo Fisher, Waltham, MA, USA). *Rpl19* RNA was chosen as the housekeeping gene. All samples were performed in duplicate, and data were analyzed according to the $2^{-\Delta\Delta CT}$ method. The identity and purity of the amplified product were assessed by melting curve analysis at the end of amplification. The primer sequences for the targeted mouse genes are presented in Table 1.

Adipocyte Histological Analysis

SAT tissues were fixed in 4% formaldehyde. Hematoxylin and eosin staining was performed using standard protocols on 5-µm adipose tissue sections. Adipocyte size was determined using ImageJ software (version 1.50a, National Institutes of Health, Bethesda, MD, USA).

Hepatic Lipid Content Analysis by Oil Red O Staining

Liver tissue was embedded in Tissue-Tek Optimal Cutting Temperature compound (Sakura Europe, Leiden, Netherlands) and flash-frozen in cold isopentane. Five µm-tick tissue sections were stained with oil red O staining for lipid content analysis. Quantification of the mean droplet size was performed using ImageJ software (version 1.50a, National Institutes of Health, Bethesda, MD, USA).

Table 1: Primers used for real-time qPCR

Gene	Protein	Forward Primer Sequence (5′-3′)	Reverse Primer Sequence (5′-3′)
Abcb11	BSEP	AGATACAACCGAAGGGGACA	TCAACTTCTTCCACAAGCACA
Abcb4	MDR2	GAGCCCGTGCTGTTCTCTAC	TCTGTTTCTGTCCCCCACTC
Abcg5	ABCG5	ACCTTACCCACGGTTCCTTT	ACGCATAATCACTGCCTGCT
Abcg8	ABCG8	CCGTCGTCAGATTTCCAATGA	GGCTTCCGACCCATGAATG
Abhd6	ABHD6	CTGTCCATAGTGGGGCAAGT	TCAGATGGGTAGTAAGCGGC
Acox1	ACOX1	CTATGGGATCAGCCAGAAAGG	AGTCAAAGGCATCCACCAAAG
Acta2	αSMA	GGCTGGAGAATTGGATCT	CCAGCAAAGGTCAGAGAAGG
Adgre1	F4/80	TGACAACCAGACGGCTTGTG	GCAGGCGAGGAAAAGATAGTGT
Baat	BAT	GCACAGGCTCATCAACAAGA	TAGAGCACACCACGTTCCTG
Ccl2	MCP1	GCAGTTAACGCCCCACTCA	TCCAGCCTACTCATTGGGATCA
Cd14	CD14	CCTGCCCTCTCCACCTTAGAC	TCAGTCCTCTCTCGCCCAAT
Cpt1a	CPT1α	AGACCGTGAGGAACTCAAACCTAT	TGAAGAGTCGCTCCCACT
Cyp27a1	CYP27A1	TCTGGCTACCTGCACTTCCT	GTGTGTTGGATGTCGTGTCC
Cyp7a1	CYP7A1	GGGATTGCTGTGGTAGTGAGC	GGTATGGAATCAACCCGTTGTC
Cyp7b1	CYP7B1	TAGGCATGACGATCCTGAAA	TCTCTGGTGAAGTGGACTGAAA
Cyp8b1	CYP8B1	GATCCGTCGCGGAGATAAGG	CGGGTTGAGGAACCGATCAT
Daglb	DAGLβ	CTCCACCAGCAACAAGACAA	GCAGTTCTCCACTTCTGCATC
Faah	FAAH	GTGAGGATTTGTTCCGCTTG	GGAGTGGGCATGGTGTAGTT
Fabp6	IBABP	CAAGGCTACCGTGAAGATGGA	CCCACGACCTCCGAAGTCT
Fgf15	FGF15	GAGGACCAAAACGAACGAAATT	ACGTCCTTGATGGCAATCG
Fgfr4	FGFR4	CTCGATCCGCTTTGGGAATTC	CAGGTCTGCCAAATCCTTGTC
Hmgcr	HMGCR	TGGTGGGACCAACCTTCTAC	GCCATCACAGTGCCACATAC
Hnf4a	HNF4α	AAGAGGTCCATGGTGTTTAAGG	ATCGAGGATGCGGATGGA
Il1b	IL1β	TCGCTCAGGGTCACAAGAAA	CATCAGAGGCAAGGAGGAAAAC
Il6	IL6	ACAAGTCGGAGGCTTAATTACACAT	TTGCCATTGCACAACTCTTTTC
Itgax	CD11c	ACGTCAGTACAAGGAGATGTTGGA	ATCCTATTGCAGAATGCTTCTTTACC
Krt19	CK19	AGCGTGATCAGCGGTTTTG	CCTGGTTCTGGCGCTCTATG
Lbp	LBP	GTCCTGGGAATCTGTCCTTG	CCGGTAACCTTGCTGTTGTT
Mgll	MGL	ATGGTCCTGATTTCACCTCTGGT	TCAACCTCCGACTTGTTCCGAGACA
Naaa	NAAA	ATTATGACCATTGGAAGCCTGCA	CGCTCATCACTGTAGTATAAATTGTGTAG
Napepld	NAPE-PLD	CTCCATCCCGAATGTGCT	AAGCCAGCCTCTCTCACTCC
Npc1l1	NPC1L1	GGCTCCATCTGGAGTAGCTG	ATCGCACTACCATCCAGGAC
Oatp1b2	OATP1B2	ATCCCGTGACTAATCCAACA	ACCAAACTGCTGCTCTATAAACT
Pecam1	CD31	GGAACGAGAGCCACAGAGAC	TGCACTGCCTTGACTGTCTT
Ppara	PPARα	CAACGGCGTCGAAGACAAA	TGACGGTCTCCACGGACAT
Rpl19	RPL19	GAAGGTCAAAGGGAATGTGTTCA	CCTTGTCTGCCTTCAGCTTGT
Saa2	SAA2	GGGGTCTGGGCTTCCTATCT	CCATTCTGAAACCCTTGTGG
Saa3	SAA3	CGCAGCACGAGCAGGAT	CCAGGATCAAGATGCAAAGAATG
Slc10a1	NTCP	GGACAAGGTGCCCTACAAAG	ACAGCCACAGAGAGGGAGAA
Slc10a2	ASBT	TGGGTTTCTTCCTGGCTAGACT	TGTTCTGCATTCCAGTTTCCAA
Slc27a5	BAL	TGTGTGTGAAGGAACCTGGA	ACCCGGACAACTTTGTGAAG
Slc51a	OSTα	TACAAGAACACCCTTTGCCC	CGAGGAATCCAGAGACCAAA
Slc51b	OSTβ	GTATTTTCGTGCAGAAGATGCG	TTTCTGTTTGCCAGGATGCTC
Tnf	TNFα	TCGAGTGACAAGCCTGTAGCC	TTGAGATCCATGCCGTTGG

Extraction of Liver Lipids

Total lipids were measured in the liver tissue after extraction in $CHCl_3$:MeOH according to the Folch method [403] and adapted as follows: briefly, 100 mg of liver tissue was homogenized in 2 mL of $CHCl_3$:MeOH (2:1) using a tissue lyser followed by an ultrasonic homogenizer. Four hundred microliter of 0.9% NaCl solution was added and lipids were then extracted by vigorous shaking. After centrifugation, the chloroform phase was recovered in glass tubes and dried under a stream of N2. Glass tubes were weighed before and after lipid extraction to quantify total lipid content. The dried residue was solubilized in 1.5 mL isopropanol.

Biochemical Analyses

Plasma non-esterified fatty acids (NEFA) and liver and plasma cholesterol and triglyceride concentrations were measured using kits coupling an enzymatic reaction with spectrophotometric detection of the reaction endproducts (Diasys Diagnostic and Systems, Holzheim, Germany) according to the manufacturer's instructions.

Lipidomic Analysis

All lipids measured are presented in Table 2.

Table 2: Lipids abbreviations.

NAEs and ECB-Related Molecules		Bile Acids	
1-AG	1-arachidonoylglycerol	CA	Cholic acid
2-AG	2-arachidonoylglycerol	CDCA	Chenodeoxycholic acid
1-LG	1-linoleoylglycerol	DCA	Deoxycholic acid
2-LG	2-linoleoylglycerol	(α, β or ω) MCA	(α, β or ω) Muricholic acid
2-OG	2-oleoylglycerol		
1-PG	1-palmitoylglycerol		
2-PG	2-palmitoylglycerol		
AA	Arachidonic acid		
AEA	*N*-arachidonoylethanolamine	**Oxysterols**	
DHA	Docosahexaenoic acid	24(*S*)-OHC	24(*S*)-hydroxycholesterol
DHA-1-G	DHA-1-glycerol	25-OHC	25-hydroxycholesterol
DHA-2-G	DHA-2-glycerol	27-OHC	27-hydroxycholesterol
DHEA	*N*-docosahexaenoylethanolamine	4β-OHC	4β-hydroxycholesterol
DPA-1-G	DPA-1-glycerol	5α6α-EC	5α,6α-epoxycholesterol
DPA-2-G	DPA-2-glycerol	5α6β-diOHC	5α,6β-dihydroxycholesterol
DPA-ω3	DPA-omega3	5β6β-EC	5β,6β-epoxycholesterol
EPA	Eicosapentaenoic acid	7α-OHCone	7α-hydroxycholestenone
EPA-1-G	EPA-1-glycerol	7-KC	7-ketocholesterol
EPA-2-G	EPA-2-glycerol	7-OHC	7-hydroxycholesterol
EPEA	*N*-eicosapentaenoylethanolamine		
LEA	*N*-linoleylethanolamine		
OEA	*N*-oleoylethanolamine		
PEA	*N*-palmitoylethanolamine		

eCBome mediators. NAEs and other eCBome mediators were quantified by LC–MS/MS as described in Everard, Plovier and Rastelli et al. [292]. Briefly, liver lipids were injected in the HPLC system interfaced with the electrospray source of a Shimadzu 8050 triple quadrupole mass spectrometer and mass spectrometric analysis was done in the positive ion mode using multiple reaction monitoring using the specific mass transitions [441].

Oxysterols. Oxysterols were analyzed by LC-MS as previously reported [231]. Briefly, lipids were extracted, in the presence of internal standards, through liquid–liquid extraction, and then samples were prepurified by solid phase extraction. The eluate was recovered and injected in the LC–MS system consisting in an Accela HPLC system (Thermo Fisher Scientific) coupled to an LTQ-Orbitrap XL mass

spectrometer (Thermo Fisher Scientific) equipped with an APCI probe used in positive mode. Lipids were quantified using calibration curves obtained using the same procedure.

Bile acids. Bile acids were quantified using a LC-MS method adapted from Guillemot-Legris et al. [230]. Liver samples were homogenized in ice-cold bi-distilled water. Proteins were then precipitated overnight at −20 °C using acetone containing deuterated internal standards. Supernatant was recovered and evaporated to dryness. The organic residue was resuspended in methanol and injected in the LC–MS system, equipped with an electrospray probe used in negative mode. Lipids were quantified using calibration curves obtained using the same procedure.

Ethics Statement

All mouse experiments were reviewed and approved by and performed in accordance with the guidelines of the local ethics committee for animal care of the Health Sector of the Université catholique de Louvain under the specific agreement numbers 2014/UCL/MD/022 and 2017/UCL/MD/005. Housing conditions were as specified by the Belgian Law of 29 May 2013 regarding the protection of laboratory animals (agreement number LA1230314). Every effort was made to minimize animal pain, suffering, and distress.

Statistical Analysis

Data were presented as the mean ± s.e.m. The difference between two groups was evaluated by a *t*-test. Differences between more than two groups were assessed by two-way ANOVA, followed by the Tukey post hoc test. Data were analyzed with GraphPad Prism (GraphPad Software).

2.7 Acknowledgments

We thank A. Barrois, H. Danthinne and A. Puel for excellent technical assistance. We thank P. Chambon for the kind gift of the Albumin Cre-ERT2 mice. P.D. Cani is a senior research associate at FRS-FNRS (Fonds de la Recherche Scientifique), Belgium. V.D. is the holder of a Canada Excellence Research Chair at Université Laval. The authors wish to thank M. Cyril Martin for his valuable technical assistance with the LC/MS-MS analyses.

2.8 Funding

This work was supported by the Fonds de la Recherche Scientifique (FNRS FRFS-WELBIO) under the grants WELBIO-CR-2017C-02 and WELBIO-CR-2019C-02R, the Funds Baillet-Latour under the grant “Grant For Medical Research 2015”. C.S. and N.F. are associated to the Canada Excellence Research

Chair on the microbiome-endocannabinoidome axis in metabolic health, held by VD and funded by the Canadian Federal Tri-Agency.

2.9 Conflicts of Interest

The authors have not conflict of interest to declare with the present study.

2.10 Author Contributions

Conceptualization: C.L. and P.D.C. Supervision: P.D.C. Methodology: C.L., P.D.C., S.L. Funding acquisition: P.D.C., G.G.M., V.D.M., C.S., N.F. Investigation: C.L., M.V.H., Martin Roumain, R.M., I.L., G.G.M., Marialetizia Rastelli, N.F., Resources: P.D.C., N.M.D., S.L., G.G.M., C.S., N.F., V.D.M., I.L. Writing - Original Draft: P.D.C. and C.L. Writing - Review & Editing: all the authors. All authors have read and agreed to the published version of the manuscript.

GENERAL DISCUSSION & PERSPECTIVES

Despite huge efforts to manage obesity and ensuing disturbances, the current available treatments remain poorly effective. Given that these metabolic disorders are rising and becoming epidemic, it is urgent to identify novel mediators in order to develop new strategies to cure these conditions. Accordingly, this thesis aimed to gain insights into two systems closely related to obesity, the innate immune system and the endocannabinoid system, in order to find new potential therapeutic targets in the context of obesity and associated comorbidities. This thesis was focused on the liver, which is an organ of the utmost metabolic relevance given its central role in multiple and crucial signaling pathways regulating energy homeostasis. In line with this, it is also a major tissue producing bioactive lipids that are involved in host metabolism regulation. Thereby, unravelling some of their actions might potentially open the avenue to new treatments.

1 Hepatocyte MyD88 is a main driver of lipid metabolism and bioactive lipid production

As low-grade inflammation is a key hallmark of obesity, a first approach was to deepen our knowledge on the role of a central adaptor of the innate immunity regulating inflammation, namely MyD88. Interestingly, this protein, in addition to mediate the inflammatory response, has also been recently reported to be involved in metabolic disturbances such as obesity and diabetes. For example, mice deleted for *MyD88* in intestinal epithelial cells, the central nervous system or more specifically astrocytes are protected against diet-induced obesity and glucose intolerance [37, 442, 443]. Conversely, other studies revealed controversial data on the impact of the deletion of whole-body *MyD88* in the context of diabetes and steatosis development [387, 444, 445]. Taken together, these findings suggest that MyD88 is a key factor involved in metabolic disorders and its metabolic action is probably organ-dependent and deserves to be further investigated.

To evaluate the impact of MyD88 in the liver, our group generated a mouse model harboring a constitutive and specific deletion of *MyD88* in hepatocytes (i.e. *MyD88*$^{\Delta Hep}$ mice). Surprisingly, these transgenic mice were predisposed to liver inflammation and exhibited a compromised energy homeostasis [391]. More precisely, *MyD88*$^{\Delta Hep}$ mice were prone to develop glucose intolerance and insulin resistance independently of body weight. Moreover, their lipid metabolism was highly affected by this deletion as reflected by their altered bile acid profile and their predisposition to accumulate lipids in the liver. Altogether, this work strongly suggested that MyD88 had a greater role than controlling host inflammation and could be an important target mediating liver metabolism. However, the molecular events behind this striking phenotype was not further explored in this study. Hence, the first part of this thesis was dedicated to the deeper examination of the underlying mechanisms

regarding the alteration of liver lipid metabolism and inflammation in these mice. To that end, two different strategies were carried out in order to challenge both lipid metabolism and immunity. The first one consisted in a short exposure to HFD (i.e. 3 days) whereas the second one included an acute LPS injection. In agreement with the first study published by Duparc and coworkers, we discovered that bile acid metabolism was deeply affected in *MyD88*$^{\Delta Hep}$ mice [391]. We hypothesized that the alteration of cholesterol-derived bioactive lipids observed in *MyD88*$^{\Delta Hep}$ mice would be due to an improper regulation of the enterohepatic loop repressing bile acid synthesis and that the accumulation of 25-OHC, an oxysterol which has been associated with metabolic disorders and inflammation, might be responsible for their predisposition to an elevated inflammatory response. Finally, we also found that *MyD88*$^{\Delta Hep}$ mice challenged with 3 days of HFD exhibited an elevated hepatic lipid accumulation compared to WT mice. Thereby, this study showed that liver innate immunity and more precisely hepatocyte MyD88 strongly contributed to lipid metabolism regulation.

To deepen our knowledge on the increased hepatic lipid accumulation observed in *MyD88*$^{\Delta Hep}$ mice challenged by 3 days of HFD compared to WT, we further explored liver lipid metabolism by performing RT-qPCR on key markers of lipogenesis (e.g. *Acaca*, *Fasn* and *Scd1*). These analyses showed that *MyD88*$^{\Delta Hep}$ mice exhibited a significant increase in three main markers of lipogenesis, already under basal conditions (i.e. normal diet). However, these markers were similarly blunted by the exposure to HFD (Figure 1).

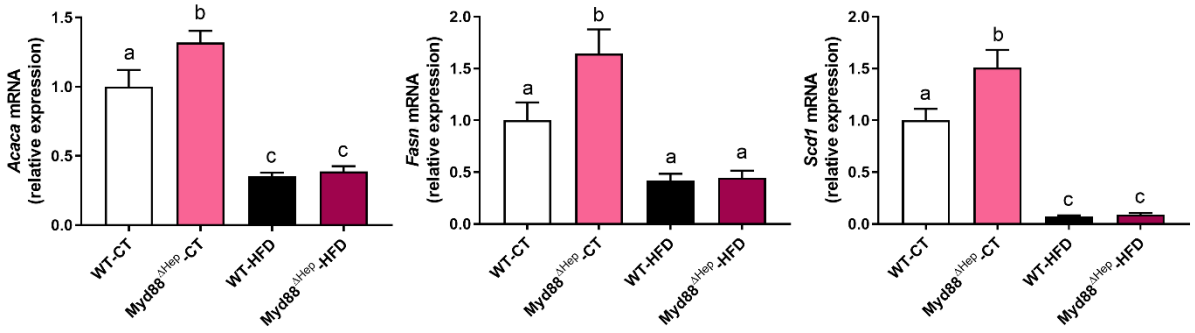

Figure 1: *MyD88*$^{\Delta Hep}$ mice exhibit an increased liver lipogenesis under basal conditions. Liver mRNA expression of lipogenic markers (i.e. *Acaca*, *Fasn* and *Scd1*) measured by real-time qPCR. Data are presented as the mean ± s.e.m. (n=6-9). Data with different superscript letters are significantly different ($p < 0.05$) according to two-way ANOVA followed by a Tukey post hoc test.

Besides the lipogenic markers, we could also have investigated lipid catabolic pathways by quantifying β-oxidation markers (e.g. *Acox1*, *Cpt1a* and *Ppara*) in the liver of both groups as well as the lipolysis process by measuring mRNA expression of *Atgl*, *Hsl* and *Mgl* in the adipose tissue and the circulating level of FFA in *MyD88*$^{\Delta Hep}$ mice and WT. Indeed, an excess of lipolysis contributes to the liver lipid

accumulation by increasing the flux of circulating FFA coming from the adipose tissue, which in turn are taken up by the liver. Finally, examining the hepatic expression of the receptor *Cd36*, which is involved in FFA uptake, from the blood to the liver would have been interesting as well.

As a reminder, we found specific differences in the level of bile acids in both the cecum and in the portal vein in the first experiment (i.e. 3 days of HFD), as well as significant changes of oxysterol levels in the liver of *MyD88*$^{\Delta Hep}$ mice compared to WT in the second experiment (i.e. LPS exposure). In the view of these results, it would have been of particular interest to fully characterize bile acid and oxysterol profiles, in both experiments, in different relevant compartments such as the liver, different intestinal segments and the blood (i.e. portal and cava veins). Such additional experiments would have allowed us to uncover the global circulation of these bioactive lipids by taking into account their absorption, synthesis and excretion. Furthermore, this would also have led to a better understanding of their local impact on metabolism. Additionally, integrating the composition of the gut microbiota to the equation would also have been relevant since there is a mutual relationship between bacteria and bile acids. Indeed, the gut microbiota is implicated in the synthesis of secondary bile acids whereas bile acids can modulate gut microbiota proliferation, composition and maturation [206, 446]. Of note, we have previously shown that *MyD88*$^{\Delta Hep}$ exhibited a specific change in the gut microbiota composition [391]. Along the same line, recent studies shed light on the fact that some of these microorganisms also participate to the metabolization of cholesterol, which is the precursor of bile acids, through specific enzymes [447, 448]. Indeed, Kenny and colleagues identified a group of bacterial cholesterol dehydrogenases encoded by *ismA* genes that convert cholesterol to coprostanol, the latter being mostly excreted in feces [448]. All of this deeply demonstrates the existence of an interconnection between cholesterol metabolism and the gut microbiota and the importance of considering both systems when working in the field of metabolism and nutrition.

Importantly, in this study, we also discovered that *MyD88*$^{\Delta Hep}$ mice were predisposed to develop liver inflammation since they displayed an increased expression of liver proinflammatory cytokines (i.e. *Tnfα*, *Il6* and *Il1β*) after LPS exposure. As 25-OHC level was more than double in the liver of *MyD88*$^{\Delta Hep}$ mice exposed to LPS compared to WT and that oxysterol was known to modulate inflammation, we hypothesized that 25-OHC might be responsible for the elevated inflammatory response seen in *MyD88*$^{\Delta Hep}$ mice challenged by LPS. However, one weakness of our study resides in the lack of demonstration that liver 25-OHC is the molecule that contributes to the increased inflammatory response in *MyD88*$^{\Delta Hep}$ mice compared to WT. Since the role of this oxysterol in mediating inflammation is still under debate and seems to depend on its concentration and localization, it is complicated to design a proper experiment which can provide evidence in favor of our assumption

[228]. Although we could imagine to administer 25-OHC at various concentrations to WT mice challenged or not with LPS and analyze the inflammatory response of the liver, we cannot exclude that circulating 25-OHC might exert other effects in other organs. In line with this, using *Cyp7b1* knockout mice or CYP7B1 inhibitors in order to increase 25-OHC level would not be a good strategy either given that CYP7B1 is also expressed in other organs than the liver, such as the brain, and does not only metabolize 25-OHC but also other steroids such as 27-OHC or dehydroepiandrosterone (DHEA) which have their own metabolic actions [230, 449-452]. It is also worth noting that blocking the synthesis of 25-OHC is rather difficult since this lipid is generated through enzymatic and non-enzymatic reactions (i.e. cholesterol 25-hydroxylase, CYP3A5 and ROS) [216]. Finally, blocking its receptor would not be relevant either because 25-OHC has different targets and shares its targeted receptors with other molecules [216]. To sum up, although of great interest, designing a clear and straightforward experiment aimed to fully delineate the impact of 25-OHC in *MyD88*$^{\Delta Hep}$ mice appears currently compromised with the available technologies and their limitations.

Then, our results suggested that the altered bile acid profile in *MyD88*$^{\Delta Hep}$ mice might be due to a defect in the enterohepatic feedback loop. Although the direct link between MyD88 and the alteration has not been fully elucidated in our study, we came to this potential explanation by measuring p-JNK and p-ERK. Indeed, under normal conditions, in response to the feedback response from the gut, FGF15 is produced in enterocytes and travels to the liver via the bloodstream to activate FGFR4. In turn, FGFR4 stimulation induces the phosphorylation of both JNK and ERK which inhibit bile acid synthesis. In our study, we found that p-ERK and p-JNK were lower in *MyD88*$^{\Delta Hep}$ fed a HFD versus WT mice. This lower activation may somehow impact the regulation of bile acid synthesis. However, the molecular connection between MyD88 and ERK remains to be deciphered.

It is worth mentioning that as compared to the second and main chapter of this thesis concerning hepatocyte NAPE-PLD, no further experiment were carried out on *MyD88*$^{\Delta Hep}$ mice. Nevertheless, we believe that a strong connection exists between the two chapters. Indeed, since bile acid composition was deeply altered in mice deleted for *MyD88* in hepatocytes and that bile acids regulate NAPE-PLD, we wondered whether its expression would have been altered in the liver of these mutant mice. To address this question, we quantified the liver mRNA expression of *Napepld* and found that *Napepld* was upregulated (about 50%) in the liver of *MyD88*$^{\Delta Hep}$ mice in basal condition suggesting that the modified bile acid profile might have influenced NAPE-PLD activity (Figure 2). However, additional experiments would have been required to explore this possibility such as measuring bile acids in the liver to highlight putative changes regarding bile acids acting as NAPE-PLD mediators. Indeed, several studies have demonstrated that bile acids were key molecules regulating NAPE-PLD. For instance, it

has been shown that DCA and CDCA enhanced NAPE-PLD activity whereas LCA, TUDCA, THDCA and α/β-MCA would likely act as NAPE-PLD inhibitors [314, 318, 322]. Moreover, quantifying bioactive lipids synthesized by NAPE-PLD, the NAEs, would also have been a good indication of the enzyme activity even though investigating the enzymes responsible for their degradation would also have been mandatory. In line with this, analyzing the NAE composition of the liver may have helped to understand better the phenotype given that NAEs are bioactive lipids involved in the regulation of inflammation and host homeostasis.

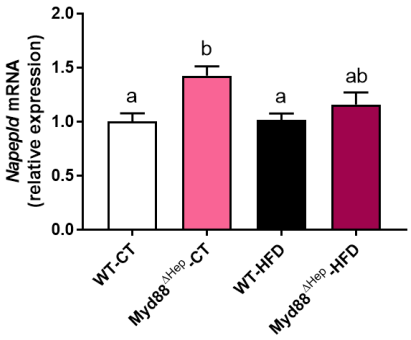

Figure 2: *MyD88*$^{\Delta Hep}$ mice display an increased liver *Napepld* expression under basal conditions. Liver mRNA expression of *Napepld* measured by real-time qPCR. Data are presented as the mean ± s.e.m. (n=6-9). Data with different superscript letters are significantly different ($p < 0.05$) according to two-way ANOVA followed by a Tukey post hoc test.

Collectively, this first set of studies provided evidence that *MyD88* deletion leads to an alteration of liver lipid metabolism and predisposes the mice to liver inflammation. This suggests that MyD88 is not only a key adaptor of immunity but also a regulator of host homeostasis. The phenotype observed here might probably be due to the alteration of liver bioactive lipids such as bile acids and their precursors, among others, highlighting the importance of a fine-tuning regulation of these liver lipid mediators.

2 Hepatocyte NAPE-PLD controls whole-body metabolism and inflammation

In accordance with the first chapter of this thesis which shed light on the relevance of some bioactive lipids on systems typically altered in metabolic disorders (i.e. liver lipid metabolism and inflammation), the second and main project of this thesis aimed to explore the role of another family of bioactive lipids, namely the NAEs, on liver metabolism.

Over the last two decades, NAEs have emerged as pivotal lipid mediators implicated in obesity and associated complications. Indeed, various metabolic disorders were correlated with an altered NAE levels in both mouse models and human beings [60, 291, 292, 453-457]. In line with this, several scientific teams, including ours, have tried to decipher their roles by working with genetic mouse models or with inhibitors of key enzymes involved in their synthesis or degradation [281, 291, 292, 458, 459]. In our laboratory, we focused our interest on NAPE-PLD, the main enzyme producing these lipid mediators, and generated several mouse models with organ-specific deletion of *Napepld* in order to investigate the impact of the diminution of the NAEs, in a particular tissue, on host homeostasis. Although whole-body *Napepld* knockout mice displayed a rather normal phenotype, we discovered that the deletion of *Napepld* in either the intestine or the adipose tissue worsened the pathophysiology of obesity [291, 292, 299, 300, 325]. However, the physiological role of NAPE-PLD in the liver remained to be elucidated. Consequently, in the frame of this thesis, a new inducible mouse model harboring a *Napepld* hepatocyte-specific deletion (i.e. *Napepld*$^{\Delta Hep}$ mice) has been generated to properly examine the function of this enzyme and related bioactive lipids, in this organ. Our results indicated that *Napepld*$^{\Delta Hep}$ mice fed with a normal diet developed a high-fat diet-like phenotype, characterized by an increased adipose tissue weight and adipocyte size as well as an elevated capacity to accumulate lipids within the liver. Moreover, we discovered that *Napepld*$^{\Delta Hep}$ mice were more prone to liver inflammation. Finally, we also demonstrated that the role of liver NAPE-PLD goes beyond the mere synthesis of NAEs, since the deletion of *Napepld* was associated with a marked modification of numerous bioactive lipids (i.e. oxysterols and bile acids) involved in several metabolic pathways. Altogether, our study demonstrated that an appropriate hepatic regulation of this enzyme is mandatory to avoid the emergence of metabolic complications. Of note, it would have been relevant to complete the whole-body bile acid and oxysterol profiles by measuring them also in the intestine, cecum and bloodstream (i.e. portal and cava veins) in order to get a full picture regarding their concentration and circulation (e.g. absorption and excretion). In addition, determining the composition of the gut microbiota in these mice would also have been pertinent for the same reasons as mentioned in the chapter devoted to MyD88 in this general discussion. Finally, it would have been

intriguing to quantify other eCBome molecules such as the precursors (i.e. NAPEs) and the derived molecules of NAEs (e.g. prostaglandins and leukotrienes) to acquire a more comprehensive view of the impact of the deletion of *Napepld* in hepatocytes. Indeed, we cannot rule out that the lack of hepatocyte *Napepld* will not activate a compensatory mechanism that will increase NAPEs availability for instance or alter somehow some NAE-metabolizing enzymes which can in turn influence inflammatory lipid mediator levels.

In the following part of this discussion, several unpublished experiments performed on *Napepld*$^{\Delta Hep}$ mice will be exposed and discussed in the context of the overall thesis and the published chapter.

2.1 Does the *Napepld* hepatocyte-specific deletion affect similarly male and female mice as well as heterozygotes and homozygotes?

Since sexual hormones influence males and females differently, and this has been linked with a different impact on obesity and metabolic disorders [460-462], we wondered whether the deletion of *Napepld* would create a sexual dimorphism among the mutant mice. Moreover, we also asked ourselves whether the deletion of one allele would be enough to induce the phenotype. In order to investigate these questions, an experiment including all these parameters was performed. Therefore, the following paragraph briefly describes the female *Napepld*$^{\Delta Hep}$ mice as well as the similarities between the heterozygotes (i.e. *Napepld*$^{\Delta Hep+/-}$ mice) and homozygotes (i.e. *Napepld*$^{\Delta Hep-/-}$ mice) regarding the development of the phenotype.

First, we discovered that comparably to male *Napepld*$^{\Delta Hep-/-}$ mice, the female *Napepld*$^{\Delta Hep-/-}$ mice displayed the same variations regarding the mRNA expression of key genes of the endocannabinoid system and exhibited a high-fat diet-like phenotype under normal diet (Figure 3A-F). This was reflected by a trend (significant with *t*-test analysis between WT and mutant female mice) of increased fat mass percentage, insulin plasma level, adipocyte size and liver lipid droplet size as well as decreased lean mass percentage (Figure 3B-F). Similarly to the male phenotype, no change has been reported regarding the body weight, food and water intake or glucose tolerance in *Napepld*$^{\Delta Hep-/-}$ females compared to WT mice (data not shown).

Regarding the heterozygosity, even though there was only one *Napepld* allele absent, as confirmed by the 50% decrease in *Napepld* mRNA expression in the liver of *Napepld*$^{\Delta Hep+/-}$ mice compared to WT, heterozygotes developed approximately a similar phenotype as homozygotes (Figure 3). This highlighted the strong importance of hepatocyte NAPE-PLD in the regulation of host homeostasis. In addition, although we did not fully characterize the other markers, the present preliminary observations suggested that there was no sexual dimorphism concerning *Napepld*$^{\Delta Hep}$ mice. The only discrepancy noted concerned the expression of liver *Cyp7b1* which was already blunted in WT females and in both *Napepld*$^{\Delta Hep+/-}$ and *Napepld*$^{\Delta Hep-/-}$ female mice compared to males. Noteworthy, this sex-specific observation has already been reported by the scientific community and is thus NAPE-PLD-independent [449].

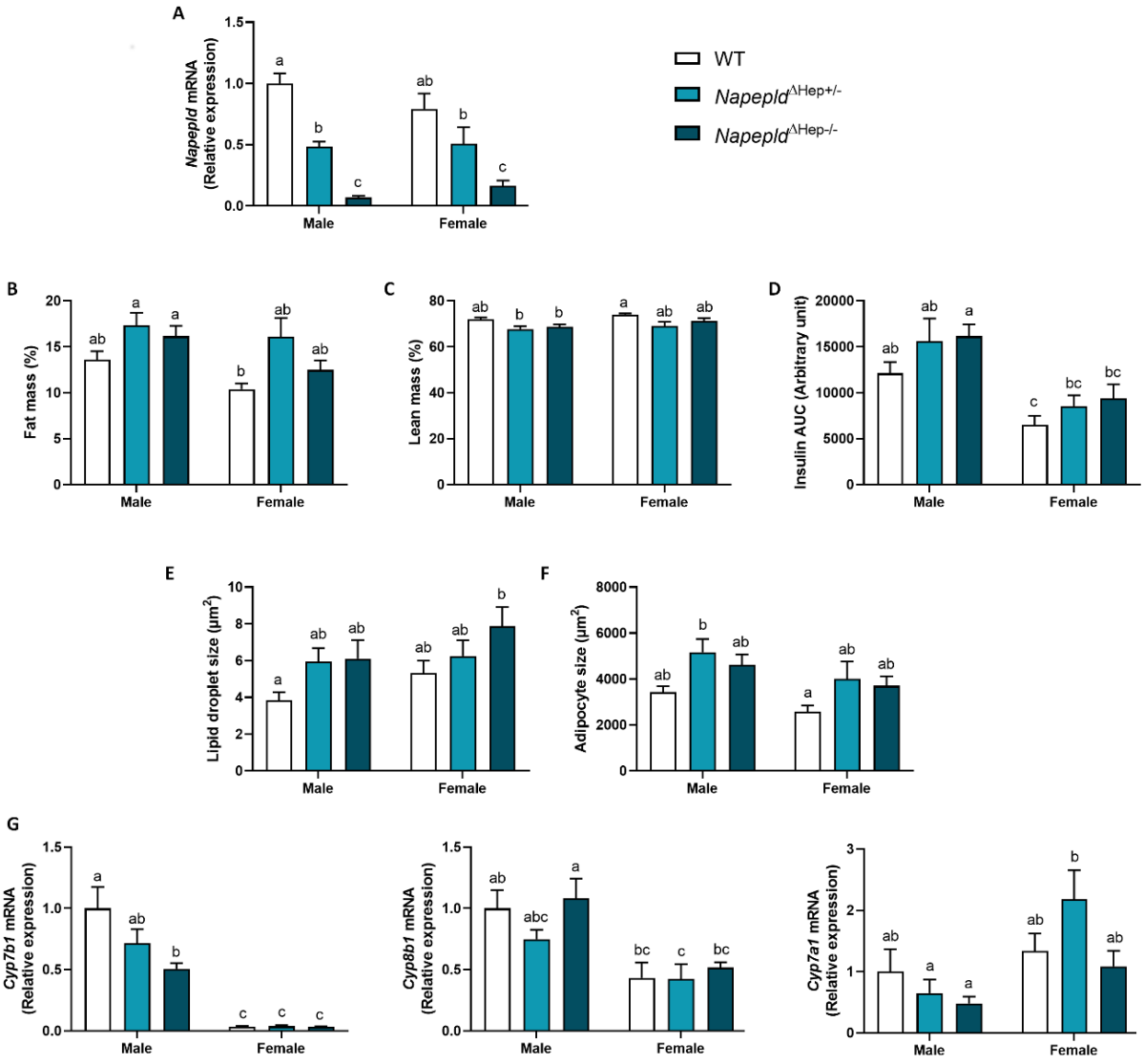

Figure 3: Heterozygotes and homozygotes from female and male *Napepld*$^{\Delta Hep}$ mice develop approximately the same phenotype. (**A**) Liver mRNA expression of *Napepld* measured by real-time qPCR. (**B**) Fat mass (%) and (**C**) lean mass (%) after a 7 weeks period on normal diet. (**D**) Mean area under the curve (AUC) of plasma insulin measured between 30 min before and 15 min after glucose loading. (**E**) Liver average lipid droplet size (µm^2) measured according to oil red O staining. (**F**) Mean adipocyte size (µm^2) quantified according to hematoxylin and eosin-stained pictures of SAT deposits. (**G**) Liver mRNA expression of bile acid synthesis markers measured by real-time qPCR. Data are presented as the mean ± s.e.m. (n = 6–10). Data with different superscript letters are significantly different ($p < 0.05$) according to two-way ANOVA followed by a Tukey post hoc test.

Because generating littermate mice of both sexes from all genotypes for all the subsequent experiments, to maintain some consistency, would have requested an enormous amount of time and a larger animal facility, the decision was to start to investigate the phenotype on male homozygotes. Indeed, although both genotypes seemed to develop the same phenotype, *Napepld*$^{\Delta Hep+/-}$ hepatocytes still produced NAPE-PLD. Therefore, the study of such model was not compatible with our primary objective, which was as a reminder, to generate a full hepatocyte-specific *Napepld* knockout mouse

model. Nevertheless, having a better understanding of the metabolism of heterozygotes is definitely of interest and warrants further research.

Likewise, since there are substantial dissimilarities between sexes regarding host metabolism (e.g. female C57Bl6 mice are less prone to diet-induced obesity, glucose intolerance and inflammation by opposition to males) [463-466], we may not rule out that the variations observed in the genes involved in bile acid synthesis in our experiment (Figure 3G), could partially contribute to these divergences. Hence, whether the impact of the deletion of *Napepld* in females might be different at the molecular level (e.g. bile acids, oxysterols, NAEs and cholesterol) requires additional investigations. Also, we may not exclude that some of the putative targets might differ according to the gender. Thus, ideally, every research, in particular in medicine, should be conducted on both sexes.

2.2 Does a long-term HFD exposure impact deeper *Napepld*$^{\Delta Hep}$ phenotype?

In the second chapter of this thesis, we reported that the obese-like phenotype exhibited by *Napepld*$^{\Delta Hep}$ mice was partially accentuated following 8 weeks of HFD exposure compared to WT. Of note, sometimes a longer exposure to HFD may help to decipher some phenotypes. Therefore, we also carried out a long-term HFD exposure of 16 weeks in order to evaluate whether a longer nutritional stress, as compared to 8 weeks HFD, would further affect the *Napepld*$^{\Delta Hep}$ phenotype. However it was not the case as we found that *Napepld*$^{\Delta Hep}$ mice fed for 16 weeks with a HFD exhibited the same phenotype as the mice treated for 8 weeks with a HFD (data not shown). Hence, this experiment strengthened our original observation that metabolic disorders were worsen in *Napepld*$^{\Delta Hep}$ male mice upon HFD exposure compared to WT mice.

2.3 Does hepatocyte NAPE-PLD control metabolism during a fasting-refeeding transition?

The discovery of the *Napepld*$^{\Delta Hep}$ phenotype led us to wonder what would be the major drivers triggering this phenotype. We thereby designed two other murine experiments on WT and *Napepld*$^{\Delta Hep}$ male after 3 weeks of follow-up, before the appearance of the phenotype. On the one hand, we placed the mice in metabolic chambers during 3 days to acquire more sensitive data regarding their metabolism (n=7). On the other hand, we challenged WT and *Napepld*$^{\Delta Hep}$ male mice with a fasting-refeeding experiment in order to further investigate their glucose and lipid metabolism (n=7).

Concerning metabolic chamber measurements, no change in locomotion activity, water intake, energy expenditure, CO_2 production and O_2 consumption were observed in *Napepld*$^{\Delta Hep}$ mice compared to WT. The only dissimilarity resided in food intake. Indeed, the results revealed that *Napepld*$^{\Delta Hep}$ mice ingested significantly more food during 3 days compared to WT (Figure 4). Nevertheless, it is worth noting that this observation has only been reported in this experiment and not in the previous ones, likely due to the method used which is more accurate and the slight magnitude of difference.

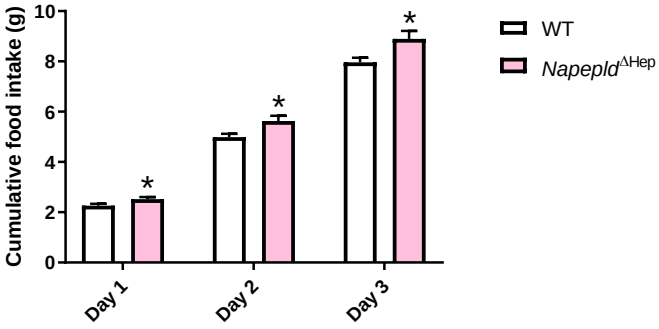

Figure 4: *Napepld*$^{\Delta Hep}$ mice have an increased food intake compared to WT before the emergence of the phenotype. Cumulative food intake (g) recorded in metabolic chambers. Data are presented as the mean ± s.e.m. (n = 7). Asterisk (*) indicates a significant difference versus WT ($p < 0.05$) according to Student's t-test.

The second study regarding the fasting-refeeding experiment has been conducted in parallel according to the protocol illustrated in Figure 5. In short, before the emergence of the phenotype, WT and *Napepld*$^{\Delta Hep}$ male mice were split in 3 groups (i.e. CT, fasted and refed) and crucial markers of the lipid and glucose metabolism were analyzed in the liver and the adipose tissue of these groups (Figure 6). Of note, since the CT groups of both genotypes behaved similarly we represented them with a single dotted green line in the graph to avoid overloading the graphics.

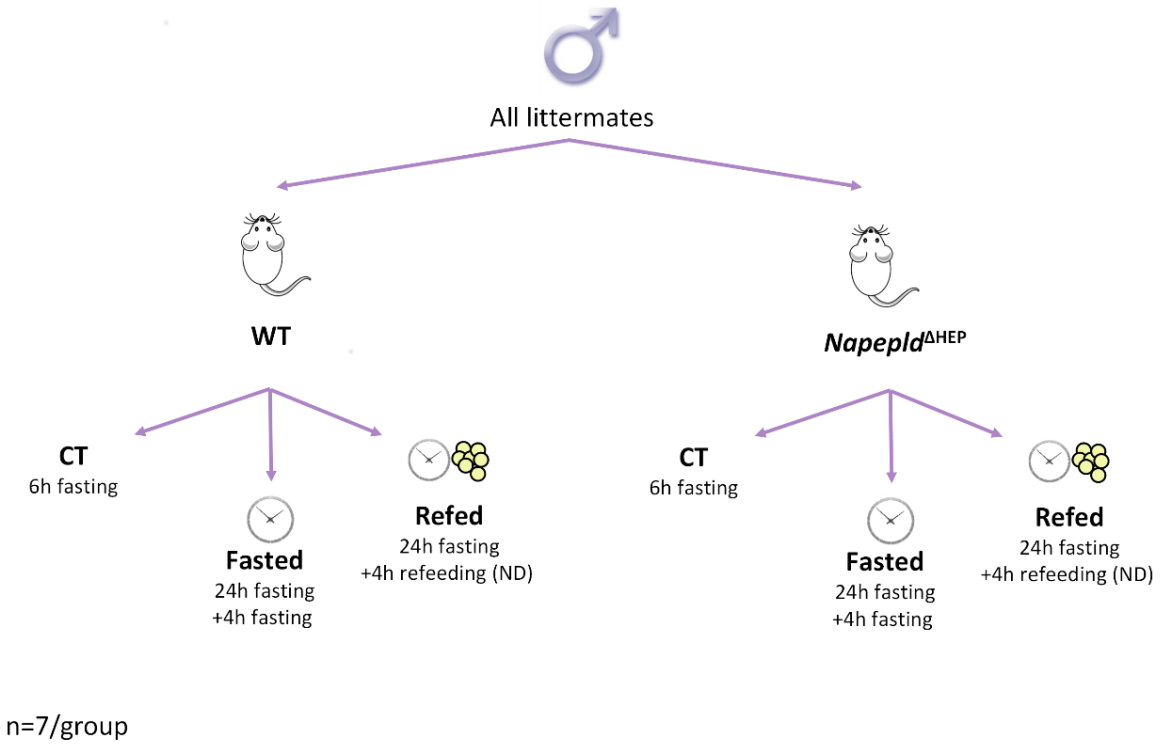

Figure 5: Experimental design regarding the fasting-refeeding experiment on *Napepld*$^{\Delta Hep}$ male and WT mice. The clock refers to 24h fasting. The yellow circles indicate that mice were refed with normal diet (ND).

First, we validated the fasting-refeeding experiment as indicated by the decrease and increase in gluconeogenesis and glycolysis markers respectively upon refeeding mice, from both genotypes, with normal diet (Figure 6A). Indeed, following food ingestion, blood glucose increases and thereby the liver stops producing glucose and initiates the glycolysis. Interestingly, some discrepancies could be noted between *Napepld*$^{\Delta Hep}$ mice and WT concerning lipid metabolism in refed condition. Indeed, the production of fatty acids tended or was significantly higher in the adipose tissue and in the liver of *Napepld*$^{\Delta Hep}$ mice compared to WT, likely contributing to the increase in fat mass perceived in mutant mice having developed the phenotype (cfr 2nd chapter of this manuscript). Moreover, markers of β-oxidation in the liver of both genotypes were similar whereas in the adipose tissue the observed tendencies were variable either for β-oxidation or lipolysis (Figure 6A-B).

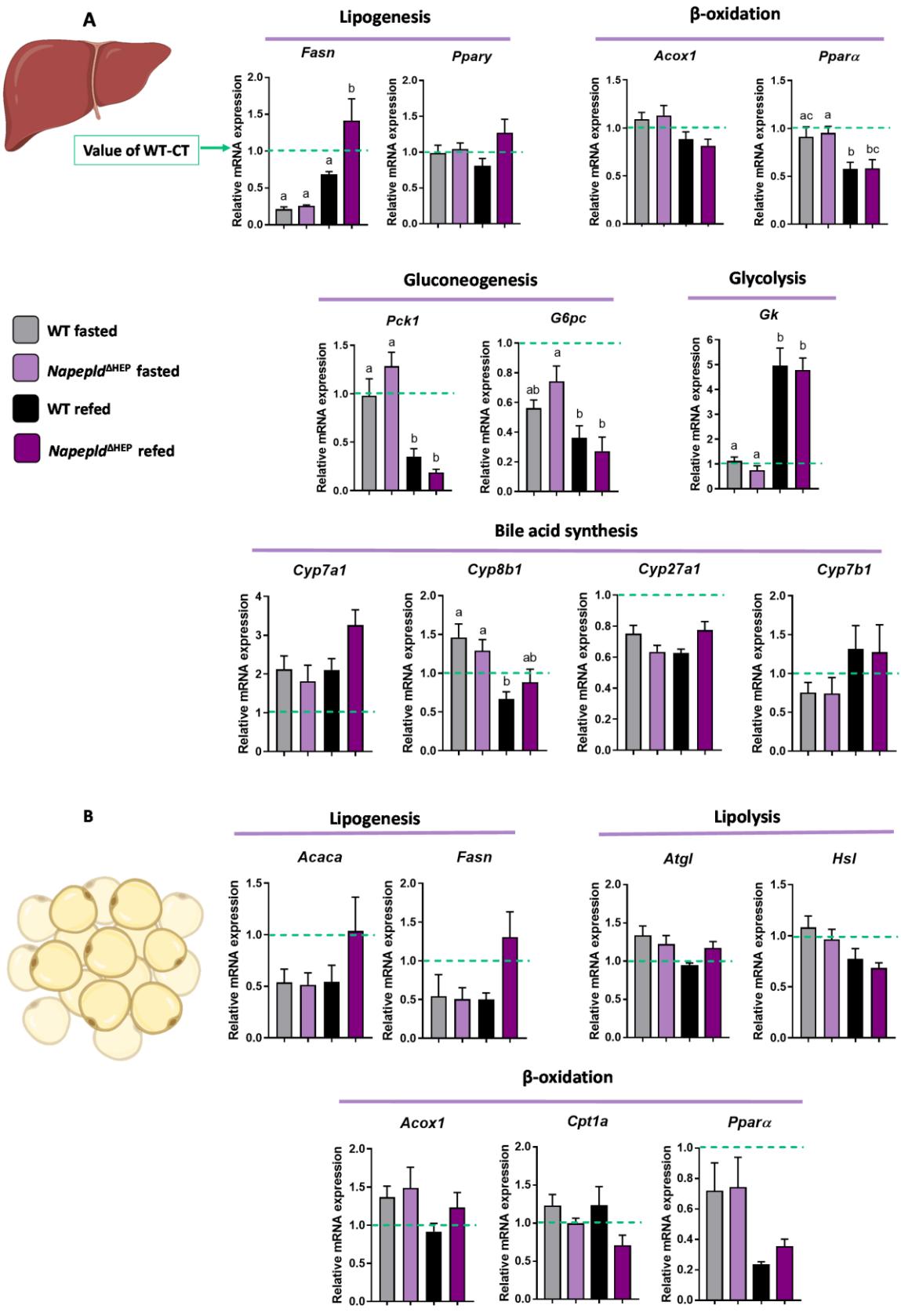
A
Value of WT-CT
WT fasted
Napepld^ΔHEP fasted
WT refed
Napepld^ΔHEP refed
Lipogenesis
Fasn
Ppary
β-oxidation
Acox1
Pparα
Gluconeogenesis
Pck1
G6pc
Glycolysis
Gk
Bile acid synthesis
Cyp7a1
Cyp8b1
Cyp27a1
Cyp7b1
B
Lipogenesis
Acaca
Fasn
Lipolysis
Atgl
Hsl
β-oxidation
Acox1
Cpt1a
Pparα
Relative mRNA expression

Figure 6: Under refeeding condition, *Napepld*$^{\Delta Hep}$ mice exhibit an altered lipid metabolism. (**A**) Liver mRNA expression of genes involved in lipogenesis, β-oxidation, gluconeogenesis, glycolysis and bile acid synthesis in *Napepld*$^{\Delta Hep}$ mice and WT under CT, fasted and refed conditions. (**B**) Subcutaneous adipose tissue (SAT) mRNA expression of genes involved in lipogenesis, lipolysis and β-oxidation in *Napepld*$^{\Delta Hep}$ mice and WT under CT, fasted and refed conditions. The dotted green line corresponds to the value of the WT-CT group. Data are presented as the mean ± s.e.m. (n = 7). Data with different superscript letters are significantly different ($p < 0.05$) according to two-way ANOVA followed by a Tukey post hoc test.

Finally, hepatic bile acid synthesis tended to be boosted in refed condition in *Napepld*$^{\Delta Hep}$ mice, suggesting that a defect in these pathways might also drive the phenotype observed a few weeks later in mutant mice. However, these last results did not reach the statistical significance under two-way ANOVA statistical analysis (Figure 6A).

Unlike lipid metabolism, no difference has been observed regarding glucose homeostasis in *Napepld*$^{\Delta Hep}$ mice compared to WT. This is in line with the appropriate response to glucose seen during the OGTT performed on mutant mice displaying the phenotype (cfr 2nd chapter of this manuscript; Figure 6A). Altogether, these two experiments suggest that the increase in food intake and the trend to an elevated lipogenesis in the liver and adipose tissue might contribute to the development of the *Napepld*$^{\Delta Hep}$ phenotype. However, the molecular mechanisms linking these effects and the absence of hepatocyte *Napepld* have not been elucidated yet and deserve further investigations.

In order to explore this crucial question, it would have been compelling to measure all the eCBome mediators, not only in the liver but also in the bloodstream and in peripheral organs of metabolic relevance such as the brain, the adipose tissue and the intestine in all experiments performed in the frame of this thesis. Since a recent study demonstrated that NAE levels varied in a time dependent-manner [467], it would have been interesting to track these changes before the emergence of the phenotype, during the phenotype as well as in mice exposed to 8 weeks and 16 weeks of HFD and compare them with WT. These data would also have revealed whether the absence of hepatocyte *Napepld* could influence the eCBome in other tissues. Finally, integrating these results with a complete quantification of bile acids and the gut microbiota composition would have been of the utmost interest and should have provided some essential clues to have a better understanding of the molecular events underlying the phenotype and its development.

2.4 Does hepatocyte NAPE-PLD affect other liver cells involved in the regulation of metabolism and inflammation?

The last results discussed in this thesis regard the putative compensation of liver non-parenchymal cells (NPC) concerning *Napepld* expression in mutant mice. Since the diminution of hepatic NAE levels was not as lower as expected in *Napepld*$^{\Delta Hep}$ mice, we wondered whether another cell type of the liver may contribute to the generation of NAEs. In the published article, we reported that non-parenchymal cells expressed *Napepld* but no difference was observed between *Napepld*$^{\Delta Hep}$ mice and WT. Given that some hepatocyte contaminations in this fraction could not be excluded, a more accurate experiment was required. Accordingly, we tried to isolate, among the dozens of different cells present in the liver, some key cell types such as Kupffer cells (KC), liver sinusoidal endothelial cells (LSEC), hepatic stellate cells (HSC) and cholangiocytes via fluorescence-activated cell sorting (FACS). More precisely, after having separated the hepatocyte and NPC fractions through simple centrifugations, specific antibodies were added in the NPC fraction of both genotypes for FACS analysis. Five antibodies were used (i.e. CD45, CD326, CD16/CD32, F4/80 and CD106) and the four cell types were isolated according to the presence or absence of these markers on their cell surface; HSC (CD45-, autofluorescence and CD106+), KC (CD45+ and F4/80+), LSEC (CD45- and CD16/CD32) and cholangiocytes (CD45- and CD326 +) [415, 468-472]. To validate the isolation of the appropriate cell types, we measured specific markers at the RNA level by RT-qPCR in the different fractions harvested [415, 416, 418, 473]. As demonstrated in the Figure 7A, the fractions were relatively pure and no significant difference was observed between *Napepld*$^{\Delta Hep}$ mice and WT except for *F4/80* which was slightly increased in mutant mice compared to WT. Finally, *Napepld* mRNA expression was quantified in the various cell-type fractions (Figure 7B). The results revealed that F4/80+ immune cells expressed globally more *Napepld* as compared to the other examined cells, strengthening the fact that NAPE-PLD plays an important role in immune function and inflammation. Indeed, it should be reminded that some NAEs exhibit pro- and anti-inflammatory properties [467, 474]. More interestingly, *Napepld* expression, in this fraction, was more than 2-fold higher in *Napepld*$^{\Delta Hep}$ mice compared to WT, suggesting that a possible compensation of immune cells to generate more NAEs could not be excluded in mutant mice. Noteworthy, we cannot either rule out that alternative pathways contributed to the formation of NAEs in hepatocytes. One interesting perspective would be to quantify NAEs in each fraction, including hepatocytes and total NPC, in order to gain insights into the potential crosstalk of the liver cell types and/or the importance of the alternative pathways. However, this remains challenging as technically, the minimal quantity of cells required to measure all the different endocannabinoid-related molecules is still a rate-limiting step for the moment.

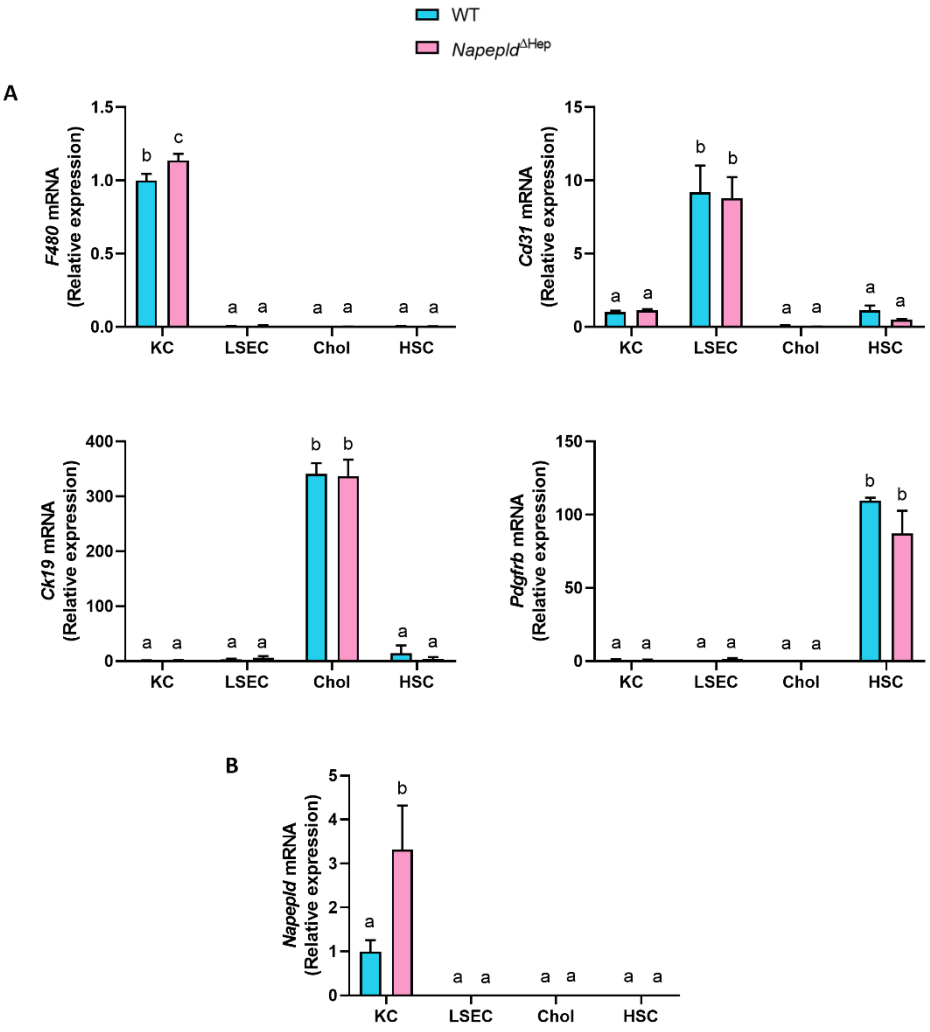

Figure 7: Kupffer cells overexpress *Napepld* mRNA expression in *Napepld*$^{\Delta Hep}$ mice. (**A**) Validation of the isolation of various cell types with different markers measured by RT-qPCR : *F4/80* for Kupffer cells (KC), *Cd31* for liver sinusoidal endothelial cell (LSEC), *Ck19* for cholangiocytes (Chol) and *Pdgfrb* for hepatic stellate cells (HSC). (**B**) *Napepld* mRNA expression measured in the different cell-type fractions. Data are presented as the mean ± s.e.m. (n=4-5). Data with different superscript letters are significantly different ($P < 0.05$) according to two-way ANOVA followed by Tukey post hoc test.

3 General conclusion

In this last paragraph of the manuscript, a conclusion highlighting some key points and future perspectives will be drawn.

In the present thesis, we discovered that a dysregulation of either hepatocyte MyD88 or hepatocyte NAPE-PLD leads to pathophysiological abnormalities in specific mouse models. Whether MyD88 or NAPE-PLD could be thereby considered as a good therapeutic target to tackle obesity and associated comorbidities is a question that should receive further attention. Although these two proteins exert a strong impact on metabolism, the present data do not allow us to confidently claim a clear answer at this stage. Indeed, these two studies shed light on the negative effects associated to their absence in hepatocytes suggesting that, instead of finding an inhibitor, future research should focus on enhancing their activity. While no specific regulator of MyD88 has been reported yet, several bile acids have been recognized to modulate, positively and negatively, NAPE-PLD activity [314, 318, 322]. Hence, one interesting experiment could consist in administrating bile acids which specifically enhance NAPE-PLD activity in obese mice, induced genetically or through HFD, and analyze the subsequent impact. Since all mouse models harboring a *Napepld* organ-specific deletion generated so far developed metabolic issues, administrating these NAPE-PLD activators without targeting a specific organ could potentially confer health benefits. More precisely, we can hypothesize that increasing NAE levels would reduce the low-grade inflammation usually observed during obesity given that most of the NAEs exhibit anti-inflammatory properties, especially PEA [379, 384, 425, 475]. Moreover, by promoting the endogenous production of OEA, one can assume that food intake would be reduced since OEA displays anorexic effects [335, 407, 476]. Nevertheless, we cannot exclude that promoting NAPE-PLD activity in specific cell types that have not been investigated yet might trigger harmful effects, since we discovered that the role of NAPE-PLD goes beyond the mere synthesis of NAEs in hepatocytes and affected the regulation of other bioactive lipids. Hence, the role of NAPE-PLD in other cell type might lead to other yet unknown phenomenon. Furthermore, one should also take into account that NAPE-PLD directly generates several bioactive lipids (i.e. NAEs) displaying beneficial and deleterious actions. Therefore, the risk to cause unwanted side effects by increasing NAPE-PLD activity cannot be excluded. Moreover, we cannot either rule out that an overproduction of potentially beneficial NAEs such as PEA or OEA might be deleterious for health given that « The dose makes the poison » as Paracelsus would say. Finally, the administration of bile acids should not be undervalued since they are themselves bioactive lipids exerting a plethora of effects on metabolism [237, 240]. Thereby, designing a specific molecule that enhances NAPE-PLD action, based on the chemical structure of DCA and CDCA, but which does

not interact with bile acid receptors or the gut microbiota, would be an ideal solution to perform the aforementioned test.

In the best of the worlds, discovering a molecule that binds to or captures a specific NAE, inhibiting it without directly altering other NAEs, would put forward the research regarding the function of those bioactive mediators which are definitely attractive candidates for the treatment of diverse metabolic disorders. However, in addition to be potentially very difficult to set up, such suggestion would require the assistance of numerous scientific disciplines including molecular and medicinal chemists to design and test such molecules first *in vitro* and then *in vivo*.

Finally, one should bear in mind that the studies conducted in the frame of this thesis were performed on rodents and that thereby these results cannot be directly translated to humans. Indeed, several differences exist between these two living organisms including the bile acid pool, the adipose tissue function as well as the gut microbiota composition and one should be careful when interpreting the data in a broader context [240, 477-479]. Even though the eCBome is also affected in obese human beings, mostly reflected by an altered plasma NAE levels in obese as compared to healthy subjects, we cannot predict that the response of the inhibition or enhancement of NAPE-PLD activity would be the same in both organisms [453-457]. Nevertheless, rodents remain good animal models to start scientific investigations that could not be directly carried out in humans.

Collectively, this thesis provided a deeper insight into the involvement of the immune system as well as the endocannabinoidome in the context of metabolic disorders and opened the way to the development of new strategies to set up in order to push forward the research in that specific field.

3.1 Main conclusions and novelties

- Hepatocyte MyD88, in addition of being a pivotal regulator of inflammation, modulates cholesterol-derived molecules (i.e. bile acids and oxysterols) likely through the enterohepatic feedback loop.

- 25-OHC might be responsible for the increased inflammatory response perceived in *MyD88*$^{\Delta Hep}$ mice challenged with LPS injection.

- Generation and validation of a new inducible mouse model harboring a *Napepld* hepatocyte-specific deletion (i.e. *Napepld*$^{\Delta Hep}$ mice).

- Hepatocyte NAPE-PLD is a key regulator of liver bioactive lipid synthesis. Aside from regulating NAE biosynthesis, this enzyme also modulates the concentration of other liver lipid mediators such as oxysterols and bile acids.

- The deletion of hepatocyte *Napepld* contributes to the emergence of metabolic disorders, in both female and male mice, under physiological condition (e.g. increased fat mass deposits, adipocyte size and liver lipid droplet size).

- The obese-like phenotype observed in *Napepld*$^{\Delta Hep}$ is worsen under HFD compared to WT mice.

- Heterozygotes and homozygotes *Napepld*$^{\Delta Hep}$ mice exhibit approximately the same high-fat diet-like phenotype, emphasizing the importance of hepatocyte NAPE-PLD on metabolism.

- Before the appearance of the phenotype, *Napepld*$^{\Delta Hep}$ mice have an increased food intake and an altered liver lipid metabolism. These effects probably contribute to the development of *Napepld*$^{\Delta Hep}$ phenotype.

3.2 Main perspectives

- Characterizing the bile acid profile not only in the liver, but also in different intestinal segments and bloodstream, in both *MyD88*$^{\Delta Hep}$ and *Napepld*$^{\Delta Hep}$ mice, would allow us to obtain a full picture of their circulation in the body. This might lead to important results that may explain the development of their respective phenotype. In line with this, integrating the gut microbiota composition would also be highly relevant.

- Measuring all eCBome mediators in the liver and in other tissues of metabolic relevance (e.g. the adipose tissue, the brain and the intestine) would enable us to have a better understanding of NAPE-PLD function in hepatocytes.

- Analyzing deeper the role of hepatocyte NAPE-PLD in female mice on metabolism would allow us to gain more insights into potential sex differences regarding the physiological action of the eCBome-related molecules.

- Exploring the role of bile acids enhancing NAPE-PLD activity in mouse models of metabolic syndrome would allow us to find out whether promoting NAPE-PLD action may confer beneficial health effects.

- Investigating further the crosstalk between KC and hepatocytes would enable us to better understand the liver function at the cellular level.

- Examining the role of overexpressing *Napepld* or *MyD88* in hepatocytes would be complementary to the loss-of-function strategy that we used.

REFERENCES

1. Abdelaal, M., C.W. le Roux, and N.G. Docherty, *Morbidity and mortality associated with obesity.* Ann Transl Med, 2017. **5**(7): p. 161.
2. Gonzalez-Muniesa, P., et al., *Obesity.* Nat Rev Dis Primers, 2017. **3**: p. 17034.
3. Speakman, J.R., *The 'Fat Mass and Obesity Related' (FTO) gene: Mechanisms of Impact on Obesity and Energy Balance.* Curr Obes Rep, 2015. **4**(1): p. 73-91.
4. Flier, J.S., *Obesity wars: molecular progress confronts an expanding epidemic.* Cell, 2004. **116**(2): p. 337-50.
5. Pineda, E., et al., *Forecasting Future Trends in Obesity across Europe: The Value of Improving Surveillance.* Obes Facts, 2018. **11**(5): p. 360-371.
6. Collaboration, N.C.D.R.F., *Worldwide trends in body-mass index, underweight, overweight, and obesity from 1975 to 2016: a pooled analysis of 2416 population-based measurement studies in 128.9 million children, adolescents, and adults.* Lancet, 2017. **390**(10113): p. 2627-2642.
7. Finkelstein, E.A., et al., *Obesity and severe obesity forecasts through 2030.* Am J Prev Med, 2012. **42**(6): p. 563-70.
8. Kelly, T., et al., *Global burden of obesity in 2005 and projections to 2030.* Int J Obes (Lond), 2008. **32**(9): p. 1431-7.
9. Lang, T., et al., *Policy councils on food, nutrition and physical activity: the UK as a case study.* Public Health Nutr, 2005. **8**(1): p. 11-9.
10. Dobbs, R., et al., *Overcoming obesity: An initial economic analysis.* McKinsey Global Institute, 2014.
11. Chen, L., et al., *Inflammatory responses and inflammation-associated diseases in organs.* Oncotarget, 2018. **9**(6): p. 7204-7218.
12. Nathan, D.M., *Long-term complications of diabetes mellitus.* N Engl J Med, 1993. **328**(23): p. 1676-85.
13. Diehl, A.M. and C. Day, *Cause, Pathogenesis, and Treatment of Nonalcoholic Steatohepatitis.* N Engl J Med, 2017. **377**(21): p. 2063-2072.
14. Chambers, J.C., et al., *C-reactive protein, insulin resistance, central obesity, and coronary heart disease risk in Indian Asians from the United Kingdom compared with European whites.* Circulation, 2001. **104**(2): p. 145-50.
15. Visser, M., et al., *Low-grade systemic inflammation in overweight children.* Pediatrics, 2001. **107**(1): p. E13.
16. Donath, M.Y. and S.E. Shoelson, *Type 2 diabetes as an inflammatory disease.* Nat Rev Immunol, 2011. **11**(2): p. 98-107.
17. Rosen, E.D. and B.M. Spiegelman, *What we talk about when we talk about fat.* Cell, 2014. **156**(1-2): p. 20-44.
18. Despres, J.P. and I. Lemieux, *Abdominal obesity and metabolic syndrome.* Nature, 2006. **444**(7121): p. 881-7.
19. Karpe, F. and K.E. Pinnick, *Biology of upper-body and lower-body adipose tissue--link to whole-body phenotypes.* Nat Rev Endocrinol, 2015. **11**(2): p. 90-100.
20. Suriano, F., M. Van Hul, and P.D. Cani, *Gut microbiota and regulation of myokine-adipokine function.* Curr Opin Pharmacol, 2020. **52**: p. 9-17.
21. Osborn, O. and J.M. Olefsky, *The cellular and signaling networks linking the immune system and metabolism in disease.* Nat Med, 2012. **18**(3): p. 363-74.
22. Shulman, G.I., *Ectopic fat in insulin resistance, dyslipidemia, and cardiometabolic disease.* N Engl J Med, 2014. **371**(23): p. 2237-8.
23. Cani, P.D., *Human gut microbiome: hopes, threats and promises.* Gut, 2018.
24. Cani, P.D., et al., *Microbial regulation of organismal energy homeostasis.* Nature Metabolism, 2019. **1**(1): p. 34-46.
25. Cani, P.D., *Gut microbiota - at the intersection of everything?* Nat Rev Gastroenterol Hepatol, 2017. **14**(6): p. 321-322.

26. Sender, R., S. Fuchs, and R. Milo, *Are We Really Vastly Outnumbered? Revisiting the Ratio of Bacterial to Host Cells in Humans.* Cell, 2016. **164**(3): p. 337-40.
27. Li, J., et al., *An integrated catalog of reference genes in the human gut microbiome.* Nat Biotechnol, 2014. **32**(8): p. 834-41.
28. Cani, P.D., *Microbiota and metabolites in metabolic diseases.* Nat Rev Endocrinol, 2019. **15**(2): p. 69-70.
29. Konig, J., et al., *Human Intestinal Barrier Function in Health and Disease.* Clin Transl Gastroenterol, 2016. **7**(10): p. e196.
30. Wells, J.M., et al., *Homeostasis of the gut barrier and potential biomarkers.* American Journal of Physiology-Gastrointestinal and Liver Physiology, 2016. **312**(3): p. G171-G193.
31. Cani, P.D., et al., *Metabolic endotoxemia initiates obesity and insulin resistance.* Diabetes, 2007. **56**(7): p. 1761-72.
32. Cani, P.D., et al., *Changes in gut microbiota control metabolic endotoxemia-induced inflammation in high-fat diet-induced obesity and diabetes in mice.* Diabetes, 2008. **57**(6): p. 1470-81.
33. Di Gioia, M. and I. Zanoni, *Toll-like receptor co-receptors as master regulators of the immune response.* Mol Immunol, 2015. **63**(2): p. 143-52.
34. Park, B.S., et al., *The structural basis of lipopolysaccharide recognition by the TLR4-MD-2 complex.* Nature, 2009. **458**(7242): p. 1191-5.
35. Lucas, K. and M. Maes, *Role of the Toll Like receptor (TLR) radical cycle in chronic inflammation: possible treatments targeting the TLR4 pathway.* Mol Neurobiol, 2013. **48**(1): p. 190-204.
36. Rocha, D.M., et al., *Saturated fatty acids trigger TLR4-mediated inflammatory response.* Atherosclerosis, 2016. **244**: p. 211-5.
37. Everard, A., et al., *Intestinal epithelial MyD88 is a sensor switching host metabolism towards obesity according to nutritional status.* Nat Commun, 2014. **5**: p. 5648.
38. Ye, D., et al., *Toll-like receptor-4 mediates obesity-induced non-alcoholic steatohepatitis through activation of X-box binding protein-1 in mice.* Gut, 2012. **61**(7): p. 1058-67.
39. Luche, E., et al., *Metabolic endotoxemia directly increases the proliferation of adipocyte precursors at the onset of metabolic diseases through a CD14-dependent mechanism.* Mol Metab, 2013. **2**(3): p. 281-91.
40. Dennis, E.A. and P.C. Norris, *Eicosanoid storm in infection and inflammation.* Nat Rev Immunol, 2015. **15**(8): p. 511-23.
41. Teng, K.T., et al., *Modulation of obesity-induced inflammation by dietary fats: mechanisms and clinical evidence.* Nutr J, 2014. **13**: p. 12.
42. Ghoshal, S., et al., *Chylomicrons promote intestinal absorption of lipopolysaccharides.* J Lipid Res, 2009. **50**(1): p. 90-7.
43. Laugerette, F., et al., *Emulsified lipids increase endotoxemia: possible role in early postprandial low-grade inflammation.* J Nutr Biochem, 2011. **22**(1): p. 53-9.
44. Pendyala, S., J.M. Walker, and P.R. Holt, *A high-fat diet is associated with endotoxemia that originates from the gut.* Gastroenterology, 2012. **142**(5): p. 1100-1101 e2.
45. Caesar, R., et al., *Crosstalk between Gut Microbiota and Dietary Lipids Aggravates WAT Inflammation through TLR Signaling.* Cell Metab, 2015. **22**(4): p. 658-68.
46. Tilg, H., et al., *The intestinal microbiota fuelling metabolic inflammation.* Nat Rev Immunol, 2020. **20**(1): p. 40-54.
47. Cani, P.D., et al., *Changes in gut microbiota control inflammation in obese mice through a mechanism involving GLP-2-driven improvement of gut permeability.* Gut, 2009. **58**(8): p. 1091-103.
48. Vijayan, A., et al., *Compartmentalized Antimicrobial Defenses in Response to Flagellin.* Trends Microbiol, 2018. **26**(5): p. 423-435.
49. Wolf, A.J. and D.M. Underhill, *Peptidoglycan recognition by the innate immune system.* Nat Rev Immunol, 2018. **18**(4): p. 243-254.

50. Belkaid, Y. and T.W. Hand, *Role of the microbiota in immunity and inflammation.* Cell, 2014. **157**(1): p. 121-41.
51. Winkler, P., et al., *Molecular and cellular basis of microflora-host interactions.* J Nutr, 2007. **137**(3 Suppl 2): p. 756S-72S.
52. Chassaing, B., et al., *Dietary emulsifiers impact the mouse gut microbiota promoting colitis and metabolic syndrome.* Nature, 2015. **519**(7541): p. 92-6.
53. Chassaing, B., et al., *Dietary emulsifiers directly alter human microbiota composition and gene expression ex vivo potentiating intestinal inflammation.* Gut, 2017. **66**(8): p. 1414-1427.
54. Cani, P.D. and B.F. Jordan, *Gut microbiota-mediated inflammation in obesity: a link with gastrointestinal cancer.* Nat Rev Gastroenterol Hepatol, 2018. **15**(11): p. 671-682.
55. Anhê, F.F., et al., *Type 2 diabetes influences bacterial tissue compartmentalisation in human obesity.* Nature Metabolism, 2020. **2**(3): p. 233-242.
56. Kolodziejczyk, A.A., et al., *The role of the microbiome in NAFLD and NASH.* EMBO Mol Med, 2019. **11**(2).
57. Cohen, L.J., et al., *Commensal bacteria make GPCR ligands that mimic human signalling molecules.* Nature, 2017. **549**(7670): p. 48-53.
58. Muccioli, G.G., et al., *The endocannabinoid system links gut microbiota to adipogenesis.* Mol Syst Biol, 2010. **6**: p. 392.
59. Cani, P.D., *Crosstalk between the gut microbiota and the endocannabinoid system: impact on the gut barrier function and the adipose tissue.* Clin Microbiol Infect, 2012. **18 Suppl 4**: p. 50-3.
60. Cani, P.D., et al., *Endocannabinoids--at the crossroads between the gut microbiota and host metabolism.* Nat Rev Endocrinol, 2016. **12**(3): p. 133-43.
61. Ze, X., et al., *Some are more equal than others: the role of "keystone" species in the degradation of recalcitrant substrates.* Gut Microbes, 2013. **4**(3): p. 236-40.
62. Louis, P. and H.J. Flint, *Formation of propionate and butyrate by the human colonic microbiota.* Environ Microbiol, 2017. **19**(1): p. 29-41.
63. Hoek, M. and R.M.H. Merks, *Emergence of microbial diversity due to cross-feeding interactions in a spatial model of gut microbial metabolism.* BMC Syst Biol, 2017. **11**(1): p. 56.
64. Donohoe, D.R., et al., *The microbiome and butyrate regulate energy metabolism and autophagy in the mammalian colon.* Cell Metab, 2011. **13**(5): p. 517-26.
65. Canfora, E.E., J.W. Jocken, and E.E. Blaak, *Short-chain fatty acids in control of body weight and insulin sensitivity.* Nat Rev Endocrinol, 2015. **11**(10): p. 577-91.
66. Cani, P.D., C. Dewever, and N.M. Delzenne, *Inulin-type fructans modulate gastrointestinal peptides involved in appetite regulation (glucagon-like peptide-1 and ghrelin) in rats.* Br J Nutr, 2004. **92**(3): p. 521-6.
67. Cani, P.D., et al., *Oligofructose promotes satiety in rats fed a high-fat diet: involvement of glucagon-like Peptide-1.* Obes Res, 2005. **13**(6): p. 1000-7.
68. Brooks, L., et al., *Fermentable carbohydrate stimulates FFAR2-dependent colonic PYY cell expansion to increase satiety.* Mol Metab, 2017. **6**(1): p. 48-60.
69. De Vadder, F., et al., *Microbiota-generated metabolites promote metabolic benefits via gut-brain neural circuits.* Cell, 2014. **156**(1-2): p. 84-96.
70. Singh, V., et al., *Microbiota-Dependent Hepatic Lipogenesis Mediated by Stearoyl CoA Desaturase 1 (SCD1) Promotes Metabolic Syndrome in TLR5-Deficient Mice.* Cell Metab, 2015. **22**(6): p. 983-96.
71. De Vadder, F., et al., *Microbiota-Produced Succinate Improves Glucose Homeostasis via Intestinal Gluconeogenesis.* Cell Metab, 2016. **24**(1): p. 151-7.
72. Cani, P.D., et al., *Improvement of glucose tolerance and hepatic insulin sensitivity by oligofructose requires a functional glucagon-like peptide 1 receptor.* Diabetes, 2006. **55**(5): p. 1484-90.
73. Rastelli, M., P.D. Cani, and C. Knauf, *The Gut Microbiome Influences Host Endocrine Functions.* Endocr Rev, 2019. **40**(5): p. 1271-1284.

74. Plovier, H., et al., *A purified membrane protein from Akkermansia muciniphila or the pasteurized bacterium improves metabolism in obese and diabetic mice.* Nat Med, 2017. **23**(1): p. 107-113.
75. Zheng, Y., S.H. Ley, and F.B. Hu, *Global aetiology and epidemiology of type 2 diabetes mellitus and its complications.* Nat Rev Endocrinol, 2018. **14**(2): p. 88-98.
76. Czech, M.P., *Insulin action and resistance in obesity and type 2 diabetes.* Nat Med, 2017. **23**(7): p. 804-814.
77. IDF, *International Diabetes Federation 9th Edition.* Diabetes Atlas 2019.
78. Buse, J.B., et al., *2019 update to: Management of hyperglycaemia in type 2 diabetes, 2018. A consensus report by the American Diabetes Association (ADA) and the European Association for the Study of Diabetes (EASD).* Diabetologia, 2020. **63**(2): p. 221-228.
79. Boucher, J., A. Kleinridders, and C.R. Kahn, *Insulin receptor signaling in normal and insulin-resistant states.* Cold Spring Harb Perspect Biol, 2014. **6**(1).
80. Roden, M. and G.I. Shulman, *The integrative biology of type 2 diabetes.* Nature, 2019. **576**(7785): p. 51-60.
81. Kasuga, M., F.A. Karlsson, and C.R. Kahn, *Insulin stimulates the phosphorylation of the 95,000-dalton subunit of its own receptor.* Science, 1982. **215**(4529): p. 185-7.
82. Sun, X.J., et al., *Structure of the insulin receptor substrate IRS-1 defines a unique signal transduction protein.* Nature, 1991. **352**(6330): p. 73-77.
83. Sun, X.J., et al., *Role of IRS-2 in insulin and cytokine signalling.* Nature, 1995. **377**(6545): p. 173-177.
84. DeFronzo, R.A., et al., *Synergistic interaction between exercise and insulin on peripheral glucose uptake.* The Journal of clinical investigation, 1981. **68**(6): p. 1468-1474.
85. DeFronzo, R.A., et al., *The effect of insulin on the disposal of intravenous glucose. Results from indirect calorimetry and hepatic and femoral venous catheterization.* Diabetes, 1981. **30**(12): p. 1000-7.
86. Donnelly, K.L., et al., *Sources of fatty acids stored in liver and secreted via lipoproteins in patients with nonalcoholic fatty liver disease.* The Journal of clinical investigation, 2005. **115**(5): p. 1343-1351.
87. Najjar, S.M. and G. Perdomo, *Hepatic Insulin Clearance: Mechanism and Physiology.* Physiology (Bethesda), 2019. **34**(3): p. 198-215.
88. Duckworth, W.C., R.G. Bennett, and F.G. Hamel, *Insulin Degradation: Progress and Potential*.* Endocrine Reviews, 1998. **19**(5): p. 608-624.
89. Meier, J.J., J.D. Veldhuis, and P.C. Butler, *Pulsatile insulin secretion dictates systemic insulin delivery by regulating hepatic insulin extraction in humans.* Diabetes, 2005. **54**(6): p. 1649-56.
90. Tokarz, V.L., P.E. MacDonald, and A. Klip, *The cell biology of systemic insulin function.* J Cell Biol, 2018. **217**(7): p. 2273-2289.
91. Poy, M.N., et al., *CEACAM1 regulates insulin clearance in liver.* Nat Genet, 2002. **30**(3): p. 270-6.
92. Polidori, D.C., et al., *Hepatic and Extrahepatic Insulin Clearance Are Differentially Regulated: Results From a Novel Model-Based Analysis of Intravenous Glucose Tolerance Data.* Diabetes, 2016. **65**(6): p. 1556-64.
93. Gurzov, E.N., et al., *Hepatic oxidative stress promotes insulin-STAT-5 signaling and obesity by inactivating protein tyrosine phosphatase N2.* Cell Metab, 2014. **20**(1): p. 85-102.
94. Yuzefovych, L., G. Wilson, and L. Rachek, *Different effects of oleate vs. palmitate on mitochondrial function, apoptosis, and insulin signaling in L6 skeletal muscle cells: role of oxidative stress.* Am J Physiol Endocrinol Metab, 2010. **299**(6): p. E1096-105.
95. Carmiel-Haggai, M., A.I. Cederbaum, and N. Nieto, *A high-fat diet leads to the progression of non-alcoholic fatty liver disease in obese rats.* FASEB J, 2005. **19**(1): p. 136-8.
96. Satapati, S., et al., *Elevated TCA cycle function in the pathology of diet-induced hepatic insulin resistance and fatty liver.* J Lipid Res, 2012. **53**(6): p. 1080-92.

97. Yokota, T., et al., *Oxidative stress in skeletal muscle impairs mitochondrial respiration and limits exercise capacity in type 2 diabetic mice.* Am J Physiol Heart Circ Physiol, 2009. **297**(3): p. H1069-77.
98. Tran, T.T., et al., *Beneficial effects of subcutaneous fat transplantation on metabolism.* Cell Metab, 2008. **7**(5): p. 410-20.
99. Min, S.Y., et al., *Human 'brite/beige' adipocytes develop from capillary networks, and their implantation improves metabolic homeostasis in mice.* Nat Med, 2016. **22**(3): p. 312-8.
100. Hocking, S.L., et al., *Subcutaneous fat transplantation alleviates diet-induced glucose intolerance and inflammation in mice.* Diabetologia, 2015. **58**(7): p. 1587-600.
101. Feingold, K.R., et al., *Effect of tumor necrosis factor (TNF) on lipid metabolism in the diabetic rat. Evidence that inhibition of adipose tissue lipoprotein lipase activity is not required for TNF-induced hyperlipidemia.* J Clin Invest, 1989. **83**(4): p. 1116-21.
102. Grunfeld, C. and K.R. Feingold, *The metabolic effects of tumor necrosis factor and other cytokines.* Biotherapy, 1991. **3**(2): p. 143-58.
103. Hotamisligil, G.S., N.S. Shargill, and B.M. Spiegelman, *Adipose expression of tumor necrosis factor-alpha: direct role in obesity-linked insulin resistance.* Science, 1993. **259**(5091): p. 87-91.
104. Uysal, K.T., et al., *Protection from obesity-induced insulin resistance in mice lacking TNF-alpha function.* Nature, 1997. **389**(6651): p. 610-4.
105. Solinas, G., et al., *JNK1 in hematopoietically derived cells contributes to diet-induced inflammation and insulin resistance without affecting obesity.* Cell Metab, 2007. **6**(5): p. 386-97.
106. Arkan, M.C., et al., *IKK-beta links inflammation to obesity-induced insulin resistance.* Nat Med, 2005. **11**(2): p. 191-8.
107. Furuhashi, M., et al., *Adipocyte/macrophage fatty acid-binding proteins contribute to metabolic deterioration through actions in both macrophages and adipocytes in mice.* J Clin Invest, 2008. **118**(7): p. 2640-50.
108. Mauer, J., et al., *Myeloid cell-restricted insulin receptor deficiency protects against obesity-induced inflammation and systemic insulin resistance.* PLoS Genet, 2010. **6**(5): p. e1000938.
109. Stephens, J.M. and P.H. Pekala, *Transcriptional repression of the GLUT4 and C/EBP genes in 3T3-L1 adipocytes by tumor necrosis factor-alpha.* J Biol Chem, 1991. **266**(32): p. 21839-45.
110. Ye, J., *Regulation of PPARgamma function by TNF-alpha.* Biochem Biophys Res Commun, 2008. **374**(3): p. 405-8.
111. Hevener, A.L., et al., *Macrophage PPAR gamma is required for normal skeletal muscle and hepatic insulin sensitivity and full antidiabetic effects of thiazolidinediones.* J Clin Invest, 2007. **117**(6): p. 1658-69.
112. Odegaard, J.I., et al., *Macrophage-specific PPARgamma controls alternative activation and improves insulin resistance.* Nature, 2007. **447**(7148): p. 1116-20.
113. Holland, W.L., et al., *Lipid-induced insulin resistance mediated by the proinflammatory receptor TLR4 requires saturated fatty acid-induced ceramide biosynthesis in mice.* J Clin Invest, 2011. **121**(5): p. 1858-70.
114. Dobrowsky, R.T., et al., *Ceramide activates heterotrimeric protein phosphatase 2A.* J Biol Chem, 1993. **268**(21): p. 15523-30.
115. Olefsky, J.M. and C.K. Glass, *Macrophages, inflammation, and insulin resistance.* Annu Rev Physiol, 2010. **72**: p. 219-46.
116. Cai, D., et al., *Local and systemic insulin resistance resulting from hepatic activation of IKK-beta and NF-kappaB.* Nat Med, 2005. **11**(2): p. 183-90.
117. Lanthier, N., et al., *Kupffer cell activation is a causal factor for hepatic insulin resistance.* Am J Physiol Gastrointest Liver Physiol, 2010. **298**(1): p. G107-16.
118. Neyrinck, A.M., et al., *Critical role of Kupffer cells in the management of diet-induced diabetes and obesity.* Biochem Biophys Res Commun, 2009. **385**(3): p. 351-6.
119. Tilg, H. and A. Kaser, *Gut microbiome, obesity, and metabolic dysfunction.* J Clin Invest, 2011. **121**(6): p. 2126-32.

120. Shi, H., et al., *TLR4 links innate immunity and fatty acid-induced insulin resistance.* J Clin Invest, 2006. **116**(11): p. 3015-25.
121. Maslowski, K.M. and C.R. Mackay, *Diet, gut microbiota and immune responses.* Nat Immunol, 2011. **12**(1): p. 5-9.
122. Yang, Q., A. Vijayakumar, and B.B. Kahn, *Metabolites as regulators of insulin sensitivity and metabolism.* Nat Rev Mol Cell Biol, 2018. **19**(10): p. 654-672.
123. Hotamisligil, G.S. and R.J. Davis, *Cell Signaling and Stress Responses.* Cold Spring Harb Perspect Biol, 2016. **8**(10).
124. Pal, D., et al., *Fetuin-A acts as an endogenous ligand of TLR4 to promote lipid-induced insulin resistance.* Nature Medicine, 2012. **18**(8): p. 1279-1285.
125. Oh, D.Y., et al., *GPR120 is an omega-3 fatty acid receptor mediating potent anti-inflammatory and insulin-sensitizing effects.* Cell, 2010. **142**(5): p. 687-98.
126. Liu, Y., et al., *The fish oil ingredient, docosahexaenoic acid, activates cytosolic phospholipase A(2) via GPR120 receptor to produce prostaglandin E(2) and plays an anti-inflammatory role in macrophages.* Immunology, 2014. **143**(1): p. 81-95.
127. Finck, B.N. and A.M. Hall, *Does Diacylglycerol Accumulation in Fatty Liver Disease Cause Hepatic Insulin Resistance?* Biomed Res Int, 2015. **2015**: p. 104132.
128. Chavez-Talavera, O., et al., *Bile Acid Control of Metabolism and Inflammation in Obesity, Type 2 Diabetes, Dyslipidemia, and Nonalcoholic Fatty Liver Disease.* Gastroenterology, 2017. **152**(7): p. 1679-1694 e3.
129. Iwasa, M., et al., *Elevation of branched-chain amino acid levels in diabetes and NAFL and changes with antidiabetic drug treatment.* Obes Res Clin Pract, 2015. **9**(3): p. 293-7.
130. Newgard, C.B., *Metabolomics and Metabolic Diseases: Where Do We Stand?* Cell Metab, 2017. **25**(1): p. 43-56.
131. Chen, Y., et al., *Insulin Receptor Trafficking: Consequences for Insulin Sensitivity and Diabetes.* Int J Mol Sci, 2019. **20**(20).
132. Kobayashi, M. and J.M. Olefsky, *Effect of experimental hyperinsulinemia on insulin binding and glucose transport in isolated rat adipocytes.* Am J Physiol, 1978. **235**(1): p. E53-62.
133. Ghadieh, H.E., et al., *Hyperinsulinemia drives hepatic insulin resistance in male mice with liver-specific Ceacam1 deletion independently of lipolysis.* Metabolism, 2019. **93**: p. 33-43.
134. DeAngelis, A.M., et al., *Carcinoembryonic antigen-related cell adhesion molecule 1: a link between insulin and lipid metabolism.* Diabetes, 2008. **57**(9): p. 2296-303.
135. Park, S.-Y., et al., *Mechanism of glucose intolerance in mice with dominant negative mutation of CEACAM1.* American journal of physiology. Endocrinology and metabolism, 2006. **291**(3): p. E517-24.
136. Huang, T.D., J. Behary, and A. Zekry, *Non-alcoholic fatty liver disease (NAFLD): a review of epidemiology, risk factors, diagnosis and management.* Intern Med J, 2019.
137. Younossi, Z., et al., *Global burden of NAFLD and NASH: trends, predictions, risk factors and prevention.* Nat Rev Gastroenterol Hepatol, 2018. **15**(1): p. 11-20.
138. Younossi, Z.M., et al., *Global epidemiology of nonalcoholic fatty liver disease-Meta-analytic assessment of prevalence, incidence, and outcomes.* Hepatology, 2016. **64**(1): p. 73-84.
139. Anstee, Q.M., et al., *From NASH to HCC: current concepts and future challenges.* Nat Rev Gastroenterol Hepatol, 2019. **16**(7): p. 411-428.
140. Boyd, A., et al., *Medical liver biopsy: background, indications, procedure and histopathology.* Frontline Gastroenterol, 2020. **11**(1): p. 40-47.
141. Younossi, Z.M., et al., *Nonalcoholic fatty liver disease in lean individuals in the United States.* Medicine (Baltimore), 2012. **91**(6): p. 319-27.
142. Birkenfeld, A.L. and G.I. Shulman, *Nonalcoholic fatty liver disease, hepatic insulin resistance, and type 2 diabetes.* Hepatology, 2014. **59**(2): p. 713-23.
143. Lewis, G.F., et al., *Disordered fat storage and mobilization in the pathogenesis of insulin resistance and type 2 diabetes.* Endocr Rev, 2002. **23**(2): p. 201-29.

144. Puri, P., et al., *A lipidomic analysis of nonalcoholic fatty liver disease.* Hepatology, 2007. **46**(4): p. 1081-90.
145. Araya, J., et al., *Decreased liver fatty acid delta-6 and delta-5 desaturase activity in obese patients.* Obesity (Silver Spring), 2010. **18**(7): p. 1460-3.
146. Min, H.K., et al., *Increased hepatic synthesis and dysregulation of cholesterol metabolism is associated with the severity of nonalcoholic fatty liver disease.* Cell Metab, 2012. **15**(5): p. 665-74.
147. Hernández, E., et al., *Acute dietary fat intake initiates alterations in energy metabolism and insulin resistance.* J Clin Invest, 2017. **127**(2): p. 695-708.
148. Luukkonen, P.K., et al., *Saturated Fat Is More Metabolically Harmful for the Human Liver Than Unsaturated Fat or Simple Sugars.* Diabetes Care, 2018. **41**(8): p. 1732-1739.
149. Parks, E., H. Yki-Järvinen, and M. Hawkins, *Out of the frying pan: dietary saturated fat influences nonalcoholic fatty liver disease.* The Journal of clinical investigation, 2017. **127**(2): p. 454-456.
150. Aron-Wisnewsky, J., et al., *Gut microbiota and human NAFLD: disentangling microbial signatures from metabolic disorders.* Nature Reviews Gastroenterology & Hepatology, 2020. **17**(5): p. 279-297.
151. Safari, Z. and P. Gérard, *The links between the gut microbiome and non-alcoholic fatty liver disease (NAFLD).* Cell Mol Life Sci, 2019. **76**(8): p. 1541-1558.
152. Brandl, K. and B. Schnabl, *Intestinal microbiota and nonalcoholic steatohepatitis.* Curr Opin Gastroenterol, 2017. **33**(3): p. 128-133.
153. Fei, N., et al., *Endotoxin Producers Overgrowing in Human Gut Microbiota as the Causative Agents for Nonalcoholic Fatty Liver Disease.* mBio, 2020. **11**(1): p. e03263-19.
154. Hoyles, L., et al., *Molecular phenomics and metagenomics of hepatic steatosis in non-diabetic obese women.* Nature Medicine, 2018. **24**(7): p. 1070-1080.
155. Sookoian, S. and C.J. Pirola, *Genetic predisposition in nonalcoholic fatty liver disease.* Clin Mol Hepatol, 2017. **23**(1): p. 1-12.
156. Liu, Y.L., et al., *TM6SF2 rs58542926 influences hepatic fibrosis progression in patients with non-alcoholic fatty liver disease.* Nat Commun, 2014. **5**: p. 4309.
157. Valenti, L., et al., *Homozygosity for the patatin-like phospholipase-3/adiponutrin I148M polymorphism influences liver fibrosis in patients with nonalcoholic fatty liver disease.* Hepatology, 2010. **51**(4): p. 1209-17.
158. Sanyal, A.J., *Past, present and future perspectives in nonalcoholic fatty liver disease.* Nat Rev Gastroenterol Hepatol, 2019. **16**(6): p. 377-386.
159. Sutti, S. and E. Albano, *Adaptive immunity: an emerging player in the progression of NAFLD.* Nat Rev Gastroenterol Hepatol, 2020. **17**(2): p. 81-92.
160. Angulo, P., et al., *The NAFLD fibrosis score: a noninvasive system that identifies liver fibrosis in patients with NAFLD.* Hepatology, 2007. **45**(4): p. 846-54.
161. Cani, P.D. and M. Van Hul, *Mediterranean diet, gut microbiota and health: when age and calories do not add up!* Gut, 2020.
162. Gibson, G.R., et al., *Expert consensus document: The International Scientific Association for Probiotics and Prebiotics (ISAPP) consensus statement on the definition and scope of prebiotics.* Nat Rev Gastroenterol Hepatol, 2017. **14**(8): p. 491-502.
163. Morissette, A., et al., *Blueberry proanthocyanidins and anthocyanins improve metabolic health through a gut microbiota-dependent mechanism in diet-induced obese mice.* Am J Physiol Endocrinol Metab, 2020.
164. Anhe, F.F., et al., *Treatment with camu camu (Myrciaria dubia) prevents obesity by altering the gut microbiota and increasing energy expenditure in diet-induced obese mice.* Gut, 2018.
165. Zhao, L., et al., *Gut bacteria selectively promoted by dietary fibers alleviate type 2 diabetes.* Science, 2018. **359**(6380): p. 1151-1156.
166. Rodriguez, J., et al., *Discovery of the gut microbial signature driving the efficacy of prebiotic intervention in obese patients.* Gut, 2020.

167. Wieers, G., et al., *How Probiotics Affect the Microbiota.* Front Cell Infect Microbiol, 2019. **9**: p. 454.
168. Hill, C., et al., *Expert consensus document. The International Scientific Association for Probiotics and Prebiotics consensus statement on the scope and appropriate use of the term probiotic.* Nat Rev Gastroenterol Hepatol, 2014. **11**(8): p. 506-14.
169. Depommier, C., et al., *Supplementation with Akkermansia muciniphila in overweight and obese human volunteers: a proof-of-concept exploratory study.* Nat Med, 2019. **25**(7): p. 1096-1103.
170. Depommier, C., et al., *Pasteurized Akkermansia muciniphila increases whole-body energy expenditure and fecal energy excretion in diet-induced obese mice.* Gut Microbes, 2020: p. 1-15.
171. Jackson, V.M., et al., *Latest approaches for the treatment of obesity.* Expert Opin Drug Discov, 2015. **10**(8): p. 825-39.
172. Rodgers, R.J., M.H. Tschop, and J.P. Wilding, *Anti-obesity drugs: past, present and future.* Dis Model Mech, 2012. **5**(5): p. 621-6.
173. Melnikova, I. and D. Wages, *Anti-obesity therapies.* Nat Rev Drug Discov, 2006. **5**(5): p. 369-70.
174. Field, B.C., O.B. Chaudhri, and S.R. Bloom, *Obesity treatment: novel peripheral targets.* Br J Clin Pharmacol, 2009. **68**(6): p. 830-43.
175. Ntambi, J.M., *Hepatic de novo lipogenesis and regulation of metabolism*. 2015: Springer.
176. Sanders, F.W. and J.L. Griffin, *De novo lipogenesis in the liver in health and disease: more than just a shunting yard for glucose.* Biol Rev Camb Philos Soc, 2016. **91**(2): p. 452-68.
177. Kuntz, E. and H.-D. Kuntz, *Morphology of the Liver.* Hepatology Textbook and Atlas: History· Morphology Biochemistry· Diagnostics Clinic· Therapy, 2008: p. 15-33.
178. McCuskey, R.S., *Morphological mechanisms for regulating blood flow through hepatic sinusoids.* Liver, 2000. **20**(1): p. 3-7.
179. Bykov, I., et al., *Functional Differences between Periportal and Perivenous Kupffer Cells Isolated by Digitonin-Collagenase Perfusion.* Comp Hepatol, 2004. **3 Suppl 1**: p. S34.
180. Malarkey, D.E., et al., *New insights into functional aspects of liver morphology.* Toxicol Pathol, 2005. **33**(1): p. 27-34.
181. Gissen, P. and I.M. Arias, *Structural and functional hepatocyte polarity and liver disease.* J Hepatol, 2015. **63**(4): p. 1023-37.
182. Piel, M., D. Fletcher, and J. Doh, *Microfluidics in Cell Biology: Part A: Microfluidics for Multicellular Systems*. 2018: Academic Press.
183. Smedsrod, B., et al., *Scavenger functions of the liver endothelial cell.* Biochem J, 1990. **266**(2): p. 313-27.
184. Poisson, J., et al., *Liver sinusoidal endothelial cells: Physiology and role in liver diseases.* J Hepatol, 2017. **66**(1): p. 212-227.
185. Dixon, L.J., et al., *Kupffer cells in the liver.* Compr Physiol, 2013. **3**(2): p. 785-97.
186. Horst, A.K., et al., *Modulation of liver tolerance by conventional and nonconventional antigen-presenting cells and regulatory immune cells.* Cellular & Molecular Immunology, 2016. **13**(3): p. 277-292.
187. Wake, K., *Karl Wilhelm Kupffer And His Contributions To Modern Hepatology.* Comp Hepatol, 2004. **3 Suppl 1**: p. S2.
188. Tsuchida, T. and S.L. Friedman, *Mechanisms of hepatic stellate cell activation.* Nat Rev Gastroenterol Hepatol, 2017. **14**(7): p. 397-411.
189. Han, H.S., et al., *Regulation of glucose metabolism from a liver-centric perspective.* Exp Mol Med, 2016. **48**: p. e218.
190. Ameer, F., et al., *De novo lipogenesis in health and disease.* Metabolism, 2014. **63**(7): p. 895-902.
191. Sassa, T. and A. Kihara, *Metabolism of very long-chain Fatty acids: genes and pathophysiology.* Biomol Ther (Seoul), 2014. **22**(2): p. 83-92.
192. Sun, Z. and M.A. Lazar, *Dissociating fatty liver and diabetes.* Trends Endocrinol Metab, 2013. **24**(1): p. 4-12.

193. Reddy, J.K. and M.S. Rao, *Lipid metabolism and liver inflammation. II. Fatty liver disease and fatty acid oxidation.* Am J Physiol Gastrointest Liver Physiol, 2006. **290**(5): p. G852-8.
194. Dentin, R., J. Girard, and C. Postic, *Carbohydrate responsive element binding protein (ChREBP) and sterol regulatory element binding protein-1c (SREBP-1c): two key regulators of glucose metabolism and lipid synthesis in liver.* Biochimie, 2005. **87**(1): p. 81-6.
195. Santoleri, D. and P.M. Titchenell, *Resolving the Paradox of Hepatic Insulin Resistance.* Cell Mol Gastroenterol Hepatol, 2019. **7**(2): p. 447-456.
196. Yecies, J.L., et al., *Akt stimulates hepatic SREBP1c and lipogenesis through parallel mTORC1-dependent and independent pathways.* Cell Metab, 2011. **14**(1): p. 21-32.
197. Nogueiras, R., M. López, and C. Diéguez, *Regulation of lipid metabolism by energy availability: a role for the central nervous system.* Obes Rev, 2010. **11**(3): p. 185-201.
198. Lee, S.B., et al., *Intermittent restraint-induced sympathetic activation attenuates hepatic steatosis and inflammation in a high-fat diet-fed mouse model.* Am J Physiol Gastrointest Liver Physiol, 2019. **317**(6): p. G811-g823.
199. Jensen, K.J., G. Alpini, and S. Glaser, *Hepatic nervous system and neurobiology of the liver.* Comprehensive Physiology, 2013. **3**(2): p. 655-665.
200. Soty, M., et al., *Gut-Brain Glucose Signaling in Energy Homeostasis.* Cell Metab, 2017. **25**(6): p. 1231-1242.
201. Troy, S., et al., *Intestinal gluconeogenesis is a key factor for early metabolic changes after gastric bypass but not after gastric lap-band in mice.* Cell Metab, 2008. **8**(3): p. 201-11.
202. Duraffourd, C., et al., *Mu-opioid receptors and dietary protein stimulate a gut-brain neural circuitry limiting food intake.* Cell, 2012. **150**(2): p. 377-88.
203. Vily-Petit, J., et al., *Intestinal gluconeogenesis prevents obesity-linked liver steatosis and non-alcoholic fatty liver disease.* Gut, 2020: p. gutjnl-2019-319745.
204. Li, T. and J.Y. Chiang, *Bile acid signaling in metabolic disease and drug therapy.* Pharmacol Rev, 2014. **66**(4): p. 948-83.
205. Chen, M.L., K. Takeda, and M.S. Sundrud, *Emerging roles of bile acids in mucosal immunity and inflammation.* Mucosal Immunol, 2019. **12**(4): p. 851-861.
206. Wahlstrom, A., et al., *Intestinal Crosstalk between Bile Acids and Microbiota and Its Impact on Host Metabolism.* Cell Metab, 2016. **24**(1): p. 41-50.
207. Luo, J., H. Yang, and B.L. Song, *Mechanisms and regulation of cholesterol homeostasis.* Nat Rev Mol Cell Biol, 2020. **21**(4): p. 225-245.
208. Spann, N.J. and C.K. Glass, *Sterols and oxysterols in immune cell function.* Nat Immunol, 2013. **14**(9): p. 893-900.
209. Radhakrishnan, A., et al., *Sterol-regulated transport of SREBPs from endoplasmic reticulum to Golgi: oxysterols block transport by binding to Insig.* Proc Natl Acad Sci U S A, 2007. **104**(16): p. 6511-8.
210. Goldstein, J.L. and M.S. Brown, *The LDL receptor.* Arterioscler Thromb Vasc Biol, 2009. **29**(4): p. 431-8.
211. Wang, B. and P. Tontonoz, *Liver X receptors in lipid signalling and membrane homeostasis.* Nat Rev Endocrinol, 2018. **14**(8): p. 452-463.
212. Hong, C. and P. Tontonoz, *Liver X receptors in lipid metabolism: opportunities for drug discovery.* Nat Rev Drug Discov, 2014. **13**(6): p. 433-44.
213. Wang, J., et al., *Relative roles of ABCG5/ABCG8 in liver and intestine.* J Lipid Res, 2015. **56**(2): p. 319-30.
214. Peet, D.J., et al., *Cholesterol and bile acid metabolism are impaired in mice lacking the nuclear oxysterol receptor LXR alpha.* Cell, 1998. **93**(5): p. 693-704.
215. Willinger, T., *Oxysterols in intestinal immunity and inflammation.* J Intern Med, 2019. **285**(4): p. 367-380.
216. Guillemot-Legris, O., V. Mutemberezi, and G.G. Muccioli, *Oxysterols in Metabolic Syndrome: From Bystander Molecules to Bioactive Lipids.* Trends Mol Med, 2016. **22**(7): p. 594-614.

217. Mutemberezi, V., O. Guillemot-Legris, and G.G. Muccioli, *Oxysterols: From cholesterol metabolites to key mediators.* Prog Lipid Res, 2016. **64**: p. 152-169.
218. Chu, K., et al., *Stearoyl-coenzyme A desaturase 1 deficiency protects against hypertriglyceridemia and increases plasma high-density lipoprotein cholesterol induced by liver X receptor activation.* Mol Cell Biol, 2006. **26**(18): p. 6786-98.
219. Joseph, S.B., et al., *Direct and indirect mechanisms for regulation of fatty acid synthase gene expression by liver X receptors.* J Biol Chem, 2002. **277**(13): p. 11019-25.
220. Yoshikawa, T., et al., *Identification of liver X receptor-retinoid X receptor as an activator of the sterol regulatory element-binding protein 1c gene promoter.* Molecular and cellular biology, 2001. **21**(9): p. 2991-3000.
221. Jakobsson, T., et al., *Liver X receptor biology and pharmacology: new pathways, challenges and opportunities.* Trends Pharmacol Sci, 2012. **33**(7): p. 394-404.
222. Patel, R., et al., *LXRβ is required for glucocorticoid-induced hyperglycemia and hepatosteatosis in mice.* J Clin Invest, 2011. **121**(1): p. 431-41.
223. Wang, Y., et al., *Modulation of retinoic acid receptor-related orphan receptor alpha and gamma activity by 7-oxygenated sterol ligands.* The Journal of biological chemistry, 2010. **285**(7): p. 5013-5025.
224. Kase, E.T., et al., *Liver X receptor antagonist reduces lipid formation and increases glucose metabolism in myotubes from lean, obese and type 2 diabetic individuals.* Diabetologia, 2007. **50**(10): p. 2171-2180.
225. Shirouchi, B., et al., *27-Hydroxycholesterol suppresses lipid accumulation by down-regulating lipogenic and adipogenic gene expression in 3T3-L1 cells.* Cytotechnology, 2017. **69**(3): p. 485-492.
226. Ito, A., et al., *LXRs link metabolism to inflammation through Abca1-dependent regulation of membrane composition and TLR signaling.* Elife, 2015. **4**: p. e08009.
227. Treuter, E., *New wrestling rules of anti-inflammatory transrepression by oxysterol receptor LXR revealed.* Cell Res, 2011. **21**(5): p. 711-4.
228. Cyster, J.G., et al., *25-Hydroxycholesterols in innate and adaptive immunity.* Nat Rev Immunol, 2014. **14**(11): p. 731-43.
229. Tremblay-Franco, M., et al., *Effect of obesity and metabolic syndrome on plasma oxysterols and fatty acids in human.* Steroids, 2015. **99**(Pt B): p. 287-92.
230. Guillemot-Legris, O., et al., *Obesity is associated with changes in oxysterol metabolism and levels in mice liver, hypothalamus, adipose tissue and plasma.* Sci Rep, 2016. **6**: p. 19694.
231. Mutemberezi, V., et al., *Development and validation of an HPLC-MS method for the simultaneous quantification of key oxysterols, endocannabinoids, and ceramides: variations in metabolic syndrome.* Anal Bioanal Chem, 2016. **408**(3): p. 733-45.
232. Murakami, H., et al., *Plasma oxysterols and tocopherol in patients with diabetes mellitus and hyperlipidemia.* Lipids, 2000. **35**(3): p. 333-8.
233. Bertolotti, M., et al., *Increased appearance rate of 27-hydroxycholesterol in vivo in hypercholesterolemia: a possible compensatory mechanism.* Nutr Metab Cardiovasc Dis, 2012. **22**(10): p. 823-30.
234. Ikegami, T., et al., *Increased serum liver X receptor ligand oxysterols in patients with non-alcoholic fatty liver disease.* J Gastroenterol, 2012. **47**(11): p. 1257-66.
235. Griffiths, W.J. and Y. Wang, *Oxysterol research: a brief review.* Biochemical Society transactions, 2019. **47**(2): p. 517-526.
236. Russell, D.W., *The enzymes, regulation, and genetics of bile acid synthesis.* Annu Rev Biochem, 2003. **72**: p. 137-74.
237. Schaap, F.G., M. Trauner, and P.L. Jansen, *Bile acid receptors as targets for drug development.* Nat Rev Gastroenterol Hepatol, 2014. **11**(1): p. 55-67.
238. Li-Hawkins, J., et al., *Cholic acid mediates negative feedback regulation of bile acid synthesis in mice.* J Clin Invest, 2002. **110**(8): p. 1191-200.

239. Pandak, W.M. and G. Kakiyama, *The acidic pathway of bile acid synthesis: Not just an alternative pathway().* Liver Res, 2019. **3**(2): p. 88-98.
240. de Aguiar Vallim, T.Q., E.J. Tarling, and P.A. Edwards, *Pleiotropic roles of bile acids in metabolism.* Cell Metab, 2013. **17**(5): p. 657-69.
241. Kurdi, P., et al., *Mechanism of growth inhibition by free bile acids in lactobacilli and bifidobacteria.* J Bacteriol, 2006. **188**(5): p. 1979-86.
242. Ridlon, J.M., et al., *Bile acids and the gut microbiome.* Curr Opin Gastroenterol, 2014. **30**(3): p. 332-8.
243. Chiang, J.Y., *Bile acids: regulation of synthesis.* J Lipid Res, 2009. **50**(10): p. 1955-66.
244. Lin, B.C., et al., *Liver-specific activities of FGF19 require Klotho beta.* J Biol Chem, 2007. **282**(37): p. 27277-84.
245. Kong, B., et al., *Mechanism of tissue-specific farnesoid X receptor in suppressing the expression of genes in bile-acid synthesis in mice.* Hepatology, 2012. **56**(3): p. 1034-43.
246. Sayin, S.I., et al., *Gut microbiota regulates bile acid metabolism by reducing the levels of tauro-beta-muricholic acid, a naturally occurring FXR antagonist.* Cell Metab, 2013. **17**(2): p. 225-35.
247. Sinal, C.J., et al., *Targeted disruption of the nuclear receptor FXR/BAR impairs bile acid and lipid homeostasis.* Cell, 2000. **102**(6): p. 731-44.
248. Kok, T., et al., *Enterohepatic circulation of bile salts in farnesoid X receptor-deficient mice: efficient intestinal bile salt absorption in the absence of ileal bile acid-binding protein.* J Biol Chem, 2003. **278**(43): p. 41930-7.
249. Zhang, Y., et al., *Activation of the nuclear receptor FXR improves hyperglycemia and hyperlipidemia in diabetic mice.* Proc Natl Acad Sci U S A, 2006. **103**(4): p. 1006-11.
250. Ma, K., et al., *Farnesoid X receptor is essential for normal glucose homeostasis.* J Clin Invest, 2006. **116**(4): p. 1102-9.
251. Pircher, P.C., et al., *Farnesoid X receptor regulates bile acid-amino acid conjugation.* J Biol Chem, 2003. **278**(30): p. 27703-11.
252. Ananthanarayanan, M., et al., *Human bile salt export pump promoter is transactivated by the farnesoid X receptor/bile acid receptor.* J Biol Chem, 2001. **276**(31): p. 28857-65.
253. Denson, L.A., et al., *The orphan nuclear receptor, shp, mediates bile acid-induced inhibition of the rat bile acid transporter, ntcp.* Gastroenterology, 2001. **121**(1): p. 140-7.
254. Watanabe, M., et al., *Bile acids lower triglyceride levels via a pathway involving FXR, SHP, and SREBP-1c.* J Clin Invest, 2004. **113**(10): p. 1408-18.
255. Caron, S., et al., *Farnesoid X receptor inhibits the transcriptional activity of carbohydrate response element binding protein in human hepatocytes.* Mol Cell Biol, 2013. **33**(11): p. 2202-11.
256. Pineda Torra, I., et al., *Bile acids induce the expression of the human peroxisome proliferator-activated receptor alpha gene via activation of the farnesoid X receptor.* Mol Endocrinol, 2003. **17**(2): p. 259-72.
257. Yamagata, K., et al., *Bile acids regulate gluconeogenic gene expression via small heterodimer partner-mediated repression of hepatocyte nuclear factor 4 and Foxo1.* J Biol Chem, 2004. **279**(22): p. 23158-65.
258. Stayrook, K.R., et al., *Regulation of carbohydrate metabolism by the farnesoid X receptor.* Endocrinology, 2005. **146**(3): p. 984-91.
259. Cariou, B., et al., *The farnesoid X receptor modulates adiposity and peripheral insulin sensitivity in mice.* J Biol Chem, 2006. **281**(16): p. 11039-49.
260. Wang, Y.D., et al., *Farnesoid X receptor antagonizes nuclear factor kappaB in hepatic inflammatory response.* Hepatology, 2008. **48**(5): p. 1632-43.
261. Mencarelli, A., et al., *Antiatherosclerotic effect of farnesoid X receptor.* Am J Physiol Heart Circ Physiol, 2009. **296**(2): p. H272-81.
262. Adorini, L., M. Pruzanski, and D. Shapiro, *Farnesoid X receptor targeting to treat nonalcoholic steatohepatitis.* Drug Discov Today, 2012. **17**(17-18): p. 988-97.

263. Cipriani, S., et al., *FXR activation reverses insulin resistance and lipid abnormalities and protects against liver steatosis in Zucker (fa/fa) obese rats.* J Lipid Res, 2010. **51**(4): p. 771-84.
264. Mudaliar, S., et al., *Efficacy and safety of the farnesoid X receptor agonist obeticholic acid in patients with type 2 diabetes and nonalcoholic fatty liver disease.* Gastroenterology, 2013. **145**(3): p. 574-82 e1.
265. Hindson, J., *Obeticholic acid for the treatment of NASH.* Nature Reviews Gastroenterology & Hepatology, 2020. **17**(2): p. 66-66.
266. Prawitt, J., et al., *Farnesoid X receptor deficiency improves glucose homeostasis in mouse models of obesity.* Diabetes, 2011. **60**(7): p. 1861-71.
267. Watanabe, M., et al., *Lowering bile acid pool size with a synthetic farnesoid X receptor (FXR) agonist induces obesity and diabetes through reduced energy expenditure.* J Biol Chem, 2011. **286**(30): p. 26913-20.
268. Jiang, C., et al., *Intestinal farnesoid X receptor signaling promotes nonalcoholic fatty liver disease.* J Clin Invest, 2015. **125**(1): p. 386-402.
269. Jiang, C., et al., *Intestine-selective farnesoid X receptor inhibition improves obesity-related metabolic dysfunction.* Nat Commun, 2015. **6**: p. 10166.
270. Fang, S., et al., *Intestinal FXR agonism promotes adipose tissue browning and reduces obesity and insulin resistance.* Nat Med, 2015. **21**(2): p. 159-65.
271. Pathak, P., et al., *Intestine farnesoid X receptor agonist and the gut microbiota activate G-protein bile acid receptor-1 signaling to improve metabolism.* Hepatology, 2018.
272. Maruyama, T., et al., *Identification of membrane-type receptor for bile acids (M-BAR).* Biochem Biophys Res Commun, 2002. **298**(5): p. 714-9.
273. Kawamata, Y., et al., *A G protein-coupled receptor responsive to bile acids.* J Biol Chem, 2003. **278**(11): p. 9435-40.
274. Watanabe, M., et al., *Bile acids induce energy expenditure by promoting intracellular thyroid hormone activation.* Nature, 2006. **439**(7075): p. 484-9.
275. Pols, T.W., et al., *TGR5 activation inhibits atherosclerosis by reducing macrophage inflammation and lipid loading.* Cell Metab, 2011. **14**(6): p. 747-57.
276. Wang, Y.D., et al., *The G-protein-coupled bile acid receptor, Gpbar1 (TGR5), negatively regulates hepatic inflammatory response through antagonizing nuclear factor kappa light-chain enhancer of activated B cells (NF-kappaB) in mice.* Hepatology, 2011. **54**(4): p. 1421-32.
277. Katsuma, S., A. Hirasawa, and G. Tsujimoto, *Bile acids promote glucagon-like peptide-1 secretion through TGR5 in a murine enteroendocrine cell line STC-1.* Biochem Biophys Res Commun, 2005. **329**(1): p. 386-90.
278. Thomas, C., et al., *TGR5-mediated bile acid sensing controls glucose homeostasis.* Cell Metab, 2009. **10**(3): p. 167-77.
279. Veilleux, A., V. Di Marzo, and C. Silvestri, *The Expanded Endocannabinoid System/Endocannabinoidome as a Potential Target for Treating Diabetes Mellitus.* Curr Diab Rep, 2019. **19**(11): p. 117.
280. Cristino, L., T. Bisogno, and V. Di Marzo, *Cannabinoids and the expanded endocannabinoid system in neurological disorders.* Nat Rev Neurol, 2020. **16**(1): p. 9-29.
281. Di Marzo, V., *New approaches and challenges to targeting the endocannabinoid system.* Nat Rev Drug Discov, 2018. **17**(9): p. 623-639.
282. Munro, S., K.L. Thomas, and M. Abu-Shaar, *Molecular characterization of a peripheral receptor for cannabinoids.* Nature, 1993. **365**(6441): p. 61-5.
283. Matsuda, L.A., et al., *Structure of a cannabinoid receptor and functional expression of the cloned cDNA.* Nature, 1990. **346**(6284): p. 561-4.
284. Mechoulam, R., et al., *Identification of an endogenous 2-monoglyceride, present in canine gut, that binds to cannabinoid receptors.* Biochem Pharmacol, 1995. **50**(1): p. 83-90.
285. Devane, W.A., et al., *Isolation and structure of a brain constituent that binds to the cannabinoid receptor.* Science, 1992. **258**(5090): p. 1946-9.

286. Sugiura, T., et al., *2-Arachidonoylglycerol: a possible endogenous cannabinoid receptor ligand in brain.* Biochem Biophys Res Commun, 1995. **215**(1): p. 89-97.
287. Di Marzo, V. and A. Fontana, *Anandamide, an endogenous cannabinomimetic eicosanoid: 'killing two birds with one stone'.* Prostaglandins Leukot Essent Fatty Acids, 1995. **53**(1): p. 1-11.
288. Pertwee, R.G., et al., *International Union of Basic and Clinical Pharmacology. LXXIX. Cannabinoid receptors and their ligands: beyond CB(1) and CB(2).* Pharmacol Rev, 2010. **62**(4): p. 588-631.
289. Ligresti, A., L. De Petrocellis, and V. Di Marzo, *From Phytocannabinoids to Cannabinoid Receptors and Endocannabinoids: Pleiotropic Physiological and Pathological Roles Through Complex Pharmacology.* Physiol Rev, 2016. **96**(4): p. 1593-659.
290. Schmid, H.H., *Pathways and mechanisms of N-acylethanolamine biosynthesis: can anandamide be generated selectively?* Chem Phys Lipids, 2000. **108**(1-2): p. 71-87.
291. Geurts, L., et al., *Adipose tissue NAPE-PLD controls fat mass development by altering the browning process and gut microbiota.* Nat Commun, 2015. **6**: p. 6495.
292. Everard, A., et al., *Intestinal epithelial N-acylphosphatidylethanolamine phospholipase D links dietary fat to metabolic adaptations in obesity and steatosis.* Nat Commun, 2019. **10**(1): p. 457.
293. Maccarrone, M., *Missing Pieces to the Endocannabinoid Puzzle.* Trends Mol Med, 2020. **26**(3): p. 263-272.
294. Yates, M.L. and E.L. Barker, *Organized trafficking of anandamide and related lipids.* Vitam Horm, 2009. **81**: p. 25-53.
295. Oddi, S., et al., *Evidence for the intracellular accumulation of anandamide in adiposomes.* Cell Mol Life Sci, 2008. **65**(5): p. 840-50.
296. Okamoto, Y., et al., *Molecular characterization of a phospholipase D generating anandamide and its congeners.* J Biol Chem, 2004. **279**(7): p. 5298-305.
297. Rahman, I.A., et al., *New players in the fatty acyl ethanolamide metabolism.* Pharmacol Res, 2014. **86**: p. 1-10.
298. Hussain, Z., et al., *Mammalian enzymes responsible for the biosynthesis of N-acylethanolamines.* Biochim Biophys Acta Mol Cell Biol Lipids, 2017. **1862**(12): p. 1546-1561.
299. Leung, D., et al., *Inactivation of N-acyl phosphatidylethanolamine phospholipase D reveals multiple mechanisms for the biosynthesis of endocannabinoids.* Biochemistry, 2006. **45**(15): p. 4720-6.
300. Tsuboi, K., et al., *Enzymatic formation of N-acylethanolamines from N-acylethanolamine plasmalogen through N-acylphosphatidylethanolamine-hydrolyzing phospholipase D-dependent and -independent pathways.* Biochim Biophys Acta, 2011. **1811**(10): p. 565-77.
301. Muccioli, G.G., *Endocannabinoid biosynthesis and inactivation, from simple to complex.* Drug Discov Today, 2010. **15**(11-12): p. 474-83.
302. Cravatt, B.F., et al., *Molecular characterization of an enzyme that degrades neuromodulatory fatty-acid amides.* Nature, 1996. **384**(6604): p. 83-7.
303. Ueda, N., et al., *An acid amidase hydrolyzing anandamide as an endogenous ligand for cannabinoid receptors.* FEBS Lett, 1999. **454**(3): p. 267-70.
304. Tsuboi, K., et al., *Molecular characterization of N-acylethanolamine-hydrolyzing acid amidase, a novel member of the choloylglycine hydrolase family with structural and functional similarity to acid ceramidase.* J Biol Chem, 2005. **280**(12): p. 11082-92.
305. Bisogno, T., et al., *Cloning of the first sn1-DAG lipases points to the spatial and temporal regulation of endocannabinoid signaling in the brain.* J Cell Biol, 2003. **163**(3): p. 463-8.
306. Dinh, T.P., et al., *Brain monoglyceride lipase participating in endocannabinoid inactivation.* Proc Natl Acad Sci U S A, 2002. **99**(16): p. 10819-24.
307. Navia-Paldanius, D., J.R. Savinainen, and J.T. Laitinen, *Biochemical and pharmacological characterization of human alpha/beta-hydrolase domain containing 6 (ABHD6) and 12 (ABHD12).* J Lipid Res, 2012. **53**(11): p. 2413-24.

308. Kozak, K.R., J.J. Prusakiewicz, and L.J. Marnett, *Oxidative metabolism of endocannabinoids by COX-2.* Curr Pharm Des, 2004. **10**(6): p. 659-67.
309. Ueda, N., et al., *Lipoxygenase-catalyzed oxygenation of arachidonylethanolamide, a cannabinoid receptor agonist.* Biochim Biophys Acta, 1995. **1254**(2): p. 127-34.
310. Snider, N.T., V.J. Walker, and P.F. Hollenberg, *Oxidation of the endogenous cannabinoid arachidonoyl ethanolamide by the cytochrome P450 monooxygenases: physiological and pharmacological implications.* Pharmacol Rev, 2010. **62**(1): p. 136-54.
311. Urquhart, P., A. Nicolaou, and D.F. Woodward, *Endocannabinoids and their oxygenation by cyclo-oxygenases, lipoxygenases and other oxygenases.* Biochim Biophys Acta, 2015. **1851**(4): p. 366-76.
312. Di Marzo, V. and J. Wang, *The endocannabinoidome: the world of endocannabinoids and related mediators*. 2014: Academic Press.
313. Schmid, P.C., et al., *Metabolism of N-acylethanolamine phospholipids by a mammalian phosphodiesterase of the phospholipase D type.* J Biol Chem, 1983. **258**(15): p. 9302-6.
314. Magotti, P., et al., *Structure of human N-acylphosphatidylethanolamine-hydrolyzing phospholipase D: regulation of fatty acid ethanolamide biosynthesis by bile acids.* Structure, 2015. **23**(3): p. 598-604.
315. Okamoto, Y., et al., *Biosynthetic pathways of the endocannabinoid anandamide.* Chem Biodivers, 2007. **4**(8): p. 1842-57.
316. McPartland, J.M., et al., *Evolutionary origins of the endocannabinoid system.* Gene, 2006. **370**: p. 64-74.
317. Wang, J., et al., *Functional analysis of the purified anandamide-generating phospholipase D as a member of the metallo-beta-lactamase family.* J Biol Chem, 2006. **281**(18): p. 12325-35.
318. Margheritis, E., et al., *Bile Acid Recognition by NAPE-PLD.* ACS Chem Biol, 2016. **11**(10): p. 2908-2914.
319. Setchell, K.D., et al., *Bile acid concentrations in human and rat liver tissue and in hepatocyte nuclei.* Gastroenterology, 1997. **112**(1): p. 226-35.
320. Northfield, T.C. and I. McColl, *Postprandial concentrations of free and conjugated bile acids down the length of the normal human small intestine.* Gut, 1973. **14**(7): p. 513-8.
321. Jiao, N., et al., *Suppressed hepatic bile acid signalling despite elevated production of primary and secondary bile acids in NAFLD.* Gut, 2018. **67**(10): p. 1881-1891.
322. Aggarwal, G., et al., *Symmetrically substituted dichlorophenes inhibit N-acyl-phosphatidylethanolamine phospholipase D.* J Biol Chem, 2020. **295**(21): p. 7289-7300.
323. Castellani, B., et al., *Synthesis and characterization of the first inhibitor of N-acylphosphatidylethanolamine phospholipase D (NAPE-PLD).* Chem Commun (Camb), 2017. **53**(95): p. 12814-12817.
324. Mock, E.D., et al., *Discovery of a NAPE-PLD inhibitor that modulates emotional behavior in mice.* Nat Chem Biol, 2020. **16**(6): p. 667-675.
325. Leishman, E., et al., *Lipidomics profile of a NAPE-PLD KO mouse provides evidence of a broader role of this enzyme in lipid metabolism in the brain.* Biochim Biophys Acta, 2016. **1861**(6): p. 491-500.
326. Inoue, M., et al., *Peripheral tissue levels and molecular species compositions of N-acyl-phosphatidylethanolamine and its metabolites in mice lacking N-acyl-phosphatidylethanolamine-specific phospholipase D.* J Biochem, 2017. **162**(6): p. 449-458.
327. Fu, J., et al., *Food intake regulates oleoylethanolamide formation and degradation in the proximal small intestine.* J Biol Chem, 2007. **282**(2): p. 1518-28.
328. Zhu, C., et al., *Proinflammatory stimuli control N-acylphosphatidylethanolamine-specific phospholipase D expression in macrophages.* Mol Pharmacol, 2011. **79**(4): p. 786-92.
329. Wangensteen, T., et al., *A common haplotype in NAPEPLD is associated with severe obesity in a Norwegian population-based cohort (the HUNT study).* Obesity (Silver Spring), 2011. **19**(3): p. 612-7.

330. Reggio, P.H., *Endocannabinoid binding to the cannabinoid receptors: what is known and what remains unknown.* Curr Med Chem, 2010. **17**(14): p. 1468-86.
331. Motter, A.L. and G.P. Ahern, *TRPV1-null mice are protected from diet-induced obesity.* FEBS Lett, 2008. **582**(15): p. 2257-62.
332. Lee, E., et al., *Transient receptor potential vanilloid type-1 channel regulates diet-induced obesity, insulin resistance, and leptin resistance.* FASEB J, 2015. **29**(8): p. 3182-92.
333. DiPatrizio, N.V., et al., *Endocannabinoid signal in the gut controls dietary fat intake.* Proc Natl Acad Sci U S A, 2011. **108**(31): p. 12904-8.
334. Avalos, B., et al., *Cannabinoid CB(1) Receptors in the Intestinal Epithelium Are Required for Acute Western-Diet Preferences in Mice.* Nutrients, 2020. **12**(9).
335. Schwartz, G.J., et al., *The lipid messenger OEA links dietary fat intake to satiety.* Cell Metab, 2008. **8**(4): p. 281-288.
336. Hansen, H.S., *Role of anorectic N-acylethanolamines in intestinal physiology and satiety control with respect to dietary fat.* Pharmacol Res, 2014. **86**: p. 18-25.
337. Everard, A., et al., *Cross-talk between Akkermansia muciniphila and intestinal epithelium controls diet-induced obesity.* Proc Natl Acad Sci U S A, 2013. **110**(22): p. 9066-71.
338. Karwad, M.A., et al., *Oleoylethanolamine and palmitoylethanolamine modulate intestinal permeability in vitro via TRPV1 and PPARalpha.* FASEB J, 2017. **31**(2): p. 469-481.
339. Lan, H., et al., *Agonists at GPR119 mediate secretion of GLP-1 from mouse enteroendocrine cells through glucose-independent pathways.* Br J Pharmacol, 2012. **165**(8): p. 2799-807.
340. Hansen, H.S., et al., *GPR119 as a fat sensor.* Trends Pharmacol Sci, 2012. **33**(7): p. 374-81.
341. Wang, P., et al., *Transient receptor potential vanilloid 1 activation enhances gut glucagon-like peptide-1 secretion and improves glucose homeostasis.* Diabetes, 2012. **61**(8): p. 2155-65.
342. Sykaras, A.G., et al., *Duodenal enteroendocrine I-cells contain mRNA transcripts encoding key endocannabinoid and fatty acid receptors.* PLoS One, 2012. **7**(8): p. e42373.
343. Argueta, D.A., et al., *Cannabinoid CB1 Receptors Inhibit Gut-Brain Satiation Signaling in Diet-Induced Obesity.* Frontiers in Physiology, 2019. **10**(704).
344. Duszka, K., et al., *PPARgamma Modulates Long Chain Fatty Acid Processing in the Intestinal Epithelium.* Int J Mol Sci, 2017. **18**(12).
345. Cluny, N.L., et al., *Naphthalen-1-yl-(4-pentyloxynaphthalen-1-yl)methanone (SAB378), a peripherally restricted cannabinoid CB1/CB2 receptor agonist, inhibits gastrointestinal motility but has no effect on experimental colitis in mice.* J Pharmacol Exp Ther, 2010. **334**(3): p. 973-80.
346. Duncan, M., et al., *Cannabinoid CB2 receptors in the enteric nervous system modulate gastrointestinal contractility in lipopolysaccharide-treated rats.* Am J Physiol Gastrointest Liver Physiol, 2008. **295**(1): p. G78-G87.
347. Lin, X.H., et al., *A novel CB receptor GPR55 and its ligands are involved in regulation of gut movement in rodents.* Neurogastroenterol Motil, 2011. **23**(9): p. 862-e342.
348. Stančić, A., et al., *The GPR55 antagonist CID16020046 protects against intestinal inflammation.* Neurogastroenterology and motility : the official journal of the European Gastrointestinal Motility Society, 2015. **27**(10): p. 1432-1445.
349. Grunewald, Z.I., et al., *Cannabinoid receptor type-1 partially mediates metabolic endotoxemia-induced inflammation and insulin resistance.* Physiol Behav, 2019. **199**: p. 282-291.
350. Karwad, M.A., et al., *The role of CB1 in intestinal permeability and inflammation.* FASEB J, 2017. **31**(8): p. 3267-3277.
351. Maccarrone, M., et al., *Endocannabinoid signaling at the periphery: 50 years after THC.* Trends Pharmacol Sci, 2015. **36**(5): p. 277-96.
352. Osei-Hyiaman, D., et al., *Endocannabinoid activation at hepatic CB1 receptors stimulates fatty acid synthesis and contributes to diet-induced obesity.* Journal of Clinical Investigation, 2005. **115**(5): p. 1298-1305.

353. Osei-Hyiaman, D., et al., *Hepatic CB1 receptor is required for development of diet-induced steatosis, dyslipidemia, and insulin and leptin resistance in mice.* J Clin Invest, 2008. **118**(9): p. 3160-9.
354. Ravinet Trillou, C., et al., *CB1 cannabinoid receptor knockout in mice leads to leanness, resistance to diet-induced obesity and enhanced leptin sensitivity.* Int J Obes Relat Metab Disord, 2004. **28**(4): p. 640-8.
355. Liu, J., et al., *Hepatic cannabinoid receptor-1 mediates diet-induced insulin resistance via inhibition of insulin signaling and clearance in mice.* Gastroenterology, 2012. **142**(5): p. 1218-1228 e1.
356. Teixeira-Clerc, F., et al., *CB1 cannabinoid receptor antagonism: a new strategy for the treatment of liver fibrosis.* Nat Med, 2006. **12**(6): p. 671-6.
357. Jourdan, T., et al., *CB1 antagonism exerts specific molecular effects on visceral and subcutaneous fat and reverses liver steatosis in diet-induced obese mice.* Diabetes, 2010. **59**(4): p. 926-34.
358. Tam, J., et al., *Peripheral cannabinoid-1 receptor inverse agonism reduces obesity by reversing leptin resistance.* Cell Metab, 2012. **16**(2): p. 167-79.
359. Tam, J., et al., *Peripheral CB1 cannabinoid receptor blockade improves cardiometabolic risk in mouse models of obesity.* J Clin Invest, 2010. **120**(8): p. 2953-66.
360. Lipina, C., et al., *CB1 receptor blockade counters age-induced insulin resistance and metabolic dysfunction.* Aging Cell, 2016. **15**(2): p. 325-35.
361. Julien, B., et al., *Antifibrogenic role of the cannabinoid receptor CB2 in the liver.* Gastroenterology, 2005. **128**(3): p. 742-55.
362. Guillot, A., et al., *Cannabinoid receptor 2 counteracts interleukin-17-induced immune and fibrogenic responses in mouse liver.* Hepatology, 2014. **59**(1): p. 296-306.
363. Louvet, A., et al., *Cannabinoid CB2 receptors protect against alcoholic liver disease by regulating Kupffer cell polarization in mice.* Hepatology, 2011. **54**(4): p. 1217-26.
364. Pawlak, M., P. Lefebvre, and B. Staels, *Molecular mechanism of PPARalpha action and its impact on lipid metabolism, inflammation and fibrosis in non-alcoholic fatty liver disease.* J Hepatol, 2015. **62**(3): p. 720-33.
365. Montagner, A., et al., *Liver PPARalpha is crucial for whole-body fatty acid homeostasis and is protective against NAFLD.* Gut, 2016. **65**(7): p. 1202-14.
366. Régnier, M., et al., *Hepatocyte-specific deletion of Pparα promotes NAFLD in the context of obesity.* Scientific Reports, 2020. **10**(1): p. 6489.
367. Yang, J.W., et al., *GPR119: a promising target for nonalcoholic fatty liver disease.* FASEB J, 2016. **30**(1): p. 324-35.
368. Li, N.X., et al., *GPR119 Agonism Increases Glucagon Secretion During Insulin-Induced Hypoglycemia.* Diabetes, 2018. **67**(7): p. 1401-1413.
369. Liu, B., et al., *GPR55-dependent stimulation of insulin secretion from isolated mouse and human islets of Langerhans.* Diabetes Obes Metab, 2016. **18**(12): p. 1263-1273.
370. Lipina, C., et al., *GPR55 deficiency is associated with increased adiposity and impaired insulin signaling in peripheral metabolic tissues.* FASEB J, 2019. **33**(1): p. 1299-1312.
371. Gonzalez-Mariscal, I., et al., *Human CB1 Receptor Isoforms, present in Hepatocytes and beta-cells, are Involved in Regulating Metabolism.* Sci Rep, 2016. **6**: p. 33302.
372. Zhang, X., et al., *Cannabinoid 2 Receptor Agonist Improves Systemic Sensitivity to Insulin in High-Fat Diet/Streptozotocin-Induced Diabetic Mice.* Cell Physiol Biochem, 2016. **40**(5): p. 1175-1185.
373. Gonzalez-Mariscal, I. and J.M. Egan, *Endocannabinoids in the Islets of Langerhans: the ugly, the bad, and the good facts.* Am J Physiol Endocrinol Metab, 2018. **315**(2): p. E174-E179.
374. Pagano, C., M. Rossato, and R. Vettor, *Endocannabinoids, adipose tissue and lipid metabolism.* J Neuroendocrinol, 2008. **20 Suppl 1**: p. 124-9.

375. Tedesco, L., et al., *Cannabinoid type 1 receptor blockade promotes mitochondrial biogenesis through endothelial nitric oxide synthase expression in white adipocytes.* Diabetes, 2008. **57**(8): p. 2028-36.
376. Perwitz, N., et al., *Cannabinoid type 1 receptor blockade induces transdifferentiation towards a brown fat phenotype in white adipocytes.* Diabetes Obes Metab, 2010. **12**(2): p. 158-66.
377. Ruiz de Azua, I., et al., *Adipocyte cannabinoid receptor CB1 regulates energy homeostasis and alternatively activated macrophages.* J Clin Invest, 2017. **127**(11): p. 4148-4162.
378. Sharma, A.M. and B. Staels, *Review: Peroxisome proliferator-activated receptor gamma and adipose tissue--understanding obesity-related changes in regulation of lipid and glucose metabolism.* J Clin Endocrinol Metab, 2007. **92**(2): p. 386-95.
379. Ambrosino, P., et al., *Activation and desensitization of TRPV1 channels in sensory neurons by the PPARalpha agonist palmitoylethanolamide.* Br J Pharmacol, 2013. **168**(6): p. 1430-44.
380. Silveira, L.S., et al., *Effect of an acute moderate-exercise session on metabolic and inflammatory profile of PPAR-alpha knockout mice.* Cell Biochem Funct, 2017. **35**(8): p. 510-517.
381. Esposito, G., et al., *Palmitoylethanolamide improves colon inflammation through an enteric glia/toll like receptor 4-dependent PPAR-alpha activation.* Gut, 2014. **63**(8): p. 1300-12.
382. Lo Verme, J., et al., *The nuclear receptor peroxisome proliferator-activated receptor-alpha mediates the anti-inflammatory actions of palmitoylethanolamide.* Mol Pharmacol, 2005. **67**(1): p. 15-9.
383. Alhouayek, M. and G.G. Muccioli, *Harnessing the anti-inflammatory potential of palmitoylethanolamide.* Drug Discov Today, 2014. **19**(10): p. 1632-9.
384. Parlar, A., et al., *The exogenous administration of CB2 specific agonist, GW405833, inhibits inflammation by reducing cytokine production and oxidative stress.* Exp Ther Med, 2018. **16**(6): p. 4900-4908.
385. Bassaganya-Riera, J., et al., *PPAR gamma is highly expressed in F4/80(hi) adipose tissue macrophages and dampens adipose-tissue inflammation.* Cell Immunol, 2009. **258**(2): p. 138-46.
386. Leung, C., et al., *The role of the gut microbiota in NAFLD.* Nat Rev Gastroenterol Hepatol, 2016. **13**(7): p. 412-25.
387. Miura, K., et al., *Role of toll-like receptors and their downstream molecules in the development of nonalcoholic Fatty liver disease.* Gastroenterol Res Pract, 2010. **2010**: p. 362847.
388. Rinella, M.E. and A.J. Sanyal, *NAFLD in 2014: Genetics, diagnostics and therapeutic advances in NAFLD.* Nat Rev Gastroenterol Hepatol, 2015. **12**(2): p. 65-6.
389. Tilg, H., P.D. Cani, and E.A. Mayer, *Gut microbiome and liver diseases.* Gut, 2016. **65**(12): p. 2035-2044.
390. O'Neill, L.A., D. Golenbock, and A.G. Bowie, *The history of Toll-like receptors - redefining innate immunity.* Nat Rev Immunol, 2013. **13**(6): p. 453-60.
391. Duparc, T., et al., *Hepatocyte MyD88 affects bile acids, gut microbiota and metabolome contributing to regulate glucose and lipid metabolism.* Gut, 2017. **66**(4): p. 620-632.
392. Inagaki, T., et al., *Fibroblast growth factor 15 functions as an enterohepatic signal to regulate bile acid homeostasis.* Cell Metab, 2005. **2**(4): p. 217-25.
393. Guarda, G., et al., *Type I interferon inhibits interleukin-1 production and inflammasome activation.* Immunity, 2011. **34**(2): p. 213-23.
394. Reboldi, A., et al., *Inflammation. 25-Hydroxycholesterol suppresses interleukin-1-driven inflammation downstream of type I interferon.* Science, 2014. **345**(6197): p. 679-84.
395. Gold, E.S., et al., *25-Hydroxycholesterol acts as an amplifier of inflammatory signaling.* Proc Natl Acad Sci U S A, 2014. **111**(29): p. 10666-71.
396. Koarai, A., et al., *25-Hydroxycholesterol enhances cytokine release and Toll-like receptor 3 response in airway epithelial cells.* Respir Res, 2012. **13**: p. 63.

397. Bauman, D.R., et al., *25-Hydroxycholesterol secreted by macrophages in response to Toll-like receptor activation suppresses immunoglobulin A production.* Proc Natl Acad Sci U S A, 2009. **106**(39): p. 16764-9.
398. Diczfalusy, U., *On the formation and possible biological role of 25-hydroxycholesterol.* Biochimie, 2013. **95**(3): p. 455-60.
399. Diczfalusy, U., et al., *Marked upregulation of cholesterol 25-hydroxylase expression by lipopolysaccharide.* J Lipid Res, 2009. **50**(11): p. 2258-64.
400. Beaumont, M., et al., *The gut microbiota metabolite indole alleviates liver inflammation in mice.* FASEB J, 2018: p. fj201800544.
401. Tall, A.R. and L. Yvan-Charvet, *Cholesterol, inflammation and innate immunity.* Nat Rev Immunol, 2015. **15**(2): p. 104-16.
402. Brandl, K., V. Kumar, and L. Eckmann, *Gut-liver axis at the frontier of host-microbial interactions.* Am J Physiol Gastrointest Liver Physiol, 2017. **312**(5): p. G413-G419.
403. Folch, J., M. Lees, and G.H. Sloane Stanley, *A simple method for the isolation and purification of total lipides from animal tissues.* J Biol Chem, 1957. **226**(1): p. 497-509.
404. Gatta-Cherifi, B. and D. Cota, *New insights on the role of the endocannabinoid system in the regulation of energy balance.* Int J Obes (Lond), 2016. **40**(2): p. 210-9.
405. Jamshidi, N. and D.A. Taylor, *Anandamide administration into the ventromedial hypothalamus stimulates appetite in rats.* Br J Pharmacol, 2001. **134**(6): p. 1151-4.
406. Hansen, H.S. and T.A. Diep, *N-acylethanolamines, anandamide and food intake.* Biochem Pharmacol, 2009. **78**(6): p. 553-60.
407. Piomelli, D., *A fatty gut feeling.* Trends Endocrinol Metab, 2013. **24**(7): p. 332-41.
408. Purohit, V., R. Rapaka, and D. Shurtleff, *Role of cannabinoids in the development of fatty liver (steatosis).* AAPS J, 2010. **12**(2): p. 233-7.
409. Simon, G.M. and B.F. Cravatt, *Characterization of mice lacking candidate N-acyl ethanolamine biosynthetic enzymes provides evidence for multiple pathways that contribute to endocannabinoid production in vivo.* Mol Biosyst, 2010. **6**(8): p. 1411-8.
410. Powell, D.R., et al., *Diacylglycerol Lipase alpha Knockout Mice Demonstrate Metabolic and Behavioral Phenotypes Similar to Those of Cannabinoid Receptor 1 Knockout Mice.* Front Endocrinol (Lausanne), 2015. **6**: p. 86.
411. Gunschmann, C., et al., *Transgenic mouse technology in skin biology: inducible gene knockout in mice.* J Invest Dermatol, 2014. **134**(7): p. e22.
412. Loomba, R. and A.J. Sanyal, *The global NAFLD epidemic.* Nat Rev Gastroenterol Hepatol, 2013. **10**(11): p. 686-90.
413. Schuler, M., et al., *Efficient temporally controlled targeted somatic mutagenesis in hepatocytes of the mouse.* Genesis, 2004. **39**(3): p. 167-72.
414. Liu, J., et al., *Multiple pathways involved in the biosynthesis of anandamide.* Neuropharmacology, 2008. **54**(1): p. 1-7.
415. Movita, D., et al., *Kupffer cells express a unique combination of phenotypic and functional characteristics compared with splenic and peritoneal macrophages.* J Leukoc Biol, 2012. **92**(4): p. 723-33.
416. Elvevold, K., B. Smedsrod, and I. Martinez, *The liver sinusoidal endothelial cell: a cell type of controversial and confusing identity.* Am J Physiol Gastrointest Liver Physiol, 2008. **294**(2): p. G391-400.
417. Carpino, G., et al., *Alpha-SMA expression in hepatic stellate cells and quantitative analysis of hepatic fibrosis in cirrhosis and in recurrent chronic hepatitis after liver transplantation.* Dig Liver Dis, 2005. **37**(5): p. 349-56.
418. Manco, R., et al., *Reactive cholangiocytes differentiate into proliferative hepatocytes with efficient DNA repair in mice with chronic liver injury.* J Hepatol, 2019. **70**(6): p. 1180-1191.
419. Cani, P.D., et al., *Glucose metabolism: focus on gut microbiota, the endocannabinoid system and beyond.* Diabetes Metab, 2014. **40**(4): p. 246-57.

420. Sugiura, T., et al., *Transacylase-mediated and phosphodiesterase-mediated synthesis of N-arachidonoylethanolamine, an endogenous cannabinoid-receptor ligand, in rat brain microsomes. Comparison with synthesis from free arachidonic acid and ethanolamine.* Eur J Biochem, 1996. **240**(1): p. 53-62.
421. Ueda, N., K. Yamanaka, and S. Yamamoto, *Purification and characterization of an acid amidase selective for N-palmitoylethanolamine, a putative endogenous anti-inflammatory substance.* J Biol Chem, 2001. **276**(38): p. 35552-7.
422. Bisogno, T., et al., *Biosynthesis, uptake, and degradation of anandamide and palmitoylethanolamide in leukocytes.* J Biol Chem, 1997. **272**(6): p. 3315-23.
423. Muccioli, G.G. and N. Stella, *Microglia produce and hydrolyze palmitoylethanolamide.* Neuropharmacology, 2008. **54**(1): p. 16-22.
424. Ohara, M., et al., *Palmitoylethanolamide Ameliorates Carbon Tetrachloride-Induced Liver Fibrosis in Rats.* Front Pharmacol, 2018. **9**: p. 709.
425. Petrosino, S. and V. Di Marzo, *The pharmacology of palmitoylethanolamide and first data on the therapeutic efficacy of some of its new formulations.* Br J Pharmacol, 2017. **174**(11): p. 1349-1365.
426. Turcotte, C., et al., *Human leukocytes differentially express endocannabinoid-glycerol lipases and hydrolyze 2-arachidonoyl-glycerol and its metabolites from the 15-lipoxygenase and cyclooxygenase pathways.* J Leukoc Biol, 2019. **106**(6): p. 1337-1347.
427. Zechner, R., et al., *FAT SIGNALS--lipases and lipolysis in lipid metabolism and signaling.* Cell Metab, 2012. **15**(3): p. 279-91.
428. Dawson, P.A. and S.J. Karpen, *Intestinal transport and metabolism of bile acids.* J Lipid Res, 2015. **56**(6): p. 1085-99.
429. Somm, E., et al., *beta-Klotho deficiency protects against obesity through a crosstalk between liver, microbiota, and brown adipose tissue.* JCI Insight, 2017. **2**(8).
430. Douglass, J.D., et al., *Global deletion of MGL in mice delays lipid absorption and alters energy homeostasis and diet-induced obesity.* J Lipid Res, 2015. **56**(6): p. 1153-71.
431. Geurts, L., et al., *Chronic endocannabinoid system stimulation induces muscle macrophage and lipid accumulation in type 2 diabetic mice independently of metabolic endotoxaemia.* PLoS One, 2013. **8**(2): p. e55963.
432. Li, Z., S.F. Schmidt, and J.M. Friedman, *Developmental role for endocannabinoid signaling in regulating glucose metabolism and growth.* Diabetes, 2013. **62**(7): p. 2359-67.
433. Ahmad, T.R. and R.A. Haeusler, *Bile acids in glucose metabolism and insulin signalling - mechanisms and research needs.* Nat Rev Endocrinol, 2019. **15**(12): p. 701-712.
434. Silvestri, C. and V. Di Marzo, *The endocannabinoid system in energy homeostasis and the etiopathology of metabolic disorders.* Cell Metab, 2013. **17**(4): p. 475-90.
435. Wahli, W. and L. Michalik, *PPARs at the crossroads of lipid signaling and inflammation.* Trends Endocrinol Metab, 2012. **23**(7): p. 351-63.
436. Piomelli, D. and O. Sasso, *Peripheral gating of pain signals by endogenous lipid mediators.* Nat Neurosci, 2014. **17**(2): p. 164-74.
437. Alhouayek, M. and G.G. Muccioli, *COX-2-derived endocannabinoid metabolites as novel inflammatory mediators.* Trends Pharmacol Sci, 2014. **35**(6): p. 284-92.
438. Mazuy, C., et al., *Nuclear bile acid signaling through the farnesoid X receptor.* Cell Mol Life Sci, 2015. **72**(9): p. 1631-50.
439. Lefort, C., et al., *Hepatic MyD88 regulates liver inflammation by altering synthesis of oxysterols.* Am J Physiol Endocrinol Metab, 2019. **317**(1): p. E99-E108.
440. Izzo, A.A., et al., *Basal and fasting/refeeding-regulated tissue levels of endogenous PPAR-alpha ligands in Zucker rats.* Obesity (Silver Spring), 2010. **18**(1): p. 55-62.
441. Manca, C., et al., *Germ-free mice exhibit profound gut microbiota-dependent alterations of intestinal endocannabinoidome signaling.* J Lipid Res, 2020. **61**(1): p. 70-85.
442. Kleinridders, A., et al., *MyD88 signaling in the CNS is required for development of fatty acid-induced leptin resistance and diet-induced obesity.* Cell Metab, 2009. **10**(4): p. 249-59.

443. Jin, S., et al., *Function of astrocyte MyD88 in high-fat-diet-induced hypothalamic inflammation.* Journal of neuroinflammation, 2020. **17**(1): p. 195-195.
444. Yokoyama, S., T. Hosoi, and K. Ozawa, *Stearoyl-CoA Desaturase 1 (SCD1) is a key factor mediating diabetes in MyD88-deficient mice.* Gene, 2012. **497**(2): p. 340-3.
445. Hosoi, T., et al., *Myeloid differentiation factor 88 (MyD88)-deficiency increases risk of diabetes in mice.* PLoS One, 2010. **5**(9).
446. van Best, N., et al., *Bile acids drive the newborn's gut microbiota maturation.* Nat Commun, 2020. **11**(1): p. 3692.
447. Gerard, P., *Metabolism of cholesterol and bile acids by the gut microbiota.* Pathogens, 2013. **3**(1): p. 14-24.
448. Kenny, D.J., et al., *Cholesterol Metabolism by Uncultured Human Gut Bacteria Influences Host Cholesterol Level.* Cell Host Microbe, 2020.
449. Li-Hawkins, J., et al., *Disruption of the oxysterol 7alpha-hydroxylase gene in mice.* J Biol Chem, 2000. **275**(22): p. 16536-42.
450. Rose, K.A., et al., *Cyp7b, a novel brain cytochrome P450, catalyzes the synthesis of neurosteroids 7alpha-hydroxy dehydroepiandrosterone and 7alpha-hydroxy pregnenolone.* Proc Natl Acad Sci U S A, 1997. **94**(10): p. 4925-30.
451. Yantsevich, A.V., et al., *Human steroid and oxysterol 7alpha-hydroxylase CYP7B1: substrate specificity, azole binding and misfolding of clinically relevant mutants.* FEBS J, 2014. **281**(6): p. 1700-13.
452. Martin, C., et al., *cyp7b1 catalyses the 7alpha-hydroxylation of dehydroepiandrosterone and 25-hydroxycholesterol in rat prostate.* Biochem J, 2001. **355**(Pt 2): p. 509-15.
453. Di Marzo, V., et al., *Changes in plasma endocannabinoid levels in viscerally obese men following a 1 year lifestyle modification programme and waist circumference reduction: associations with changes in metabolic risk factors.* Diabetologia, 2009. **52**(2): p. 213-7.
454. Di Marzo, V., et al., *Role of insulin as a negative regulator of plasma endocannabinoid levels in obese and nonobese subjects.* Eur J Endocrinol, 2009. **161**(5): p. 715-22.
455. Sipe, J.C., et al., *Biomarkers of endocannabinoid system activation in severe obesity.* PLoS One, 2010. **5**(1): p. e8792.
456. Bluher, M., et al., *Dysregulation of the peripheral and adipose tissue endocannabinoid system in human abdominal obesity.* Diabetes, 2006. **55**(11): p. 3053-60.
457. Engeli, S., et al., *Activation of the peripheral endocannabinoid system in human obesity.* Diabetes, 2005. **54**(10): p. 2838-43.
458. Cravatt, B.F., et al., *Functional disassociation of the central and peripheral fatty acid amide signaling systems.* Proc Natl Acad Sci U S A, 2004. **101**(29): p. 10821-6.
459. Vaitheesvaran, B., et al., *Peripheral effects of FAAH deficiency on fuel and energy homeostasis: role of dysregulated lysine acetylation.* PLoS One, 2012. **7**(3): p. e33717.
460. Brown, L.M., et al., *Metabolic impact of sex hormones on obesity.* Brain research, 2010. **1350**: p. 77-85.
461. Chella Krishnan, K., M. Mehrabian, and A.J. Lusis, *Sex differences in metabolism and cardiometabolic disorders.* Current opinion in lipidology, 2018. **29**(5): p. 404-410.
462. Guarner-Lans, V., et al., *Relation of aging and sex hormones to metabolic syndrome and cardiovascular disease.* Exp Gerontol, 2011. **46**(7): p. 517-23.
463. Dakin, R.S., et al., *Estrogens protect male mice from obesity complications and influence glucocorticoid metabolism.* International Journal of Obesity, 2015. **39**(10): p. 1539-1547.
464. Noonan, W.T. and R.O. Banks, *Renal Function and Glucose Transport in Male and Female Mice with Diet-Induced Type II Diabetes Mellitus (44568).* Proceedings of the Society for Experimental Biology and Medicine, 2000. **225**(3): p. 221-230.
465. Hwang, L.L., et al., *Sex differences in high-fat diet-induced obesity, metabolic alterations and learning, and synaptic plasticity deficits in mice.* Obesity (Silver Spring), 2010. **18**(3): p. 463-9.

466. Stubbins, R.E., et al., *Estrogen modulates abdominal adiposity and protects female mice from obesity and impaired glucose tolerance.* European Journal of Nutrition, 2012. **51**(7): p. 861-870.
467. Lacroix, S., et al., *Rapid and Concomitant Gut Microbiota and Endocannabinoidome Response to Diet-Induced Obesity in Mice.* mSystems, 2019. **4**(6).
468. Kubota, H., H.L. Yao, and L.M. Reid, *Identification and characterization of vitamin A-storing cells in fetal liver: implications for functional importance of hepatic stellate cells in liver development and hematopoiesis.* Stem Cells, 2007. **25**(9): p. 2339-49.
469. Knittel, T., et al., *Expression and regulation of cell adhesion molecules by hepatic stellate cells (HSC) of rat liver: involvement of HSC in recruitment of inflammatory cells during hepatic tissue repair.* The American journal of pathology, 1999. **154**(1): p. 153-167.
470. Fomin, M.E., et al., *Coexpression of CD14 and CD326 discriminate hepatic precursors in the human fetal liver.* Stem Cells Dev, 2011. **20**(7): p. 1247-57.
471. Strauss, O., et al., *Immunofluorescence identifies distinct subsets of endothelial cells in the human liver.* Sci Rep, 2017. **7**: p. 44356.
472. Lacombe, F., et al., *Flow cytometry CD45 gating for immunophenotyping of acute myeloid leukemia.* Leukemia, 1997. **11**(11): p. 1878-86.
473. Kocabayoglu, P., et al., *Induction and contribution of beta platelet-derived growth factor signalling by hepatic stellate cells to liver regeneration after partial hepatectomy in mice.* Liver Int, 2016. **36**(6): p. 874-82.
474. Turcotte, C., et al., *Regulation of inflammation by cannabinoids, the endocannabinoids 2-arachidonoyl-glycerol and arachidonoyl-ethanolamide, and their metabolites.* J Leukoc Biol, 2015. **97**(6): p. 1049-70.
475. Szafran, B., et al., *Lipopolysaccharide suppresses carboxylesterase 2g activity and 2-arachidonoylglycerol hydrolysis: A possible mechanism to regulate inflammation.* Prostaglandins Other Lipid Mediat, 2015. **121**(Pt B): p. 199-206.
476. Rodriguez de Fonseca, F., et al., *An anorexic lipid mediator regulated by feeding.* Nature, 2001. **414**(6860): p. 209-12.
477. Chusyd, D.E., et al., *Relationships between Rodent White Adipose Fat Pads and Human White Adipose Fat Depots.* Front Nutr, 2016. **3**: p. 10.
478. Nguyen, T.L., et al., *How informative is the mouse for human gut microbiota research?* Dis Model Mech, 2015. **8**(1): p. 1-16.
479. Luong, Q., J. Huang, and K.Y. Lee, *Deciphering White Adipose Tissue Heterogeneity.* Biology (Basel), 2019. **8**(2).

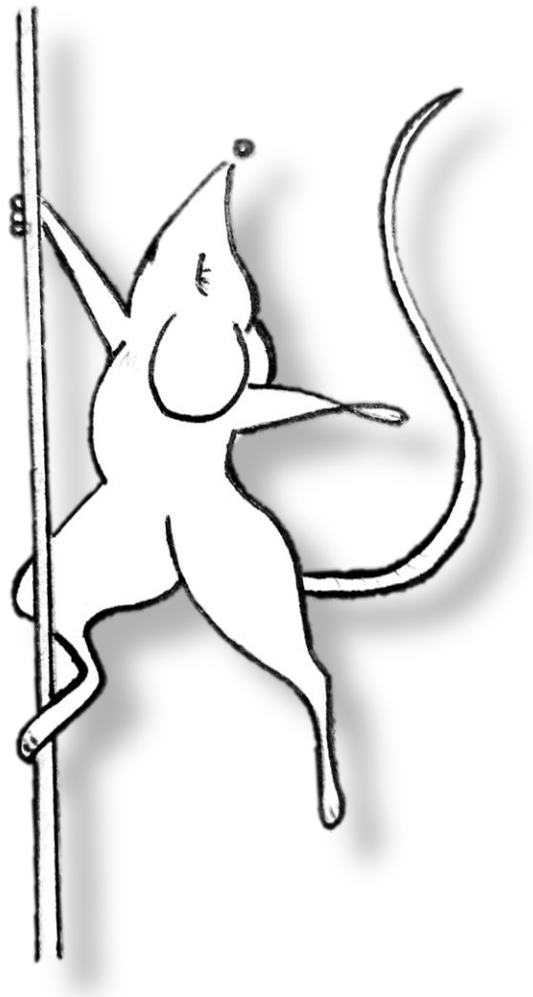

Figure emblématique de la thèse [Depommier & Lefort, *Bureau de la folie*, 2019]. Représentation du Yin et du Yang revisité. Merci Cla d'avoir dessiné ce chef-d'œuvre ;) qui regroupe mes deux passions et qui est devenu ma signature.